

NASA CR-72163
Aerojet 3392

FINAL REPORT

IMPROVED CRYOGENIC
RESIN/GLASS-FILAMENT-WOUND COMPOSITES

by

A. Lewis and G.E. Bush

prepared for

NATIONAL AERONAUTICS AND SPACE ADMINISTRATION

April 1967

Contract NAS 3-6297

Technical Management
NASA Lewis Research Center
Cleveland, Ohio
Chemical Rocket Division
R. F. Lark

Von Karman Center
AEROJET-GENERAL CORPORATION
Azusa, California

FOREWORD

This final report is submitted in fulfillment of the work under the contract. It covers the period from 29 June 1965 to 29 March 1967.

The work was conducted by the Glass Technology and Applications Department of the Structural Products Division, Aerojet-General Corporation, with assistance from the Composite Structures Department. The program was managed by A. Lewis, Program Manager, and G. E. Bush, Project Engineer. Major contributions were made by H. Buday, L. W. Kelley, and R. Molho, and further assistance was provided by E. E. Morris, R. F. Borden, J. Garancovsky, R. J. Robinson, P. B. Guhl, and A. I. Taoyama.

R. F. Lark, Program Manager, Liquid Rocket Technology Branch, Lewis Research Center, National Aeronautics and Space Administration, provided guidance throughout the program.



A. Lewis, Manager
Glass Technology and Applications Department



W. T. Cox, Manager
Structural Products Division

IMPROVED CRYOGENIC RESIN/GLASS-FILAMENT-WOUND COMPOSITES

by

A. Lewis and G. E. Bush

ABSTRACT

Composites fabricated with Aerojet Hi-Stren glass filaments and newly developed finish and resin systems yielded improved properties at room and cryogenic temperatures. Naval Ordnance Laboratory rings, flat filament-wound laminates, and 8-in.-dia filament-wound pressure vessels were tested. The glass reinforcement consisted of monofilaments, single-end roving, or 12-end roving. The finishes developed were compatible with both the glass surface and the matrix resins under evaluation.

CONTENTS

	<u>Page</u>
SUMMARY _____	xiii
I. INTRODUCTION _____	1
A. Background _____	1
B. Program Tasks _____	1
II. SELECTION OF MATERIALS AND PROCESSING TECHNIQUES _____	3
III. UNIAXIAL MONOFILAMENT COMPOSITES (TASK I) _____	7
IV. UNIAXIAL SINGLE-END COMPOSITES (TASK II) _____	8
A. Material Selection _____	8
B. Specimen Fabrication _____	11
C. Evaluation _____	19
V. BIAXIAL AND UNIAXIAL COMPOSITES (TASK III) _____	81
A. Material Selection _____	81
B. Specimen Fabrication _____	81
C. Evaluation _____	86
VI. FABRICATION AND EVALUATION OF FILAMENT-WOUND COMPOSITE (FWC) PRESSURE VESSELS (TASK IV) _____	104
A. Design _____	104
B. Fabrication _____	107
C. Instrumentation _____	112
D. Test Results _____	116
VII. SUPPLEMENTARY WORK _____	140
A. Glass-Boron Composites _____	140
B. Glass-Fiber/Whisker Composites _____	140
C. Void-Free NOL Rings _____	143
D. Ultrasonic Agitation _____	143
VIII. CONCLUSIONS _____	145
IX. RECOMMENDATIONS _____	146
References _____	147

CONTENTS (cont.)

<u>Table</u>		<u>Page</u>
1	Candidate Resins _____	4
2	Candidate Flexibilizers and Lubricants _____	4
3	Candidate Coupling Agents _____	5
4	Materials for Evaluation in Task II _____	9
5	Properties of Resin Systems Selected for Task II Evaluation _____	10
6	Strength and Modulus, Hi-Stren Glass Monofilaments _____	12
7	Data from Process and Control Study _____	20
8	Composite Tensile Strengths, Coupling-Agent Study _____	34
9	Composite Flexural Strengths, Coupling-Agent Study _____	35
10	Composite Horizontal Shear Strengths, Coupling-Agent Study _____	36
11	Control-Resin Study, Effect of Thermal Shock on Horizontal Shear Strength _____	45
12	Linear Thermal Contraction of Cast Resins _____	46
13	Cast-Resin Properties _____	48
14	Resin Study, NOL-Ring Composite Properties (Epon 828/LP-3/Curing Agent D) _____	50
15	Resin-Comparison Study, NOL-Ring Composite Properties _____	54
16	Resin Study, Effect of Thermal Shock on Horizontal Shear Strength _____	56
17	Resin Study, Flexural Fatigue _____	57
18	Resin Study, NOL-Ring Composite Properties (Epon 815/Versamid 140/Curing Agent D) _____	63
19	Resin Study, NOL-Ring Composite Properties (Araldite 6005/957 Hardener) _____	66
20	Resin Study, NOL-Ring Composite Properties (Epon 828/DSA/Empol 1040/BDMA) _____	71
21	Resin Study, NOL-Ring Composite Properties (Epon 826/Epon 871/L-100/MOCA) _____	76
22	Materials for Evaluation in Task III _____	82
23	Composite Test Results, Unidirectional 1:0 Orientation _____	91
24	Composite Test Results, Bidirectional 1:1 Orientation _____	92

CONTENTS (cont.)

<u>Table</u>		<u>Page</u>
25	Composite Test Results, Bidirectional 1:2 Orientation _____	93
26	Resin Study, Effect of Thermal Shock on Short-Span-Shear Strength _____	97
27	Impact Strength _____	97
28	Linear Thermal Contraction of Bidirectional 1:2 Composites _____	98
29	Evaluation of Improved, Cast, Epoxy/Polyurethane Resins _____	102
30	Composite Test Results, Improved Epoxy/Polyurethane Resin (Unidirectional 1:0 Orientation) _____	103
31	Test-Vessel Design Criteria _____	105
32	Test-Vessel Dimensional and Material Parameters _____	106
33	Test-Vessel Weight Analysis _____	110
34	Test-Vessel Fabrication Data _____	113
35	Pressure-Vessel Data and Burst-Test Results _____	118
36	Structural-Test Results, Pressure Vessels _____	119
37	Test-Temperature Measurements, Cryogenic Pressure Vessels _____	138
38	Composite Properties, Glass Fibers/Silicon Carbide Whiskers and Glass Fibers/Boron Filaments _____	141
39	Glass-Fiber/Whisker-Reinforced Composites, Horizontal Shear _____	142
 <u>Figure</u>		
1	Glass-Melting Furnace _____	13
2	Marble Furnace _____	14
3	Winding Machine _____	16
4	NOL-Ring Cutting Fixture _____	17
5	Cake Package _____	18
6	Winding-Tension Study, Resin Content vs Tension Load _____	21
7	Winding-Tension Study, Resin Content vs Specific Gravity _____	22
8	Coupling Agent A-1100, Composite Tensile Strength _____	24
9	Coupling Agent A-1100, Composite Flexural Strength _____	25

CONTENTS (cont.)

<u>Figure</u>		<u>Page</u>
10	Coupling Agent A-1100, Composite Horizontal Shear Strength _____	26
11	Coupling Agent A-186, Composite Tensile Strength _____	27
12	Coupling Agent A-186, Composite Flexural Strength _____	28
13	Coupling Agent A-186, Composite Horizontal Shear Strength _____	30
14	Coupling Agent Z-6020, Composite Tensile Strength _____	31
15	Coupling Agent Z-6020, Composite Flexural Strength _____	32
16	Coupling Agent Z-6020, Composite Horizontal Shear Strength _____	33
17	Coupling Agent Z-6040, Composite Tensile Strength _____	37
18	Coupling Agent Z-6040, Composite Flexural Strength _____	38
19	Coupling Agent Z-6040, Composite Horizontal Shear Strength _____	39
20	Typical Cross Section, Task II NOL Ring _____	40
21	Wetting Study, Contact Angle 31° _____	40
22	Wetting Study, Contact Angle 61° _____	41
23	Wetting Study, Contact Angle 77° _____	41
24	Wetting Study, Single-End Roving (Epon 828/LP-3/ Curing Agent D) _____	43
25	Wetting Study, Single-End Roving (VHS Finish) _____	43
26	Wetting Study, Single-End Roving (Epon 828/NMA/BDMA) _____	44
27	Wetting Study, Single-End Roving (Epon 828/LP-3/ Curing Agent D), Effect of Increased Pressurization _____	44
28	Linear Thermal Contraction, Cryogenic Resin Systems _____	47
29	Resin Study (Epon 828/LP-3/Curing Agent D), Tensile Strength _____	51
30	Resin Study (Epon 828/LP-3/Curing Agent D), Flexural Strength _____	52
31	Resin Study (Epon 828/LP-3/Curing Agent D), Horizontal Shear Strength _____	53
32	Resin-Comparison Study, Tensile Strength _____	55
33	Resin Study (Epon 815/Versamid 140/Curing Agent D), Tensile Strength _____	60

CONTENTS (cont.)

<u>Figure</u>		<u>Page</u>
34	Resin Study (Epon 815/Versamid 140/Curing Agent D), Flexural Strength _____	61
35	Resin Study (Epon 815/Versamid 140/Curing Agent D), Horizontal Shear Strength _____	62
36	Resin-Comparison Study, Flexural Strength _____	64
37	Resin-Comparison Study, Horizontal Shear Strength _____	65
38	Resin Study (Araldite 6005/957 Hardener), Tensile Strength _____	67
39	Resin Study (Araldite 6005/957 Hardener), Flexural Strength _____	68
40	Resin Study (Araldite 6005/957 Hardener), Horizontal Shear Strength _____	69
41	Resin Study (Epon 828/DSA/Empol 1040/BDMA), Tensile Strength _____	72
42	Resin Study (Epon 828/DSA/Empol 1040/BDMA), Flexural Strength _____	73
43	Resin Study (Epon 828/DSA/Empol 1040/BDMA), Horizontal Shear Strength _____	74
44	Resin Study (Epon 826/Epon 871/L-100/MOCA), Tensile Strength _____	77
45	Resin Study (Epon 826/Epon 871/L-100/MOCA), Flexural Strength _____	78
46	Resin Study (Epon 826/Epon 871/L-100/MOCA), Horizontal Shear Strength _____	79
47	Filament-Wound Sheet, Cured Laminate, and Test Specimens _____	84
48	Filament-Orientation Patterns _____	85
49	Typical Cross Section, Unidirectional 1:0 Composite _____	87
50	Typical Cross Section, Bidirectional 1:1 Composite _____	88
51	Typical Cross Section, Bidirectional 1:2 Composite _____	88
52	Specimens After Testing _____	89
53	Resin-Finish Study, Flat Composite (Tensile Strength) _____	94
54	Resin-Finish Study, Composite Flat Coupons (Flexural Strength) _____	95
55	Resin-Finish Study, Composite Flat Coupons (Short-Span-Shear Strength) _____	96
56	Welded Liner, 8-in.-dia Pressure Vessel _____	108

CONTENTS (cont.)

<u>Figure</u>		<u>Page</u>
57	Filament-Wound Pressure Vessel _____	109
58	Test Setup, Showing Chamber for Cryogenic Pressure-Vessel Testing _____	114
59	Location of Instruments on Test Vessels _____	115
60	Pressure-Vessel Test Assembly _____	117
61	Vessel B-2 After Burst Test at Ambient Temperature _____	120
62	Vessel B-5, Showing Leak Area _____	122
63	Longitudinal Tensile Strength, Pressure Vessels with Hi-Stren Glass _____	123
64	Hoop Tensile Strength, Pressure Vessels with Hi-Stren Glass _____	124
65	Pressure vs Longitudinal Strain, Pressure Vessels at +75°F _____	125
66	Pressure vs Hoop Strain, Pressure Vessels at +75°F _____	126
67	Design vs Actual Strain, Pressure Vessels at +75°F _____	127
68	Pressure vs Longitudinal Strain, Pressure Vessels at -320°F _____	129
69	Pressure vs Hoop Strain, Pressure Vessels at -320°F _____	130
70	Pressure Vessel Assembled for Cryogenic Testing _____	131
71	Pressure Vessel After Burst Test at -320°F _____	133
72	Pressure vs Longitudinal Strain, Pressure Vessels at -423°F _____	134
73	Pressure vs Hoop Strain, Pressure Vessels at -423°F _____	135
74	Pressure Vessel After Burst Test at -423°F _____	137

APPENDIX A - TEST METHODS _____ A-1

<u>Figure</u>		
A-1	Routing Fixture, Tensile-Test Specimen _____	A-2
A-2	Clamp Fixture, Tensile-Test Specimen _____	A-3
A-3	Cryostat/Tensile-Machine Facility _____	A-4
A-4	Cryostat/Tensile-Test Machine _____	A-5
A-5	Tensile-Test Specimen _____	A-6
A-6	Tensile-Test-Fixture Setup _____	A-7

CONTENTS (cont.)

<u>Figure</u>	<u>Page</u>
A-7 Cryogenic Tester, Interlaminar Shear _____	A-10
A-8 Short-Span-Shear Test-Fixture Setup _____	A-12
A-9 Horizontal-Shear Test-Fixture Setup _____	A-14
APPENDIX B - DESIGN ANALYSIS, 8-IN.-DIA FILAMENT-WOUND PRESSURE VESSELS FOR CRYOGENIC-RESIN EVALUATION _____	B-1
APPENDIX C - PROCESSING, FABRICATION, AND TEST INSTRUCTIONS FOR IMPROVED RESIN/GLASS-FILAMENT-WOUND PRESSURE VESSELS _____	C-1
APPENDIX D - TEMPERATURE AND STRAIN MEASUREMENT, DATA AND ANALYSIS _____	D-1
<u>Table</u>	
D-1 Temperature Measurements During Burst Testing of 8-in.-dia Tankage _____	D-2
<u>Figure</u>	
D-1 Bow-Tie Extensometer, Schematic _____	D-5
D-2 Calibration Tool and Support Band _____	D-7
D-3 Calibration Curve for Bow-Tie Extensometer _____	D-9
APPENDIX E - CALCULATION OF FILAMENT AND COMPOSITE TENSILE STRESS _____	E-1
<u>Figure</u>	
E-1 Glass Weight/Volume Relationships in Resin Composites _____	E-3
APPENDIX F - EVALUATION OF PRESSURE-VESSEL WALL-TEMPERATURE MEASUREMENT _____	F-1
<u>Figure</u>	
F-1 Temperature-Sensor Locations _____	F-2
F-2 Temperature Evaluation, Test 1 _____	F-3
F-3 Temperature Evaluation, Test 2 _____	F-4
F-4 Temperature Evaluation, Test 3 _____	F-5
Distribution List _____	G-1

IMPROVED CRYOGENIC RESIN/GLASS-FILAMENT-WOUND COMPOSITES

by A. Lewis and G. E. Bush
Aerojet-General Corporation

SUMMARY

The objective of this work was the development of an improved glass/resin composite for cryogenic use through investigation of glass-filament finishes, suitable resins, and/or improved processing techniques for composite fabrication.

Task I of the four-task program consisted of evaluation of state-of-the-art materials and techniques using NOL rings fabricated from newly formed glass monofilaments. Task II covered evaluations, employing NOL rings made from single-end roving, of the materials and/or techniques selected on the basis of Task I work. Selections based on Task II work were then evaluated in Task III with uniaxially and biaxially wound composites made from single-end roving. Task IV covered the final evaluation of selected materials using 8-in.-dia pressure vessels wound with 12-end roving.

An Aerojet-developed high-strength glass fiber (Hi-Stren), a magnesia aluminosilicate, was selected as the reinforcement for all work in the program.

In Task I glass monofilaments were formed into composites direct from the fiber furnace. Materials and techniques were evaluated in tests of these composites [Naval Ordnance Laboratory (NOL) rings] for their tensile-strength and interlaminar-shear properties. The results showed that superior strength and shear properties were attainable at ambient and cryogenic temperatures when composites were fabricated direct from the furnace. Twelve materials and processing techniques were selected for evaluation in Task II. The prime resin candidates were the epoxies and modified epoxies; the selected finishes were those that used the matrix resins as film formers. A coupling-agent study showed agent effectiveness only in a wet environment. It was also found that lubricants and flexibilizers have little or no effect on composite properties.

In Tasks II and III Hi-Stren glass was formed into single-end rovings (204 filaments) and fabricated into composites. The fibers were coated with the selected finishes immediately after filament formation. Task II employed uniaxial composites consisting of NOL rings. In Task III, parallel-fiber

resin-impregnated sheets were wound from the rovings and were fabricated into unidirectional and bidirectional flat laminates, from which specimens were cut. The testing in both tasks was at +75, -320, and -423° F.

Task II resulted in the selection of three epoxy and modified-epoxy resin systems and two silane-type coupling agents for Task III evaluation. In addition, it was determined in processing-technique investigations that fiber tension and resin impregnation were the most effective factors in producing good composites having the least voids. The technique studies were therefore discontinued, and subsequent effort was concentrated on materials.

The Task III evaluations, which also included two modifications of an epoxy system that was developed under another National Aeronautics and Space Administration Contract (NAS 3-6287), resulted in the selection of two modified-epoxy-resin/finish systems and an epoxy control finish/resin system, with one coupling agent, for evaluation in Task IV.

The evaluation criteria in the earlier work were primarily shear, tensile, and flexural strength; Task IV featured burst tests of thin-walled, metal-lined, filament-wound, pressure vessels. At ambient temperature, six vessels exhibited circumferential and longitudinal filament stresses equivalent to the state of the art. At temperatures of -320 and -423° F, improved performance was obtained with Hi-Stren glass and the newly developed resin/finish systems. The highest longitudinal and hoop-filament stresses were exhibited by the system consisting of epichlorohydrin-bisphenol A (Epon 828), dodecenyl succinic anhydride (DSA), aliphatic tricarboxy acid (Empol 1040), and benzyldimethylamine (BDMA).

The program demonstrated that improved cryogenic filament-wound composites can be obtained through the use of Hi-Stren glass filaments and new low-temperature resin/finish systems. In addition, improved fabricating techniques, tooling, and test methods were developed for filament-wound composites.

I. INTRODUCTION

A. BACKGROUND

This work was initiated for the purpose of developing improved materials to use in fabricating high-performance composite tankage capable of containing cryogenic liquids at high stress levels. Glass filaments and epoxy resins were considered the prime candidate materials. A review of previous work revealed only a limited amount of cryogenic data for composites made of these materials, but showed that higher performance could be expected at cryogenic temperatures than is normally obtained at ambient temperature (Ref. 1). Preliminary experiments at Aerojet indicated that the room-temperature strength of a glass filament is increased by approximately 50% and the elastic modulus by 10% when tested at cryogenic temperatures (Ref. 2). This is in agreement with current literature.

Resin crazing at cryogenic temperatures is attributed to an increase in elastic modulus and brittleness at such temperatures. To achieve resin improvement, it was suggested that the epoxies normally used in filament-wound composites be modified to increase flexibility (Ref. 3). Materials such as nylon, polyamides, and polyurethanes were considered as offering great promise for such modifications.

In addition to flexibility improvement, Aerojet gave consideration to resin-processing characteristics (pot life, viscosity) in terms of filament winding. This aspect had not heretofore been investigated, because the reported work dealt primarily with test specimens made of glass cloth or cast resin.

B. PROGRAM TASKS

The present program initially consisted of a three-task, 16-month effort and was modified during Task III to a four-task, 21-month effort. The overall objective was to develop glass/resin composites having improved cryogenic properties attained through the use of an improved glass filament, finish, resin, and/or processing technique. Glass/finish/resin investigations at room temperature and cryogenic temperatures received primary emphasis, and processing techniques were allocated a less important role.

This report describes the work performed in Tasks II, III, and IV and summarizes Task I, which was covered separately (in Ref. 2) at the request of the National Aeronautics and Space Administration.

Task I effort revealed a substantial improvement in interlaminar shear strength using material combinations and processing techniques developed and evaluated in this task. Tasks II and III verified the findings in work under Contract NAS 3-6287 that resins having greater flexibility exhibit increased performance at cryogenic temperatures. Task IV demonstrated the superiority of cryogenic pressure vessels fabricated with the glass, finish, and resins developed in this program.

With regard to comparative strengths at room and cryogenic temperatures, the average values for the longitudinal- and hoop-filament stresses in the pressure vessels were 434,200 psi at -423°F, 437,400 psi at -320°F, and 343,200 psi at +75°F. An improvement of 26% was thus obtained at -423°F and one of 28% at -320°F.

II. SELECTION OF MATERIALS AND PROCESSING TECHNIQUES

At the outset of the program, a search of the literature on state-of-the-art resins was conducted (Ref. 2) to select materials for the development of an improved cryogenic resin/glass-filament-wound structure. In addition, information was sought by letter from 26 resin manufacturers and/or suppliers (Ref. 2) on their candidate materials. The survey yielded 31 resins, 9 flexibilizers, 5 wetting agents, and 9 coupling agents (Tables 1, 2, and 3).

These materials, along with processing techniques, were physically and mechanically examined with Naval Ordnance Laboratory (NOL) rings fabricated from newly formed glass monofilaments. The evaluations consisted of (a) filament-coating studies employing coupling agents, film formers, and wetting agents, (b) a study of resins as the matrix for NOL-ring specimens, and (c) glass investigations dealing with virgin-filament tensile strength and the horizontal-shear and tensile strengths of composites.

Twelve combinations of materials and processing techniques were ultimately selected for continued evaluation. The selections were based on the preliminary screening and evaluation studies demonstrating the properties most desirable for the fabrication of cryogenic glass/resin composites. The techniques and materials were evaluated at ambient and cryogenic temperatures (+75, -320, and -423°F), and five combinations of resins and/or finishes were selected for additional evaluation in the form of unidirectional and bidirectional, single-end, filament-wound composites.

Processing techniques were deleted from further evaluation during the remainder of the program. This permitted efforts to be concentrated on other areas relating to glass-multifilament fiberization, finish applications, and single-end and multiple-end roving manufacture.

The NOL rings were subsequently replaced by flat laminates for material evaluations. The laminates were fabricated by laying up a series of single-end filament-wound sheets to a required filament orientation and thickness. Production of the sheets served to evaluate the handling characteristics of the glass fibers and the matrix resin by simulating the winding process normally used to fabricate a pressure vessel. The uniaxially and biaxially fabricated glass-filament/resin composites were tested at ambient temperature, -320, and -423°F.

Three candidate resin-finish systems displaying improvement at cryogenic temperatures were then used, in combination with Aerojet 12-end Hi-Stren glass roving, to fabricate 18 filament-wound pressure vessels (plus one spare). They were

Epon 828/NMA/BDMA (100/80/0.5 parts by weight, pbw)
Epon 828/DSA/Empol 1040/BDMA (100/115.9/20/1 pbw)
Epon 826/Epon 871/DDI/Curalon L (35/15/14.7/35.1 pbw)

TABLE 1
CANDIDATE RESINS

Type	Trade Designation	Supplier
Epoxy	Epon 815, 826, 828, 871, 872, 949A & B, 1028-B-70	Shell Chemical Company
Epoxy	Isochemrez 405, 408	Isochem Resins Company
Epoxy	DEN 438, DER 331	Dow Chemical Company
Epoxy	Araldite 6005	Ciba Products Company
Epoxy	ELS-3001, ERRA 0300	Union Carbide Corporation
Epoxy	Oxiron 2000	FMC Corporation
Urethane	Uralane 5721-A	Furane Plastics, Inc.
Urethane	Adiprene L-100	E. I. du Pont de Nemours & Company
Urethane	Narmco 7343	Narmco Materials Division
Silicone	DC-2106	Dow Corning Corporation
Polyamide	XPI-182	American Cyanamid Company
Polyamide	XPI-185	American Cyanamid
Butadiene-styrene	Buton-100	Enjay Chemical Company
Polybutadiene	Buton-150	Enjay
Phenolic	SC 1008	Monsanto Chemical Company
Phenolic elastomer	Narmco 2021	Narmco
Epoxy-nylon	Epon 949	Shell
Polyester	Paraplex P-13	Rohm & Haas Company
Polyester	Paraplex P-43	Rohm & Haas
Polyester	Selectron 5016	Pittsburgh Plate Glass Company
Fluorocarbons	Teflon T-30	Du Pont

TABLE 2
CANDIDATE FLEXIBILIZERS AND LUBRICANTS

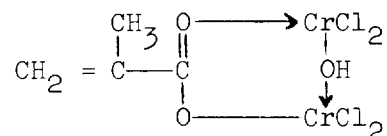
Type	Trade Designation	Supplier
Flexibilizers		
Aliphatic amide amine	Epi-Cure 855	Jones-Dabney Company
Polyamids	Versamid 100, 115, 125, and 140	General Mills, Inc.
Polysulfides	LP-3, LP-8, and LP-33	Thiokol Chemical Corporation
Trimer acid	Empol 1040 (formerly designated 3162-D)	Emery Industries, Inc.
Lubricants		
-	AHCO-185	ICI Organics Company
-	Cirrasol 220	ICI Organics
-	Cirrasol 838	ICI Organics
-	Y-4186	Union Carbide Corporation
-	L-527	Union Carbide

TABLE 3

CANDIDATE COUPLING AGENTS

Trade Designation	Chemical Name and Formula	Supplier
A-1100	γ -aminopropyltriethoxy silane $\text{NH}_2\text{CH}_2\text{CH}_2\text{CH}_2\text{Si}(\text{OC}_2\text{H}_5)_3$	Union Carbide Corporation
A-172	Vinyltris(2-methoxyethoxy) silane $\text{H}_2\text{C}=\text{C}-\text{Si}(\text{OC}_2\text{H}_4\text{OCH}_3)_3$	Union Carbide
A-174	γ -methacryloxypropyltrimethoxy silane $\text{CH}_2=\text{C}(\text{CH}_3)-\text{C}(=\text{O})-\text{OCH}_2\text{CH}_2\text{CH}_2\text{Si}(\text{OCH}_3)_3$	Union Carbide
A-186	β -3,4-(epoxycyclohexyl)ethyltrimethoxy silane $\text{O} \begin{array}{c} \diagup \diagdown \\ \text{S} \end{array} \text{CH}_2\text{CH}_2\text{Si}(\text{OCH}_3)_3$	Union Carbide
Z-6020	η -(trimethoxysilylpropyl)ethylenediamine $(\text{CH}_3\text{O})_3\text{Si}(\text{CH}_2)_3\text{NH}(\text{CH}_2)_2\text{NH}_2$	Dow Corning Corporation
Z-6030	γ -methacryloxypropyltrimethoxy silane $\text{CH}_2=\text{C}(\text{CH}_3)-\text{COO}(\text{CH}_2)_3\text{Si}(\text{OCH}_3)_3$	Dow Corning
Z-6040	γ -glycidoxypopyltrimethoxy silane $\text{OCH}_2\text{CH}(\text{CH}_2\text{O}(\text{CH}_2)_3\text{Si}(\text{OCH}_3)_3)$	Dow Corning
Volan E	Organic acid chrome complex*	E. I. du Pont de Nemours & Company
Volan L	Methacrylato chromic chloride*	Du Pont

* Structural formula for Volan E and L (which respectively contain 17 to 19 and 19 to 21% chrome complex):



The closed-end, cylindrical, test vessels were of conventional design and were 8 in. in diameter by 13 in. long. They were constructed, by wet filament winding on a metal liner and mandrel assembly, for evaluation at ambient temperature, -320, and -423^oF, using a single-cycle burst test to failure by increasing the internal pressure at a rate of 500 psig/min.

III. UNIAXIAL MONOFILAMENT COMPOSITES (TASK I)

The objective of Task I was to select candidate materials and processing techniques for the development of an improved resin/glass-filament-wound structure suitable for cryogenic pressure vessels. This was accomplished by evaluation of commercially available filament-coating materials (finishes), resins, plasticizers or flexibilizers, and/or processing techniques.

State-of-the-art materials for consideration in Task I were selected after a thorough literature search and a survey of applicable manufacturers and/or suppliers. The materials and various processing techniques were evaluated with NOL rings fabricated from newly formed monofilaments.

Hi-Stren glass, a magnesia aluminosilicate developed by Aerojet, was selected as the reinforcement. The rings were fabricated as the glass was drawn from the fiber furnace, with the finish and resin being applied just before the fiber was wound into the composite. The resin and finish performance (interfacial-bond strength) was determined by subjecting the rings to interlaminar-shear tests at room temperature, at room temperature after a 6-hour water boil, and at -423°F .

Application and processing techniques were evaluated to improve the deposition of a uniform protective coating on the fiber and the application of the matrix resin in the winding of monofilament NOL rings. Other parameters investigated included (a) resin and finish concentrations, (b) resin viscosities with temperature variations, (c) filament-winding speeds, (d) filament tension, and (e) solvent carriers. In addition, a filament-traversing mechanism was developed that minimized the entrainment of air bubbles and voids in the composite (Ref. 4).

The investigation showed that improved cryogenic properties were obtained through the proper selection of materials. Epoxy or modified-epoxy resins* provided the highest properties at room temperature, after a 6-hour water boil, and at -423°F . Coupling Agent Z-6020 or Z-6040 with Epon 828 epoxy resin provided some of the best combinations of properties at the three environmental conditions.

This work is reported in detail in Ref. 2.

* Epon 828/NMA/BDMA and Epon 828/LP-3/Curing Agent D.

IV. UNIAXIAL SINGLE-END COMPOSITES (TASK II)

The 12 materials and processing techniques that displayed improved cryogenic properties during Task I were evaluated in Task II with single-end, multi-filament, glass/resin, NOL-ring composites.

A. MATERIAL SELECTION

The materials evaluated in Task II, including resin and finish formulations and concentrations, are shown in Table 4. The mixes and concentrations in the resin and finish systems were based on Task I work.

The resin-matrix materials were epoxy and modified-epoxy systems with a wide range of properties (Table 5). Two were unmodified epoxies used previously in the filament winding of high-strength pressure vessels. They served as controls for comparison with the performance levels of the other resins. Modified-epoxy resins were selected on the basis of their increased horizontal shear strength at -423°F as compared with their room-temperature strength. Toughness and flexibility were considered also, because they reportedly increase the strength of filament-wound pressure vessels (Ref. 3).

The epoxy and epoxy-modified resins produced superior room-temperature and cryogenic mechanical properties in comparison with the other resins evaluated during Task I. Their handling characteristics were also superior to those of the other systems with regard to filament winding.

The Task II film formers were selected on the basis of use with specific resin systems, to obtain compatibility and/or crosslinking between the finish-coated glass fiber and the matrix system. A finish system normally consists of a film former, a coupling agent, a lubricant, and a plasticizer. These give the fibers a bonding surface, a moisture barrier, flexibility, and protection during processing.

The selection of coupling agents was governed by the film formers. All finishes used in this program were dispersed in a solvent carrier, because the film formers were not water-soluble. Under these conditions, it is believed, hydrolysis of the silane to the glass surface is obtained with bound surface water or silanol groups on the glass fiber. Chemical interaction of coupling agents with epoxy film formers was obtained by reacting the active groups with the active hardeners. The widely used Union Carbide A-1100 coupling agent was selected as the control.

1. Resins

The Shell Epon 815, 826, and 828 and Ciba Araldite 6005 resins used as matrix resins and film formers are epichlorohydrin/bisphenol A, low-molecular-weight epoxies. They can be cured with a variety of curing agents, such as amines, anhydrides, or other hardeners, producing a wide latitude in processing parameters and physical properties. The epoxy resins bond well to glass filaments and have less shrinkage than most resins, low water-absorption properties, and high tensile strength with good extensibility.

TABLE 4

MATERIALS FOR EVALUATION IN TASK II

Basic Ingredients	System Formulations ¹	Concentrations ²
	<u>Matrix Resins</u>	
Epon 828	Epon 828/NMA/BDMA ³	100/80/0.5 pbw
Epon 828/LP-3	Epon 828/LP-3/Curing Agent D ⁴	100/33/12 pbw
Epon 815/Versamid 140	Epon 815/Versamid 140/Curing Agent D ⁴	100/33/12 pbw
Araldite 6005	Araldite 6005/957 Hardener ⁵	100/20 pbw
Epon 828/Empol 1040	Epon 828/DSA/Empol 1040/BDMA ⁶	100/115.9/20/1 pbw
Epon 826/Epon 871	Epon 826/Epon 871/C-100/MOCA ⁷	35/15/50/27.6 pbw
	<u>Finish Film Formers</u>	
VHS (control)	-	-
Epon 828/Versamid 140	Epon 828/Versamid 140/coupling agent/acetone	12.6/5.4/5/77 wt%
Epon 815/L-100	Epon 815/L-100/coupling agent/BDMA/acetone	15/4/5/1/75 wt%
Epon 828/LP-3	Epon 828/LP-3/coupling agent/Z hardener/acetone	10/4.5/5/1.5/80 wt%
Araldite 6005	Araldite 6005/957 hardener/coupling agent/acetone	14.4/3.6/5/75 wt%
	<u>Coupling Agents</u>	
A-1100 (control)	-	-
Z-5040	-	5 wt%
Z-6020	-	5 wt%
A-186	-	5 wt%

1. NMA = nadic methyl anhydride. BDMA = benzylidimethylamine. DSA = dodecenyl succinic anhydride.
MOCA = 4,4'-methylene-bis-(2-chloroaniline). Curing Agent D = polyamine salt.
2. pbw = parts by weight. 3. Cure: 1 hour 200°F, 2 hours 350°F. 4. Cure: 1 hour 150°F, 1 hour 300°F. 5. Cure: 2 hours 200°F, 2 hours 300°F. 6. Cure: 2 hours 150°F, 4 hours 300°F. 7. Cure: 5 hours 285°F.

TABLE 5

PROPERTIES OF RESIN SYSTEMS SELECTED FOR TASK II EVALUATION

Resin		Coupling Agent	Horizontal Shear Strength, psi			Strength Ratio, %			Resin Content wt%	Specific Gravity	Water Absorption wt%	Voids vol%
System	Type		At Room Temp	After 6-Hour Water Boil	At -423°F	At Room Temp	After 6-Hour Water Boil	At -423°F				
Epon 828/MDA/BDMA	Epoxy	A-1100	10,800	8,790	19,200	100	81.0	177	13.4	2.18	0.09	0.05
Same		Z-6040	10,700	8,520	26,000	100	80.0	244	11.8	2.21	0.24	Neg.
Same		Z-6020	12,800	8,840	26,000	100	69.0	203	11.9	2.21	0.054	0.075
Same		A-186	11,400	8,940	21,900	100	78.2	192	12.5	2.18	0.13	0.52
Epon 828/IP-3/ Curing Agent D	Modified Epoxy	A-1100	4,140	1,810	19,500	100	44.0	473	11.3	2.22	0.082	Neg.
Epon 828/ Versamid 140/ Curing Agent D	Modified Epoxy	A-1100	9,790	5,110	23,200	100	52.0	237	11.3	2.20	0.104	-
Araldite 6005/ Araldite 957	Epoxy	A-1100	9,190	-	26,600	100	-	289	11.8	2.18	0.12	-
Epon 828/BSA/ Epon 1040/BDMA*	Modified Epoxy	HTS	6,650	14,110	16,110	100			17.86	1.90	-	4.70
Epon 826/Epon 871/L-100/MOCA	Epoxy-urethane	A-1100	2,320	2,300	13,000	100	99.5	564	7.1	2.12	-	-

* Values taken from Cryogenic Resins for Glass-Filament-Wound Composites, NASA CR-72114 (Aerojet-General Report 3343).
Glass reinforcement was S-901 20-end roving.

It is possible to combine epoxy resins with a wide range of modifying agents to improve the impact resistance, toughness, and flexibility of the cured resin. Materials used to impart higher flexibility to the cured resin become an integral part of the cured system (Ref. 5). The flexibilizers used in this program were LP-3, Versamid 140, Empol 1040, and Adiprene L-100.

2. Glass

To ensure very high composite-strength values, Aerojet Hi-Stren glass was selected as the reinforcing filament. Its average room-temperature tensile strength and modulus are 700,000 psi and 13.5×10^6 psi, respectively. These data were obtained with virgin filaments tested within 30 min after fiberization.

Hi-Stren monofilaments were tested at -320°F to establish a benchmark for use in comparing composite-property data. Fifteen randomly selected glass-fiber control specimens tested at room temperature had an average tensile strength of 732,000 psi and an average modulus of 13.4×10^6 psi. Fifteen additional specimens were tested at -320°F by complete submersion in liquid nitrogen (LN_2). The tensile strength was increased by approximately 50% (to 1,097,000 psi) and the tensile modulus by approximately 10% (to 14.7×10^6 psi). The data are given in Table 6.

B. SPECIMEN FABRICATION

1. Equipment

a. Fiberizing Equipment

The glass-manufacturing equipment used in Task II included a glass-melting furnace and a marble-making facility consisting of a fining furnace and a marble machine. The glass-melting furnace (Figure 1), fired by natural gas, has a glass-melt capacity of 2000 lb and a melting area of approximately 36 cu ft.

The marble facility consists of a remelt furnace (Figure 2) having a glass-holding capacity of 700 lb, fired with natural gas, and controlled by an automatic firing mechanism consisting of temperature controllers and recorders, thermocouples, a gas-air mixer, and regulators. The marble machine, at the discharge end of the fining furnace, consists of an air-regulated shear and a pair of counter-rotating screws capable of producing a $3/4$ -in.-dia marble. The marble machine has a production capacity of 35 lb/hour.

The multifilament fiberizing furnace consists of a precious-metal bushing having a 12-lb remelt capacity. The electrically heated bushing acts as the heating element and a container for the molten glass. A hopper feeds marbles into the bushing at a specified rate.

TABLE 6

STRENGTH AND MODULUS, HI-STREN GLASS MONOFILAMENTS*

Fiber Diameter in.	Tensile and Modulus Properties, psi				Ratio of Properties	
	At Room Temp		At -320° F		-320° F/Room Temp	
	Strength	Modulus	Strength	Modulus	Strength	Modulus
1 0.000361	594,000	13,050,000	1,054,000	14,640,000	1.77	1.12
2 0.000361	739,000	13,690,000	No test	-	-	-
3 0.000361	767,000	13,580,000	1,261,000	14,370,000	1.71	1.06
4 0.000361	771,000	14,150,000	1,318,000	15,570,000	1.71	1.10
5 0.000354	301,000**	13,090,000	1,099,000	14,460,000	-	1.10
6 0.000354	709,000	13,130,000	647,000**	14,380,000	-	1.10
7 0.000355	688,000	13,100,000	826,000	14,620,000	1.20	1.12
8 0.000377	857,000	15,220,000**	1,024,000	17,500,000**	1.19	-
Av	732,000	13,400,000	1,097,000	14,670,000	1.51	1.10

* Gage length = 1.00 in. Strain rate = 20%/min. Room-temperature tests at 100° F and a relative humidity of 60%.

** Value considered not representative of batch and not included in ratios or averages.



564-444

Figure 1. Glass-Melting Furnace



Figure 2. Marble Furnace

465-426

A roller coater was used to apply the finish (sizing). It consists of a roller applicator rotating at a surface velocity of approximately 100 ft/min through a finish bath.

A take-up machine was used to gather the fibers onto a 6-3/8-in. cardboard forming tube. It was driven by a variable-speed motor capable of operating at 0 to 10,000 ft/min (fpm). A constant-speed traversing mechanism provided a uniform buildup of the strand (single-end roving) into a cake package.

b. NOL-Ring Winder

The NOL-ring winder was designed and built by the Aerojet Glass Technology Department and consisted of (1) a creel designed to accommodate a cake package or a ball of roving, (2) a heated-resin reservoir, and (3) a variable-speed takeup and traversing mechanism. Tensioning of the glass strand was controlled within 1/4 lb by varying a dead-weight load on the glass-fiber package. The temperature of the matrix resin was controlled by heating the resin reservoir with a resistant heating element. The winding mandrel and strand-traversing mechanism were powered by a variable-speed motor that provided control over the winding. Figure 3 shows this winding machine (including at right a takeup drum that was substituted in Task III for the mandrel used in Task II).

An electrically heated, air-circulating oven was employed to cure the composite rings. A routing fixture was designed and built to machine the rings. Test specimens were secured in a cutting fixture (Figure 4) and were cut with an 8-in. table saw equipped with a water-cooled diamond blade.

2. Procedures

NOL-ring test specimens were fabricated from a cake package (Figure 5). The finish was applied to the multifilament strand during fiberization. The NOL-ring winder was used; the single-end roving was drawn from the outside of the cake package and was passed over a series of rollers and through a resin bath. The impregnated strand was then wound onto an NOL-ring mandrel. A filament buildup of 1/32 in. over the prescribed ring thickness was added to ensure the proper dimensions. Experience with impregnation of single-end fibers in the fabrication of NOL rings has shown that uniform resin distribution and low void content are functions of the resin viscosity and strand tension. The viscosity was controlled by means of temperature, and tension control was achieved with a mechanically weighted brake. Teflon guide rollers were used to control the fiber in the resin bath.

The high interlaminar shear strength obtained for NOL rings wound with single-end fibers resulted from good processing techniques that ensured proper wetting of the fibers. The proper combination of resin viscosity and strand tension resulted in good resin distribution and low voids in the composite.

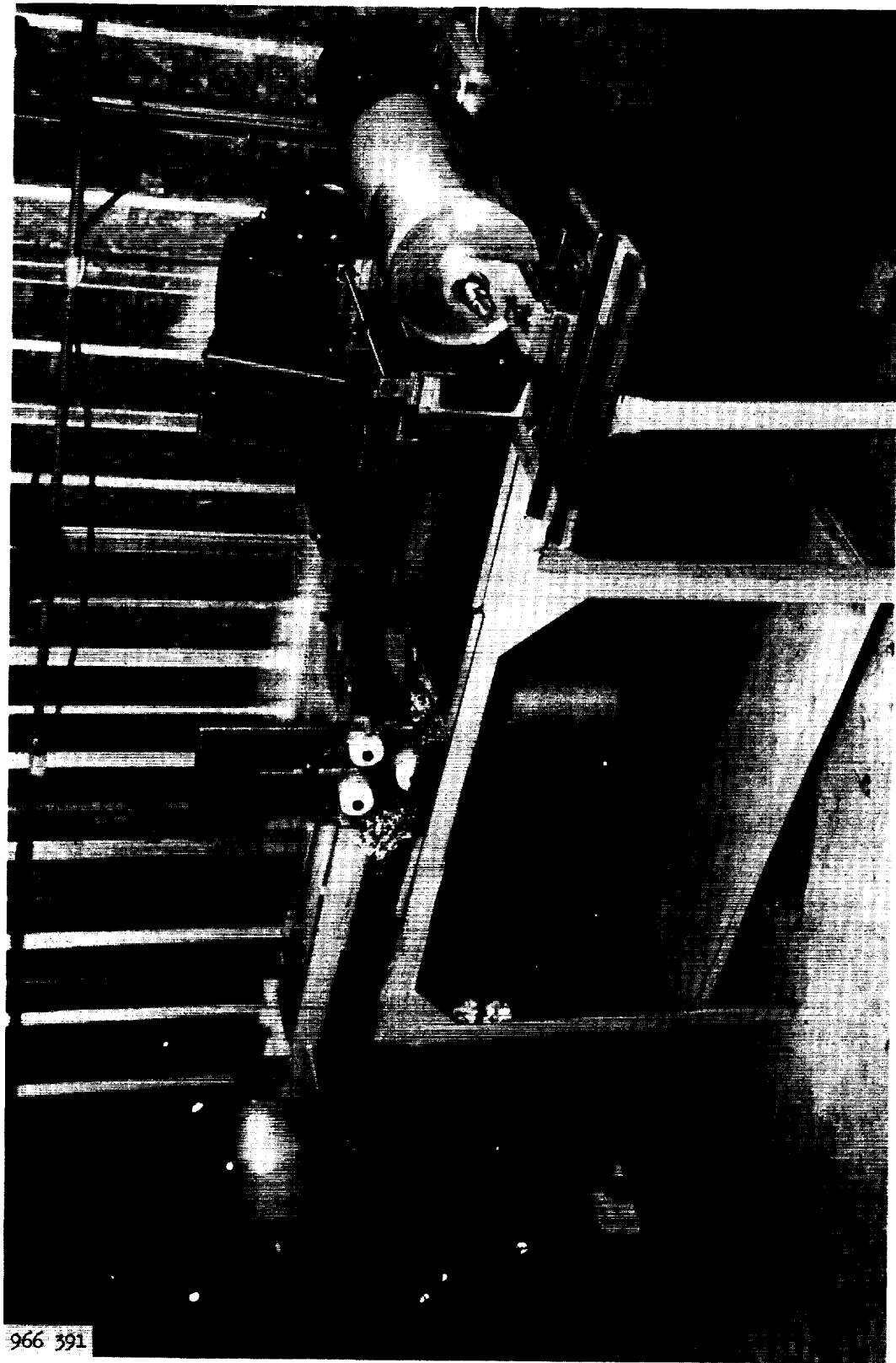
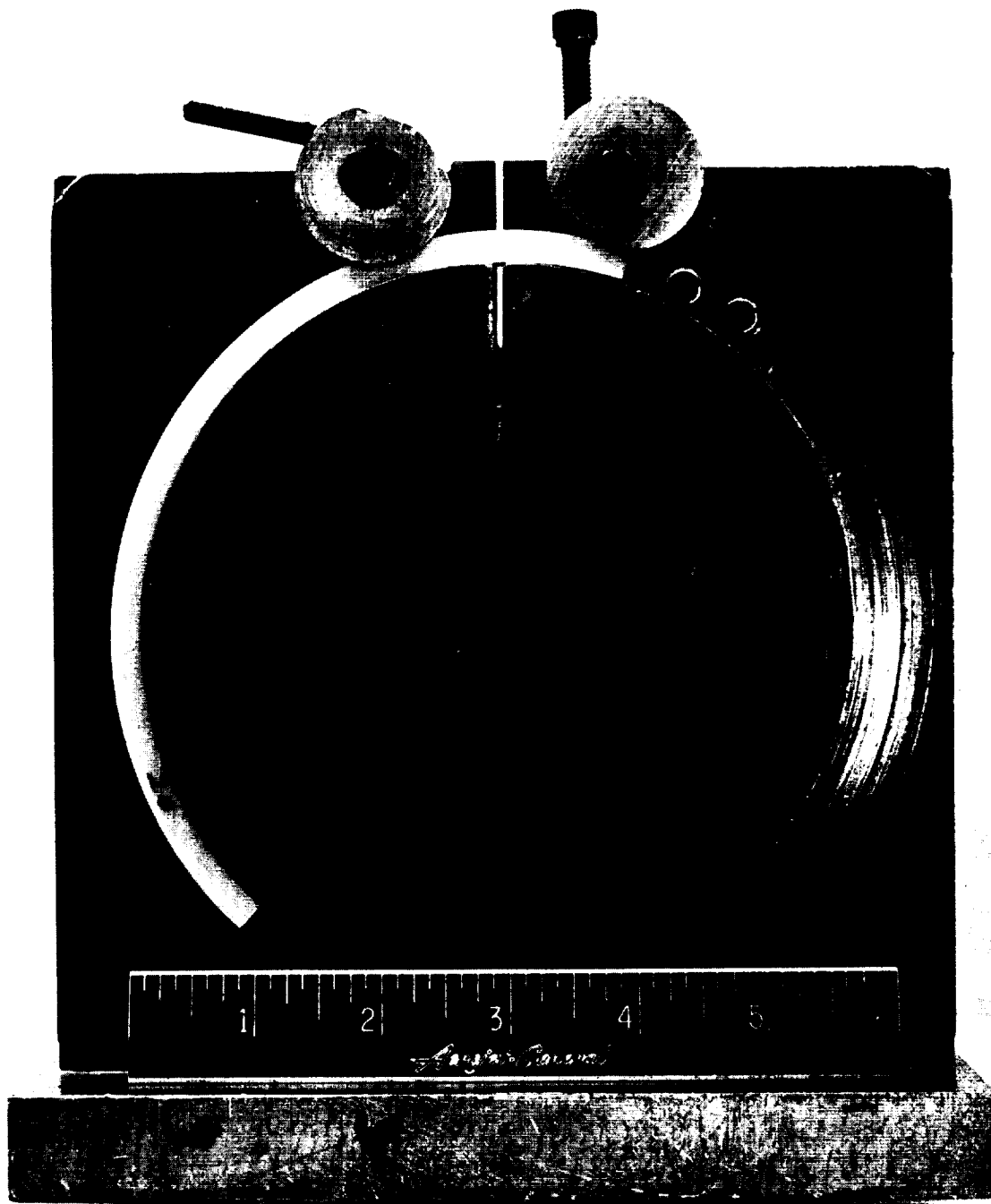


Figure 3. Winding Machine

966 391



1065-007

Figure 4. NOL-Ring Cutting Fixture

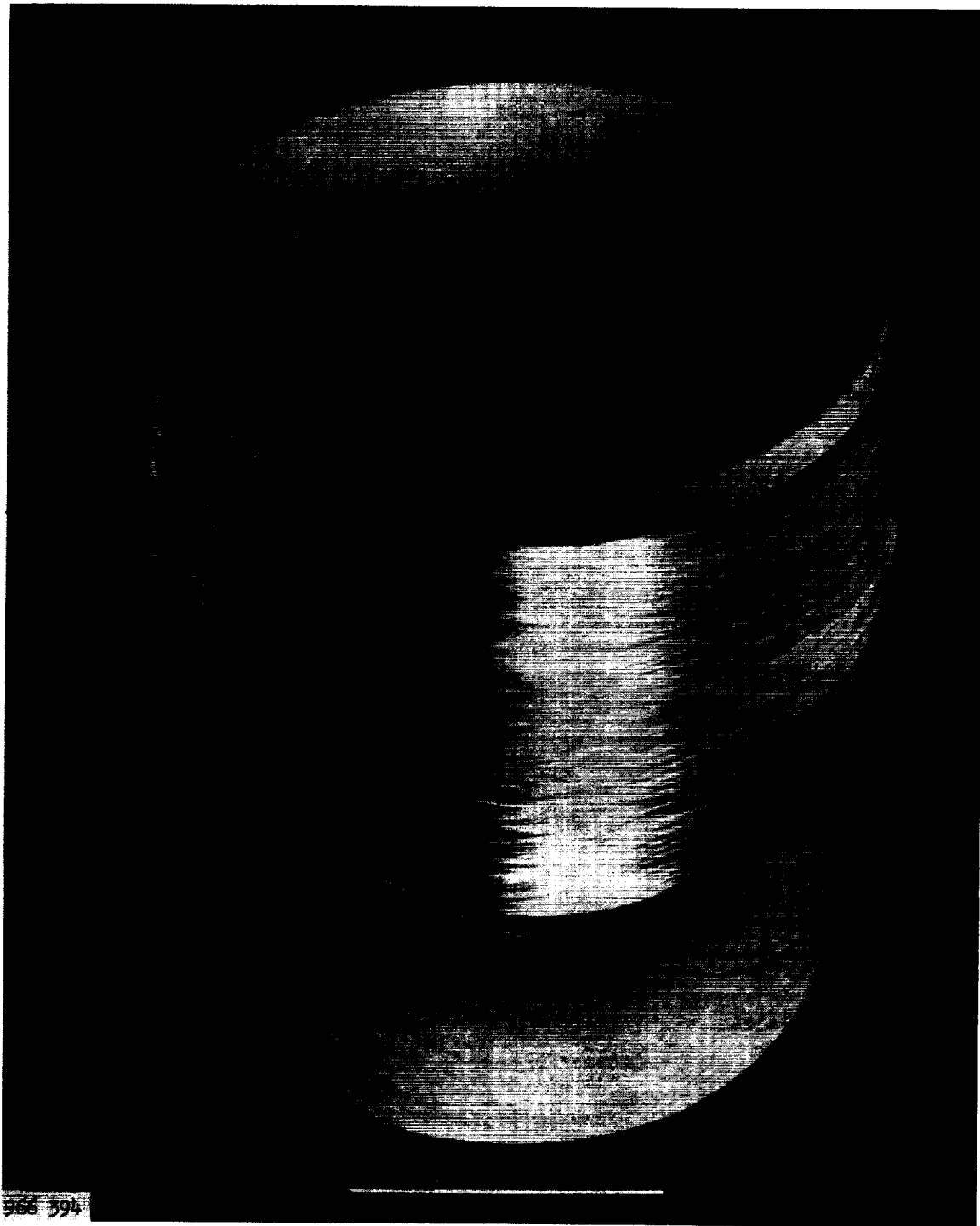


Figure 5. Cake Package

The filament-wound NOL rings were overwrapped with a Teflon tape and were oven-cured in accordance with the recommendations of the resin manufacturer. After curing, each ring was mounted on a router and was machined to the required tolerance. The rings were then hand-sanded to ensure a smooth surface. The NOL-ring composites were mounted on a shop-aid cutting fixture and were cut with a water-cooled diamond saw. This cutting method was adopted to ensure that the specimens were dimensionally accurate and to prevent the formation of defects that could result in premature failure.

Approximately 120 NOL rings were fabricated during Task II, the first of them to establish fabrication techniques for epoxy, butadiene-styrene, and modified-epoxy resins. Horizontal-shear and tensile-strength rings were fabricated (Table 7).

The winding tension was varied by varying a dead-weight load at the payoff creel. This was done to determine the amount of tension (weight) required to produce the desired resin content in the composite, which was measured by resin-content and specific-gravity determinations. The data are presented in Figures 6 and 7.

C. EVALUATION

1. Test Requirements

The tests listed below were performed on matrix resins or NOL-ring composites at the temperatures given.

- a. Standard composite NOL-ring tensile tests at +70, -320, and -423°F
- b. Flexural and horizontal-shear tests with composite NOL-ring segments at +70, -320, and -423°F
- c. Thermal-shock tests in which horizontal-shear specimens were multicycled from +70 to -423°F, followed by shear testing at +70°F
- d. Coefficient-of-thermal-contraction tests of the matrix resin at +70, -320, and -423°F
- e. Flexibility tests of cast resin at room temperature
- f. Determinations of resin shrinkage (%) during cure (at +70°F)
- g. Determinations of resin-system viscosity and pot life at +70°F
- h. Wetting tests of filament coatings and resins, including verification of uniform and satisfactory wetting

TABLE 7

DATA FROM PROCESS AND CONTROL STUDY*
SINGLE-END HI-STREN ROVING

Ring No.	Resin System	Horizontal Shear Strength, psi		Strength Retention, %					Water Absorption wt%	Void Content vol%	
		Room Temp	6-Hour Water Boil	At Room Temp	After 6-Hour Water Boil	At -423°F	Specific Gravity	Resin Content wt%			
S-1	Epon 828/NMA/BDMA	10,270	10,600	26,000	100	103	253	2.05	21.2	0.15	0.68
S-3	Epon 828/NMA/BDMA	6,040	5,210	10,800	100	86.3	179	1.94	21.4	0.55	4.09
S-4	Epon 828/NMA/BDMA	(237,700, tensile strength)			-	-	-	-	-	-	-
S-5	Epon 828/NMA/BDMA	(250,700, tensile strength)			-	-	-	-	-	-	-
S-6	Epon 828/NMA/BDMA	10,100	10,500	21,000	100	105	210	2.13	15.2	0.14	0.64
S-9	Buton-100	1,420	**	3,800	100	-	268	1.98	12.0	10.63	-
S-10	Epon 815/LP-3/A-186/D	2,400	1,110	4,800	100	46.2	200	2.14	10.5	1.31	-
S-12	Epon 826/Epon 871/L-100/MOCA	2,430	***	6,300	100	-	260	2.08	14.2	-	-
S-13	Epon 826/Epon 871/L-100/MOCA	(240,300, tensile strength)			-	-	-	-	-	-	-
S-14	Epon 815/LP-3/A-186/D	3,600	1,000	4,820	100	27.7	134	-	-	0.54	-
S-15	Epon 828/LP-3/A-186/D	7,390	5,720	12,060	100	77.3	162	2.18	12.4	0.36	-
S-16	Epon 826/Epon 871/L-100/MOCA	(194,700, tensile strength)			-	-	-	-	-	-	-
S-17	Epon 826/Epon 871/L-100/MOCA	1,630	-	5,150	100	-	315	-	-	-	-
S-18	Epon 826/Epon 871/L-100/MOCA	1,650	-	5,330	100	-	322	-	-	-	-
S-901****	828/NMA/BDMA	9,240	9,230	17,900	100	99.8	194	-	-	-	-

* Property values reported are not considered optimum for the various resin systems. D in Resin System column = Curing Agent D.

** Specimens swelled and cracked during water boil (no test).

*** Ring damaged by warping, preventing the cutting of enough satisfactory test specimens (no test).

**** Ring fabricated of resin system shown, with S-901 roving, by the Aerojet Materials Evaluation Laboratory in accordance with Specification WS-1126-B.

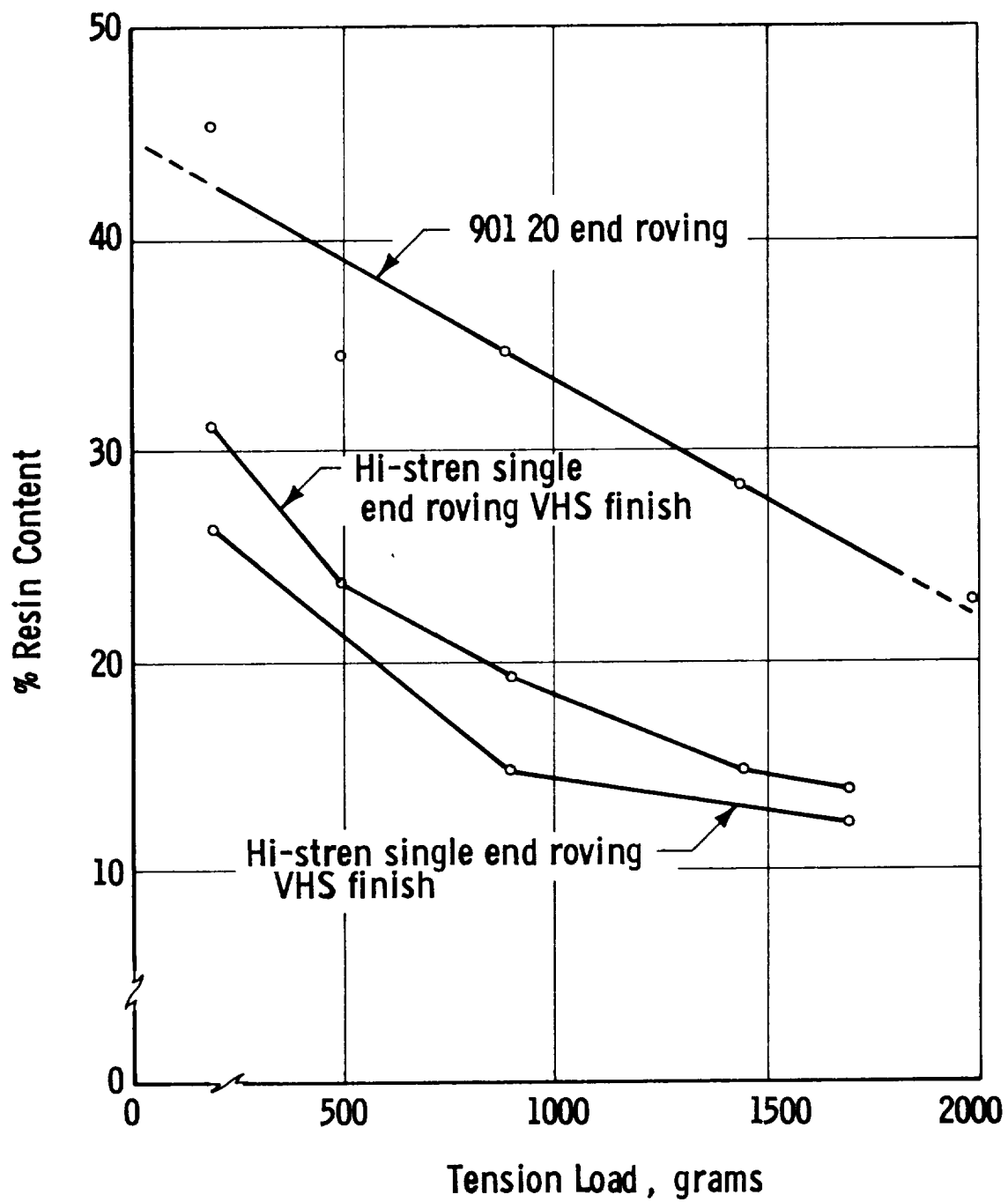


Figure 6. Winding-Tension Study, Resin Content vs Tension Load

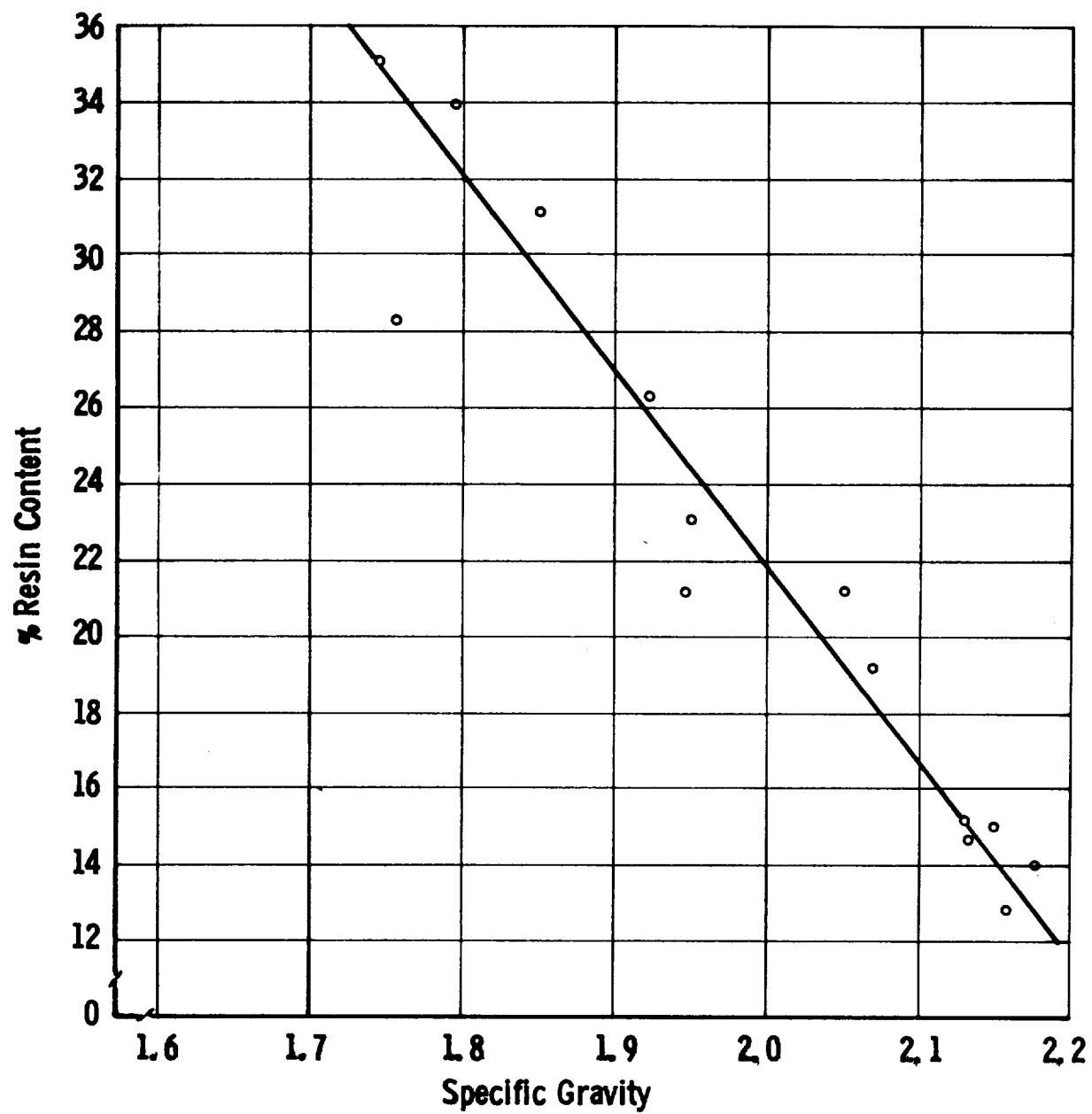


Figure 7. Winding-Tension Study, Resin Content vs Specific Gravity

of all filaments in the freshly drawn multifilament strand by optical microscopy

i. Flexural fatigue.

2. Analysis and Selection

a. Glass Finish (Sizing) and Coupling Agents

(1) A-1100 Coupling Agent

On the basis of Task I work, the control-finish/resin system was evaluated with only the A-1100 coupling agent, by comparing composites made using glass treated with the control finish, the control resin, and the five selected resin systems. The major properties used in determining the effectiveness of the finishes were (a) tensile strength, (b) horizontal shear strength, and (c) flexural strength.

The tensile strengths of composites using the control-finish/resin system were lower (Figure 8) in comparison with the other resin candidates, but the flexural strength (Figure 9) was generally higher at ambient and cryogenic temperatures. The flexural tests resulted in tensile-shear rather than tension-compression failure; this is believed to have occurred because the specimens were too short. The specimen length (2 in.) was designed to accommodate existing cryogenic-test equipment; the specimens were tested using a 1-in. span with center loading.

A survey disclosed that only relatively few NOL-ring flexural tests had been conducted in the industry. The U.S. Naval Ordnance Laboratory, probably the most advanced in this field, recommended the following test conditions (Ref. 6): (a) a specimen length of 7.6 cm, (b) four-point loading, (c) a major span of 6.35 cm, and (d) a minor span of 1.26 cm. Because Aerojet was using its NOL-ring flexural-test results only to compare the various resin systems, the data obtained were considered useful in this program.

The horizontal shear strength of the control-finish/resin system was superior at all three test conditions in comparison with the other candidate resins in this experiment (Figure 10). The strength showed a straight-line increase from 10,300 psi at room temperature, through 18,600 psi at -320°F, to 20,600 psi at -423°F. As compared with the best competitive system, the increases amount to approximately 13% at room temperature, 11% at -320°F, and 12% at -423°F.

(2) A-186 Coupling Agent

The finish that employed the A-186 coupling agent [β -3,4-(epoxycyclohexyl)ethyltrimethoxy silane] displayed good tensile and flexural properties when used with the Epon 828/Versamid 140/Curing Agent D system (Figures 11 and 12). The horizontal-shear properties of composites made

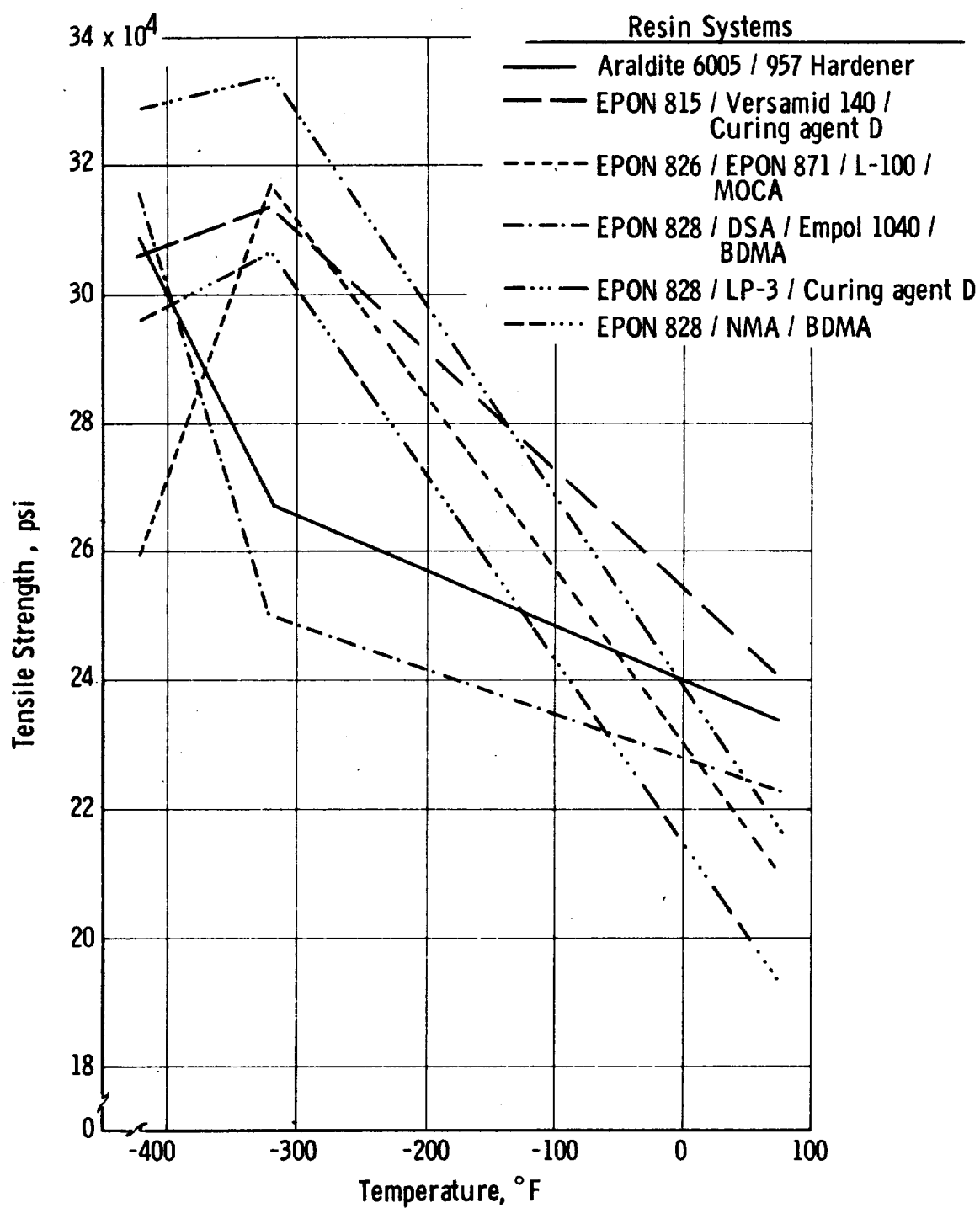


Figure 8. Coupling Agent A-1100, Composite Tensile Strength

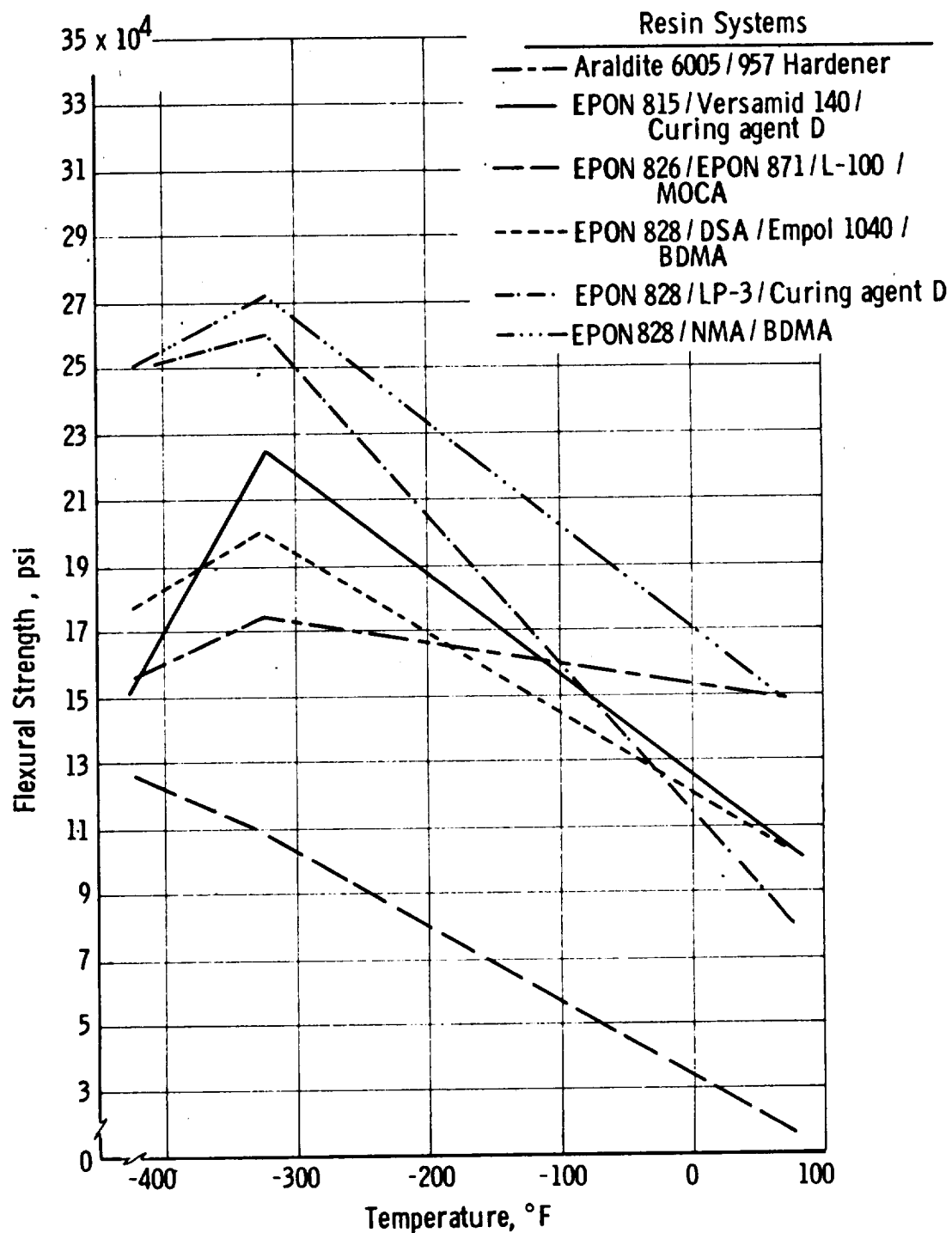


Figure 9. Coupling Agent A-1100, Composite Flexural Strength

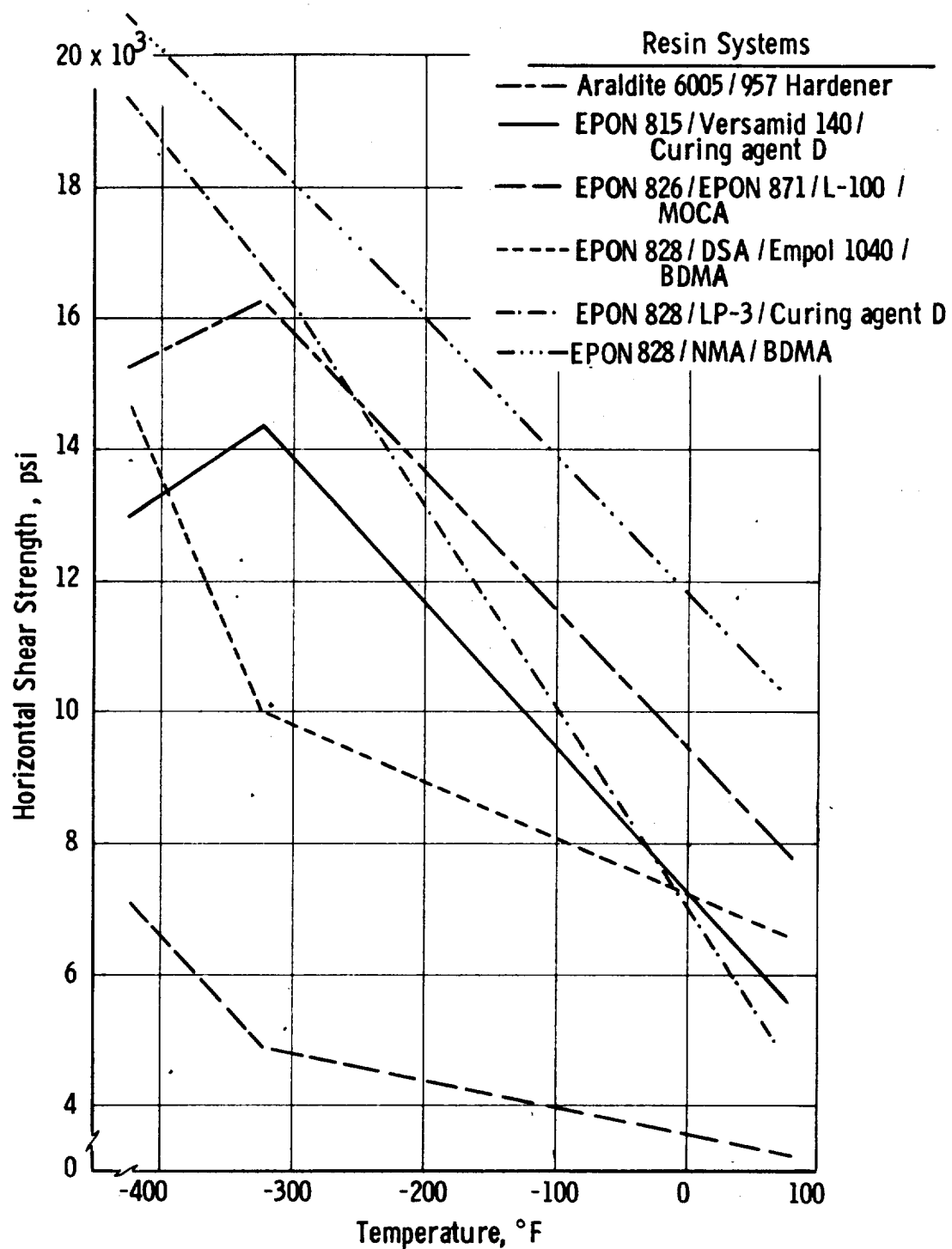


Figure 10. Coupling Agent A-1100, Composite Horizontal Shear Strength

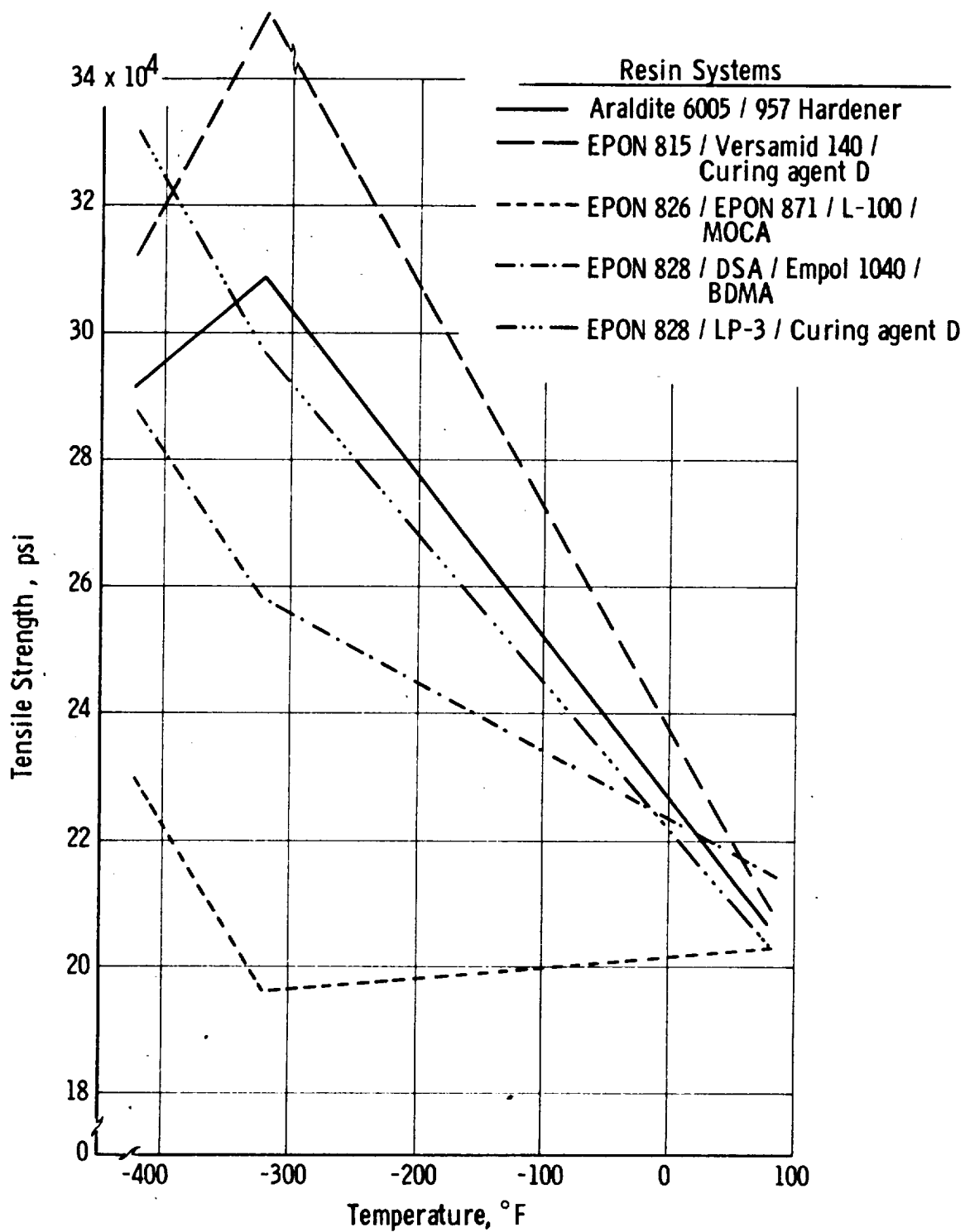


Figure 11. Coupling Agent A-186, Composite Tensile Strength

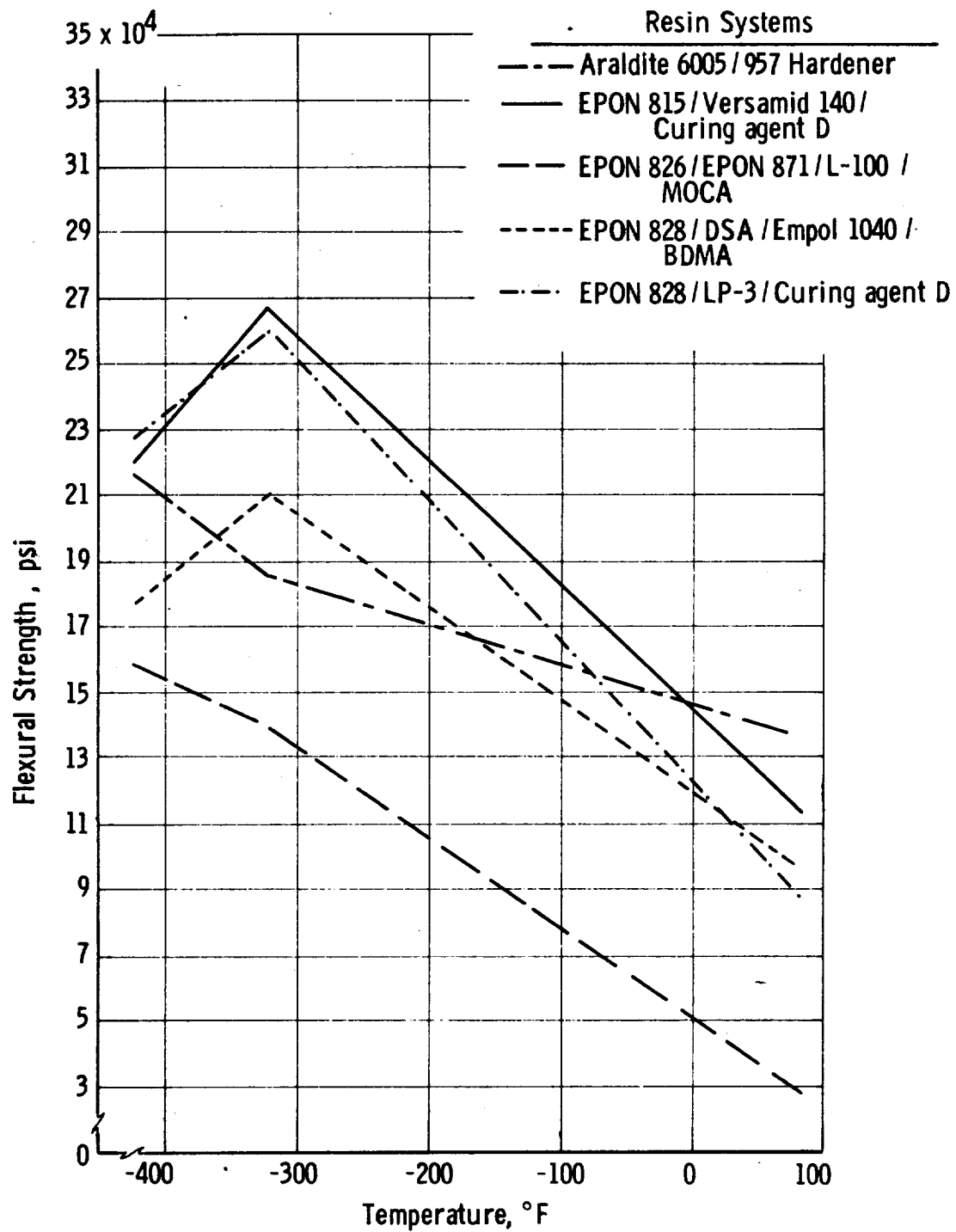


Figure 12. Coupling Agent A-186, Composite Flexural Strength

with this agent were low as compared with A-1100, but were equivalent as compared with the others (Figure 13).

The A-186 coupling agent was discarded at the conclusion of Task II because the Epon 815/Versamid 140 system was deleted.

(3) Z-6020 Coupling Agent

The Z-6020 agent presented difficulties when used with several of the resin film-forming materials. A reaction occurred between the materials in the finish, causing it to polymerize in the cake package and preventing fiber removal. The data in Figures 14 to 16 and Tables 8 to 10 indicate tensile and flexural strengths equivalent to those of the Araldite 6005 system, as well as good horizontal-shear properties. Because of the difficulties encountered, however, Z-6020 was dropped as a candidate.

(4) Z-6040 Coupling Agent

As shown in Figures 17 to 19, and Tables 8 to 10, the Z-6040 coupling agent exhibited good cryogenic-temperature properties when used with the flexibilized resin system (Epon 828/LP-3/Curing Agent D). The ambient-temperature properties of composites made with Z-6040 and all the matrix resins were generally low.

The material was selected for further study in Task III because of its good performance at low temperature with the LP-3 flexibilized system, which was also selected for further study.

b. Filament Wetting

To assist in coupling-agent selection, wetting studies were conducted to augment the physical and mechanical evaluation of composites made with the various coupling agents.

The low void content of NOL rings tested in Task II is attributed to good resin distribution throughout the composite (Figure 20). Some of the factors that contribute to low voids are the glass finish, matrix resin, and processing variables (fiber tension, impregnation techniques, and resin viscosity). Microscopic examinations of single-end fibers were undertaken to examine some of these parameters in detail.

It was difficult to discern any difference in the wetting of Hi-Stren single-end fibers as a function of different coupling agents (finish/resin compositions). Further substantiation was obtained by comparing the wetting characteristics of the various materials through contact-angle measurements on monofilaments coated with the various finishes and matrix resins. The contact angles varied from 31 to 77° for each finish/resin combination (Figures 21 to 23).

The measurements were made on finish-coated specimens of single-end roving; the fibers were mounted on the standard monofilament

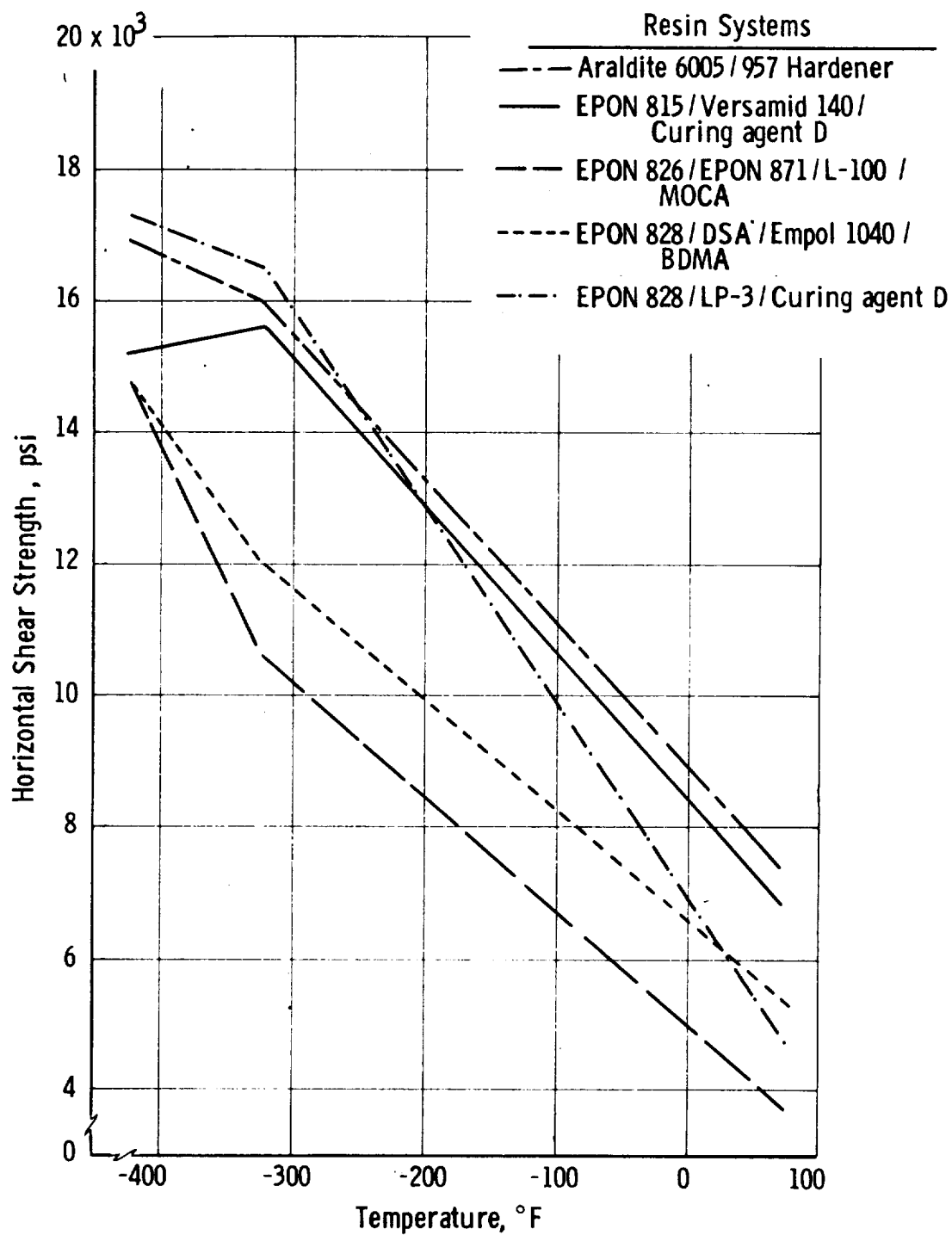


Figure 13. Coupling Agent A-186, Composite Horizontal Shear Strength

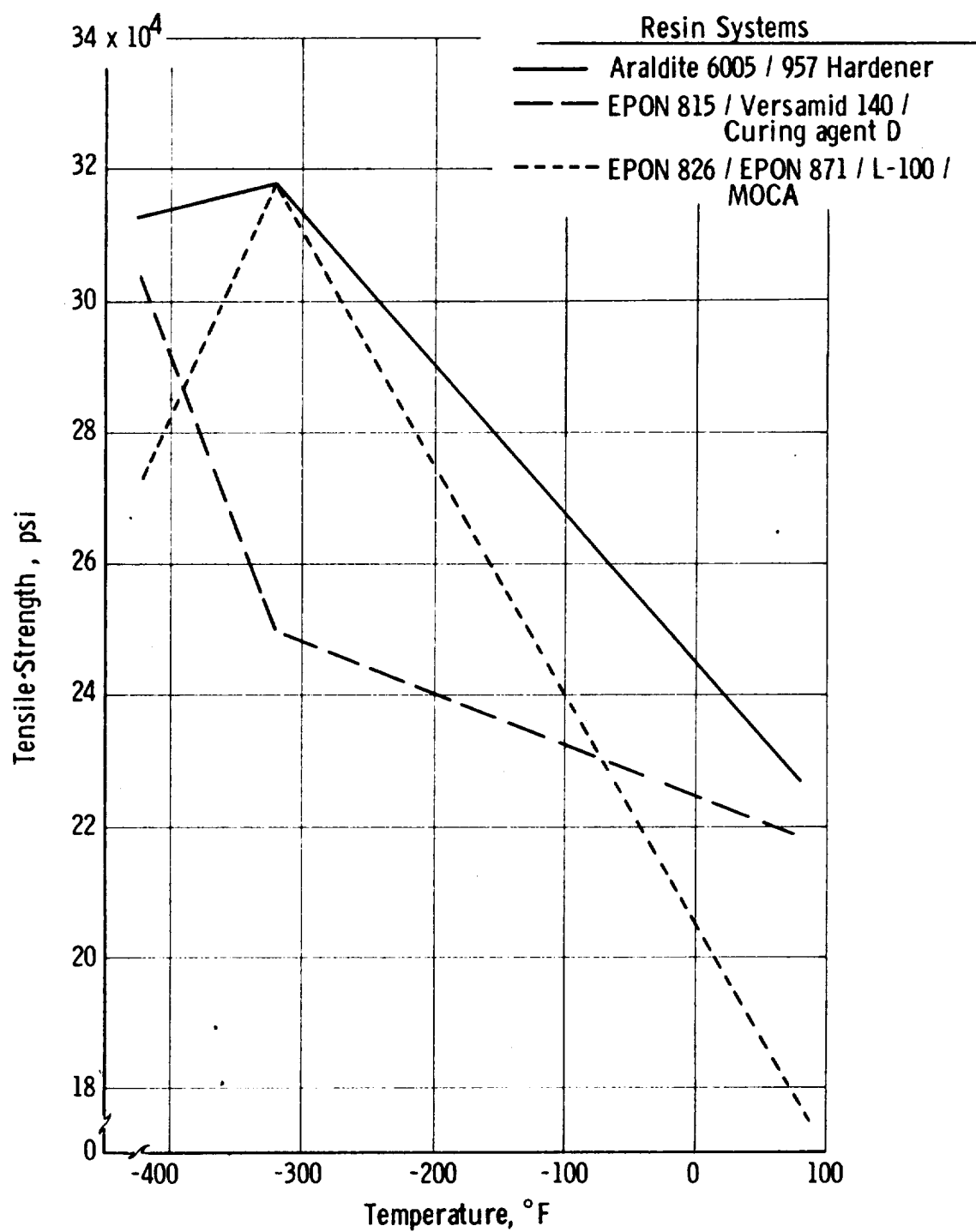


Figure 14. Coupling Agent Z-6020, Composite Tensile Strength

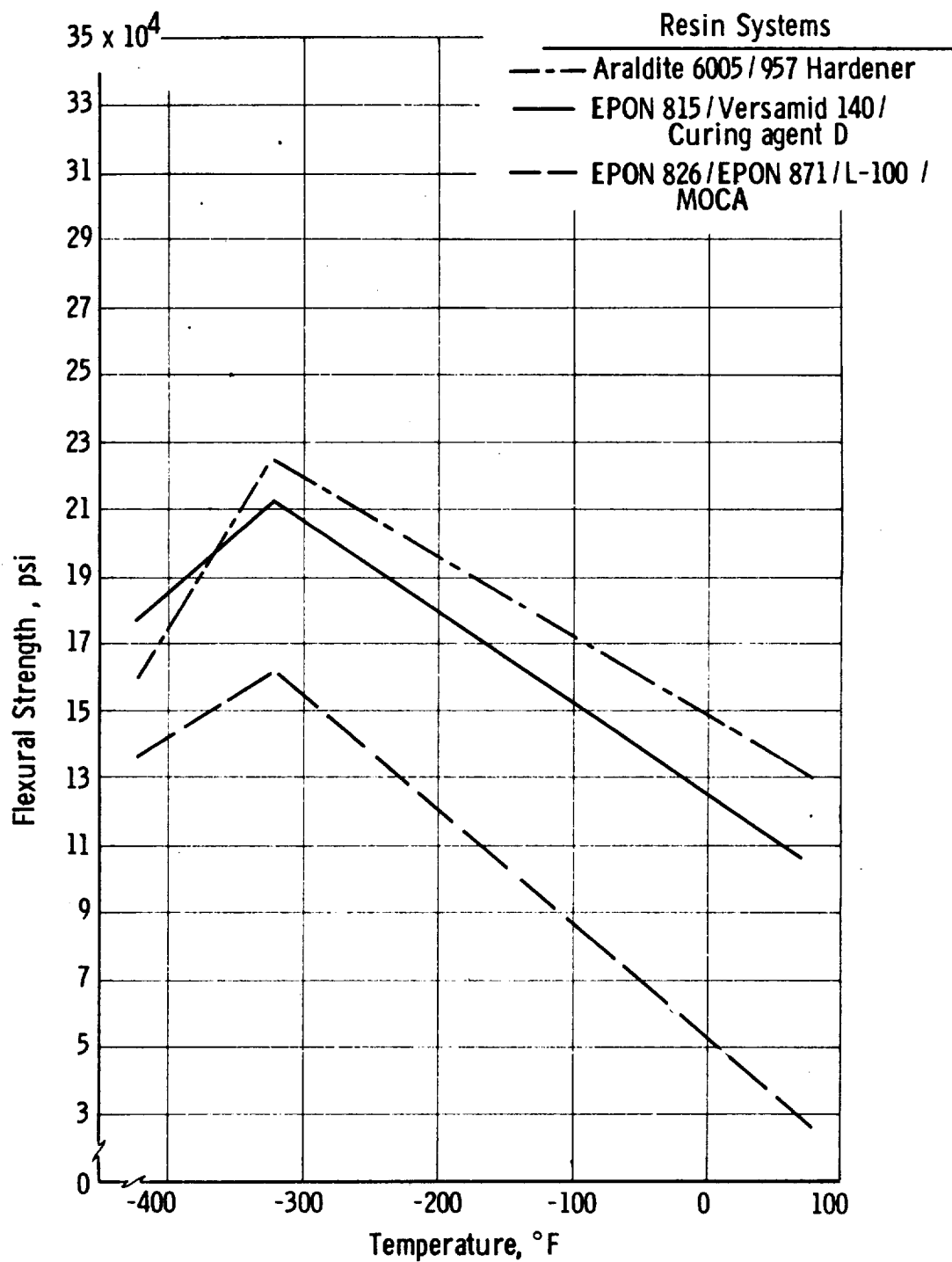


Figure 15. Coupling Agent Z-6020, Composite Flexural Strength

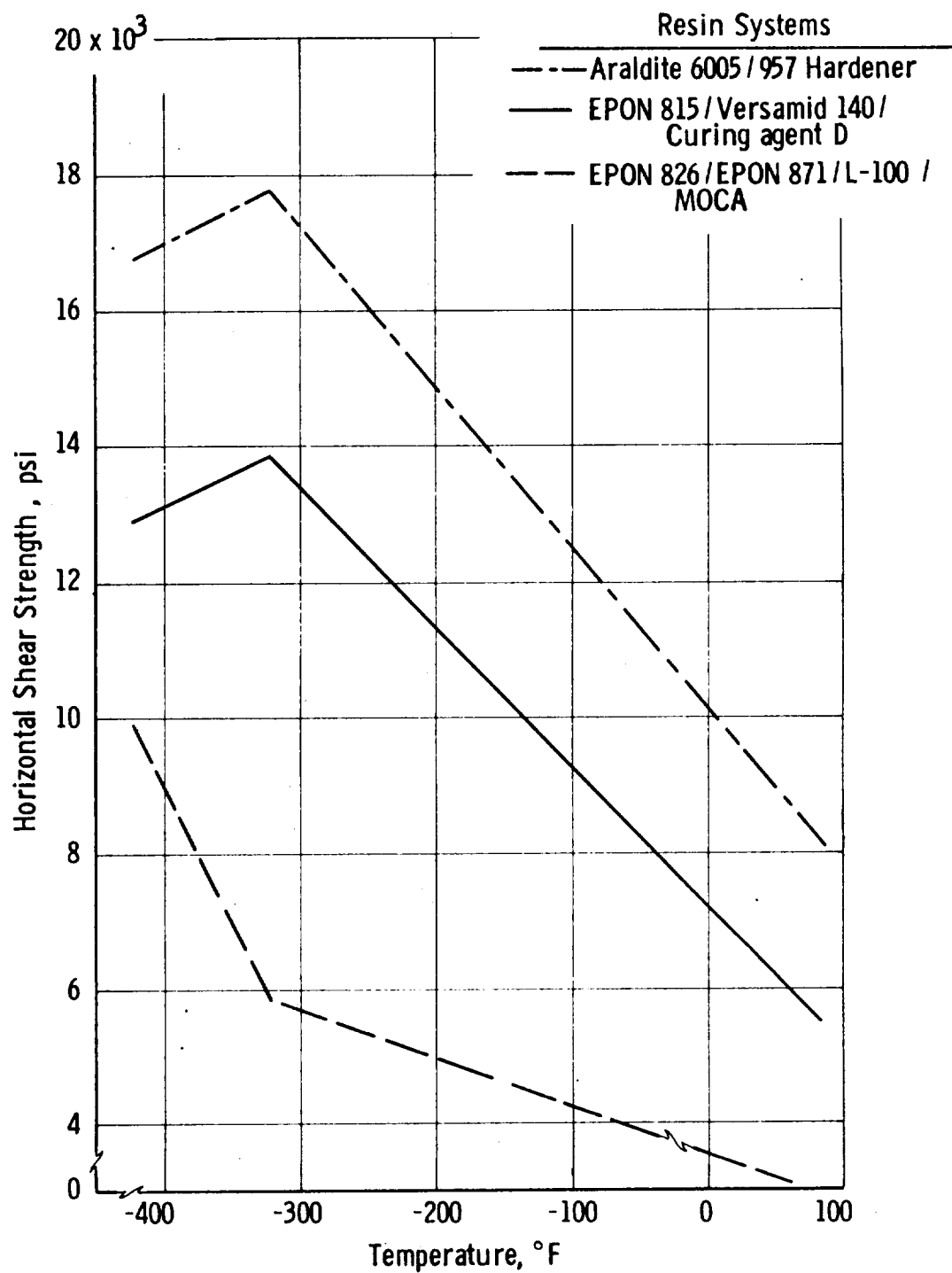


Figure 16. Coupling Agent Z-6020, Composite Horizontal Shear Strength

TABLE 8
COMPOSITE TENSILE STRENGTHS, COUPLING-AGENT STUDY*

Resin System	Tensile Strength, psi											
	At Room Temp				At -320°F				At -423°F			
	A-1100	A-186	Z-6020	Z-6040	A-1100	A-186	Z-6020	Z-6040	A-1100	A-186	Z-6020	Z-6040
Epon 826/Epon 871/ L-100/MOCA	210,400	203,600	178,100	160,000	317,700	196,000	318,300	280,000	259,700	230,900	273,800	222,300
Epon 815/Versamid 140/Curing Agent D	240,300	211,500	219,300	263,500	314,300	362,500	250,000	275,000	306,000	312,000	304,100	310,700
Epon 828/DSA/Empol 1040/BDMA	227,600	215,900	--	210,300	250,000	258,300	--	237,900	316,400	288,200	--	306,500
Epon 828/IP-3/ Curing Agent D	217,300	205,200	--	220,900	334,400	297,500	--	323,300	329,100	332,400	--	316,400
Araldite 6005/ 957 Hardener	233,800	208,400	228,800	191,600	268,000	309,000	318,200	263,200	309,100	292,300	311,300	225,300
Epon 828/NMA/ BDMA	192,400	--	--	--	307,300	--	--	--	396,000	--	--	--

* All results: averages of three tests for each condition.

TABLE 2
COMPOSITE FLEXURAL STRENGTHS, COUPLING-AGENT STUDY*

Resin System	Flexural Strength, psi											
	At Room Temp				At -320°F				At -423°F			
	A-1100	A-186	Z-6020	Z-6040	A-1100	A-186	Z-6020	Z-6040	A-1100	A-186	Z-6020	Z-6040
Epon 826/Epon 871/ L-100/MOCA	17,100	30,900	27,800	40,700	109,800	140,300	162,200	115,500	126,300	159,100	137,100	124,800
Epon 815/Versamid 140/Curing Agent D	103,000	117,400	105,500	122,000	225,200	268,400	213,900	223,500	153,600	220,500	178,000	177,400
Epon 828/DSA/Empol 1040/EDMA	102,500	98,700	--	89,200	201,800	211,700	--	187,300	177,400	184,200	--	197,600
Epon 828/LP-3/ Curing Agent D	81,000	91,800	--	93,700	261,600	260,800	--	252,700	249,000	228,400	--	231,000
Araldite 6005/ 957 Hardener	149,800	139,400	131,200	146,400	174,700	186,000	225,400	232,300	156,700	217,800	160,400	236,700
Epon 828/NMA/ BDMA	147,300	--	--	--	272,700	--	--	--	251,700	--	--	--

*Room-temperature results: average of four tests. Results at -320 and -423°F: average of three tests.

TABLE 10
COMPOSITE HORIZONTAL SHEAR STRENGTHS, COUPLING-AGENT STUDY*

Resin System	Horizontal Shear Strength, psi											
	At Room Temp				At -320°F				At -423°F			
	A-1100	A-186	Z-6020	Z-6040	A-1100	A-186	Z-6020	Z-6040	A-1100	A-186	Z-6020	Z-6040
Epon 826/Epon 871/ L-100/MOCA	1,300	3,700	1,300	1,100	4,900	10,600	5,800	6,000	7,100	14,800	9,900	11,100
Epon 815/Versamid 140/Curing Agent D	5,600	6,800	5,700	6,800	14,400	15,600	13,900	8,700	13,000	15,200	12,900	15,400
Epon 828/DSA/Empol 1040/BDMA	6,600	5,400	--	5,500	10,000	12,000	--	11,200	14,700	14,800	--	13,200
Epon 828/IP-3/ Curing Agent D	4,800	4,800	--	5,300	16,900	16,500	--	16,900	19,400	17,300	--	17,400
Araldite 6005/ 957 Hardener	7,900	7,300	8,400	8,100	16,300	16,000	17,800	17,200	15,300	16,900	16,800	16,300
Epon 828/WMA/ BDMA	10,300	--	--	--	18,600	--	--	--	20,600	--	--	--

* Room-temperature results: average of five tests. Results at -320 and -423°F: average of three tests.

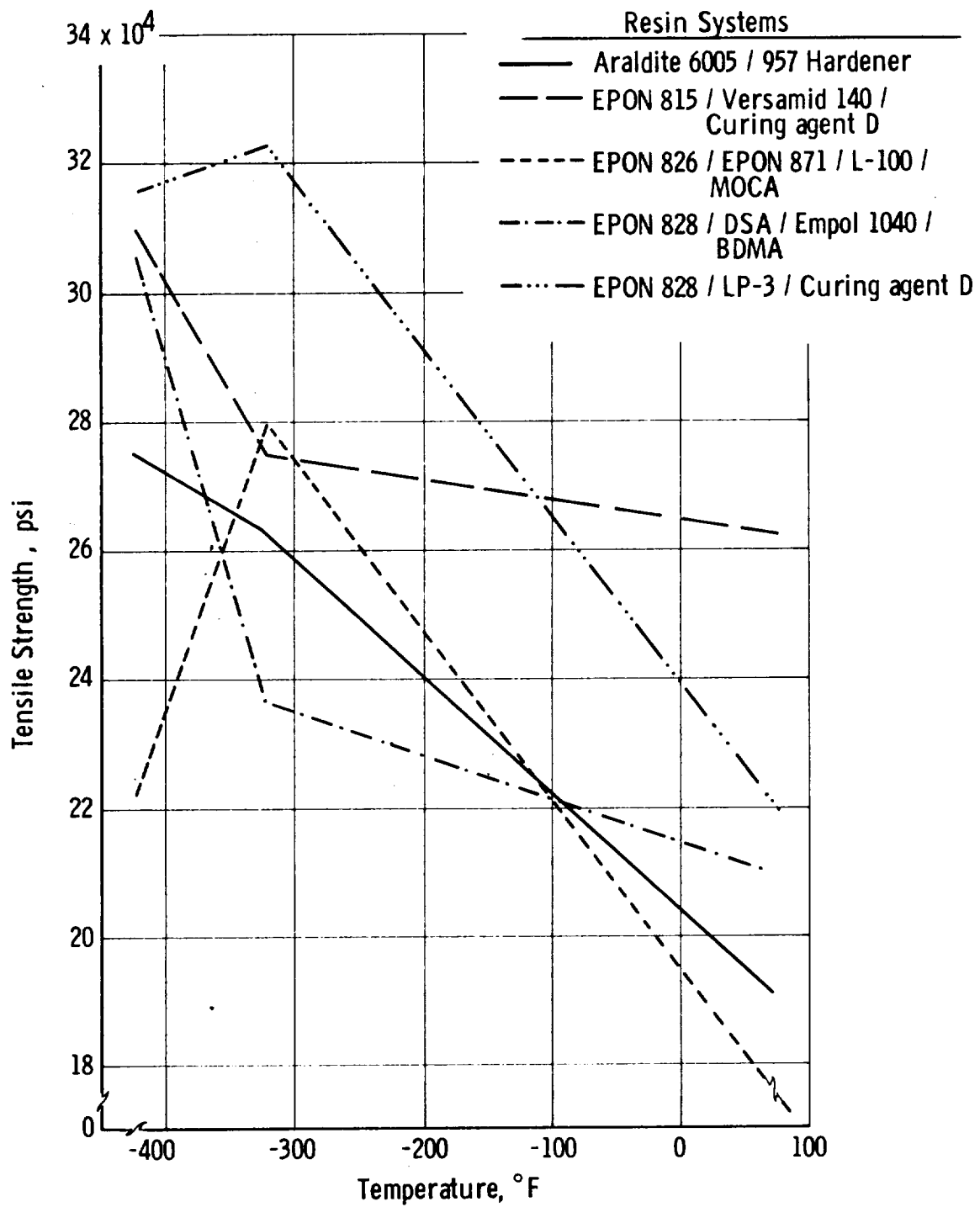


Figure 17. Coupling Agent Z-6040, Composite Tensile Strength

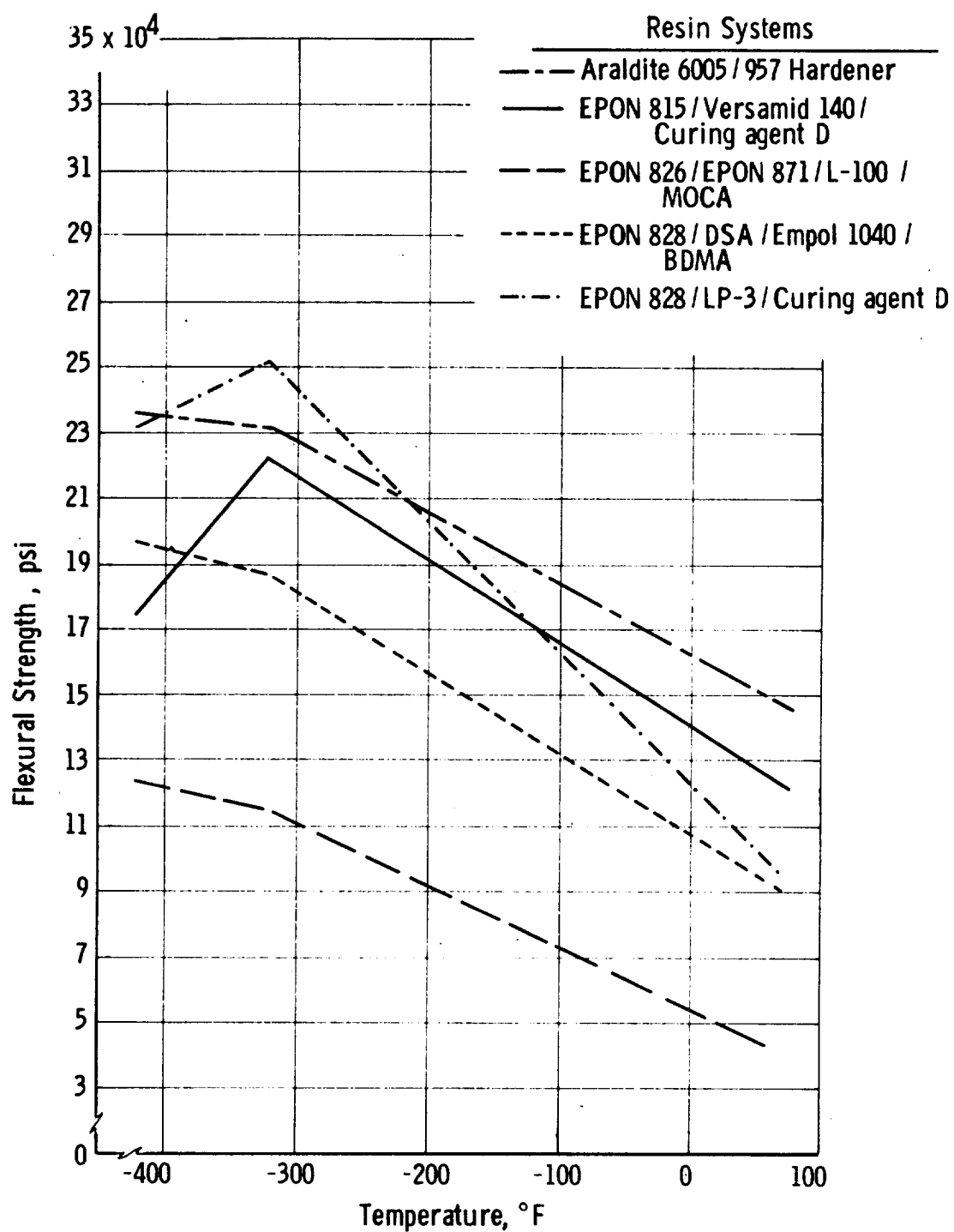


Figure 18. Coupling Agent Z-6040, Composite Flexural Strength

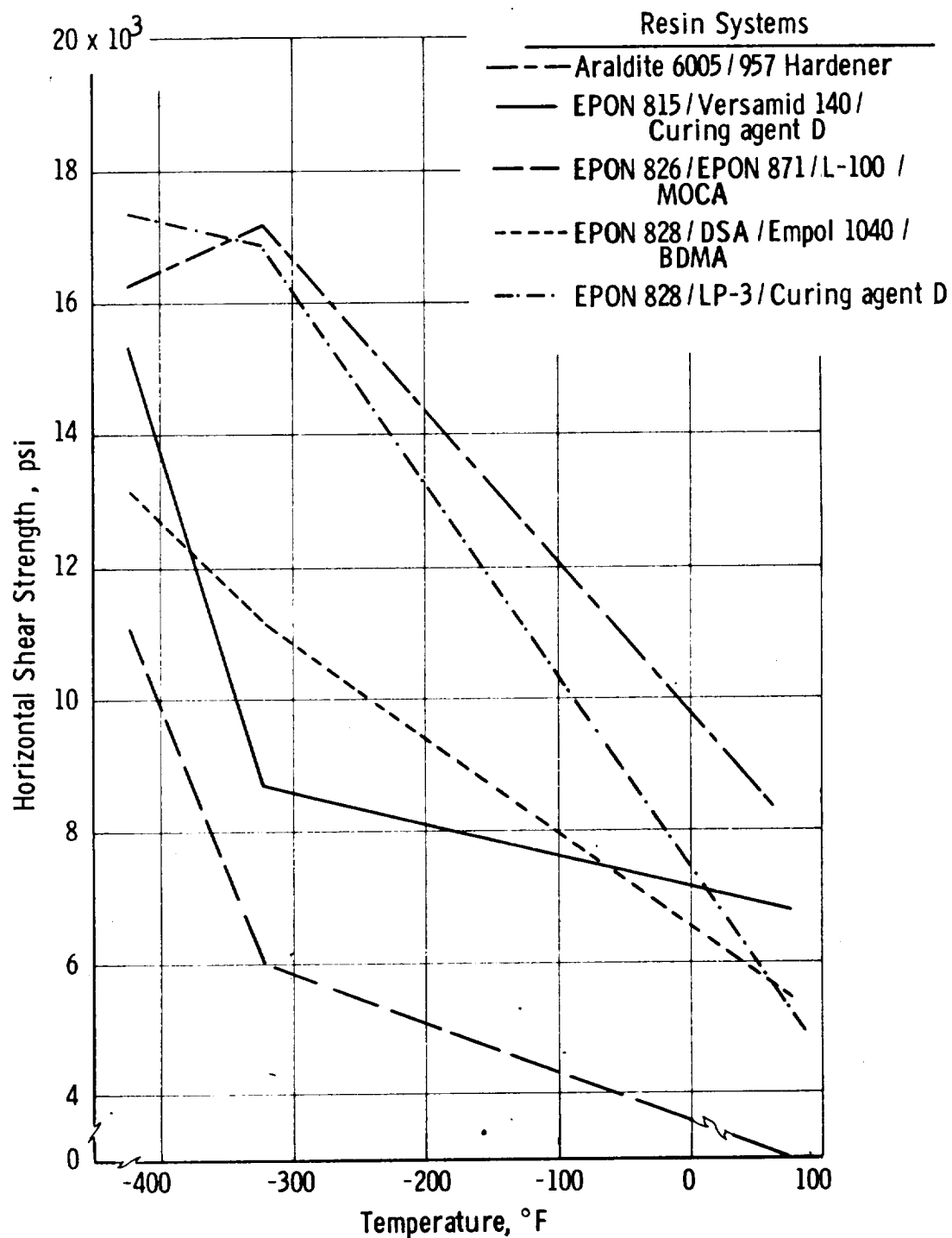
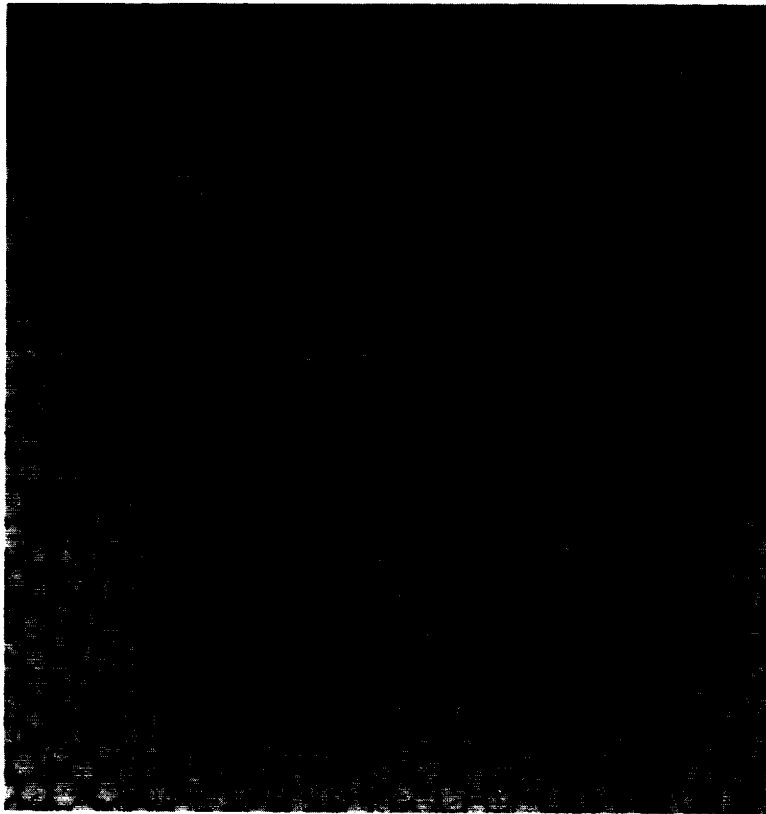
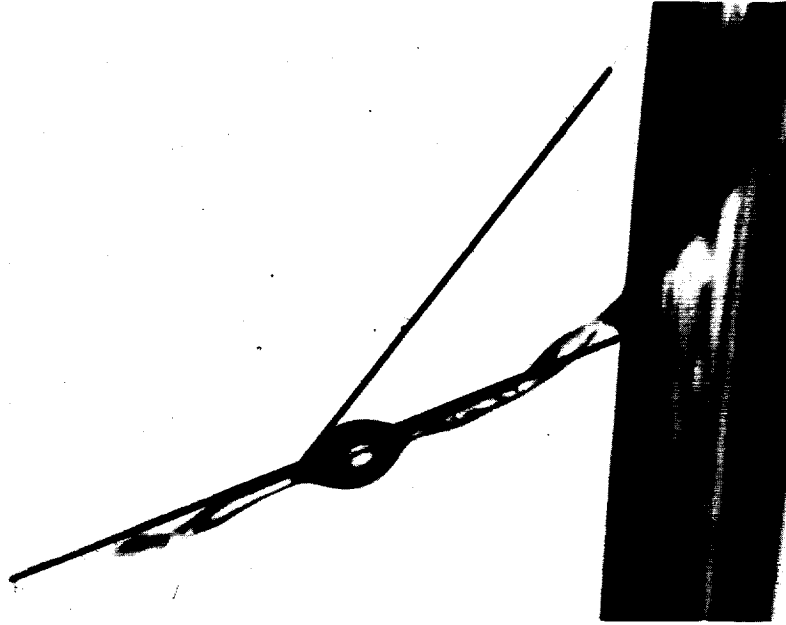


Figure 19. Coupling Agent Z-6040, Composite Horizontal Shear Strength



250x

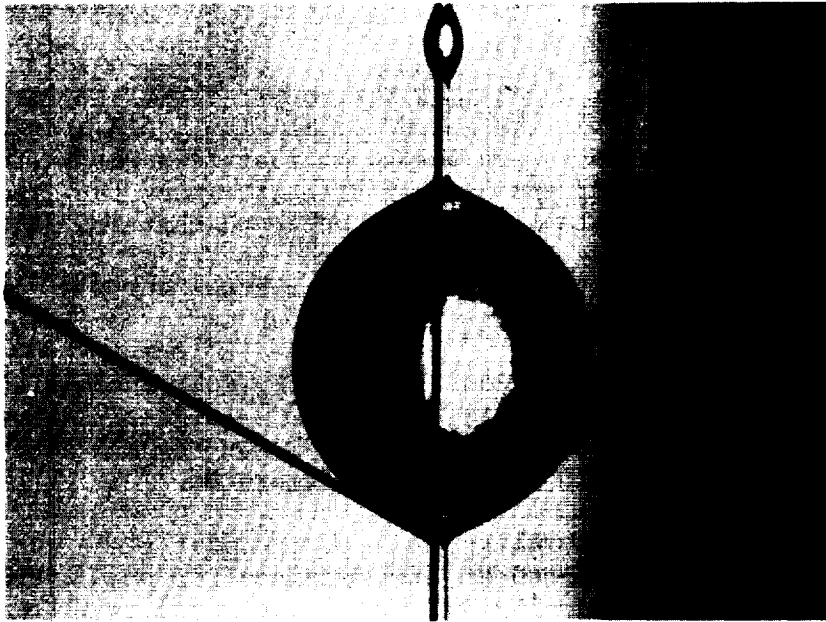
Figure 20. Typical Cross Section
Task II NOL Ring



140x

Finish - 828 / Versamid 140 / A-186
Resin - 815 / Versamid 140 / D

Figure 21. Wetting Study
Contact Angle 31



120x

Finish - VHS

Resin - 828 / DSA / Empol 1040 / BDMA

Figure 22. Wetting Study
Contact Angle 61°



120x

Finish - VHS

Resin - 815 / Versamid 140 / D

Figure 23. Wetting Study
Contact Angle 77°

tensile holder. A few drops of the matrix resin were applied to the specimen at ambient temperature. Photomicrographs revealed considerable difference in contact angle with the same finish/matrix-resin combination. The low void content of the composite probably resulted from the use of suitable processing techniques; Figures 24 to 26, for example, show the poor wetting of the glass fiber when no tension or pressure was applied. During winding, resin wet-out was a function of fiber tension and resin viscosity. A dead weight of 1000 g was selected for tensioning the rings fabricated in Task II. The resin viscosity was controlled by varying the temperature between 85 and 120°F. Fiber samples were taken from the uncured rings for microscopic examination of resin distribution. It was believed that pressure (tension) in the NOL-ring composite probably produces good wetting and resin distribution.

When single-end fibers were placed between glass slides and examined microphotographically it was found that the resin on the surface of the fibers formed spheres and the resin between the fibers assumed a cylindrical shape when no pressure was applied (Figure 24). As the pressure on the fibers was increased to approximately 280 psi, the cylinders increased in length (Figure 27), providing better resin distribution and lower void content. The results of this study indicate the importance of pressure obtained by proper fiber tensioning during ring fabrication.

c. Resins

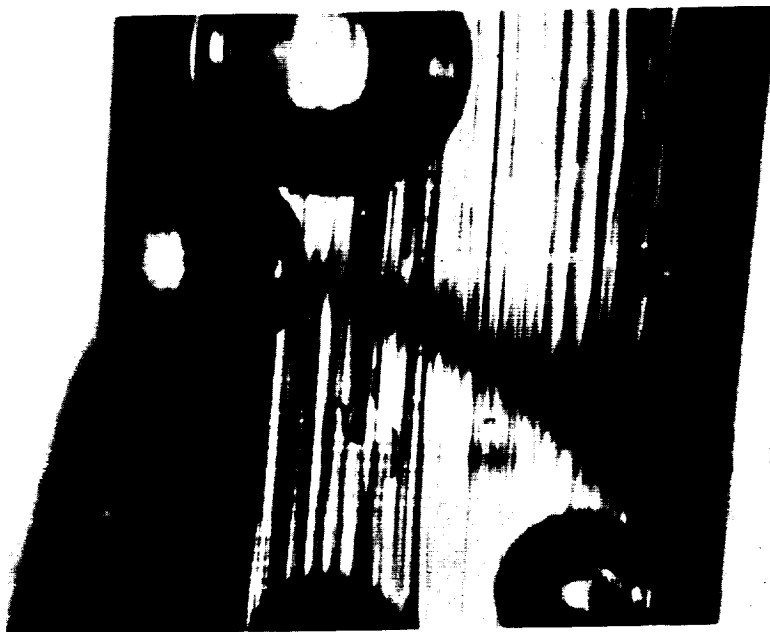
(1) Epon 828/NMA/BDMA (Control)

Composites made with this resin system yielded generally superior flexural and horizontal-shear properties in comparison with the other systems using the same finish.

Thermal shock of a horizontal-shear specimen produced a slight edge discoloration after the third cycling in liquid hydrogen (LH_2). When horizontal-shear specimens were tested at room temperature, however, this resin system again produced the highest strength among the candidates in the control-resin study (Table 11). It is believed that the edge discoloration was caused by the sawing of specimens from the ring; it was observed to be associated with both of the brittle resin systems but not with the flexible systems.

The average coefficient of linear thermal contraction for cast specimens of this resin was 25.04×10^{-6} in./in./°F (compared with a range from 20.69 to 34.16×10^{-6} in./in./°F for the six candidate resins). Test results are presented in Table 12 and Figure 28.

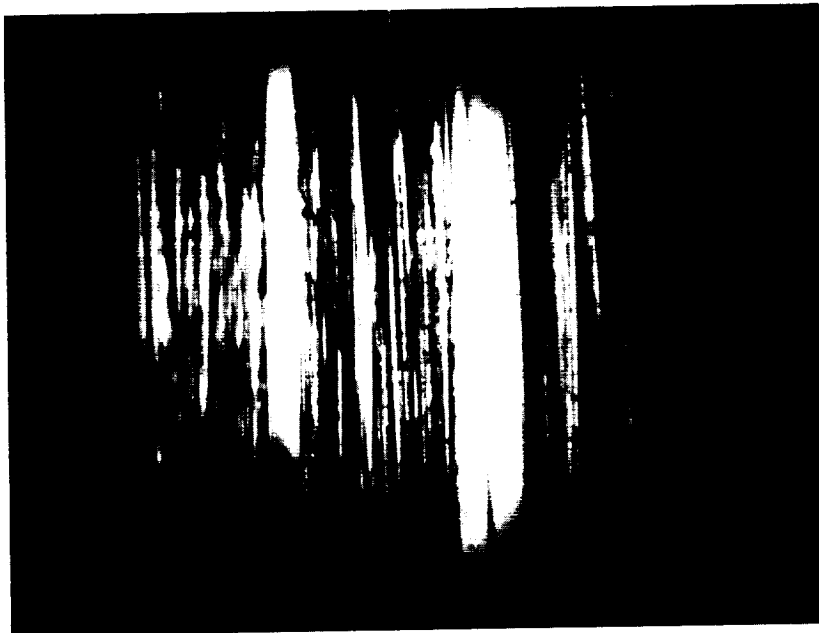
The flexural strength of the cast resin was 12,000 psi at room temperature, the second highest obtained for the candidates. The resin shrinkage was 5.4%, the viscosity 365 centipoises (cp) at 110°F, and the working pot life in excess of 12 hours. Resin-evaluation results are presented in Table 13.



140x

Finish - 828 / LP-3 / A-1100
Resin - 828 / LP-3 / D

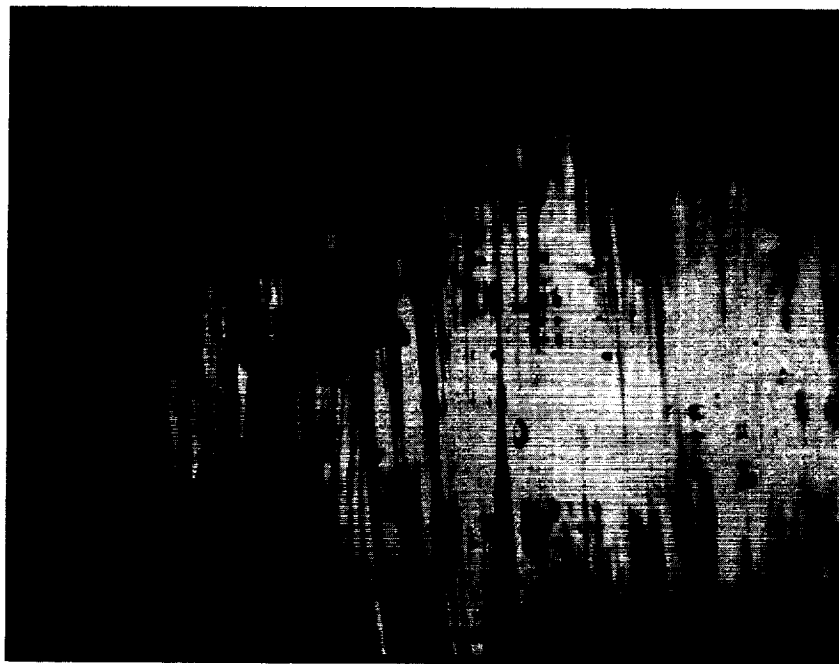
Figure 24. Wetting Study, Single-End Roving
(Epon 828/LP-3/Curing Agent D)



48x

Finish - VHS

Figure 25. Wetting Study, Single-End Roving
(VHS Finish)

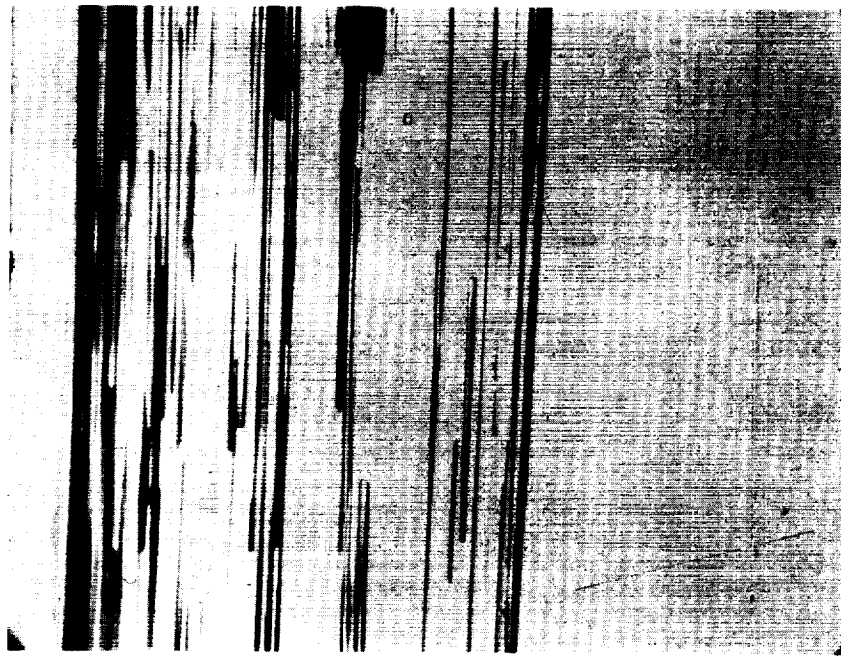


36x

Finish - VHS

Resin - 828 / NMA / BDMA

Figure 26. Wetting Study, Single-End Roving
(Epon 828/NMA/BIMA)



90x

Finish - 828 / LP-3 / A-1100

Resin - 828 / LP-3 / D

Figure 27. Wetting Study, Single-End Roving
(Epon 828/LP-3/Curing Agent D)
Effect of Increased Pressurization

TABLE 11

CONTROL-RESIN STUDY, EFFECT OF THERMAL SHOCK ON
HORIZONTAL SHEAR STRENGTH*

Resin System	Results of Visual Examination of Specimens After Number of Cycles Shown				Horizontal Shear Strength, psi, at Room Temperature	
	1	2	3	4	5	Before Cycling**
Epon 828/NMA/BDMA	N	N	D	D	D	10,300
Araldite 6005/957 hardener	D	D	D	D	D	6,400
Epon 828/IP-3/Curing Agent D	N	N	D	D	D	6,200
Epon 828/DSA/Empol 1040/BDMA	N	N	N	N	N	7,800
Epon 815/Versamid 140/Curing Agent D	N	N	N	N	N	5,100
Epon 828/Epon 871/L-100/MOCA	N	N	N	N	N	1,000
						9,500
						6,100
						5,000
						7,500
						5,100
						2,200

* A-1100 coupling agent and VHS film former. Visual examination: N = no change, and D = edge discoloration.

** Average of five specimens.

*** Average of three specimens.

TABLE 12

LINEAR THERMAL CONTRACTION OF CAST RESINS*

Temp °F	Linear Thermal Contraction, in./in.					
	Epon 828/ NMA/BDMA	Araldite 6005/ 957 Hardener	Epon 828/LP-3/ Curing Agent D	Epon 815/Versamid 140/Curing Agent D	Epon 828/DSA/ Empol 1040/BDMA	Epon 826/Epon 871/ L-100/MOCA
+70	0	0	0	0	0	0
0	0.002740	0.002172	0.002914	0.002961	0.003521	0.004680
-50	0.004324	0.003541	0.004844	0.004940	0.005990	0.006951
-100	0.005874	0.004876	0.006698	0.006658	0.008258	0.008942
-150	0.007238	0.005948	0.008161	0.008312	0.01029	0.01079
-200	0.008441	0.006913	0.009359	0.009232	0.01204	0.01228
-250	0.009524	0.007763	0.01036	0.01092	0.01342	0.01349
-300	0.01040	0.008601	0.01113	0.01194	0.01449	0.01442
-350	0.01125	0.009216	0.01171	0.01264	0.01528	0.01498
-400	0.01177	0.009727	0.01238	0.01299	0.01606	0.01571
-410	-	-	0.01242	-	-	-

* Values are averages of three determinations. Calculated average coefficients of linear thermal contraction between +70 and -400°F are as follows:

System	in./in./°F	System	in./in./°F
Epon 828/NMA/BDMA	25.04 x 10 ⁻⁶	Epon 815/Versamid 140	27.63 x 10 ⁻⁶
Araldite 6005	20.69	Epon 828/DSA/Empol 1040/BDMA	34.16
Epon 828/LP-3	25.87	Epon 826/Epon 871/L-100/MOCA	33.41

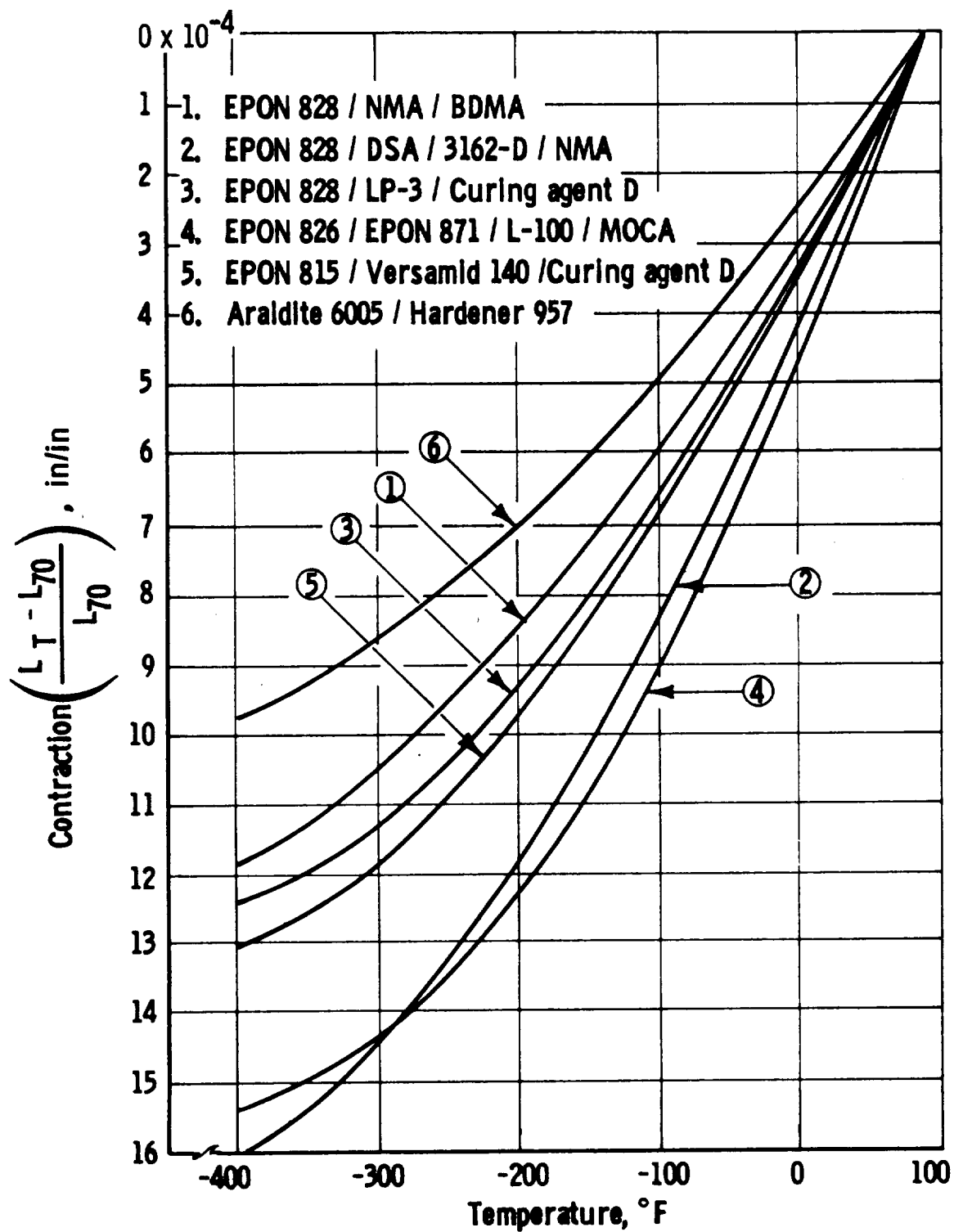


Figure 28. Linear Thermal Contraction, Cryogenic Resin Systems

TABLE 13

CAST-RESIN PROPERTIES

Resin System	Resin Shrinkage %	Viscosity		Working Pot Life hours	Fiber Wetting	Cast-Resin Flexural Strength * psi
		Centi- poises	Temp °F			
Epon 828/NMA/BDMA	5.4	356	110	>12	Good	12,200
Araldite 6005/957 hardener	8.0	860	110	2.5	Good	20,500
Epon 828/IP-3/ Curing Agent D	1.0	680	110	1.5	Good	10,700
Epon 828/DSA/Empol 1040/ BDMA	6.1	355	110	>12	Good	11,600
Epon 815/Versamid 140/ Curing Agent D	1.0	610	120	3/4	Good	11,300
Epon 828/Epon 871/ L-100/MOCA	6.0	1887	150	1/3	Good	336

* Average of four tests.

Because of its extremely good properties and its use as the control, this resin system was advanced to additional study in Task III.

(2) Epon 828/LP-3/Curing Agent D

This flexibilized epoxy-resin system was evaluated with four coupling agents (A-1100, Z-6020, A-186, and Z-6040). A common film former of Epon 828/LP-3 in a solvent carrier with these agents was used to coat the virgin fibers. A combination of the film former and Z-6020 resulted in polymerization of the finish on the glass; the fibers could not be used, and Z-6020 was discarded as a coupling agent.

This resin system exhibited good low-temperature properties, particularly with a finish containing A-1100 coupling agent (Table 14 and Figures 29 to 31).

Because earlier work had indicated that no significant benefits were obtained at ambient and low temperatures with coupling agents (Ref. 2), the overall resin performance was compared in a study that disregarded coupling-agent effectiveness. This was done by taking averages of mechanical-property data without consideration for coupling-agent differences.

An average of the tensile values, with all coupling agents considered, showed this system superior to the other candidate resins at cryogenic temperature (Table 15 and Figure 32).

The coupling agents had a minimal effect on the flexural strength of this system. The greatest differences in strengths associated with different agents were 13.5% at room temperature, 3% at -320°F, and 8.5% at -423°F. The average cryogenic strength determined in the coupling-agent study was slightly higher than those of the other candidate resins.

Thermal shocking showed no visual defects on the horizontal-shear specimens after five cycles in liquid hydrogen. When the shear specimens were tested after cycling, no difference was found (before, 4900 psi; after, 5200 psi). Test results are presented in Table 16. Flexural-fatigue testing of this system yielded good data in comparison with the A-1100 and A-186 coupling agents (Table 17).

The average coefficient of linear thermal contraction for cast-resin specimens was 25.87×10^{-6} in./in./°F (range, 20.69 to 34.16×10^{-6} in./in./°F for the six candidates; see Table 12 and Figure 28).

This system had resin shrinkage of 1.0%, a viscosity of 680 cp at 110°F, a working pot life of approximately 1.5 hours, and a flexural strength of 10,700 psi, which was the second-lowest strength obtained (Table 13).

TABLE 14

RESIN STUDY, NOL-RING COMPOSITE PROPERTIES
EPON 828/LP-3/CURING AGENT D
(100/33/12 FBW)*

Finish System: Film Former (Coupling Agent)	Resin Content wt%	Specific Gravity	Voids Vol %	Composite Strength, psi**							
				Tensile				Horizontal Shear			
				At Room Temp	At -320°F	At -423°F	At Room Temp	At -320°F	At -423°F	At Room Temp	At -320°F
Epon 828/LP-3 (A-1100)	16.0	2.07	1.2	217,300	334,400	329,100	4,800	16,900	19,400	81,000	261,600
Epon 828/LP-3 (A-186)	18.0	2.01	1.6	205,200	297,500	332,400	4,800	16,500	17,300	91,800	260,800
Epon 828/LP-3 (Z-6020)	Finish polymerized on the cake package										
Epon 828/LP-3 (Z-6040)	16.9	2.05	1.0	220,900	323,300	316,400	5,300	16,900	17,400	93,700	252,700

* Composite cure: 1 hour at 150°F and 1 hour at 300°F.

** Values shown are averages as follows: tensile at all temperatures, three tests; horizontal shear at room temperature, five tests, and at -320 and -423°F, three tests; flexural at room temperature, four tests, and -320 and -423°F, three tests.

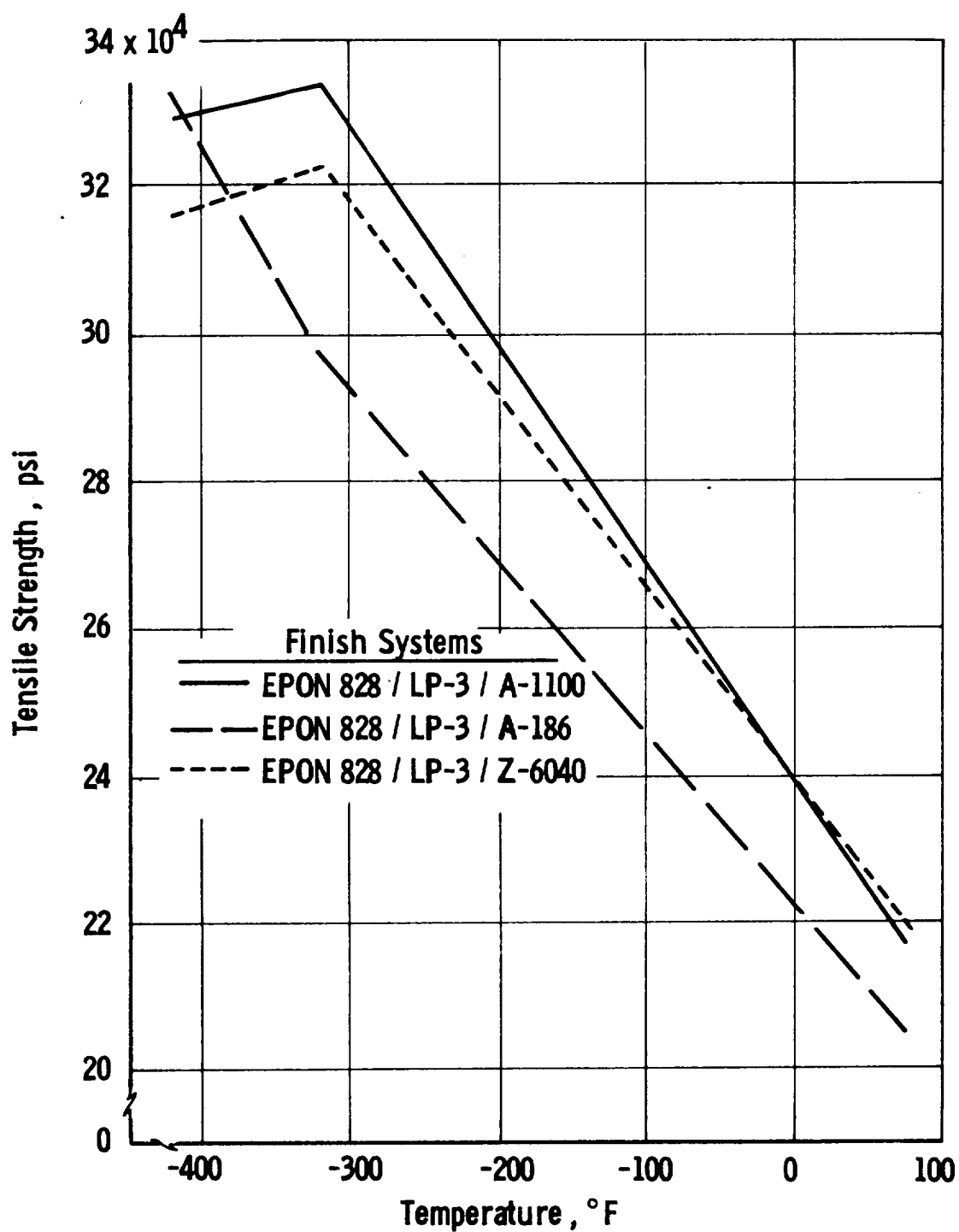


Figure 29. Resin Study (Epon 828/LP-3/Curing Agent D)
Tensile Strength

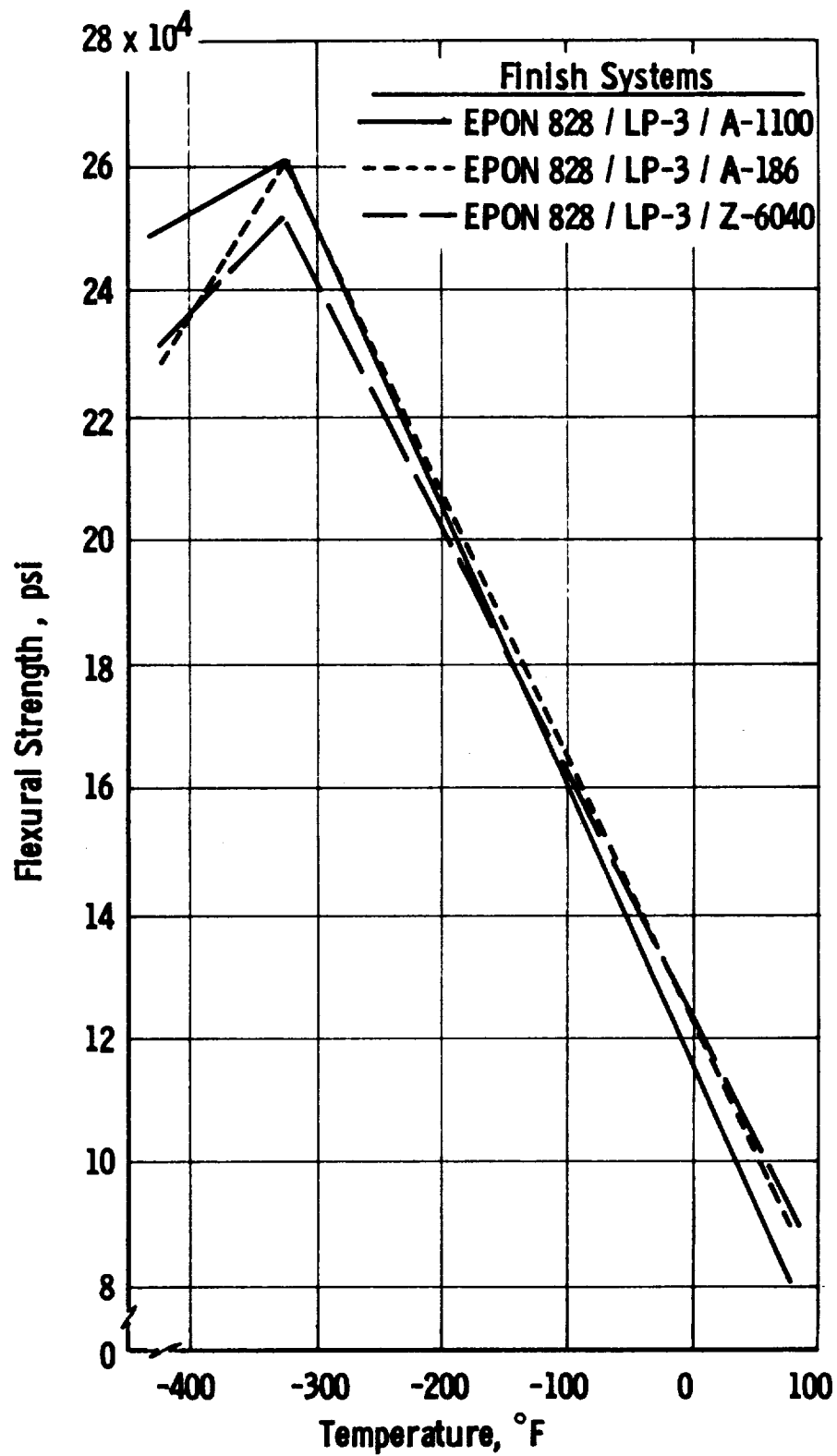


Figure 30. Resin Study (Epon 828/LP-3/Curing Agent D)
Flexural Strength

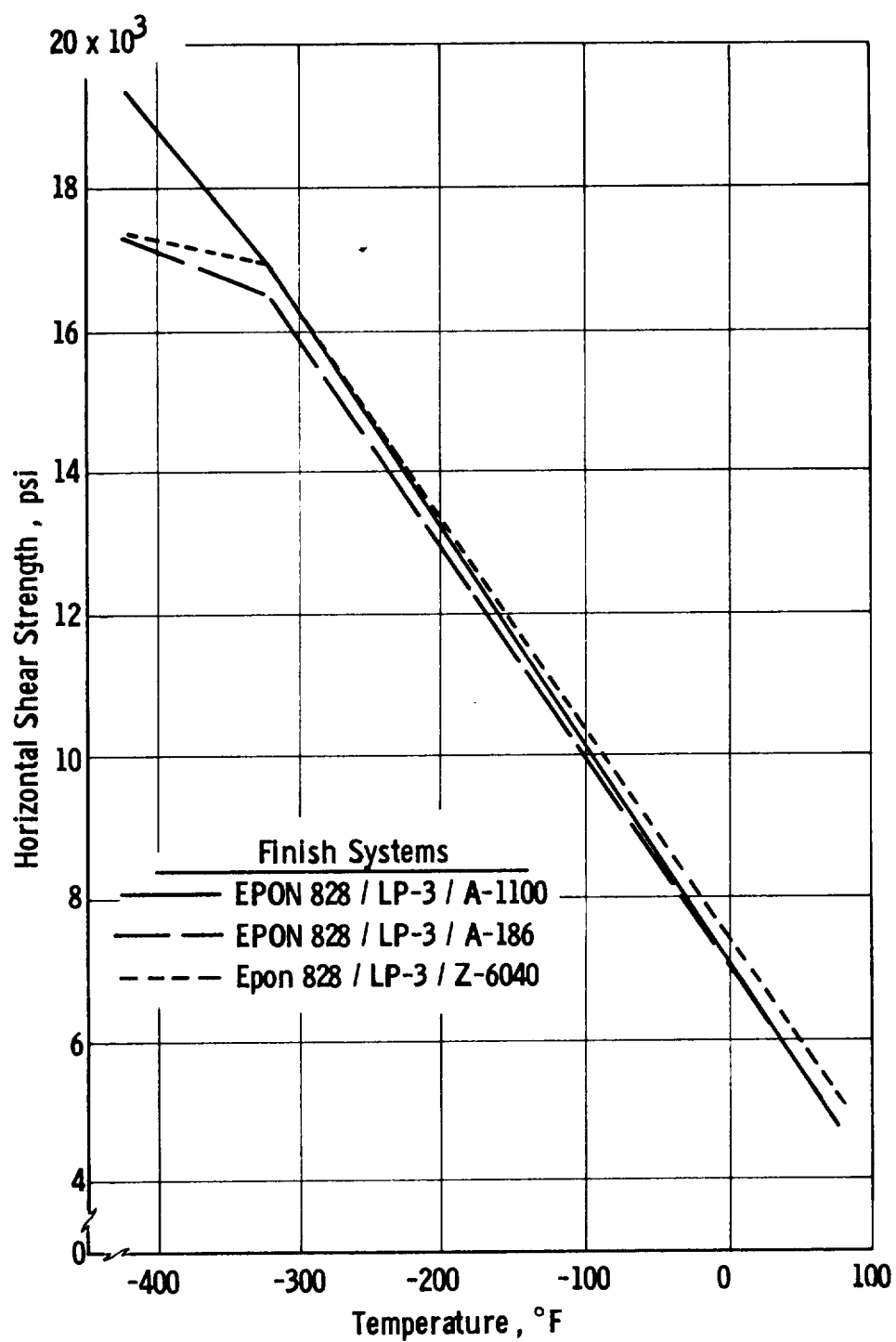


Figure 31. Resin Study (Epon 828/LP-3/Curing Agent D)
Horizontal Shear Strength

TABLE 15

RESIN-COMPARISON STUDY, NOL-RING COMPOSITE PROPERTIES*

Resin System	Composite Strength, psi									
	Tensile			Flexural			Horizontal Shear			
	At Room Temp	At -320°F	At -423°F	At Room Temp	At -320°F	At -423°F	At Room Temp	At -320°F	At -423°F	
Epon 826/Epon 871/L-100/MOCA	188,000	278,000	246,700	29,100	131,900	136,800	1,800	6,800	10,700	
Epon 815/Versamid 140/Curing Agent D	233,600	300,400	305,700	112,000	232,700	182,400	6,200	13,100	14,100	
Epon 828/DSA/ Empol 1040/EDMA **	216,300	248,700	303,700	96,800	200,300	186,400	5,800	11,100	14,200	
Epon 828/LP-3/ Curing Agent D **	244,500	318,400	325,900	88,800	258,400	236,100	4,900	16,800	18,000	
Araldite 6005/ 957 hardener	215,600	289,600	297,000	141,700	204,600	202,900	7,900	16,800	16,300	

* Values shown are averages as follows (except as noted below): tensile, 12 tests; flexural, 16 tests; horizontal shear, 20 tests.

** Z-6020 coupling agent not compatible. Values shown are averages as follows: tensile, 9 tests; flexural, 12 tests; horizontal shear, 15 tests.

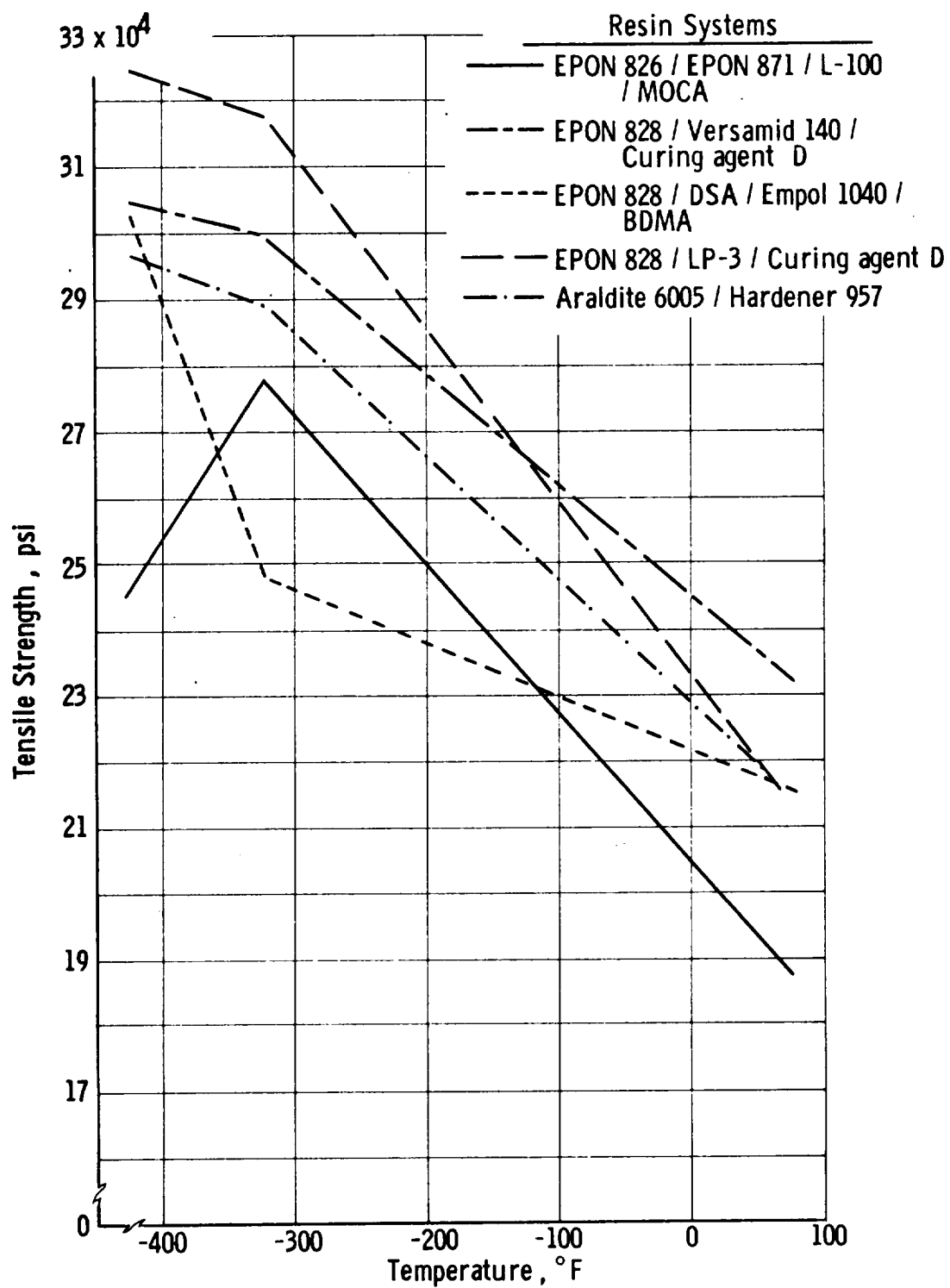


Figure 32. Resin-Comparison Study, Tensile Strength

TABLE 16

RESIN STUDY, EFFECT OF THERMAL SHOCK ON
HORIZONTAL SHEAR STRENGTH*

<u>Resin System</u>	<u>Coupling Agent</u>	<u>Room-Temperature Horizontal Shear Strength, psi**</u>	
		<u>Before Cycling</u>	<u>After Cycling</u>
Epon 828/DSA/ Empol 1040/BDMA	A-1100	6600	6100
	A-186	5400	4800
	Z-6040	5500	5000
Epon 815/ Versamid 140/ Curing Agent D	A-1100	5600	5300
	A-186	6800	6300
	Z-6020	5700	5700
	Z-6040	6800	6700
Epon 828/LP-3/ Curing Agent D	A-1100	4800	5200
	A-186	4800	5100
	Z-6040	5300	5300
Araldite 6005/ 957 hardener	A-1100	7900	7600
	A-186	-	7300
	Z-6020	8400	6600
	Z-6040	-	8700
Epon 826/ Epon 871/ L-100/MOCA	A-1100	1300	1000
	A-186	3700	3700
	Z-6020	1300	1300
	Z-6040	1100	1300

* No change noted in specimens on visual examination after each of five cycles.

** Values are averages as follows: before cycling, five specimens; after cycling, three specimens.

TABLE 17

RESIN STUDY, FLEXURAL FATIGUE*

<u>Finish System: Film Former</u> <u>(Coupling Agent)</u>	<u>80% of Predetermined</u> <u>Ultimate Load, lb</u>	<u>Ultimate Load</u> <u>After Cycling, lb</u>
Epon 828/LP-3/Curing Agent D		
Epon 828/LP-3	550	685
(A-1100)		815
		600
Epon 828/LP-3	583	775
(A-186)		860
		720
Epon 828/LP-3**	-	-
(Z-6020)		
Epon 828/LP-3	525	600
(Z-6040)		680
		680
Epon 815/Versamid 140/Curing Agent D		
Epon 828/Versamid 140	443	410
(A-1100)		600
		470
Epon 828/Versamid 140	605	855
(A-186)		820
		695
Epon 828/Versamid 140	500	610
(Z-6020)		585
		480
Epon 828/Versamid 140	460	350
(Z-6040)		350
		360

* All specimens subjected to 48 cycles at -320°F.

** Finish system polymerized.

TABLE 17 (cont.)

<u>Finish System: Film Former</u> <u>(Coupling Agent)</u>	<u>80% of Predetermined</u> <u>Ultimate Load, lb</u>	<u>Ultimate Load</u> <u>After Cycling, lb</u>
Araldite 6005/957 Hardener		
Araldite 6005 (A-1100)	516	660 525 425
Araldite 6005 (A-186)	565	600 655 630
Araldite 6005 (Z-6020)	516	670 700 530
Araldite 6005 (Z-6040)	580	815 650 815
Epon 828/DSA/Empol 1040/BDMA		
Epon 828 (A-1100)	500	550 640 610
Epon 828 (A-186)	500	615 480 500
Epon 828 (Z-6040)	500	500 610 575
Epon 826/Epon 871/L-100/MOCA		
Epon 815/L-100 (A-1100)	334	285 350 260
Epon 815/L-100 (A-186)	333	205 675 215
Epon 815/L-100 (Z-6020)	300	440 470 555
Epon 815/L-100 (Z-6040)	333	390 240 245

On the basis of good physical and mechanical properties and favorable comparison with the other Task II systems, this resin was selected for additional study in Task III.

(3) Epon 815/Versamid 140/Curing Agent D

This flexible resin system was evaluated with four coupling agents (A-1100, A-186, Z-6020, and Z-6040). A film former of Epon 828/Versamid 140 and a solvent carrier were used in coating the virgin filaments. Although the composite properties were generally low, this system had average to good cryogenic strengths (Figures 33 to 35). The tensile strength using the A-186 coupling agent (Table 18 and Figure 33) was considered good in comparison with the other systems.

When an average tensile strength for this resin with the four coupling agents was compared with averages for the other candidates (Table 15 and Figure 32), the system was considered satisfactory.

An average composite flexural strength (Figure 36), disregarding the coupling agents, disclosed good low-temperature properties (-320°F), but the horizontal shear strength (Figure 37) was considered unsatisfactory with regard to the load-transfer mechanism between adjoining fibers. In comparison with the other systems, this resin was considered average (Table 15).

Thermal shock had no visual effect on this system, nor did it affect the horizontal shear strength after cycling (Table 16). The flexural-fatigue data (Table 17) were considered to indicate poor low-temperature performance.

The coefficient of linear thermal contraction for cast-resin specimens was 27.63×10^{-6} in./in./ $^{\circ}\text{F}$ (range, 20.69 to 34.16×10^{-6} in./in./ $^{\circ}\text{F}$ for the candidates). Test results are presented in Table 12 and Figure 28.

The cast resin had a flexural strength of 11,300 psi (approximately average for the candidates) and a shrinkage of 1.0% (comparable to that of the LP-3 resin system, which had the lowest resin shrinkage). At 120°F , it had a viscosity of 610 cp and a working pot life of approximately 45 min. Test results are presented in Table 13.

In most cases this resin system had slightly better than average test results, but was not selected for Task III because of the wide range in its test data and its relatively short pot life, which is not conducive to good filament winding.

(4) Araldite 6005/Araldite 957 Hardener

This brittle resin system was evaluated with the four coupling agents. Araldite 6005 resin in a solvent carrier was used as the film former in the finish system. Test results are given in Table 19 and Figures 38 to 40.

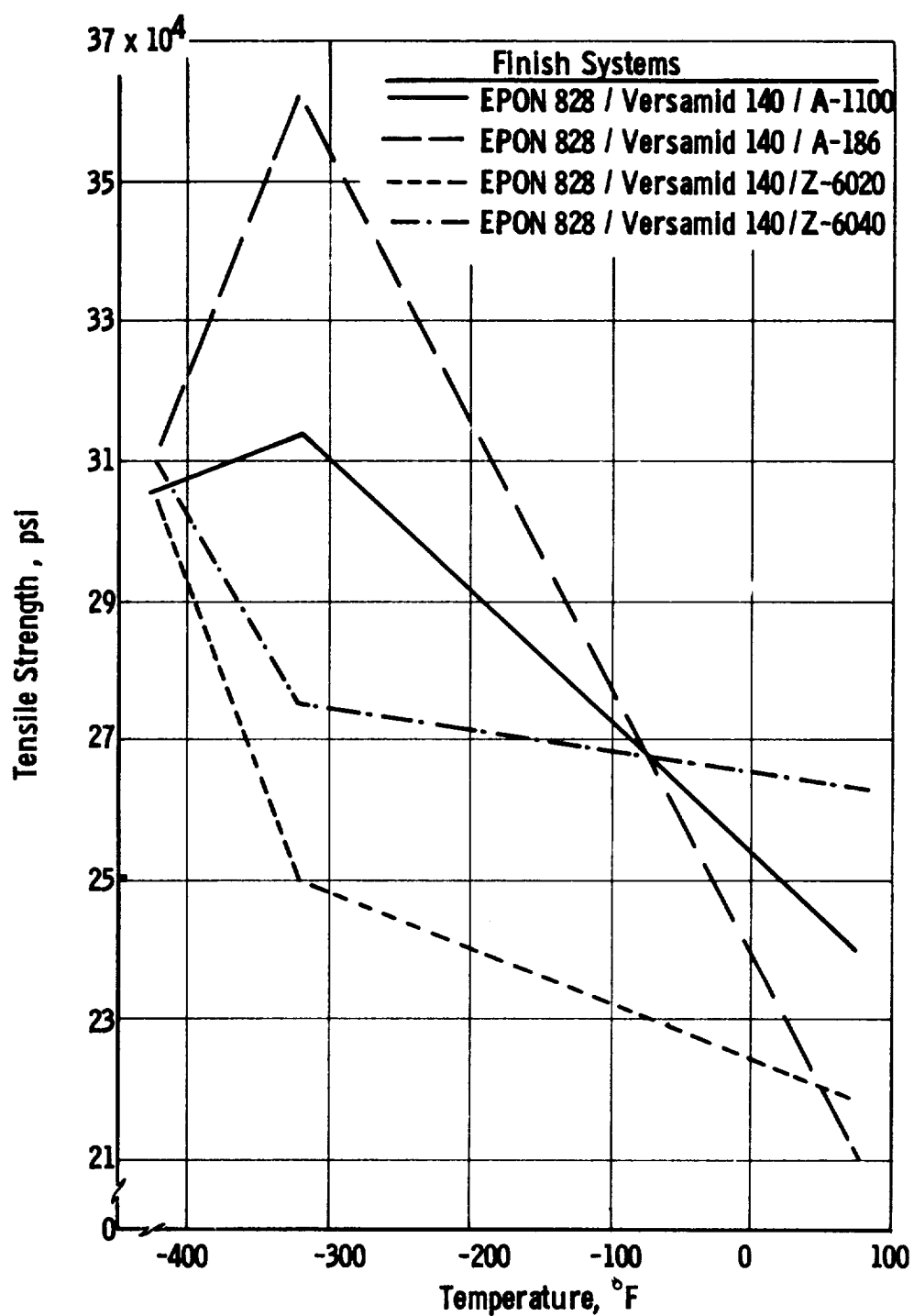


Figure 33. Resin Study (Epon 815/Versamid 140/Curing Agent D)
Tensile Strength

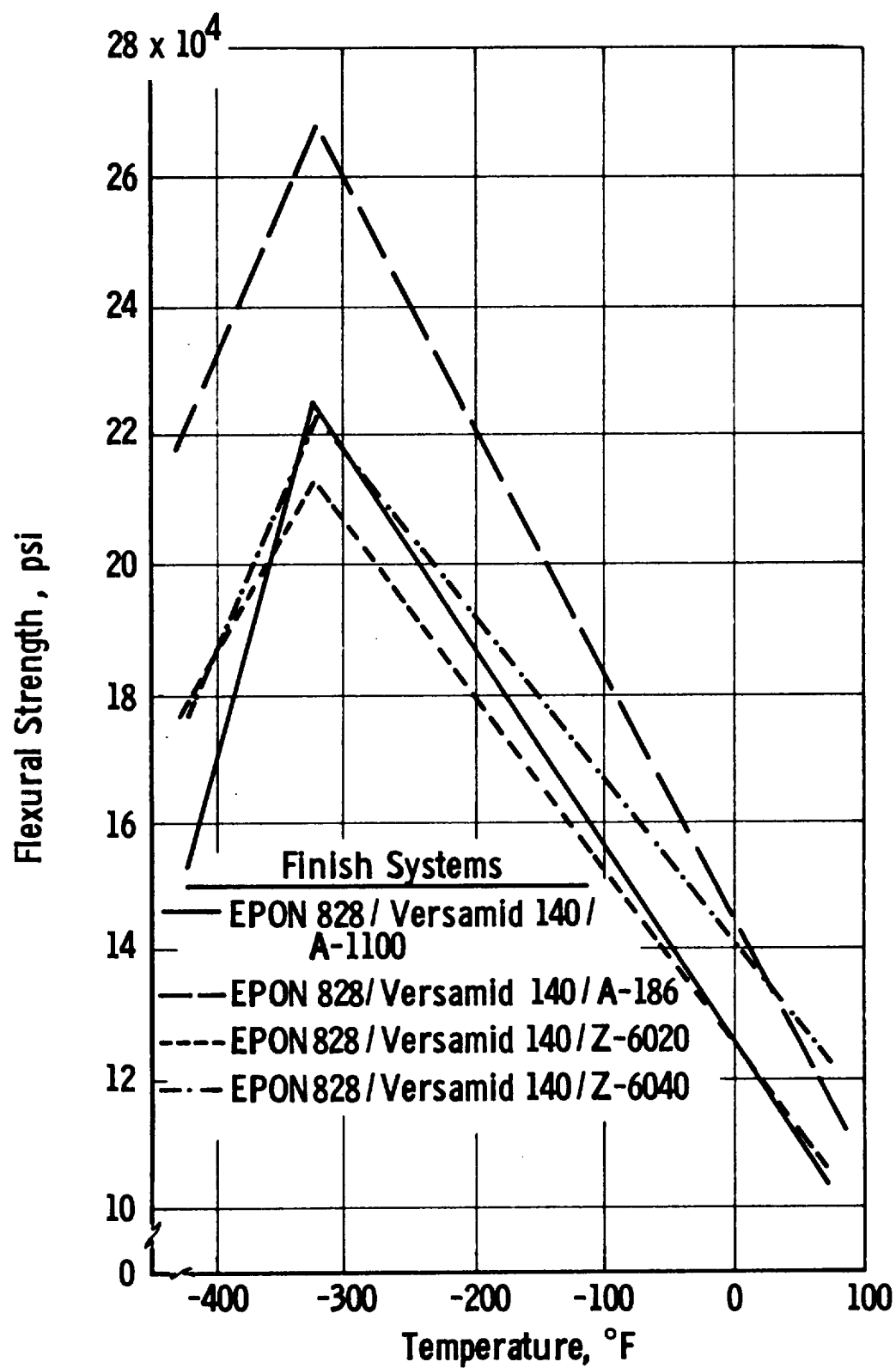


Figure 34. Resin Study (Epon 815/Versamid 140/Curing Agent D)
Flexural Strength

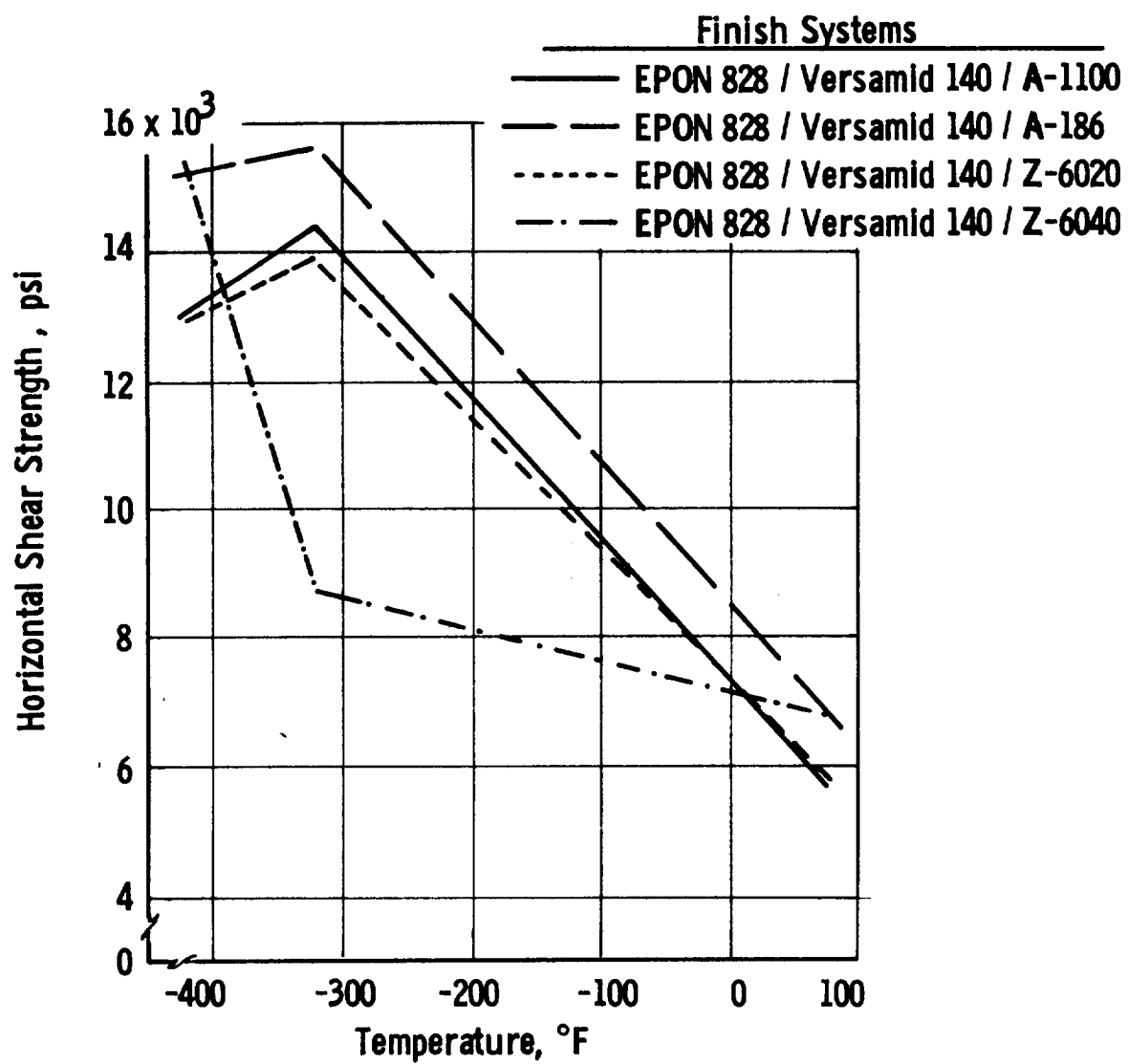


Figure 35. Resin Study (Epon 815/Versamid 140/Curing Agent D)
Horizontal Shear Strength

TABLE 18

RESIN STUDY, MOL-RING COMPOSITE PROPERTIES
EPON 815/VERSAMID 140/CURING AGENT D (100/30/12 PBW)*

Finish System: Film Former (Coupling Agent)	Resin Content wt%	Specific Gravity	Voids vol%	Composite Strength, psi**							
				Tensile				Horizontal Shear			
				At Room Temp	At -320°F	At -423°F	At Room Temp	At -320°F	At -423°F	At Room Temp	At -320°F
Epon 828/ Versamid 140 (A-1100)	15.9	2.03	1.2	240,300	314,300	306,000	5,600	14,400	13,000	103,000	225,200
Epon 828/ Versamid 140 (A-186)	12.8	2.13	2.7	211,500	362,500	312,000	6,800	15,600	15,200	117,400	268,400
Epon 828/ Versamid 140 (Z-6020)	15.0	2.02	3.9	219,300	250,000	304,100	5,700	13,900	12,900	105,500	213,900
Epon 828/ Versamid 140 (Z-6040)	-	-	-	263,500	275,000	310,700	6,800	8,700	15,400	122,000	223,500
											177,400

* Composite cure: 1 hour at 150°F and 1 hour at 300°F.

** Values shown are averages as follows: tensile at all temperatures, three tests; horizontal shear at room temperature, five tests, and at -320 and -423°F, three tests; flexural at room temperature, four tests, and at -320 and -423°F, three tests.

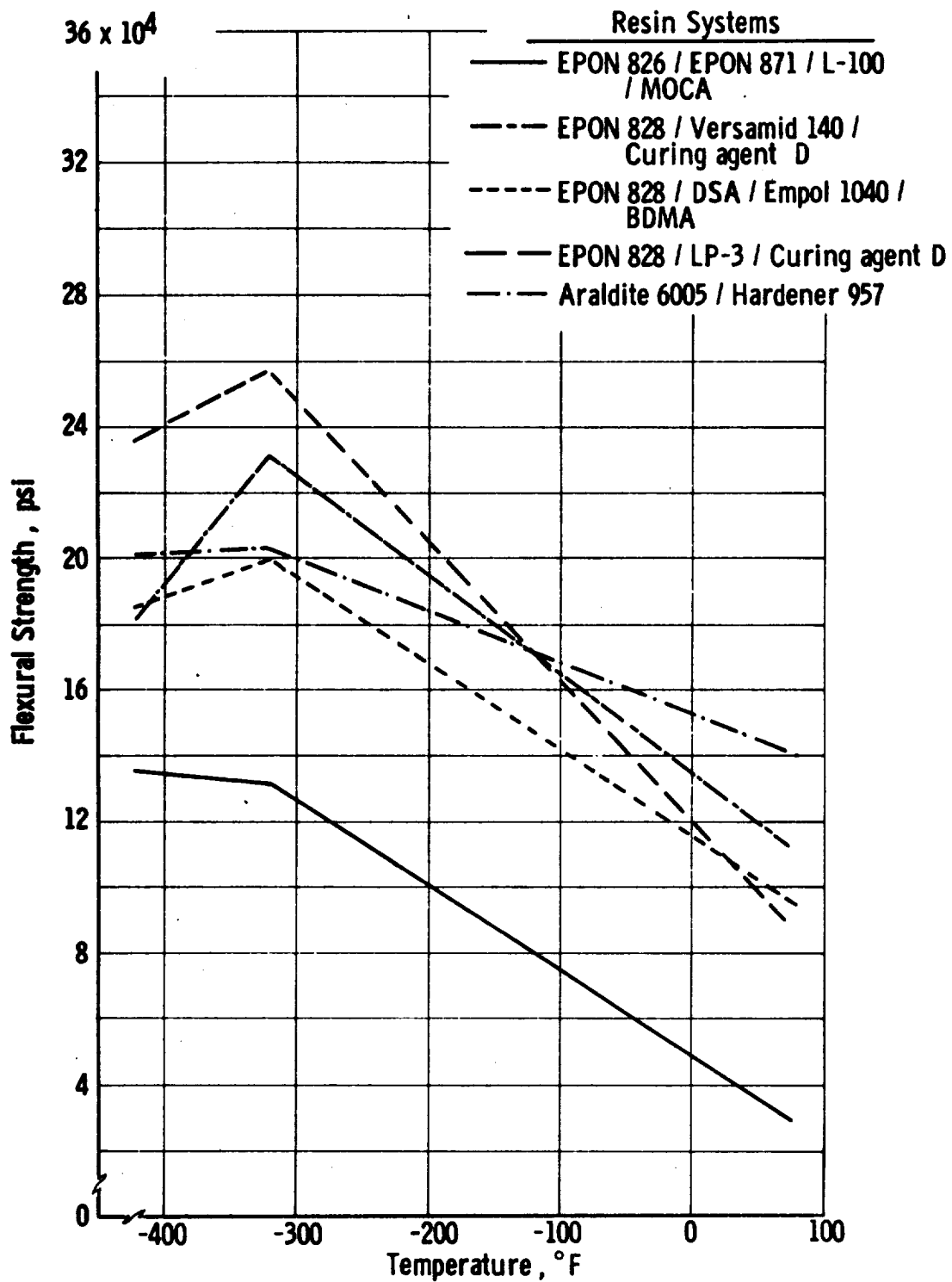


Figure 36. Resin-Comparison Study, Flexural Strength

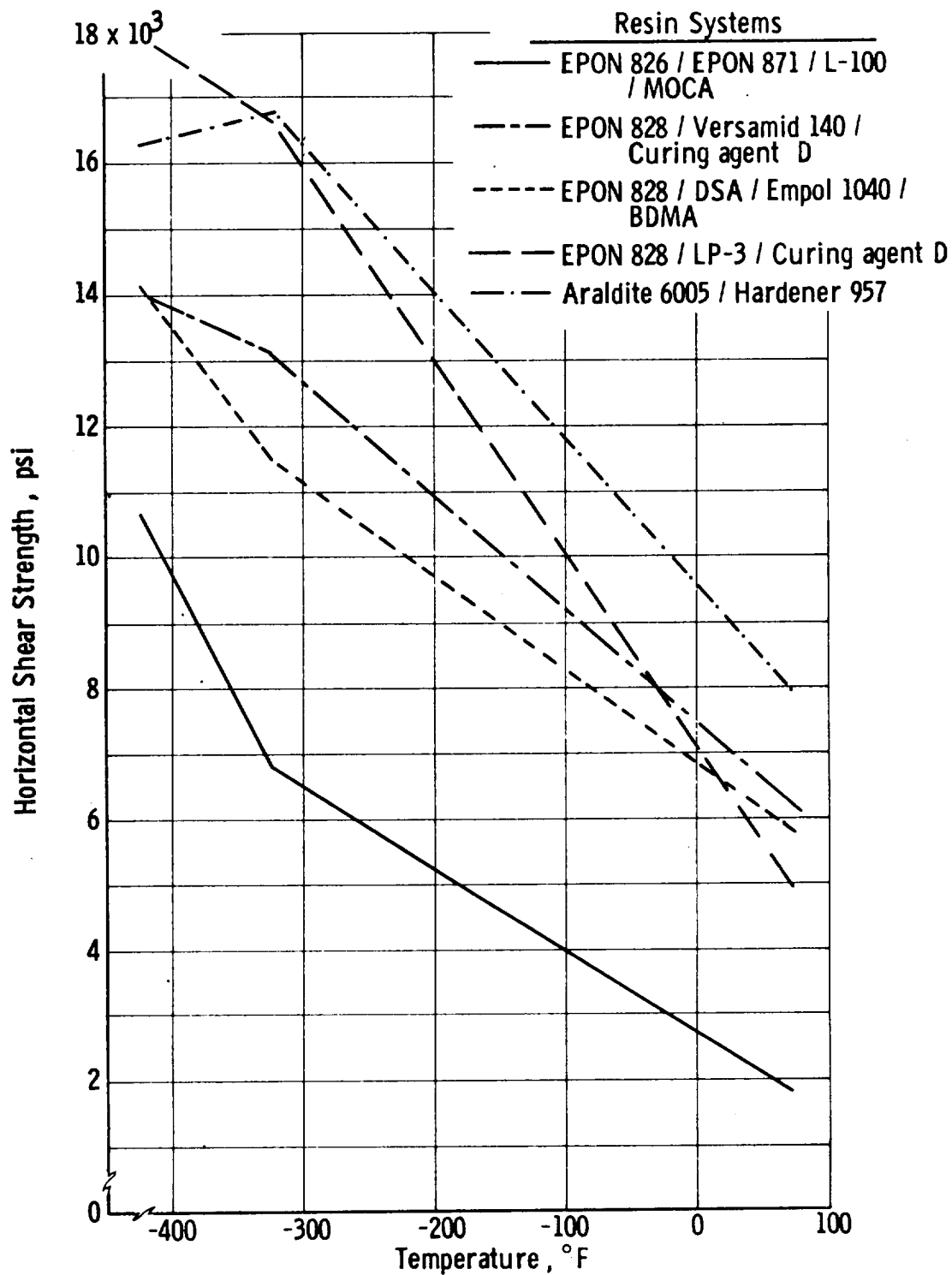


Figure 37. Resin-Comparison Study, Horizontal Shear Strength

TABLE 19

RESIN STUDY, MOL-RING COMPOSITE PROPERTIES
 ARAldITE 6005/957 HARDENER
 (100/20 FBW)*

Finish System: Film Former (Coupling Agent)	Resin Content wt%	Specific Gravity	Voids vol%	Composite Strength, psi**									
				Tensile			Horizontal Shear				Flexural		
				At Room Temp	At -320°F	At -423°F	At Room Temp	At -320°F	At -423°F	At Room Temp	At -320°F	At -423°F	At Room Temp
Araldite 6005 (A-1100)	16.1	2.00	3.6	233,800	268,000	309,100	7,900	16,300	15,300	149,800	174,700	156,700	
Araldite 6005 (A-186)	16.5	1.98	6.0	208,400	309,000	292,300	7,300	16,000	16,900	139,400	186,000	217,800	
Araldite 6005 (Z-6040)	16.7	2.02	5.4	191,600	263,200	275,300	8,100	17,200	16,300	146,400	232,300	236,700	
Araldite 6005 (Z-6020)	14.8	2.05	3.5	228,800	318,200	311,300	8,400	17,800	16,800	131,200	225,400	160,400	

* Composite Cure: 2 hours at 200°F and 2 hours at 350°F.

** Values shown are averages as follows: tensile at all temperatures, three tests; horizontal shear at room temperature, five tests, and at -320 and -423°F, three tests; flexural at room temperature, four tests, and at -320 and -423°F, three tests.

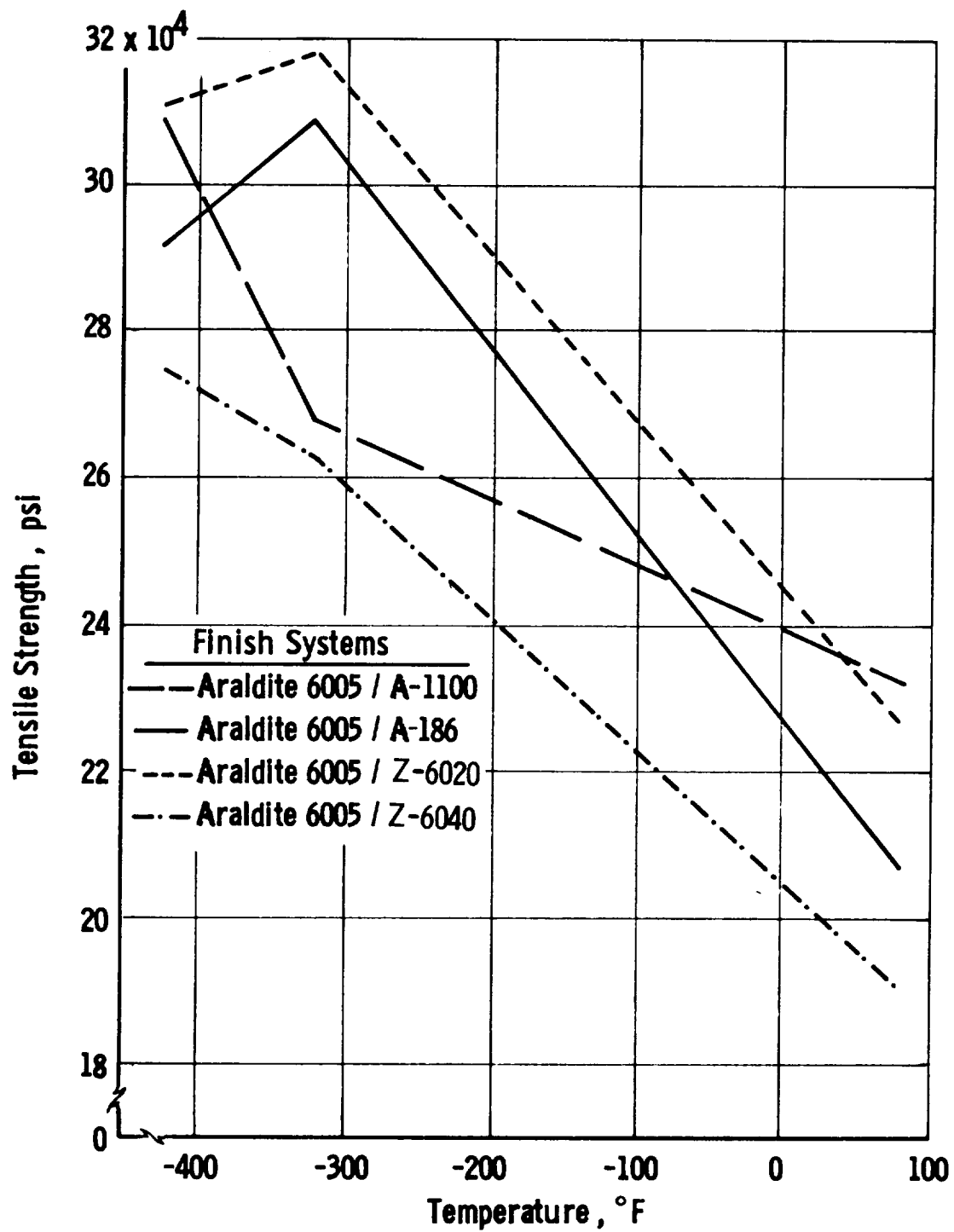


Figure 38. Resin Study (Araldite 6005/957 Hardener)
Tensile Strength

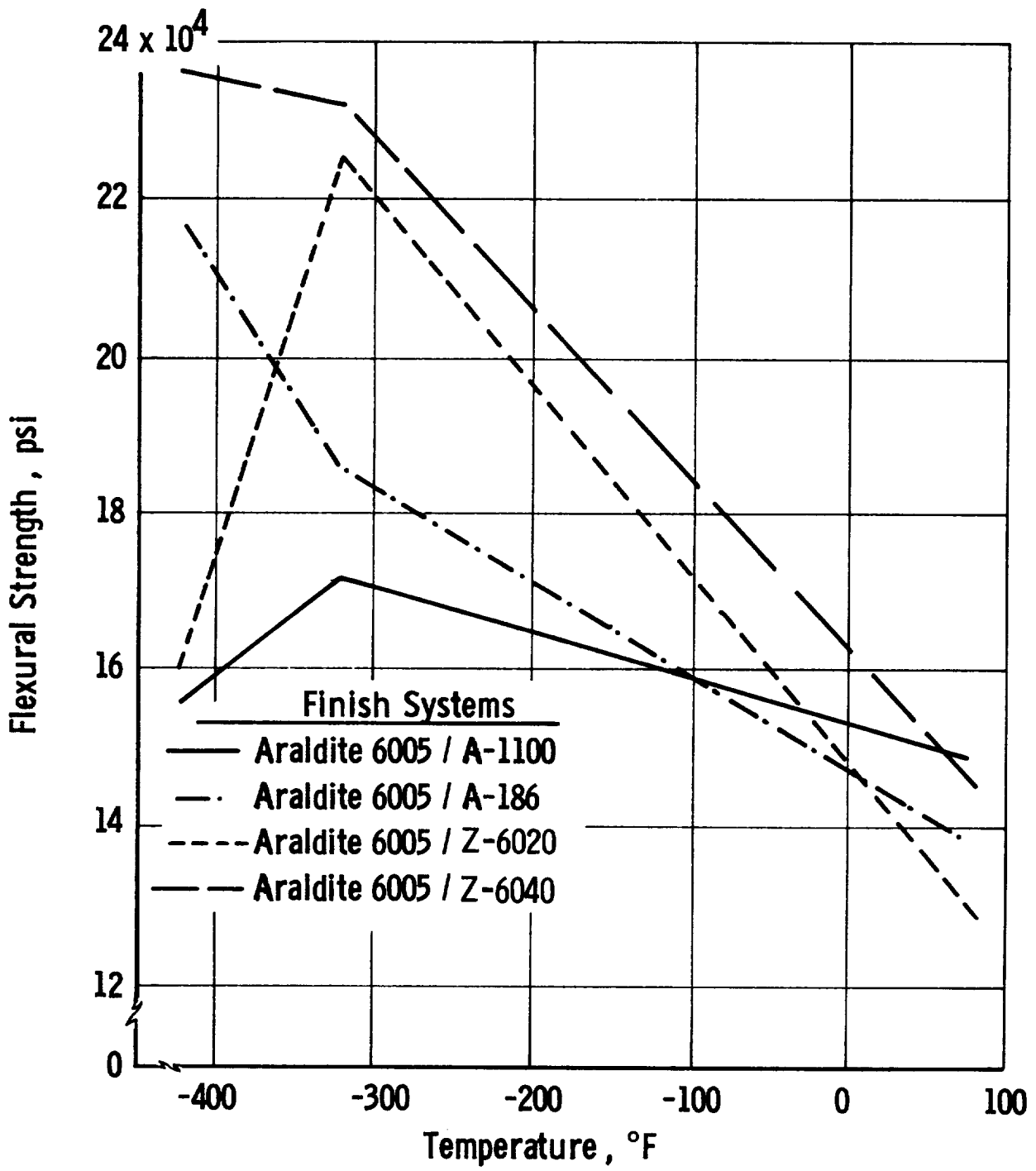


Figure 39. Resin Study (Araldite 6005/957 Hardener)
Flexural Strength

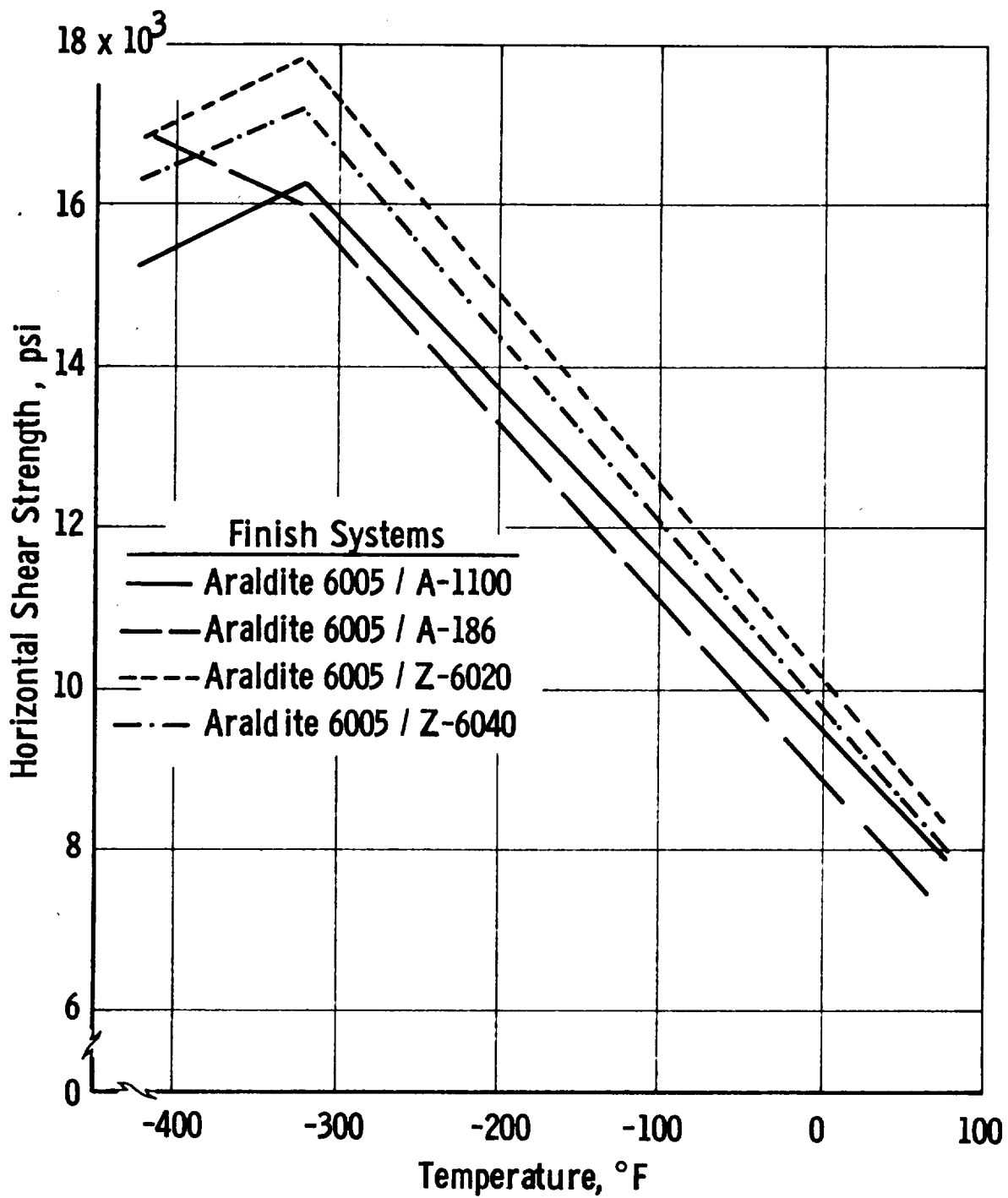


Figure 40. Resin Study (Araldite 6005/957 Hardener)
Horizontal Shear Strength

The composite tensile strength was good with the Z-6020 agent, good flexural strength was obtained with Z-6040, and good shear properties were obtained with all the coupling agents. The average composite tensile strength with the various agents was 7.7% lower at room temperature than the highest average for all the other systems (Table 15 and Figure 32). A 9.5% spread existed at -320°F, and the resin was 8.5% below the high value at -423°F.

Averaged composite flexural strengths for the four systems presented in Figure 36 showed the highest room-temperature strength for this system (21% greater than that of the highest average strength of the other systems). At -320°F, this system had a strength 20% below that of the LP-3 system. At -423°F, it had the second highest average strength (14% below that of the LP-3 system).

The average horizontal shear strength at room temperature was 22% higher than that of the next highest resin (Epon 815/Versamid 140) and was equivalent to that of LP-3 at -320°F. At -423°F, the strength of this system was 4% lower than the highest obtained (with LP-3).

This system showed edge discoloration in one thermal-shock experiment (Table 11), but none in a second (Table 16). In neither case did thermal cycling reduce the horizontal shear strength. Generally good flexural-fatigue properties were obtained (Table 17).

The average coefficient of linear thermal contraction for cast-resin specimens was 20.69×10^{-6} in./in./°F (range, 20.69 to 34.16×10^{-6} in./in./°F for the candidates). Test results are presented in Table 12 and Figure 28.

The cast resin had a flexural strength (20,500 psi) 40% greater than that of the most competitive system (Table 13) and a resin shrinkage of 8%, the highest of all the resins. Its viscosity was 860 cp at 110°F and its working pot life 2.5 hours.

Although this system yielded some rather high values, it was not considered for further evaluation because of the wide spread in its test data and its heavier than desired viscosity.

(5) Epon 828/DSA/Empol 1040/BDMA

This modified, flexible, epoxy-resin system was formulated and evaluated in work under Contract NAS 3-6287, where its test results were promising. It was evaluated in Task II with three coupling agents and an Epon 828 film former. With Agent Z-6020, the finish system polymerized during mixing and Z-6020 was dropped from the study.

The fabricated composites yielded the most uniform data in this study (Table 20 and Figures 41 to 43) and had good tensile strength at -423°F and average flexural and horizontal-shear strengths. The tensile strength was average in comparison with the other systems at room

TABLE 20

RESIN STUDY, MOL-RING COMPOSITE PROPERTIES
 EPON 828/DSA/EMPOL 1040/EDMA
 (100/115.9/20/1 PBW)*

Finish System: Film Former (Coupling Agent)	Resin Content wt%	Specific Gravity	Voids vol%	Composite Strength, psi**								
				Tensile			Horizontal Shear			Flexural		
				At Room Temp	At -320°F	At -423°F	At Room Temp	At -320°F	At -423°F	At Room Temp	At -320°F	At -423°F
Epon 828 (A-1100)	16.4	2.05	-	222,600	250,000	316,400	6,600	10,000	14,700	102,500	201,800	177,400
Epon 828 (A-186)	14.7	2.02	-	215,900	258,300	288,200	5,400	12,000	14,800	98,700	211,700	184,200
Epon 828 (Z-6020)	Finish system polymerized											
Epon 828 (Z-6040)	10.6	2.11	-	210,300	237,900	306,500	5,500	11,200	13,200	89,200	187,300	197,600

* Composite cure: 2 hours at 150°F and 4 hours at 300°F.

** Values shown are averages as follows: tensile at all temperatures, three tests; horizontal shear at room temperature, five tests, and at -320 and -423°F, three tests; flexural at room temperature, four tests, and at -320 and -423°F, three tests.

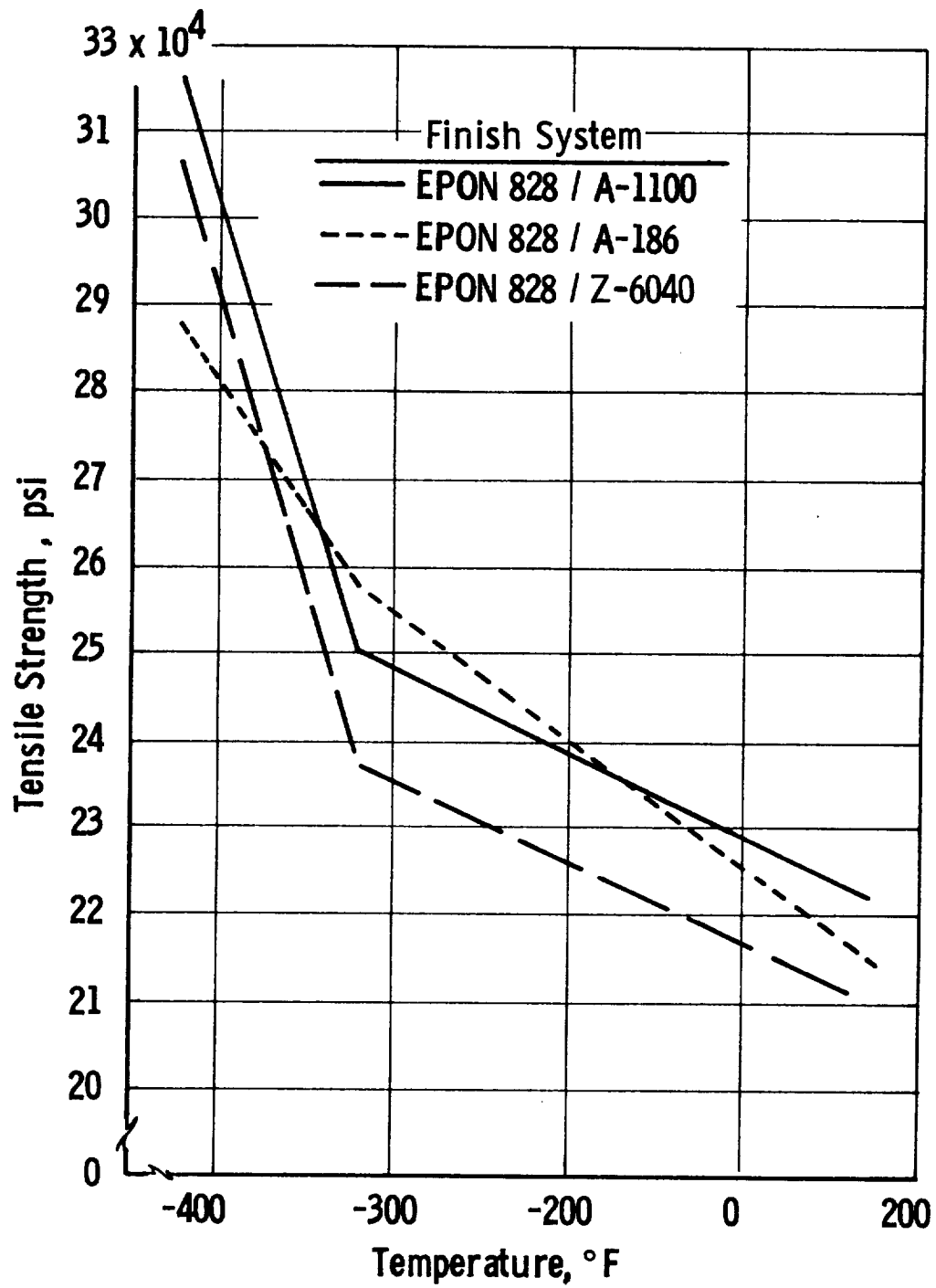


Figure 41. Resin Study (Epon 828/DSA/Empol 1040/BDMA)
Tensile Strength

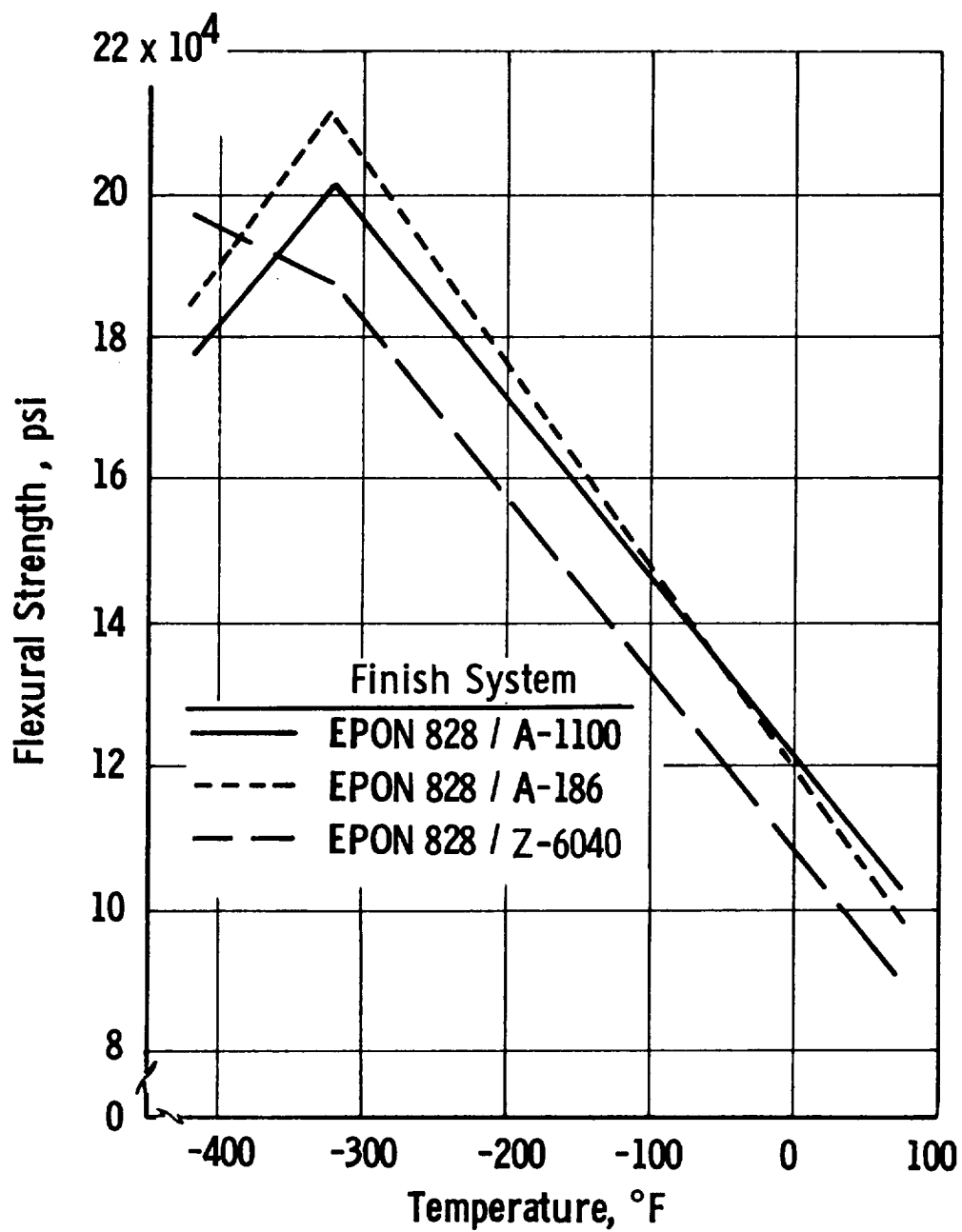


Figure 42. Resin Study (Epon 828/DSA/Empol 1040/BDMA)
Flexural Strength

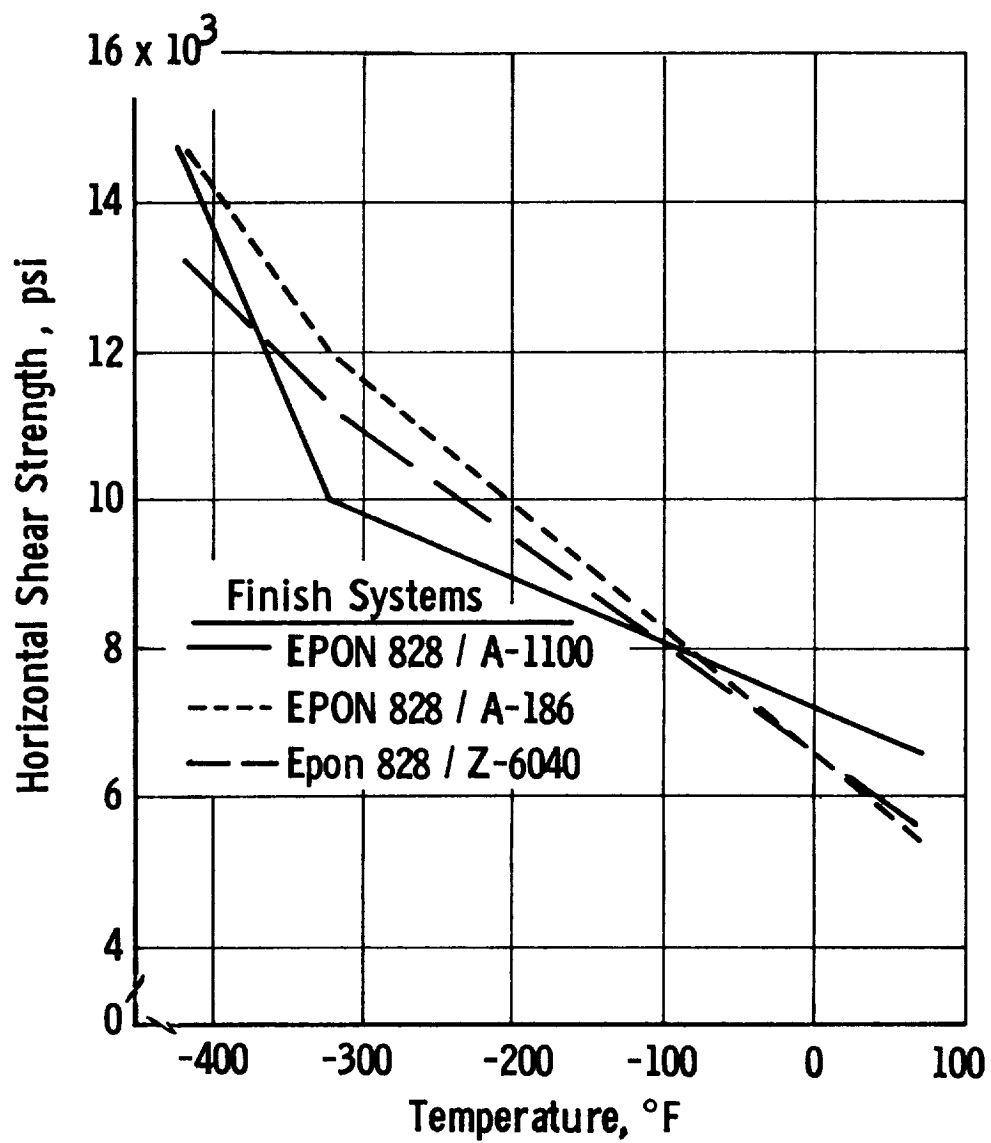


Figure 43. Resin Study (Epon 828/DSA/Empol 1040/BDMA)
Horizontal Shear Strength

temperature and -423°F . Averaged flexural and horizontal-shear data revealed composite strengths comparable to those of the other candidates.

Thermal shock had no visual effect and did not reduce the horizontal shear strength after cycling (Table 16). The low flexural-fatigue properties (Table 17) are hard to understand; the only logical explanation appears to be the possibility of test-specimen misalignment in the test fixture, resulting in erroneous test data.

The average coefficient of linear thermal contraction for cast-resin specimens was 34.16×10^{-6} in./in./ $^{\circ}\text{F}$ (range, 20.69 to 34.16×10^{-6} in./in./ $^{\circ}\text{F}$ for the candidates). Test results are presented in Table 12 and Figure 28.

The cast resin had a flexural strength of 11,600 psi, which is considered average for the candidates. It had a shrinkage of 6.1%, a viscosity of 355 cp at 110°F , and a working pot life of more than 12 hours (Table 13).

Satisfactory performance at cryogenic temperatures and data obtained from the work under Contract NAS 3-6287 led to the selection of this system for continued evaluation in Task III.

(6) Epon 826/Epon 871/L-100/MOCA

This modified, flexible, epoxy-resin system was also developed under Contract NAS 3-6287. It was evaluated in the present program, employing Hi-Stren glass fiber coated with finishes containing the four coupling agents and an Epon 815/L-100 film former in a solvent carrier. The test results are given in Table 21 and Figures 44 to 46.

The test data for composite tensile strength had considerable scatter, as the result of winding difficulties caused by an extremely short pot life. Good tensile strength was obtained at -320°F with the A-1100 and Z-6020 coupling agents. Poor flexural and horizontal-shear results are again attributed to short pot life. The average composite tensile strength with all the coupling agents was the lowest at room temperature and -423°F in comparison with the other candidate materials; at -320°F , it was only 12% lower than the highest strength obtained, which indicates a good low-temperature matrix material. The average flexural and horizontal-shear strengths with the four coupling agents was the the lowest among the candidates.

No visual defects were disclosed in thermal-shock testing, and the horizontal shear strength was unaffected (Table 16).

The system had poor flexural-fatigue properties (Table 17), which can be explained on the basis of inferior test laminates as the result of an extremely short pot life.

TABLE 21

RESIN STUDY, NOL-RING COMPOSITE PROPERTIES
 EPON 826/EPON 871/L-100/MOCA
 (35/15/50/27.6 PBW)*

Finish System: Film Former (Coupling Agent)	Resin Content wt%	Specific Gravity	Voids vol%	Composite Strength, psi**									
				Tensile			Horizontal Shear				Flexural		
				At Room Temp	At -320°F	At -423°F	At Room Temp	At -320°F	At -423°F	At Room Temp	At -320°F	At -423°F	At Room Temp
Epon 815/L-100 (A-1100)	11.8	2.09	5.0	210,400	317,700	259,700	1,300	4,900	7,100	17,100	109,800	126,300	
Epon 815/L-100 (A-186)	10.2	2.19	2.4	203,600	196,000	230,900	3,700	10,600	14,800	30,900	140,300	159,100	
Epon 815/L-100 (Z-6020)	13.5	2.07	3.7	178,100	318,300	273,800	1,300	5,800	9,900	27,800	162,200	137,100	
Epon 815/L-100 (Z-6040)	10.5	2.12	4.6	160,000	280,000	222,300	1,100	6,000	11,100	40,700	115,500	124,800	

* Composite cure: 5 hours at 285°F.

** Values shown are averages as follows: tensile at all temperatures, three tests; horizontal shear at room temperature, five tests, and at -320 and -423°F, three tests; flexural at room temperature, four tests, and at -320 and -423°F, three tests.

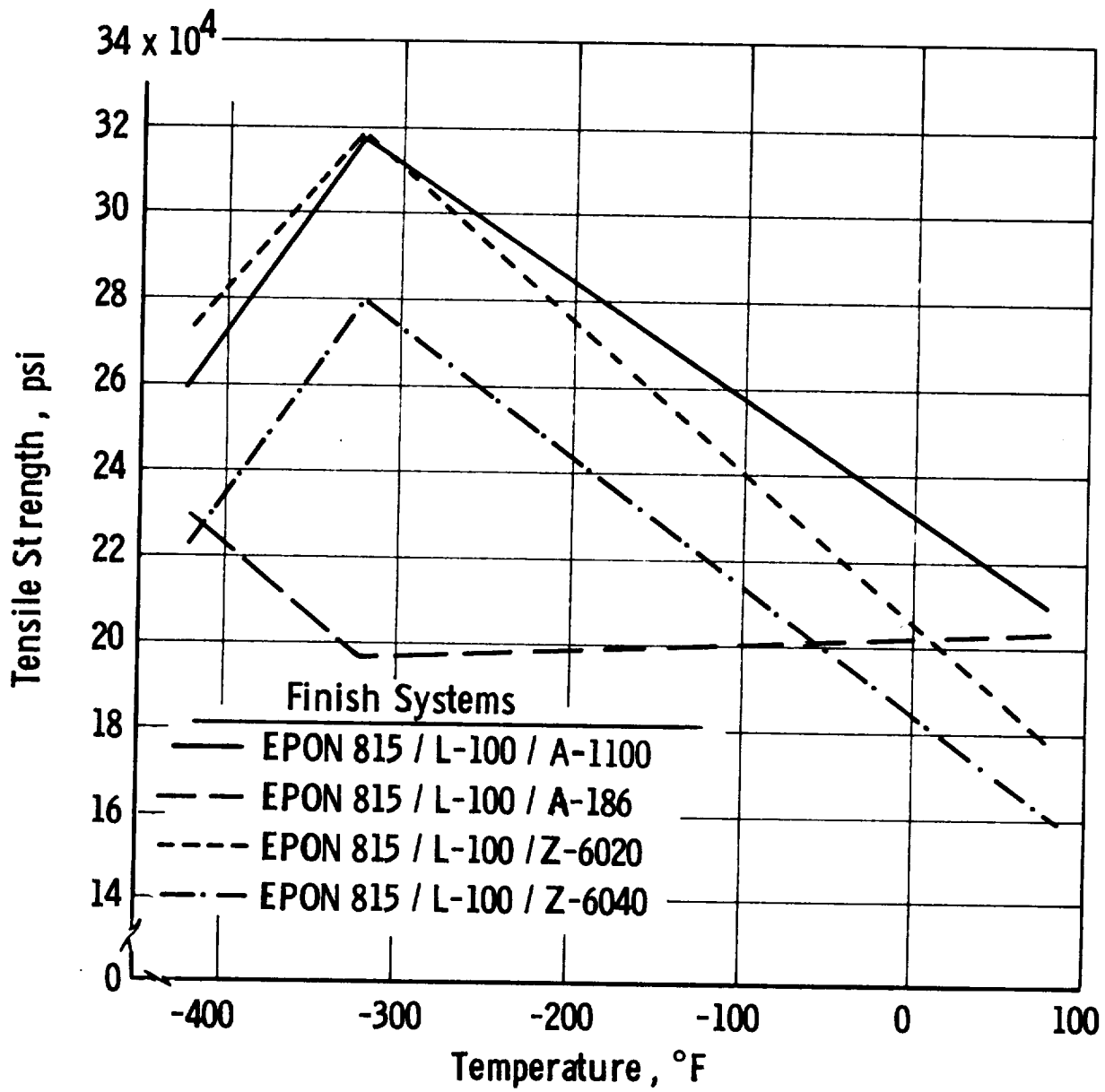


Figure 44. Resin Study (Epon 826/Epon 871/L-100/MOCA)
Tensile Strength

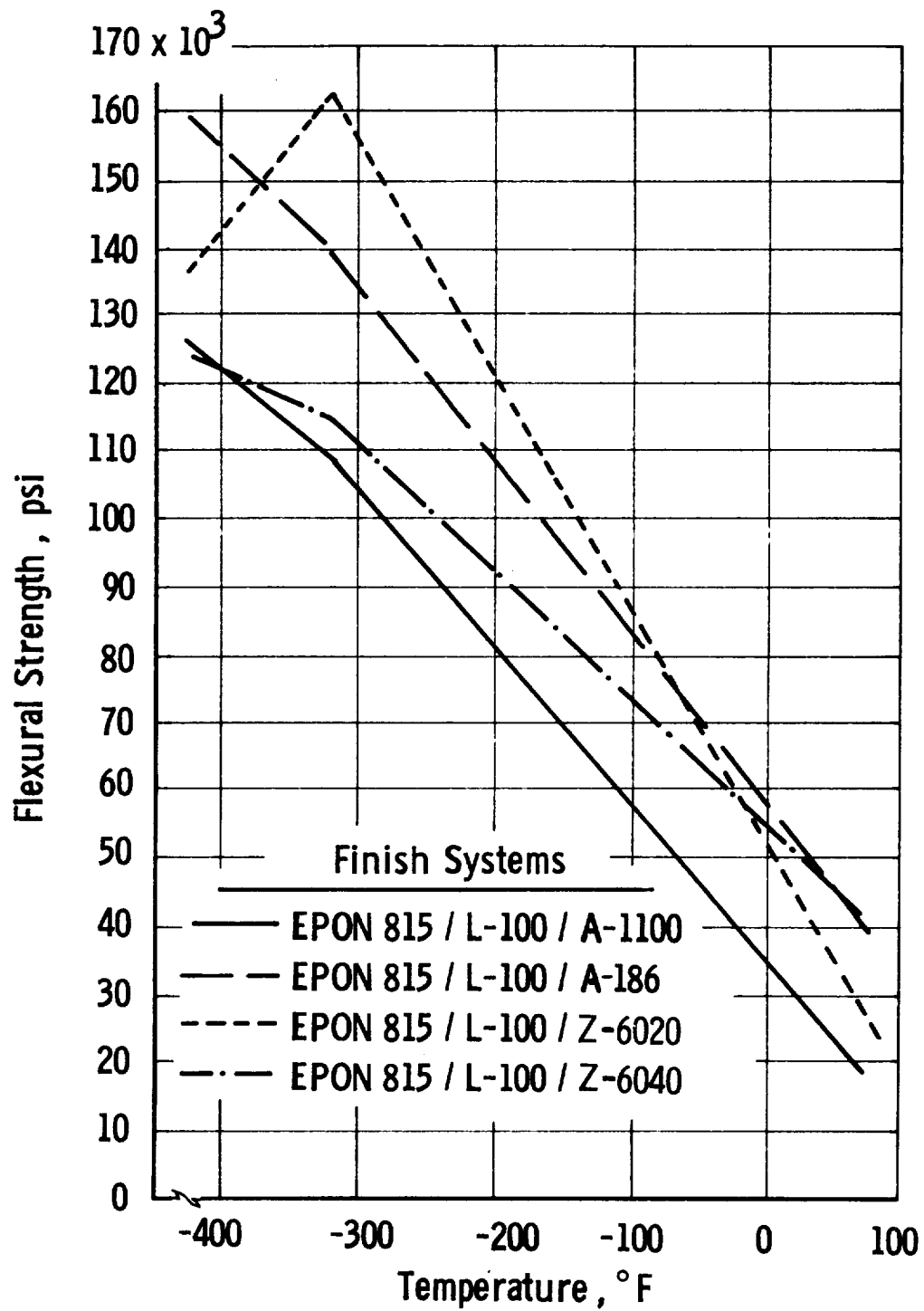


Figure 45. Resin Study (Epon 826/Epon 871/L-100/MOCA)
Flexural Strength

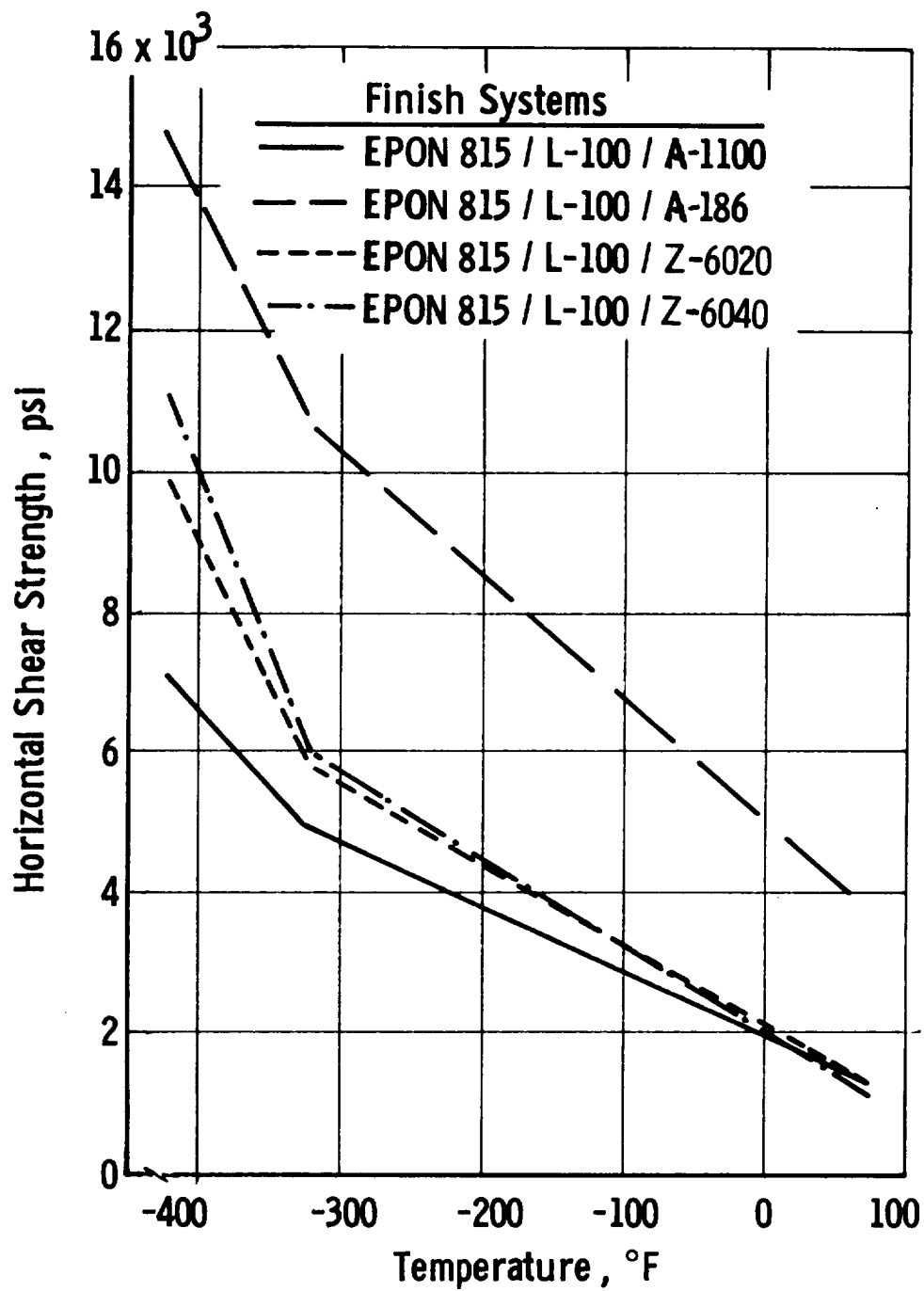


Figure 46. Resin Study (Epon 826/Epon 871/L-100/MOCA)
Horizontal Shear Strength

The average coefficient of linear thermal contraction for cast-resin specimens was 33.41×10^{-6} in./in./°F (range, 20.69 to 34.16×10^{-6} in./in./°F for the candidates). Test results are presented in Table 12 and Figure 28.

The cast resin had a flexural strength of 336 psi, a resin shrinkage of 6.0%, a viscosity of 1887 cp at 150°F, and a working pot life of 20 min (Table 13).

Because of considerable data scatter, high viscosity, and short pot life, this system was not considered for further evaluation.

V. BIAXIAL AND UNIAXIAL COMPOSITES (TASK III)

Task III initially covered evaluation of three resin systems, two coupling agents, and two film formers. The work was later expanded to include two additional resin systems developed by Aerojet.

The evaluations employed filament-wound flat laminates with Hi-Stren glass-fiber reinforcement. The laminates were prepared with the following filament ratios: unidirectional 1:0 and bidirectional 1:1 and 1:2.

A. MATERIAL SELECTION

The Task III resinous materials and finishes are shown in Table 22.

Hi-Stren single-end glass-fiber roving was manufactured for this task in a direct-melt furnace with a 204-hole bushing. Immediately after fiberization, the fibers were coated with the selected film formers and coupling agents. Cake packages in polyethylene bags were stored in a 0°F refrigerator to ensure glass of consistent quality.

B. SPECIMEN FABRICATION

1. Equipment

a. Glass-Fiber Furnace

A direct-melt glass-fiber furnace was used to produce the required single-end roving. Its melting, refining, and forming sections were constructed of high-temperature refractories. These sections were heated with natural gas and air, using a premix burner system. A 204-orifice bushing was mounted in the forming section and was heated electrically by a high-amperage, low-voltage, power supply. The fibers were drawn from the forming section, which was fed continuously by a molten pool in the refining section. The latter was fed continuously with new glass from the melting section, which was fed raw batch material automatically with the aid of a time-controlled batch charger. The glass was fiberized at the rate of 4000 ft/min.

b. Filament-Winding Machine

The single-end NOL-ring winding equipment used in Task II was modified to accommodate the winding of parallel fiber sheets (Figure 3). A stainless steel cylinder, approximately 11 in. long and 6 in. in diameter, replaced the NOL-ring mandrel. The rest of the unit was essentially the same as that used to wind single-end NOL rings.

The winding-drum and strand-traversing mechanisms were powered by a variable-speed motor, which provided an exact butt-joint layup. A creel containing a single-end roving package (Figure 5) was mounted on the extreme left side of the filament-winding machine. The roving was paid off at the top of the clockwise-turning package, and filament tension was

TABLE 22
MATERIALS FOR EVALUATION IN TASK III

<u>Basic Ingredients</u>	<u>System Formulations¹</u>	<u>Concentration</u>
Matrix Resins		
Epon 828 (control)	Epon 828/NMA/BDMA ²	100/80/0.5 pbw
Epon 828/Empol 1040	Epon 828/DSA/Empol 1040/BDMA ³	100/115.9/20/1 pbw
Epon 828/LP-3	Epon 828/LP-3/Curing Agent D ⁴	100/33/12 pbw
Epon 826/Epon 871	Epon 828/Epon 871/DDI/Curalon L ⁵	35/15/14.7/35.1 pbw
DER 332/Epon 871	DER 332/Epon 871/DDI/Curalon L ⁵	35/15/14.7/35.1 pbw
Finish Film Formers		
VHS	VHS and A-1100	--
Epon 828/LP-3	Epon 828/LP-3/Z-6040/Curing Agent Z/acetone	10/3.5/5/1.5/80 wt%
Coupling Agents		
A-1100	--	--
Z-6040	--	5 wt%

¹DDI = fatty acid diisocyanate. Curalon L = diamine curing agent.

²Cure: 1 hour at 200°F, 2 hours at 350°F.

³Cure: 2 hours at 150°F, 4 hours at 300°F.

⁴Cure: 1 hour at 150°F, 1 hour at 300°F.

⁵Cure: 5 hours at 285°F.

controlled by a predetermined dead-weight load suspended from the unwinding creel by a nylon cord, which in turn acted as a friction brake. The single-end roving was then guided by a series of Teflon rollers through a resin bath, which was heated to (1) control the viscosity, (2) provide better wetting of the fiber bundle, and (3) prevent abrasion as the fiber strand passed through the guides. As the impregnated single-end roving left the resin bath, it was passed between a pair of rubber blankets, which acted as a squeegee and removed the excess resin.

The single-end roving was then passed through the strand-traversing mechanism and was wound onto the take-up drum, which was covered with a Teflon-coated glass cloth prior to winding. The cloth was used as a release and handling medium for the filament-wound sheet. (The take-up drum is shown at the extreme right side of Figure 3.) After four layups of the single-end roving across the take-up drum, the exposed surface was also covered with Teflon cloth. The filaments were then cut from the drum to produce a flat sheet 19 in. long by 10 in. wide (Figure 47). These sheets provided two 9-in.-square plies of oriented fibers.

2. Procedures

Test laminates were fabricated by laying up a series of sheets with the filament winding having a unidirectional or a bidirectional orientation (Figure 48). The sheets were prepared by winding a single-end roving onto a Teflon-cloth-covered drum. Processing studies established that four traverses of the roving across the width of the drum produced the most satisfactory sheets. (Fewer plies cause the sheet to split or come apart during handling; more cause the sheet to wrinkle on removal from the winding drum.) The single-end finish-coated roving was impregnated with the selected resin during winding. Teflon cloth was placed over the exposed surface of the sheet, which was then cut from the winding drum at right angles to the fiber layup and was fastened to a cardboard holder with $3/4$ -in. masking tape. Fabricated sheets were placed in 0°F storage until enough were on hand for the fabrication of test panels.

Preliminary unidirectional-panel experiments indicated that approximately 36 plies or nine sheets (10 by 10 in.) would produce the required laminate thickness ($0.125 \pm .005$ in.) with a resin content of 20 +3%. The laminates were prepared on release-treated aluminum caul plates, $3/8$ in. thick, with an aluminum frame around the layup to maintain fiber orientation and reduce fiber washing. The laminate was covered with one ply of Dacron cloth, and a bleeder cloth was placed around the periphery of the laminate. The layup was then placed in a polyvinyl alcohol bag, sealed, and cured under vacuum in an air-circulating electric oven.

Three test panels (shown in Figure 47) were used to evaluate each resin system; to assure reproducibility, they were cured simultaneously in one vacuum bag.

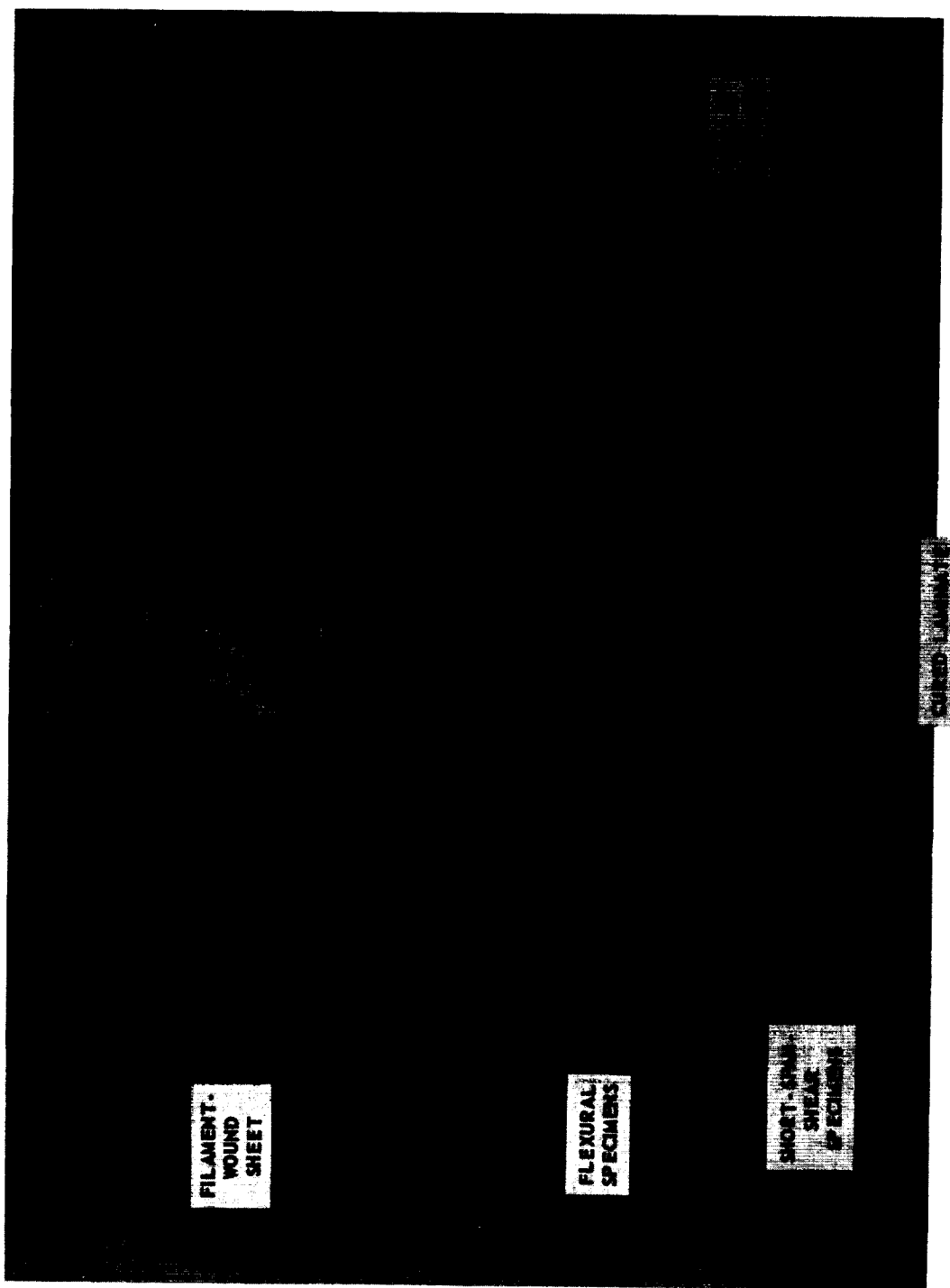
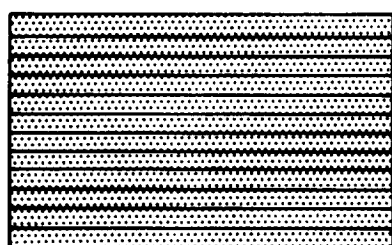


Figure 47. Filament-Wound Sheet, Cured Laminate, and Test Specimens

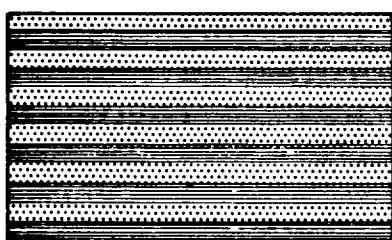


12 TH LAYER



1 ST LAYER

Unidirectional (1:0)

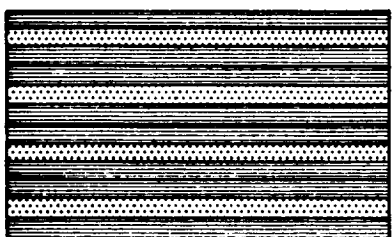


12 TH LAYER



1 ST LAYER

Bidirectional (1:1)



12 TH LAYER



1 ST LAYER

Bidirectional (1:2)

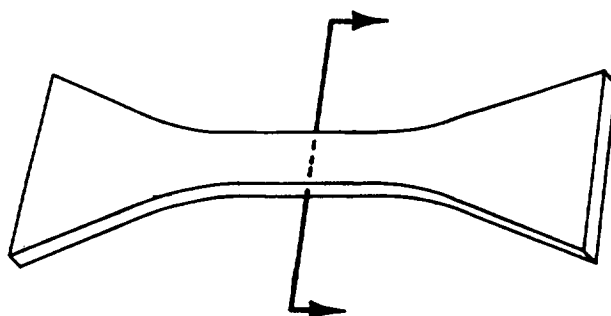


Figure 48. Filament-Orientation Patterns

Typical filament orientations (unidirectional 1:0, bidirectional 1:1, and bidirectional 1:2) are illustrated in Figures 49 to 51.

C. EVALUATION

1. Test Requirements

The Task III plan called for the testing of unidirectional and bidirectional laminates for the following properties at +70, -320, and -423°F: (a) tensile strength and strain, (b) extensibility of the composite, (c) flexural strength, (d) interlaminar shear (short-span shear), (e) thermal shock (interlaminar specimens), (f) impact strength, and (g) coefficient of thermal contraction.

These tests are described in detail in Appendix A. In general, they adhered to the methods described in the latest standards of the American Society for Testing Materials (ASTM) or in Federal Test Methods (FTM) Standard 406.

The room-temperature-test specimens were cut from one of the three simultaneously cured laminates, the -320°F specimens from another, and the -423°F specimens from the third. To obtain the proper tensile failure (shown in Figure 52), it was necessary to add four plies of 181 glass cloth, equally spaced, throughout the grip area of the specimen.

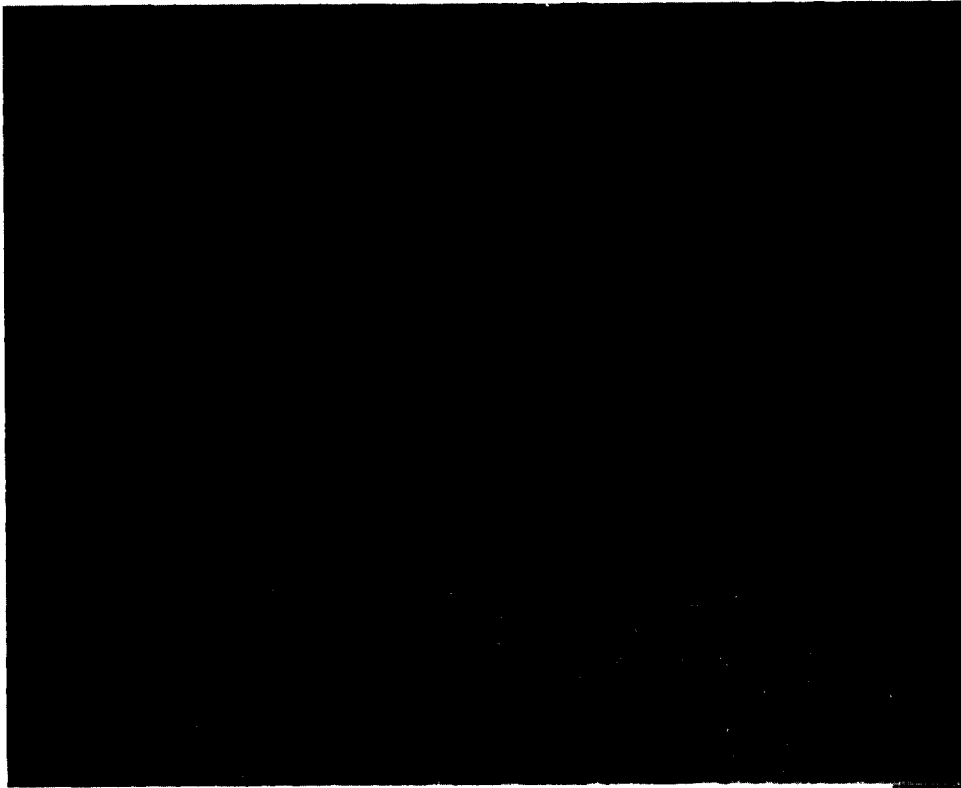
The following types of specimens (see Figure 47) were cut from each of the cured test panels: three tensile, three flexural, three short-span-shear, and three short-span-shear for thermal shock (room-temperature panel only). Resin content and specific gravity were determined for each test panel. The ignition-loss method was used to determine resin content, and specific gravity was determined gravimetrically. These data formed the basis for calculation of the void content of each panel.

The impact strength and coefficient of thermal contraction were determined with separately fabricated panels, because these tests require a greater specimen thickness.

The Task III tensile specimens were originally designed to be 0.400 in. wide throughout the necked-down (flat) test area. It became necessary to reduce the width to 0.125 in., because of the high loads obtained in the unidirectional room-temperature tests and the greater loads obtained at cryogenic temperatures.

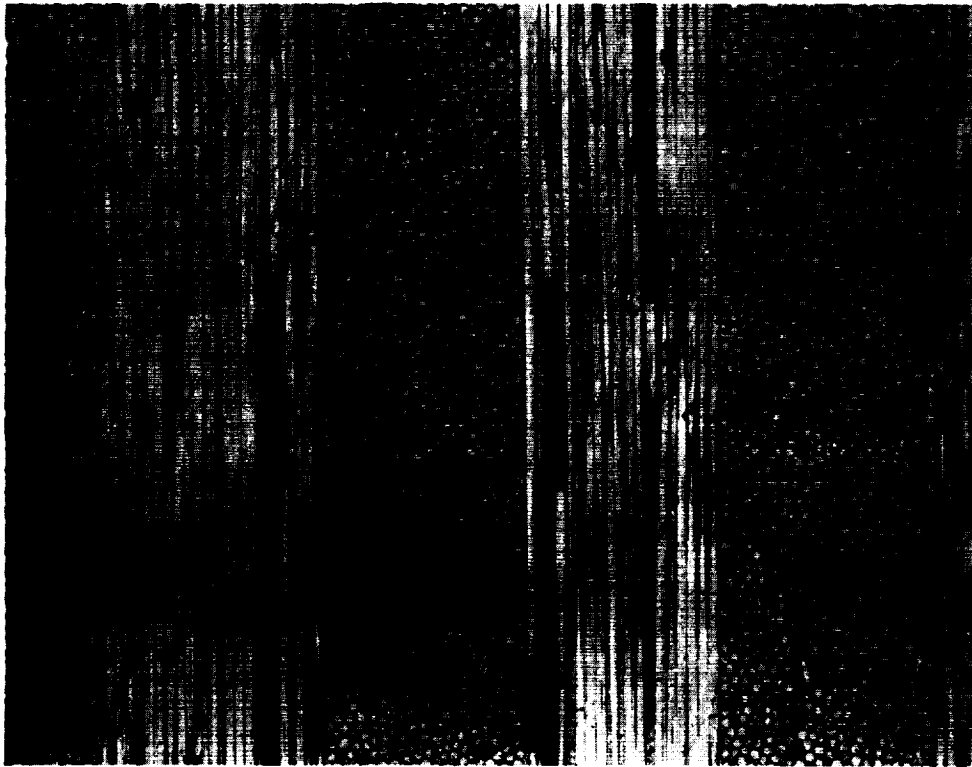
The tensile-test fixture was modified slightly by the addition of abrasive, serrated, metal inserts in the grip portion, on both sides of the specimen. When tightened in place, the inserts eliminated slippage by causing the serrations to bite into test specimens.

The inserts and the reduced test-area width eliminated grip failure (pull-through of the tensile specimen) and produced the desired tensile failure (Figure 52).



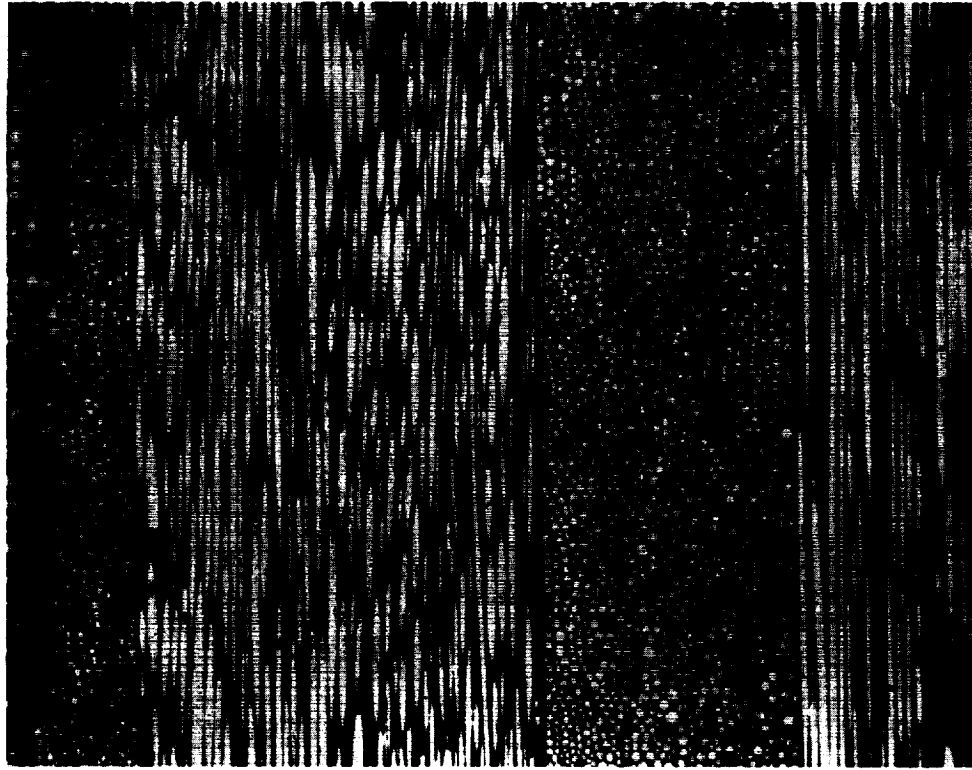
250x

Figure 49. Typical Cross Section, Unidirectional 1:0 Composite



100x

Figure 50. Typical Cross Section,
Bidirectional 1:1 Composite



100x

Figure 51. Typical Cross Section,
Bidirectional 1:2 Composite

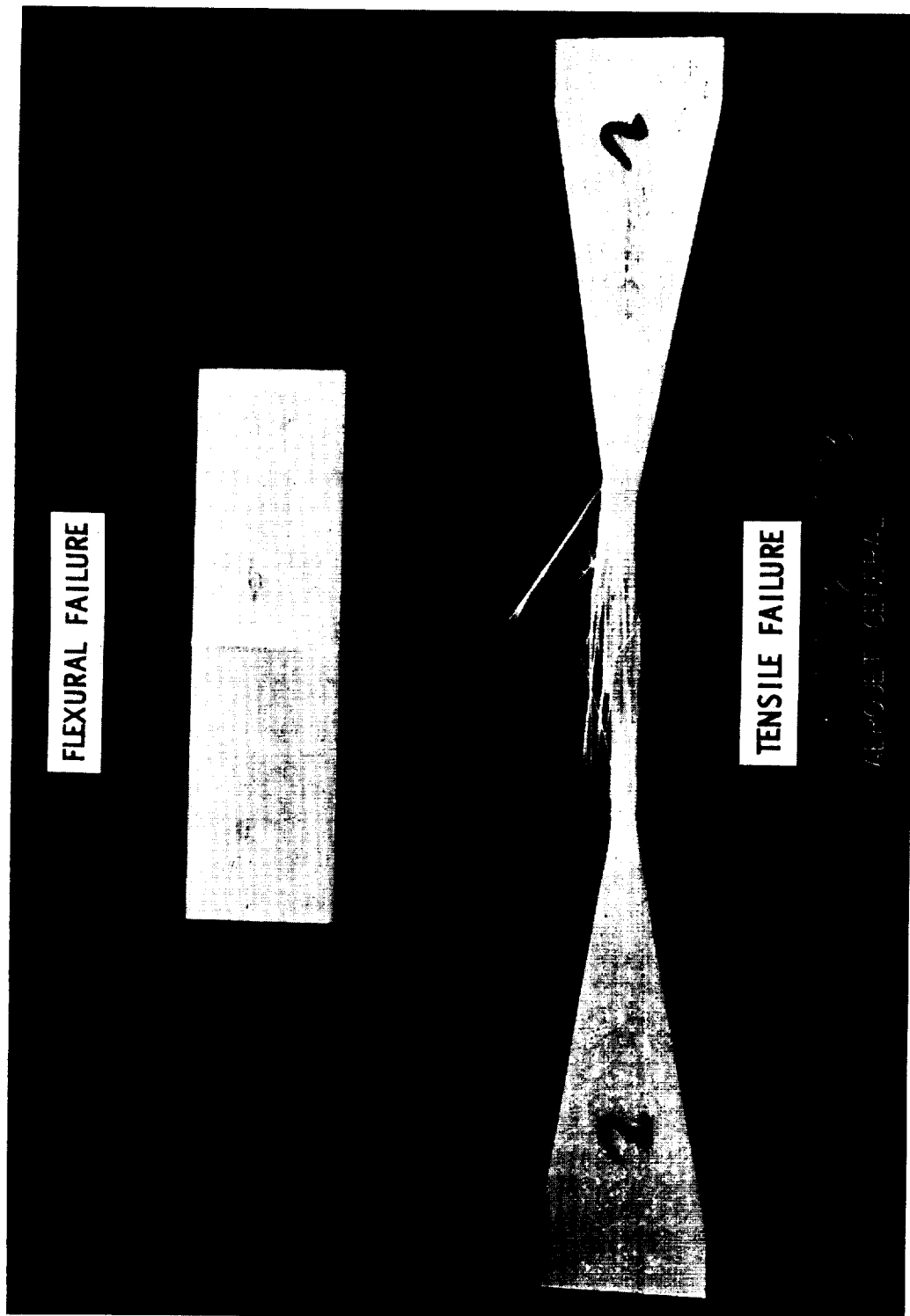


Figure 52. Specimens After Testing

To permit the use of existing -423°F flexural-test fixtures, all flexural specimens (room temperature, -320°F , and -423°F) were reduced in length from 4 in. to 3 in., with the test span held constant. The room-temperature mode of failure was flexural (definite compression failure on the top of the specimen and tensile on the bottom).

2. Analysis and Selection

a. Epon 828/NMA/BDMA (Control)

This unmodified epoxy-resin system (control) was evaluated with Hi-Stren glass filaments coated with an epoxy film former and a coupling agent in a solvent carrier. The test results are shown in Tables 23 to 25 and Figures 53 to 55.

The composite tensile strength was generally slightly lower in comparison with the highest-strength system (Epon 828/DSA/Epcol 1040/BDMA). In the unidirectional composites (1:0), as compared with that system, the control resin yielded 2% lower strengths at room temperature, 19% lower at -320°F , and 11% lower at -423°F . For the bidirectional 1:1 composites, the control was 12.5% lower at room temperature, equivalent at -320°F , and 6% higher at -423°F . For the bidirectional 1:2 composites, the control was 4% lower at room temperature, 12% lower at -320°F , and 6% lower at -423°F .

In flexural strength, the control resin displayed a unidirectional 1:0 strength value, in comparison with the best obtained, that was 15% lower at room temperature, 20% lower at -320°F , and 41% lower at -423°F . The bidirectional 1:1 tests, however, showed the control resin to be the strongest at room temperature and at -423°F ; its strength at -320°F was 19% below that of the strongest. The bidirectional 1:2 tests revealed very good properties at room temperature, but below-average strength at cryogenic temperatures.

The short-span-shear data revealed good unidirectional 1:0 properties. Bidirectional 1:1 composites yielded the highest values at room temperature and -423°F , but values 50% lower than those of the LP-3 system at -320°F . The bidirectional 1:2 tests gave data with considerable spread: In comparison with the best system, the room-temperature value was 5% lower and the -320°F value 48% lower, but the -423°F strength was the highest.

Thermal shocking (-423°F) of short-span-shear specimens resulted in no visual or mechanical deterioration after five cycles (Table 26). The impact strengths (Table 27) for the three configurations were the most consistent of all, averaging approximately 30% higher at -320°F than at room temperature for each configuration.

The coefficient of linear thermal contraction was determined with bidirectional 1:2 specimens (Table 28). An effort was made to obtain thermal-contraction data on unidirectional 1:0 specimens, but the relatively low resin content and the orientation in the direction of measurement caused the measurement to be less than the quartz correctional factor.

TABLE 23
COMPOSITE TEST RESULTS, UNIDIRECTIONAL 1:0 ORIENTATION*

Resin System	Temp OF	Resin Content wt%	Specific Gravity	Voids vol%	Tensile		Elonga- tion %	Strength, psi		Izod Impact Strength ft-lb/in. of notch
					Strength psi	Modulus psi		Flexural	Short- Span Shear	
Epon 828/NMA/BDMA**	+72	13.4	1.96	10.5	194,500	10,400,000	2.9	141,300	4,100	84
	-320	13.0	1.99	9.0	244,200	-	2.6	300,000	10,100	122
	-423	13.3	1.95	11.4	227,100	12,000,000	1.9	245,400	11,400	-
Epon 828/DGA/Empol 1040/BDMA**	+72	15.0	2.05	1.5	198,100	9,100,000	2.75	165,900	4,600	82
	-320	14.0	2.03	4.1	301,900	11,140,000	2.7	376,700	11,900	67
	-423	14.7	2.06	1.4	254,600	10,310,000	2.4	418,000	9,000	-
Epon 828/IP-3/Curing Agent D***	+72	20.8	1.98	6.6	194,700	7,450,000	5.8	88,800	3,700	128
	-320	19.5	2.00	10.0	213,200	8,040,000	2.7	324,000	9,000	162
	-423	20.6	1.90	1.0	215,700	8,240,000	2.7	381,900	12,400	-

* Each value represents an average of three tests.

** Used with VHS/A-1100, single-end, Hi-Stren, glass fibers.

*** Used with Epon 828/IP-3/Z-6040, single-end, Hi-Stren, glass fibers.

TABLE 24
COMPOSITE TEST RESULTS, BIDIRECTIONAL 1:1 ORIENTATION*

Resin System	Temp Of	Resin Content wt%	Specific Gravity	Voids vol%	Tensile		Elonga- tion %	Strength, psi		Izod Impact Strength ft-lb/in. of notch
					Strength psi	Modulus psi		Flexural	Short- Span Shear	
Epon 828/NMA/BDMA**	+72	16.4	1.99	6.2	106,600	4,100,000	3.0	121,400	4,000	49
	-320	15.8	2.01	6.1	141,200	4,500,000	3.18	170,200	5,300	67
	-423	15.8	2.03	4.7	157,000	5,700,000	2.85	252,400	10,300	-
Epon 828/DSA/Empol 1040/BDMA**	+72	15.5	2.06	0.16	122,000	5,000,000	2.7	112,600	3,800	67
	-320	15.4	2.07	0.27	142,000	4,000,000	3.5	144,600	5,700	59
	-423	16.0	2.05	0.62	147,000	6,500,000	1.9	244,500	6,300	-
Epon 828/LP-3/Curing Agent D***	+72	29.8	1.87	Neg	82,000	3,000,000	2.9	71,200	3,200	96
	-320	19.0	2.0	1.25	111,400	2,930,000	3.7	209,300	10,700	76
	-423	22.2	2.02	Neg	128,200	5,630,000	2.3	223,600	9,500	-

* Each value represents an average of three tests.

** Used with VHS/A-1100, single-end, Hi-Stren, glass fibers.

*** Used with Epon 828/LP-3/Z-6040, single-end, Hi-Stren, glass fibers.

TABLE 25
COMPOSITE TEST RESULTS, BIDIRECTIONAL 1:2 ORIENTATION*

Resin System	Temp Of	Resin Content wt%	Specific Gravity	Voids vol%	Tensile		Elonga- tion %	Strength, psi			Izod Impact Strength ft-lb/in. of notch
					Strength psi	Modulus psi		Flexural	Short- Span Shear		
Epon 828/WMA/BDMA**	+72	14.3	2.00	7.5	78,400	2,800,000	4.4	95,500	4,000		38
	-320	14.5	1.99	7.5	99,400	3,400,000	2.8	111,000	4,600		55
	-423	14.1	1.99	7.7	85,900	3,900,000	2.2	147,600	9,700		-
Epon 828/DSA/Empol 1040/BDMA**	+72	15.6	2.05	0.95	81,800	3,170,000	2.9	92,000	4,200		67
	-320	14.8	2.07	Neg	113,700	3,960,000	2.8	84,000	2,500		65
	-423	15.4	2.06	0.8	91,600	4,200,000	2.0	117,100	3,500		-
Epon 828/IP-3/Curing Agent D***	+72	24.4	1.96	Neg	77,800	2,750,000	3.5	74,100	3,900		66
	-320	22.3	1.99	0.71	73,700	2,160,000	3.3	190,000	8,900		72
	-423	19.5	2.02	Neg	84,000	3,700,000	2.4	206,000	6,800		-

* Each value represents an average of three tests.

** Used with VHS/A-1100, single-end, Hi-Stren, glass fibers.

*** Used with Epon 828/IP-3/Z-6040, single-end, Hi-Stren, glass fibers.

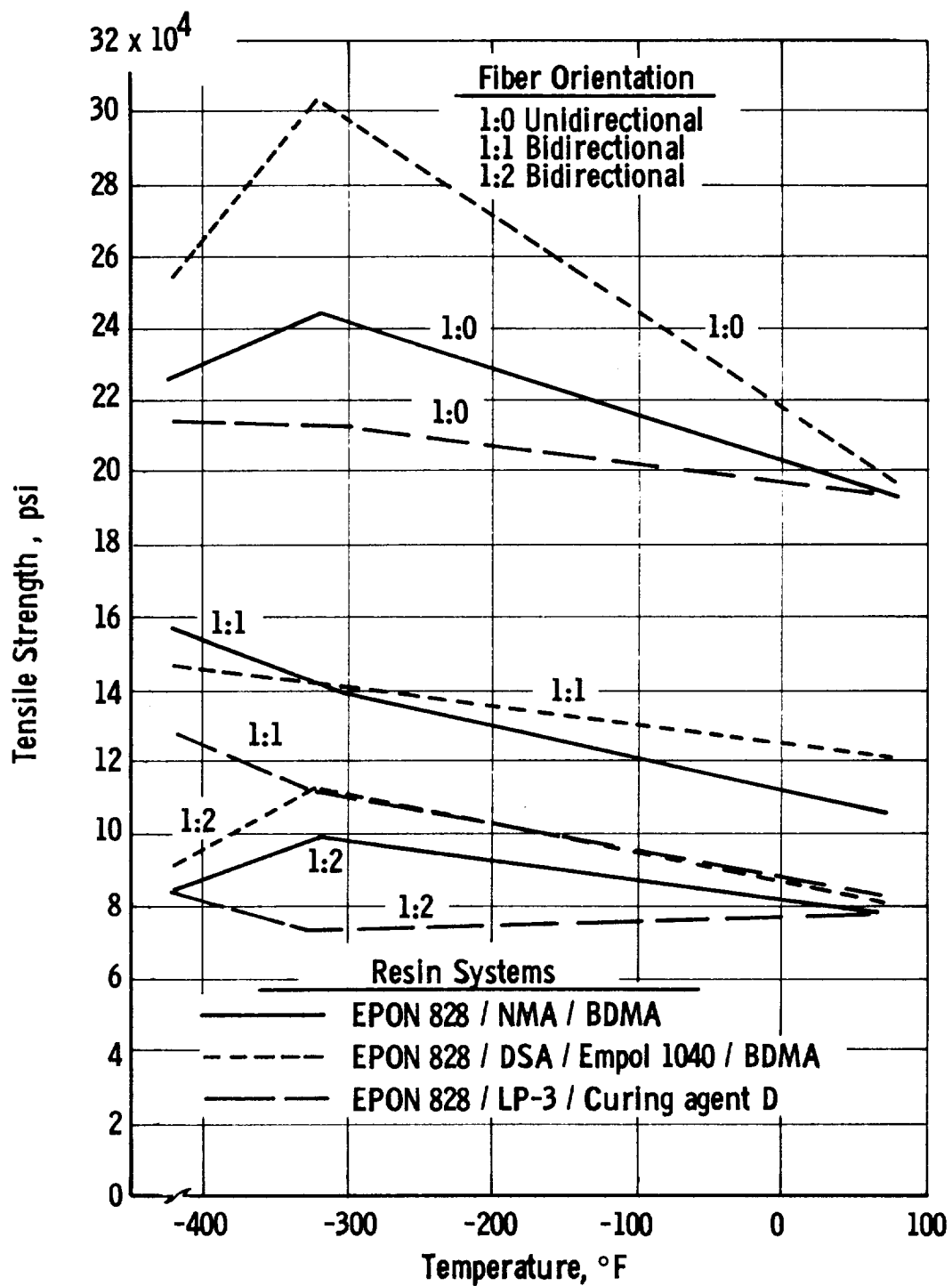


Figure 53. Resin-Finish Study, Flat Composite
(Tensile Strength)

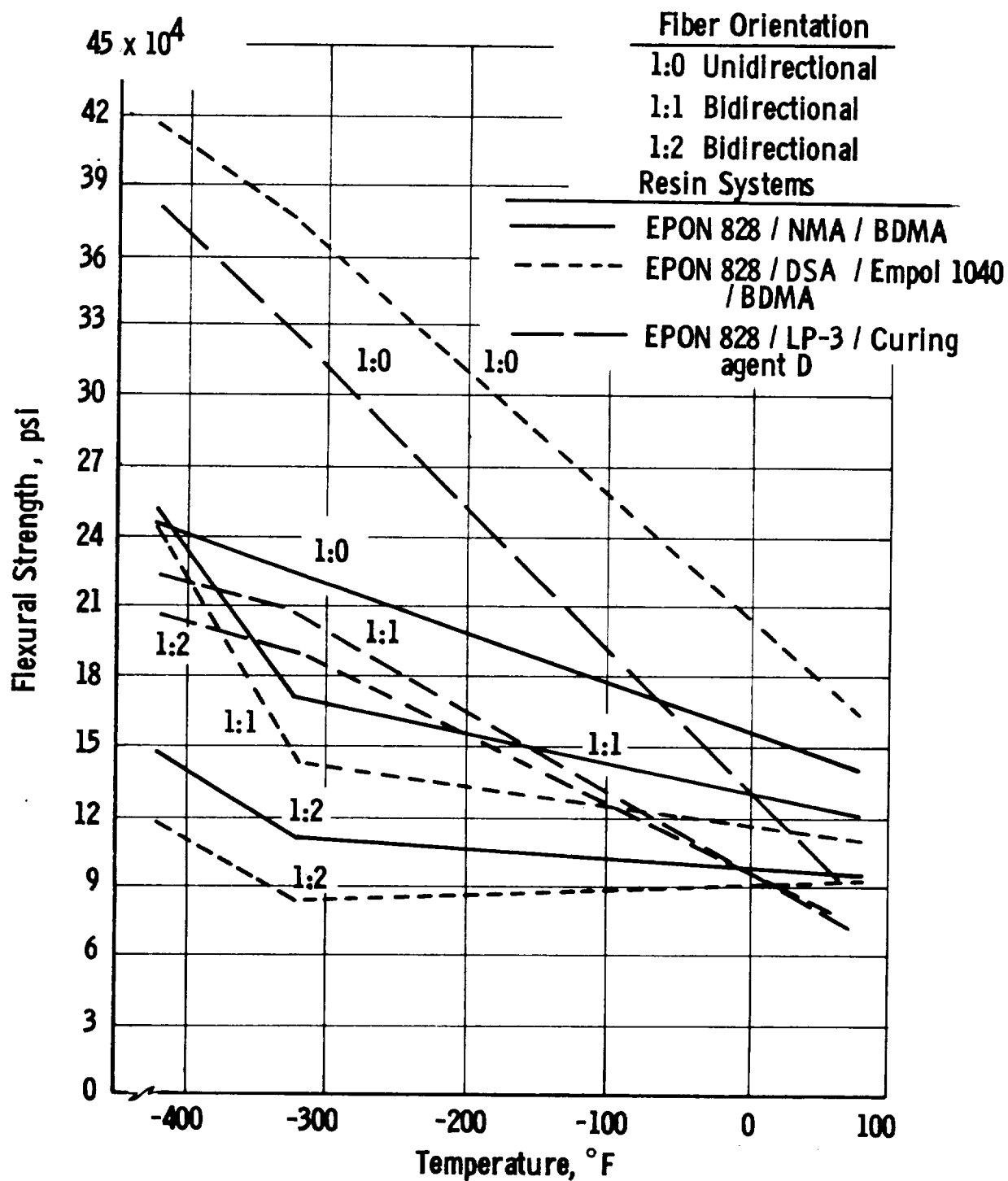


Figure 54. Resin-Finish Study, Composite Flat Coupons (Flexural Strength)

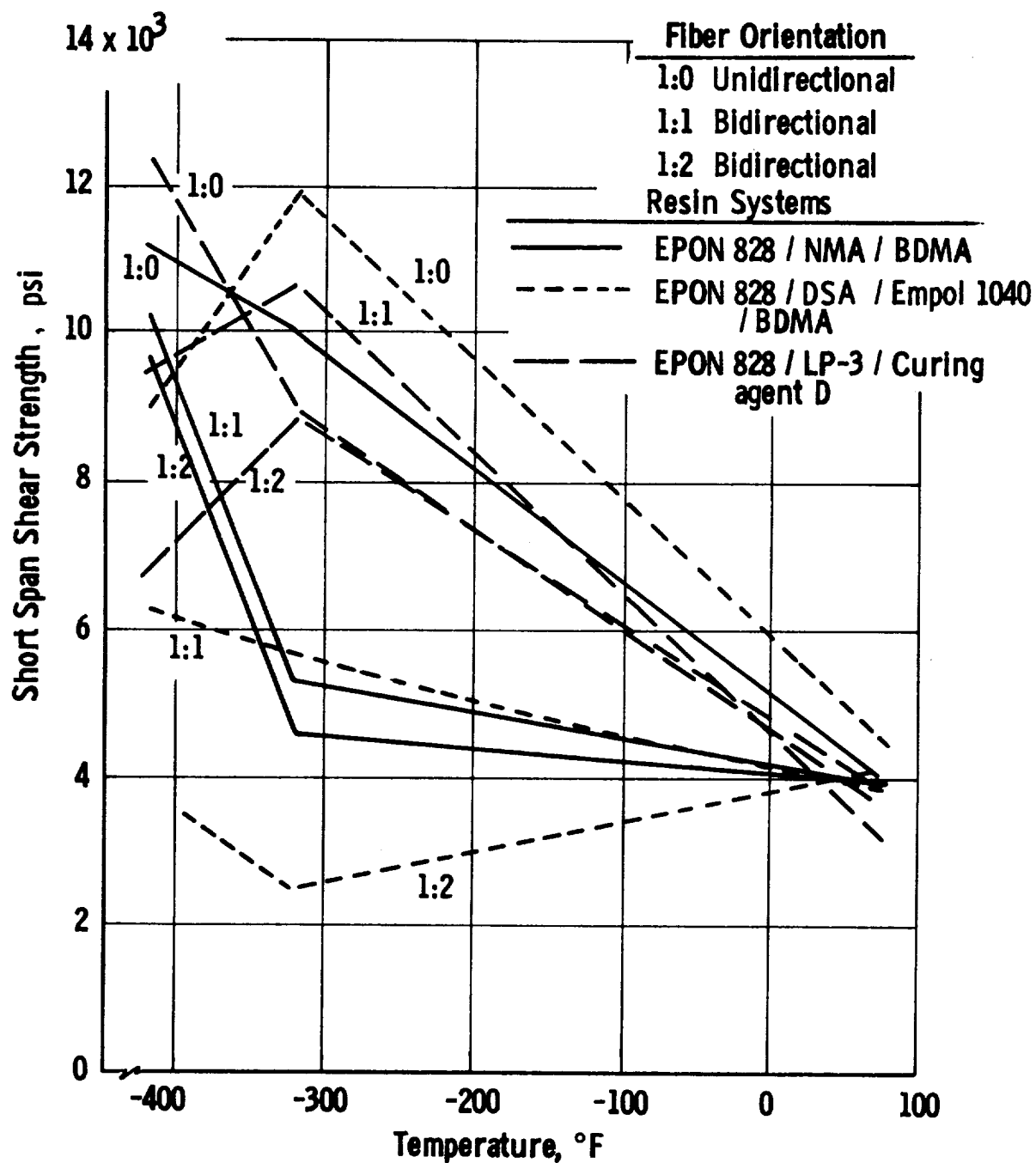


Figure 55. Resin-Finish Study, Composite Flat Coupons
(Short-Span-Shear Strength)

TABLE 26

RESIN STUDY, EFFECT OF THERMAL SHOCK ON SHORT-SPAN-SHEAR STRENGTH*

Resin System	Short-Span-Shear Strength, psi	
	Before Cycling	After Cycling
Epon 828/NMA/BDMA	4100	4120
Epon 828/Empol 1040/BDMA	4600	4380
Epon 828/LP-3/Curing Agent D	3700	3240

*

No change noted in specimens on visual examination after each of five cycles. Room-temperature tests. Values are averages for three specimens.

TABLE 27

IMPACT STRENGTH

Resin System	Izod Impact Strength, ft-lb/in. of notch					
	Unidirectional 1:0		Bidirectional 1:1		Bidirectional 1:2	
	At Room Temp	At -320°F	At Room Temp	At -320°F	At Room Temp	At -320°F
Epon 828/NMA/BDMA	84	122	49	67	38	55
Epon 828/DSA/ Empol 1040/BDMA	82	67	67	59	67	65
Epon 828/LP-3/ Curing Agent D	128	162	92	76	66	72

TABLE 28

LINEAR THERMAL CONTRACTION, BIDIRECTIONAL 1:2 COMPOSITES*

Temp °F	Linear Thermal Contraction, in./in.			
	Epon 828/NMA/ BDMA (Control)	Epon 828/DSA/ Empol 1040/BDMA	Epon 828/LP-3/ Curing Agent D	Epon 826/Epon 871/ DDI/Curalon L
+70	0	0	0	0
0	0.000191	0.000761	0.000316	0.000782
-50	0.000366	0.001305	0.000642	0.001359
-100	0.000528	0.001875	0.000888	0.001927
-150	0.000647	0.002374	0.001121	0.002466
-200	0.000757	0.002811	0.001242	0.002983
-250	0.000867	0.003219	0.001442	0.003461
-300	0.000962	0.003547	0.001537	0.003842
-350	0.001046	0.003709	0.001608	0.004111
-400	0.001131	0.004009	0.001733	0.004299
Resin, wt%	14.2	15.0	22.0	19.7

* Each value represents an average of three determinations. Calculated average coefficients of linear thermal contraction between +70 and -400°F:

System	in./in./°F
Epon 828/NMA/BDMA	2.41×10^{-6}
Epon 828/DSA/Empol 1040/BDMA	8.52
Epon 828/LP-3/Curing Agent D	3.68
Epon 826/Epon 871/DDI/Curalon L	9.13

The average coefficient of linear thermal contraction was 2.41×10^{-6} in./in./°F, the lowest value obtained; the high was 9.13×10^{-6} in./in./°F.

Although the composite tensile and flexural strengths of this resin were below those of the others, the horizontal-shear and impact properties were superior.

b. Epon 828/DSA/Empol 1040/BDMA

When this modified-epoxy system was used in conjunction with Hi-Stren coated single-end roving, it exhibited the highest overall composite tensile strength, considering filament orientation and test temperature. The test results are shown in Tables 23 to 25 and Figures 53 to 55.

The flexural-strength results for the unidirectional 1:0 laminates were the highest of all the systems at the three test temperatures. The bidirectional 1:1 flexural strength was slightly lower at room temperature and -423°F than the highest strength obtained (7 and 3%, respectively). The bidirectional 1:2 composites had low strengths.

The short-span-shear strengths were considered good for the unidirectional composites (1:0), which yielded the highest values at room temperature and -320°F. The bidirectional 1:1 properties were low in comparison with the other systems, but the bidirectional 1:2 composites had the highest value at room temperature. Erratic properties at -320 and -423°F are considered to have resulted from test difficulties.

Thermal shocking produced no visual or mechanical deterioration in short-span-shear specimens after five cycles in LH₂ (Table 26).

The impact strengths (Table 27) for the three configurations were lower at -320°F than at room temperature in each case.

The average coefficient of linear thermal contraction was 8.52×10^{-6} in./in./°F (range, 2.41 to 9.13×10^{-6} in./in./°F for the three candidate systems). Test results are shown in Table 28.

The excellent performance of this system led to its selection for further evaluation in Task IV.

c. Epon 828/LP-3/Curing Agent D

This flexibilized epoxy-resin system was used with Hi-Stren single-end roving coated with an epoxy film former and the Z-6040 coupling agent. The test results are shown in Tables 23 to 25 and Figures 53 to 55.

The composite tensile strength was the lowest at each test condition among the resins evaluated. In comparison with the highest-strength system, it was 2% lower for the unidirectional composite at room temperature, 29% lower at -320°F, and 15% lower at -423°F. The bidirectional 1:1 values were 33% lower at room temperature, 21% lower at -320°F, and 18% lower at -423°F. The bidirectional 1:2 values were 5% lower at room temperature, 35% lower at -320°F, and 8% lower at -423°F.

The unidirectional 1:0 flexural strengths were low throughout, while the bidirectional 1:1 values ranged from the highest at -320°F to the lowest at room temperature and -423°F. Among the three resin systems, the bidirectional 1:2 composites had the highest strengths at -320 and -423°F.

The short-span-shear data had considerable scatter. The unidirectional 1:0 value was the highest at -423°F, but the lowest at room temperature and -320°F (19 and 24% lower, respectively, in comparison with the highest-strength system). The bidirectional 1:1 value was the highest at -320°F, but was low at room temperature and -423°F. Bidirectional 1:2 composites also had low strength.

Thermal shocking produced no visual or mechanical deterioration in short-span-shear specimens after five cycles in LH₂ (Table 26). The impact-strength data (Table 27) were somewhat erratic for the three configurations. The bidirectional 1:1 results were lower at -320°F than at room temperature. The average coefficient of linear thermal contraction was 3.68×10^{-6} in./in./°F (range, 2.41 to 9.13 in./in./°F for all the resins). Table 28 presents the data.

This system, because of its generally poor properties, was dropped from further consideration in favor of the I-5 resin system (discussed below).

d. Improved Epoxy/Polyurethane Resins

With Aerojet funds, Resin System 4A (Epon 826/Epon 871/L-100/MOCA), developed under Contract NAS 3-6287 and tested in Task II of the present program, was modified to improve its handling characteristics (Ref. 7) by the Applied Chemistry Department of the Chemical Products Division. This department submitted the following improved epoxy/polyurethane resin formulations for evaluation by the Glass Technology Department of the Structural Products Division.

Resin System		
No.	Formulation	Parts by Weight
I-5	Epon 826/Epon 871/DDI/Curalon L	35/15/14.7/35.1
I-6	DER 332/DER 736/DDI/MOCA	35/5.9/14.7/27.6
I-9	DER 332/DER 736/DDI/Curalon L	35/5.9/14.7/35.1
I-10	Epon 826/DER 736/DDI/Curalon L	35/5.9/14.7/35.1

(cont.)

Resin System		
No.	Formulation	Parts by Weight
I-11	DER 332/Epon 871/DDI/Curalon L	35/15/14.7/35.1
I-12	DER 332/DER 732/DDI/Curalon L	35/10.5/14.7/35.1
I-13	Epon 826/DER 732/DDI/Curalon L	35/10.5/14.7/35.1
I-14	DER 332/DER 732/DDI/MOCA	35/10.5/14.7/27.6

Cast-resin panels were made for each system and were evaluated for tensile strength, tensile modulus, elongation, flexural strength, and processing characteristics. The results are summarized in Table 29.

Several resin castings were attempted with the modified epoxy/urethane systems utilizing DDI, a fatty-acid diisocyanate, and Curalon L, a diamine curing agent from U.S. Rubber Company. The original castings attempted with DER 332/DER 732/DDI/Curalon L (35/10.5/14.7/35.1 pbw) contained an excessive amount of trapped air, preventing their use as test specimens. The curing temperature appeared to influence the formation of trapped air in the cured panel. Subsequent cast-resin panels were prepared by gelling the resin at 200°F and curing the specimen at 285°F. These panels were suitable for strength determinations; they were cut into test specimens and mechanical properties were determined. The specimens with good properties were used to fabricate unidirectional glass-reinforced composites for evaluation.

Resin Systems I-5 and I-11 were selected for evaluation as the matrix resin for glass-reinforced unidirectional (1:0) composites. The test composites were fabricated from filament-wound sheets of the type used throughout Task III. Tensile, flexural, and short-span-shear tests were conducted at room temperature, -320, and -423°F. They indicated that the I-5 system was the best choice for the third resin to be evaluated in Task IV (Table 30).

This selection was based on good mechanical properties obtained from an I-5 composite containing 20 wt% of resin. This resin content is representative of that required in a filament-wound pressure vessel. The I-5 handling characteristics were found to be superior to those of Resin I-11 during the fabrication of filament-wound sheets.

TABLE 29

EVALUATION OF IMPROVED, CAST, EPOXY/POLYURETHANE RESINS
ROOM-TEMPERATURE TESTING*

No.	Resin System Formulation	Pot Life at 150°F hours	Tensile		Elongation %	Flexural Strength psi
			Strength psi	Modulus psi		
I-5	Epon 826/Epon 871/ DDI/Curalon L (35/15/14.7/35.1 pbw)	6	9,065	324,100	13.6	18,400
I-11	DER 332/Epon 871/ DDI/Curalon L (35/15/14.7/35.1 pbw)	5	8,565	326,000	12.1	14,375
I-12	DER 332/DER 732/ DDI/Curalon L (35/10.5/14.7/ 35.1 pbw)	6	8,659	-	2.26	15,600
I-13	Epon 826/DER 732/ DDI/Curalon L (35/10.5/14.7/35.1 pbw)	5	9,845	429,600	5.2	16,360

* Mechanical-property values are averages for four test specimens. Cure for all resin systems: 5 hours at 285°F.

TABLE 30

COMPOSITE TEST RESULTS, IMPROVED EPOXY/POLYURETHANE RESIN
UNIDIRECTIONAL 1:0 ORIENTATION*

No.	Resin System Formulation	Temp °F	Resin Content wt %	Specific Gravity	Tensile		Elongation %	Strength, psi	
					Strength psi	Modulus psi		Flexural	Short-Span Shear
I-5	Epon 828/Epon 87L/ DDI/Curalon L	+75	20.0	1.85	181,050	6,500,000	7.5	102,100	4,626
		-320	19.6	1.81	248,500	7,000,000	3.0	195,100	9,300
		-423	19.5	1.78	199,800	8,500,000	2.3	208,800	7,942
I-11	DER 332/Epon 87L/ DDI/Curalon L	+75	15.0	1.94	180,500	8,000,000	2.3	107,000	4,670
		-320	15.4	1.92	231,500	9,100,000	2.6	163,300	8,069
		-423	14.7	1.94	200,800	10,000,000	1.8	208,900	7,745

* Mechanical-property values are averages for three test specimens.

VI. FABRICATION AND EVALUATION OF FILAMENT-WOUND COMPOSITE (FWC) PRESSURE VESSELS (TASK IV)

The performance characteristics of the materials selected in Task III were evaluated in Task IV. Tests at +75, -320, and -423°F defined the performance levels and provided structural-property data required for comparison of the selected resins with the control system.

Six vessels were fabricated with the control resin (No. 1, composed of Epon 828/NMA/BDMA) six with Resin 2 (Epon 828/DSA/Empol 1040/BDMA), and six with Resin 3 (Epon 826/871/DDI/Curalon L). The control resin has been widely used in various filament-wound pressure-vessel structures and was therefore suitable for use as a standard of comparison.

Forty pounds of Aerojet Hi-Stren glass roving was used to wet-wind 19 vessels (the required 18 plus a spare). Pressure-vessel design, fabrication, and test results are discussed below.

A. DESIGN

The test vessel was an 8-in.-dia by 13-in.-long, closed-end cylinder. It was designed to achieve a 2.5% strain with a longitudinal-to-circumferential strain ratio of 1 at as low an internal pressure as possible with current winding processes. This type of vessel, fabricated from longitudinally and circumferentially oriented filaments wound over a 0.006-in.-thick Type 304 stainless-steel-foil liner, was selected on the basis of experience acquired in previous development efforts (Ref. 8).

A cylindrical, filament-wound, pressure vessel requires at least two longitudinal layers (produced by one rotation of the liner during the winding) and a specified number of complementing circumferential layers in the cylindrical section. It has been determined experimentally that a cured single layer of glass roving will produce an average composite thickness of approximately 0.0075, 0.0055, and 0.0035 in. for 20-end, 12-end, and single-end material, respectively. Calculations showed that the 20-end-roving structure would produce a higher burst pressure (approximately 2800 psig) than is normally associated with cryogenic tankage.

A vessel wound with the minimum number of layers of single-end roving, although exhibiting the lower burst pressure applicable to cryogenic tankage, nevertheless requires additional fabrication time and increases the winding complexity, in comparison with the use of multiple-end roving. The 12-end material was therefore selected as a logical compromise.

Dimensional coordinates of the pressure-vessel heads and other vessel characteristics were defined with the aid of a computer program that analyzed and designed the vessels. Input variables were based on design criteria presented in Table 31. Other dimensional and material parameters are summarized in Table 32. The computer program, developed by Aerojet under Contract NAS 3-6292, analyzes the filament shell by means of a netting analysis that assumes constant stresses along the path of the filament and a negligible structural contribution of the resin matrix.

TABLE 31

TEST-VESSEL DESIGN CRITERIA

Dimensions, in.	
Diameter	7.766
Length	12.250
Polar-boss diameter	2.900
Metal-liner thickness	0.006
Longitudinal-filament-wound-composite thickness	0.011
Design burst pressures, psi*	
At +75°F	1338
At -320°F	2087
At -423°F	1922

Properties	Type 304 Stainless Steel, Annealed	Glass-Filament-Wound Composite
Density, lb/in. ³	0.289	0.075
Coefficient of thermal expansion, in./in./°F at +75 to -423°F	6.760×10^{-6}	2.010×10^{-6}
Tensile-yield strength, psi	38,000	-
Derivative of yield strength with respect to temperature, psi/°F	-116.0	-
Elastic modulus, psi	29.4×10^6	13.5×10^6
Derivative of elastic modulus with respect to temperature, psi/°F	-8030	-2410
Plastic modulus, psi	800,000	-
Derivative of plastic modulus with respect to temperature, psi/°F	-0.1	-
Poisson's ratio	0.295	-
Derivative of Poisson's ratio with respect to temperature, 1/°F	0.0	-
Volume fraction of filament in composite	-	0.673
Hoop and longitudinal filaments, design allowable stress, psi		
At +75°F	-	330,000
At -320°F	-	495,000
At -423°F	-	445,000

* Determined from analysis of other design criteria.

TABLE 32

TEST-VESSEL DIMENSIONAL AND MATERIAL PARAMETERS

Cryogenic-resin specimens, Aerojet drawing number	178156-5
Standard-resin specimens, Aerojet drawing number	178156-7
Internal volume, cu in.	510.0
Dimensions, in.	
Outside diameter	7.832
Inside diameter	
Metal heads	7.766
Metal cylinder	7.754
Metal-liner thickness	0.006
Total composite cylinder-wall thickness	0.033
Hoop-wound composite	0.022
Longitudinal-wound composite	0.011
Boss-to-boss length	13.16
Cylinder length (tangent to tangent)	7.08
Forward-boss outside diameter	2.90
Aft-boss outside diameter	2.90
Liner and boss material	Type 304 stainless steel (annealed)
Glass filaments	Aerojet Hi-Stren
Roving type	12-end
Matrix resins	Epon 828/Epon 871/ DDI/Curalon L (70/30/ 29.4/70.2 pbw) Epon 828/DSA/Empol 1040/BDMA (100/115.9/ 20/1 pbw) Epon 828/MNA/BDMA (100/80/0.5 pbw)
Liner-to-composite adhesive	Epon 828/NMA/BDMA (100/80/0.5 pbw)

The filament-wound shell and the metal shell were combined in the analysis by equating strains in the longitudinal and hoop directions and by adjusting the radii of curvature of the shells to match the combined material strengths at the design pressure. The computer program also defined the filament and metal-shell stresses and strains at zero pressure and at the design pressure, the required hoop-wrap thickness for the cylindrical portion of the vessel, the filament-path length, and the weight and volume of the components and complete vessel. The test vessel was designed to fail in the heads, because earlier Aerojet studies of glass/resin interaction demonstrated that the resin has more influence on the structural integrity of the heads than on the cylindrical section.

Because the computer program contains optional input variables, the design vessel-burst pressures at the test temperature (1338 psi at +75°F, 2087 psi at -320°F, and 1922 psi at -423°F) were established on the basis of (1) a longitudinal-composite thickness of 0.011 in. for the 12-end glass-roving structure, and (2) single-cycle design-allowable strengths for the glass filaments amounting to 330,000 psi at +75°F, 495,000 psi at -320°F, and 445,000 psi at -423°F. These strengths were selected after a review of composite-property data indicated that the strength of glass laminates increases approximately 50% at -320°F and 35% at -423°F over the strengths at +75°F.

The designs prepared for the metal-foil liner and the filament-wound pressure vessel are shown in Figures 56 and 57. A vessel-weight analysis is presented in Table 33.

Appendix B summarizes the pressure-vessel design analysis and presents winding-pattern calculations for the longitudinal and circumferential filaments, as well as a structural analysis of critical metal components and high-stress areas.

B. FABRICATION

1. Metal Liner

The head sections of the welded-metal-foil liners were fabricated by hydroforming. The 0.006-in.-thick foil (Type 304 stainless steel, annealed) was cut to the required size and was placed between thin mild-steel plates. A pressure dome was lowered onto the steel plates, and hydraulic pressure was applied.

A male punch was moved upward, forcing the steel plates against a rubber diaphragm backed by hydraulic fluid under a controlled high pressure. As the punch moved upward, proper control of the pressure in the dome (or forming cavity) caused the diaphragm to form the metal to the exact configuration of the punch. The punch was then lowered, the dome was lifted, and the part was removed. Because this was a forming rather than a drawing operation, negligible part thin-out occurred. After each hydroforming operation, the mild-steel plates were discarded. Each formed metal-foil head section was stress-relieved and trimmed to the required dimensions. A center opening was cut to accommodate the boss.

INSIDE HEAD CONTINUE	X ₅	Y
	3.553	0.000
	3.571	0.232
	3.624	0.503
	3.755	0.736
	3.694	0.891
	3.688	1.007
	3.575	1.123
	3.392	1.394
	3.224	1.587
	3.020	1.780
	2.708	2.011
	2.516	2.126
	2.290	2.240
	2.021	2.353
	1.815	2.456
	1.627	2.481
	1.567	2.493
	1.502	2.493

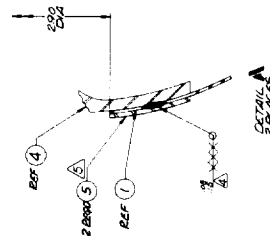
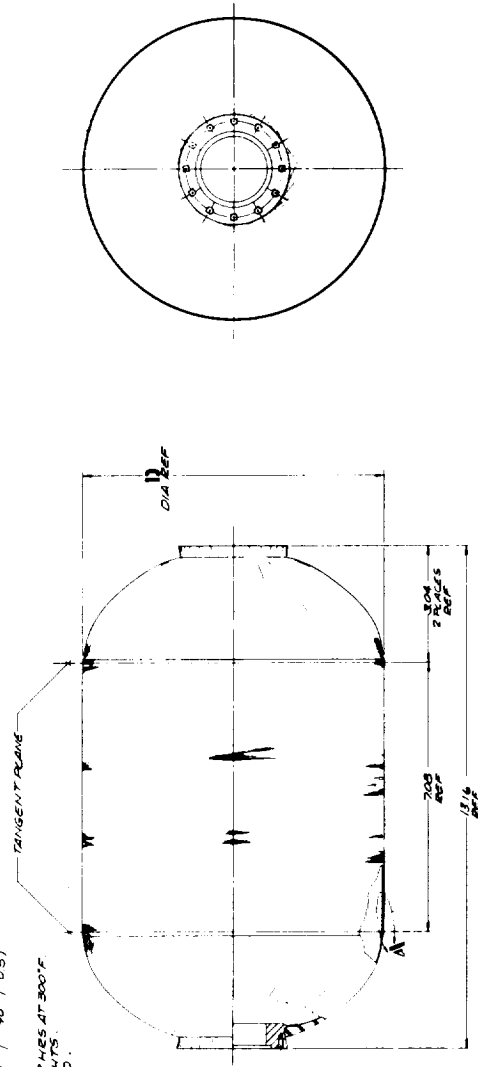
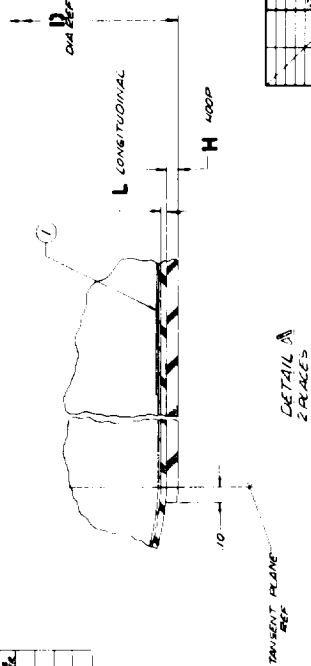
[illegible]

Figure 56. Welded Liner, 8-in.-dia Pressure Vessel

1. 2. 3. 4. 5. 6. 7. 8. 9. 10. 11. 12. 13. 14. 15. 16. 17. 18. 19. 20. 21. 22. 23. 24. 25. 26. 27. 28. 29. 30. 31. 32. 33. 34. 35. 36. 37. 38. 39. 40. 41. 42. 43. 44. 45. 46. 47. 48. 49. 50. 51. 52. 53. 54. 55. 56. 57. 58. 59. 60. 61. 62. 63. 64. 65. 66. 67. 68. 69. 70. 71. 72. 73. 74. 75. 76. 77. 78. 79. 80. 81. 82. 83. 84. 85. 86. 87. 88. 89. 90. 91. 92. 93. 94. 95. 96. 97. 98. 99. 100. 101. 102. 103. 104. 105. 106. 107. 108. 109. 110. 111. 112. 113. 114. 115. 116. 117. 118. 119. 120. 121. 122. 123. 124. 125. 126. 127. 128. 129. 130. 131. 132. 133. 134. 135. 136. 137. 138. 139. 140. 141. 142. 143. 144. 145. 146. 147. 148. 149. 150. 151. 152. 153. 154. 155. 156. 157. 158. 159. 160. 161. 162. 163. 164. 165. 166. 167. 168. 169. 170. 171. 172. 173. 174. 175. 176. 177. 178. 179. 180. 181. 182. 183. 184. 185. 186. 187. 188. 189. 190. 191. 192. 193. 194. 195. 196. 197. 198. 199. 200. 201. 202. 203. 204. 205. 206. 207. 208. 209. 210. 211. 212. 213. 214. 215. 216. 217. 218. 219. 220. 221. 222. 223. 224. 225. 226. 227. 228. 229. 230. 231. 232. 233. 234. 235. 236. 237. 238. 239. 240. 241. 242. 243. 244. 245. 246. 247. 248. 249. 250. 251. 252. 253. 254. 255. 256. 257. 258. 259. 260. 261. 262. 263. 264. 265. 266. 267. 268. 269. 270. 271. 272. 273. 274. 275. 276. 277. 278. 279. 280. 281. 282. 283. 284. 285. 286. 287. 288. 289. 290. 291. 292. 293. 294. 295. 296. 297. 298. 299. 300. 301. 302. 303. 304. 305. 306. 307. 308. 309. 310. 311. 312. 313. 314. 315. 316. 317. 318. 319. 320. 321. 322. 323. 324. 325. 326. 327. 328. 329. 330. 331. 332. 333. 334. 335. 336. 337. 338. 339. 340. 341. 342. 343. 344. 345. 346. 347. 348. 349. 350. 351. 352. 353. 354. 355. 356. 357. 358. 359. 360. 361. 362. 363. 364. 365. 366. 367. 368. 369. 370. 371. 372. 373. 374. 375. 376. 377. 378. 379. 380. 381. 382. 383. 384. 385. 386. 387. 388. 389. 390. 391. 392. 393. 394. 395. 396. 397. 398. 399. 400. 401. 402. 403. 404. 405. 406. 407. 408. 409. 410. 411. 412. 413. 414. 415. 416. 417. 418. 419. 420. 421. 422. 423. 424. 425. 426. 427. 428. 429. 430. 431. 432. 433. 434. 435. 436. 437. 438. 439. 440. 441. 442. 443. 444. 445. 446. 447. 448. 449. 450. 451. 452. 453. 454. 455. 456. 457. 458. 459. 460. 461. 462. 463. 464. 465. 466. 467. 468. 469. 470. 471. 472. 473. 474. 475. 476. 477. 478. 479. 480. 481. 482. 483. 484. 485. 486. 487. 488. 489. 490. 491. 492. 493. 494. 495. 496. 497. 498. 499. 500. 501. 502. 503. 504. 505. 506. 507. 508. 509. 510. 511. 512. 513. 514. 515. 516. 517. 518. 519. 520. 521. 522. 523. 524. 525. 526. 527. 528. 529. 530. 531. 532. 533. 534. 535. 536. 537. 538. 539. 540. 541. 542. 543. 544. 545. 546. 547. 548. 549. 550. 551. 552. 553. 554. 555. 556. 557. 558. 559. 560. 561. 562. 563. 564. 565. 566. 567. 568. 569. 570. 571. 572. 573. 574. 575. 576. 577. 578. 579. 580. 581. 582. 583. 584. 585. 586. 587. 588. 589. 590. 591. 592. 593. 594. 595. 596. 597. 598. 599. 600. 601. 602. 603. 604. 605. 606. 607. 608. 609. 610. 611. 612. 613. 614. 615. 616. 617. 618. 619. 620. 621. 622. 623. 624. 625. 626. 627. 628. 629. 630. 631. 632. 633. 634. 635. 636. 637. 638. 639. 640. 641. 642. 643. 644. 645. 646. 647. 648. 649. 650. 651. 652. 653. 654. 655. 656. 657. 658. 659. 660. 661. 662. 663. 664. 665. 666. 667. 668. 669. 670. 671. 672. 673. 674. 675. 676. 677. 678. 679. 680. 681. 682. 683. 684. 685. 686. 687. 688. 689. 690. 691. 692. 693. 694. 695. 696. 697. 698. 699. 700. 701. 702. 703. 704. 705. 706. 707. 708. 709. 710. 711. 712. 713. 714. 715. 716. 717. 718. 719. 720. 721. 722. 723. 724. 725. 726. 727. 728. 729. 730. 731. 732. 733. 734. 735. 736. 737. 738. 739. 740. 741. 742. 743. 744. 745. 746. 747. 748. 749. 750. 751. 752. 753. 754. 755. 756. 757. 758. 759. 760. 761. 762. 763. 764. 765. 766. 767. 768. 769. 770. 771. 772. 773. 774. 775. 776. 777. 778. 779. 780. 781. 782. 783. 784. 785. 786. 787. 788. 789. 790. 791. 792. 793. 794. 795. 796. 797. 798. 799. 800. 801. 802. 803. 804. 805. 806. 807. 808. 809. 810. 811. 812. 813. 814. 815. 816. 817. 818. 819. 820. 821. 822. 823. 824. 825. 826. 827. 828. 829. 830. 831. 832. 833. 834. 835. 836. 837. 838. 839. 840. 841. 842. 843. 844. 845. 846. 847. 848. 849. 850. 851. 852. 853. 854. 855. 856. 857. 858. 859. 860. 861. 862. 863. 864. 865. 866. 867. 868. 869. 870. 871. 872. 873. 874. 875. 876. 877. 878. 879. 880. 881. 882. 883. 884. 885. 886. 887. 888. 889. 890. 891. 892. 893. 894. 895. 896. 897. 898. 899. 900. 901. 902. 903. 904. 905. 906. 907. 908. 909. 910. 911. 912. 913. 914. 915. 916. 917. 918. 919. 920. 921. 922. 923. 924. 925. 926. 927. 928. 929. 930. 931. 932. 933. 934. 935. 936. 937. 938. 939. 940. 941. 942. 943. 944. 945. 946. 947. 948. 949. 950. 951. 952. 953. 954. 955. 956. 957. 958. 959. 960. 961. 962. 963. 964. 965. 966. 967. 968. 969. 970. 971. 972. 973. 974. 975. 976. 977. 978. 979. 980. 981. 982. 983. 984. 985. 986. 987. 988. 989. 990. 991. 992. 993. 994. 995. 996. 997. 998. 999. 1000.



| Assembly | D | L | H | S | T |
|----------|-------|-------|-------|-----|-----|
| -1 | 7.856 | 0.015 | 0.030 | 290 | 85 |
| -3 | 7.856 | 0.015 | 0.030 | 290 | 85 |
| -5 | 7.832 | 0.011 | 0.022 | 346 | 112 |
| -7 | 7.832 | 0.011 | 0.022 | 346 | 112 |



| Assembly | D | L | H | S | T |
|----------|-------|-------|-------|-----|-----|
| -1 | 7.856 | 0.015 | 0.030 | 290 | 85 |
| -3 | 7.856 | 0.015 | 0.030 | 290 | 85 |
| -5 | 7.832 | 0.011 | 0.022 | 346 | 112 |
| -7 | 7.832 | 0.011 | 0.022 | 346 | 112 |

Figure 57. Filament-Wound Pressure Vessel

TABLE 33

TEST-VESSEL WEIGHT ANALYSIS

| | | |
|---|------|----------|
| Cryogenic-resin specimens, Aerojet drawing number | | 178156-5 |
| Standard-resin specimens, Aerojet drawing number | | 178156-7 |
| Internal volume, cu in. | | 510.0 |
| Outside diameter, in. | | 7.832 |
| Estimated weight, lb | | 2.69 |
| Composite structure | | 0.64 |
| Forward head | 0.10 | |
| Aft head | 0.10 | |
| Cylinder section | 0.44 | |
| Metal hardware | | 2.05 |
| Metal liner | 0.56 | |
| Forward head | 0.13 | |
| Aft head | 0.13 | |
| Cylinder section | 0.30 | |
| Bosses (2) | 1.46 | |
| Doublers (2) | 0.03 | |

The cylindrical section of the liner was fabricated from 0.006-in.-thick foil that was cut to the required size, roll-formed to the desired diameter, and joined by a single-seam weld down the length. The bosses were machined from stainless steel plate (Type 304, annealed).

Resistance-roll-seam welding was used to join each boss fitting to the center opening of the head, to join the cylindrical section to each head section, and to join the cylindrical section with a longitudinal seam. The weld thus produced consists of a series of overlapping spot welds made progressively along a lapped joint with roller-type electrodes. A doubler ring was used in the boss-to-head-section joint to position the weld nugget that joined the relatively thick boss flange to the thin liner. The doubler ring, cut and formed to fit the head contour in the area where it was used, was tack-welded to position the components prior to final roll-seam welding.

Each welded-metal liner was subjected to a total of three separate pressure tests before filament winding was initiated. The first test was performed as an initial check on weld soundness and the absence of leakage across or through joints under pressure loading. In this test the tank was pressurized with Freon gas (Type F-12) to 7 ± 1 psig, and all welded areas were examined with a General Electric Model H-2 halogen leak detector (sensitivity, 60 parts per million per division).

Two additional, more sensitive, pressure tests were then performed. The first subjected the liner to a pressure load of 20 psig with nitrogen gas for 2 min to establish liner integrity under a differential pressure of 5 psi. In the second, the liner was placed in an enclosed aluminum tank, and a vacuum was created inside and outside the liner. Helium gas was used to pressurize the liner to 5 psig, while the area between the liner and aluminum tank was monitored with a Veeco Model MS-9AB leak detector (helium-mass-spectrometer technique) for traces of helium leakage. The equipment is capable of detecting one part of helium in 10^6 parts of air. The maximum acceptable leakage rate for the liners was set at 10×10^{-5} standard cu cm/sec. All metal-foil liners successfully passed each of the three tests.

2. Filament-Wound Pressure Vessel

A detailed fabrication procedure for the FWC structures was written to facilitate planning, data collection, and all phases of filament winding (see Appendix C). The leak-tested metal-foil liners were first internally coated with Kerr DMM (washout) plaster to provide a firm mandrel support for filament winding. After the cast plaster was adequately cured to remove moisture, the exterior of the metal liner was chemically cleaned to remove contaminants and to provide a suitable bonding surface. The liners were then overwrapped with resin-impregnated glass filaments. The composite structure was heated for the prescribed resin-cure schedule; after cooling to the ambient temperature, the plaster mandrel was removed with a warm, dilute, acetic-acid solution. (The vessel was then prepared for testing, at the specified temperature, in accordance with the NASA-approved test procedure.)

To prevent winding slippage, a Type 104 glass-cloth layer (0.001 in. thick) was placed over the knuckle area, and a 1-in.-wide strip of the glass cloth was also used between the weld joints and the FWC structure to minimize damage that might be produced in the glass fibers by the overlapped, seam-welded, liner edges during vessel pressurization. Fabrication data for each vessel are presented in Table 34.

C. INSTRUMENTATION

Tests were conducted in conformance with a NASA-approved plan, which defined in detail all elements of the test facility and the methods to be used for vessel instrumentation and pressurization. The facility (Figure 58) and vessels were prepared to accommodate instruments to monitor test-specimen temperature, longitudinal and circumferential strain, and internal pressure throughout the pressurization cycle. Figure 59 shows the location of test-vessel instrumentation.

Temperature was monitored with copper-constantan thermocouples in the -320°F tests. Platinum resistance thermometers were used for the -423°F tests. Two temperature measurements were made on the exterior of the vessels (90° apart circumferentially) near the center of the cylindrical section. In addition, the temperatures of the cryogenic test fluids inside and outside the vessel were measured and recorded.

Measurements of strain in the vessels were obtained with Aerojet-developed "bow-tie" extensometers. This instrument consists of a piece of beryllium-copper sheet metal in a configuration that provides two cantilever beams fitted with bonded strain gages. Metal-foil strip, approximately 0.25 in. wide, was used to link the ends of the cantilever beams to the ends of the gage. Both the extensometer and the foil strip were positioned against the test-vessel surface. For longitudinal-strain measurements, the foil was extended around the circumference and to the ends of the cylindrical section. Each extensometer was calibrated before testing (see Appendix D). Any increase or decrease in vessel girth or cylinder length produced a proportional change in strain-gage bridge output.

Hoop strain was measured at the center of the cylindrical section, and longitudinal along the cylinder at two locations 180° apart. The average of these two measurements was the axial (longitudinal) strain.

A vacuum chamber was used in the cryogenic-temperature tests. Vessels were tested at 10^{-3} mm Hg to assure attainment of the required LN_2 and LH_2 temperatures at the test-vessel walls.

The accuracy of the strain gages on the extensometers depends on the gage factor, which is extremely sensitive to cryogenic temperature variations. To provide the required extensometer accuracy, the concept of controlled-temperature strain transduction was employed: Heaters were provided to maintain the gages within the strain-gage compensation range, and a sensor was added to record the vessel-surface temperature in the vicinity of the extensometer. This sensor was used to verify that the heat input did

TABLE 34

Test-Vessel Fabrication Data

| Vessel
No. | Resin
System | Temp
°F | Metal-
Liner
Weight
g | Longitudinal Wrap | | Hoop Wrap | | Vessel
Wt, g |
|---------------|-----------------|------------|--------------------------------|-------------------|-----------------|----------------|-----------------|-----------------|
| | | | | Glass
Wt, g | No. of
Turns | Glass
Wt, g | No. of
Turns | |
| B-1 | Control | -423 | 928.7 | 135 | 370 | 110 | 447 | 1264 |
| B-2 | Control | +75 | 932.0 | 130 | 370 | 110 | 446 | 1289 |
| B-4 | 2 | +75 | 929.2 | 135 | 370 | 112 | 447 | 1271 |
| B-5 | 2 | +75 | 931.6 | 140 | 370 | 115 | 445 | 1282 |
| B-6 | Control | -423 | 934.5 | 130 | 370 | 130 | 448 | 1294 |
| B-7 | I-5 | -320 | 934.2 | 140 | 370 | 120 | 448 | 1322 |
| B-8 | Control | +75 | 927.8 | 140 | 370 | 120 | 446 | 1241 |
| B-9 | 2 | -320 | 936.9 | 140 | 370 | 125 | 445 | 1298 |
| B-10 | 2 | -423 | 930.7 | 138 | 369 | 117 | 447 | 1283 |
| B-11 | 2 | -423 | 932.5 | 134 | 371 | 118 | 444 | 1252 |
| B-12 | Control | -320 | 935.8 | 145 | 370 | 120 | 448 | 1306 |
| B-13 | I-5 | +75 | 933.8 | 135 | 370 | 130 | 446 | 1295 |
| B-14 | Control | -320 | 933.9 | 143 | 370 | 122 | 448 | 1294 |
| B-15 | I-5 | -423 | 925.7 | 135 | 370 | 115 | 449 | 1302 |
| B-16 | I-5 | -423 | 933.2 | 135 | 370 | 120 | 444 | 1284 |
| B-17 | I-5 | -320 | | | | | | |
| B-18 | I-5 | +75 | 934.2 | 140 | 370 | 115 | 446 | 1286 |
| B-19 | I-5 | -423 | 931.3 | 145 | 371 | 115 | 448 | 1317 |
| B-20 | 2 | -320 | 937.0 | 138 | 370 | 114 | 447 | 1281 |

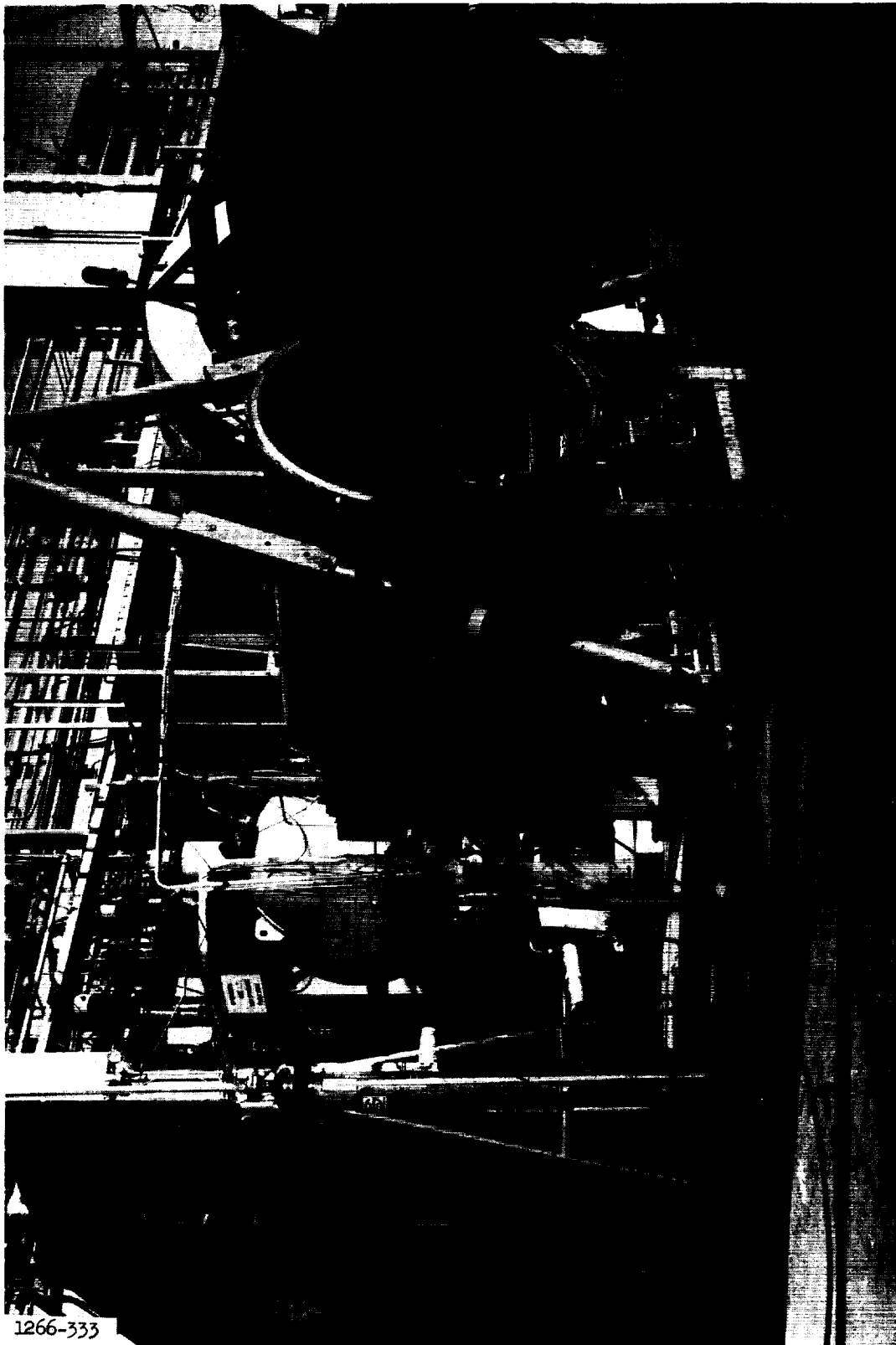


Figure 58. Test Setup, Showing Chamber for
Cryogenic Pressure-Vessel Testing

| Symbol | Measurement |
|-----------------|------------------------------------|
| P_s | Supply Pressure |
| P_c | Specimen Pressure |
| T_s | Supply Temperature |
| T_o | Specimen Temperature |
| SG_1 | Specimen Deflection, Hoop |
| $SG_{2, 3}$ | Specimen Deflections, Longitudinal |
| $TSG_{1, 2, 3}$ | Deflection Beam Temperatures |
| $TC_{1, 2}$ | Specimen (Skin) Temperatures |

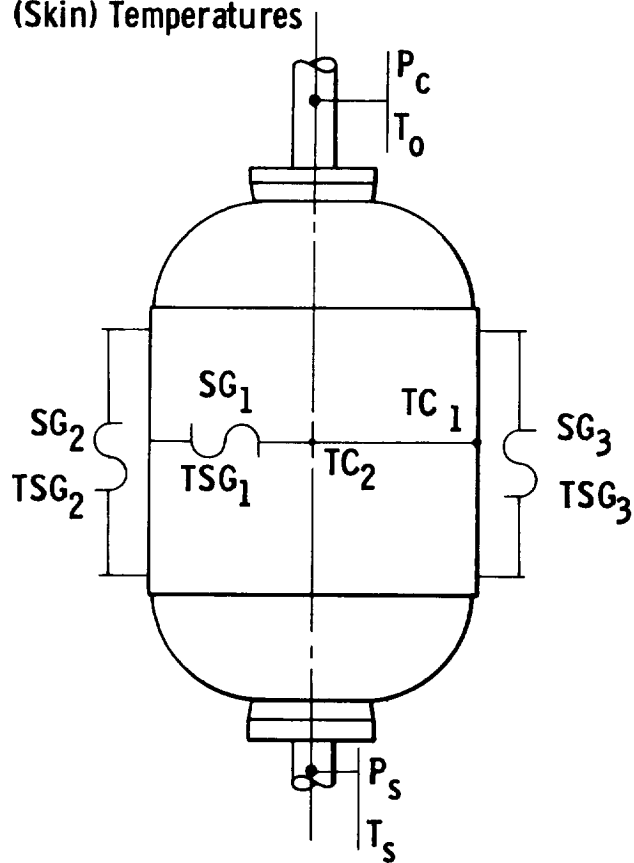


Figure 59. Location of Instruments on Test Vessels

not generate excessive temperature discontinuity in the region of the transducer. Thermal insulation was also used under the heated extensometers to reduce heat transfer to the test vessel and to reduce or eliminate the need for power application during pressurization when strain readings were taken.

As the result of the rapid temperature rise during pressurization, an extensive investigation was undertaken to determine the cause of this phenomenon. The study is covered in Appendix D.

D. TEST RESULTS

Tests were performed on 22, metal-lined, filament-wound pressure vessels. These include the 18 required vessels, a spare, and three of the original vessels that failed prematurely because of pinhole leaks and were repaired and retested. The only parameter variation was the resin/finish used as the matrix material. A system was provided to fill and test six vessels fabricated from each resin system for single-cycle burst strength, using water (+75°F), LN₂ (-320°F), or LH₂ (-423°F). Pressure was applied at a rate that produced approximately 1% strain/min in the test vessels. The pressure-vessel test assembly is shown in Figure 60.

1. Room Temperature (75°F)

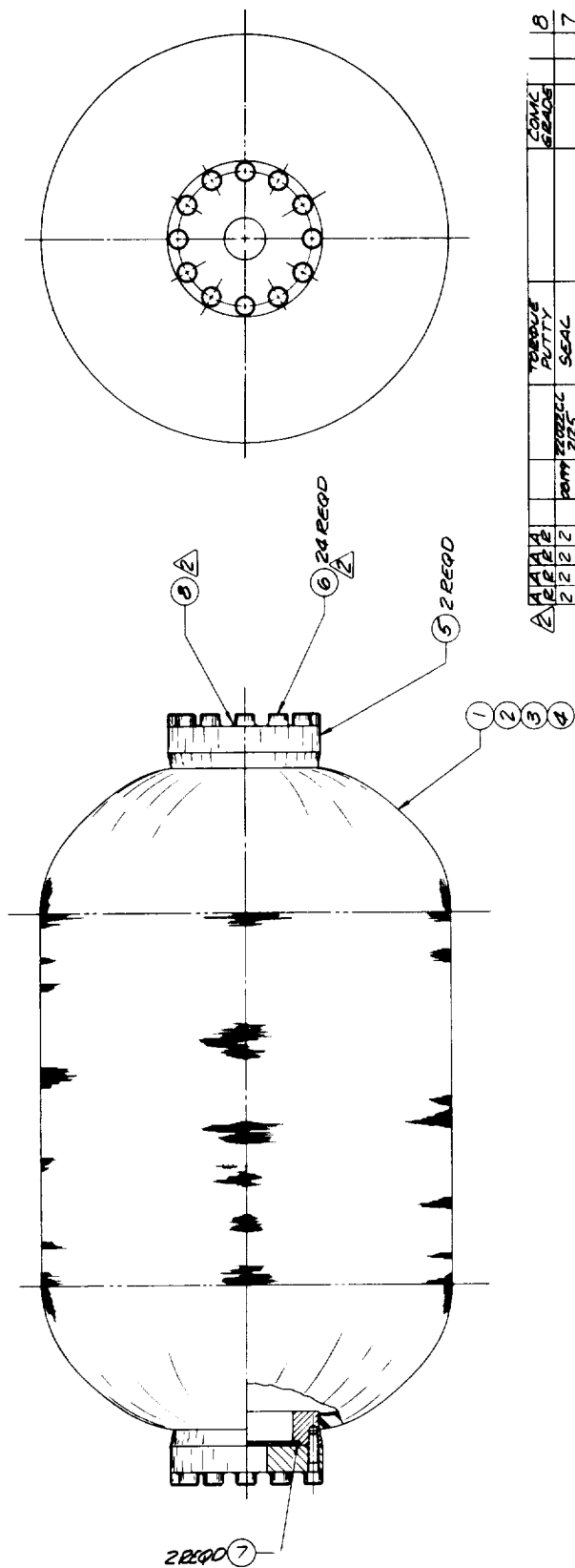
Six vessels (two with each resin system) were subjected to single-cycle burst tests by increasing the internal pressure at an average rate of 500 psig/min until failure occurred. Test data, including the vessel weight, internal volume, burst pressure, and type of failure, are summarized in Table 35. Structural-strength data, including the pressure-vessel performance factor (defined below), filament and composite stresses,* and longitudinal and hoop strains, are presented in Table 36.

The vessels burst at high filament-stress levels in the area where the detrimental effects of filament crossovers, buildup, and bridging were particularly evident. The metal bosses in the failed heads were blown free of the metal liners (see Figure 61), and the opposite head section collapsed inward during the sudden explosive reaction. The hoop filaments remained intact, indicating a degree of design redundancy.

The appearance of the burst vessels suggested simultaneous failures of the filament-wound composite and the liner, it is believed that the filaments failed first and the metal boss in the same area was then blown out.

* See Appendix E for calculation method.

NOTES:
 REMOVE ALL BURRS AND SHARP EDGES
 APPLY ITEM 8 PUTTY IN AREAS SHOWN
 AFTER TIGHTENING ITEM 6, BOLTS TO 48
 IN. LBS TORQUE.



| UNLESS OTHERWISE SPECIFIED | | DIMENSIONS ARE IN INCHES | | TOLERANCES UNLESS OTHERWISE SPECIFIED | | FINISHES UNLESS OTHERWISE SPECIFIED | | TREATMENT | | MATERIALS | | ITEM NO. | |
|----------------------------|-------------|--------------------------|-------------|---------------------------------------|-------------|-------------------------------------|-------------|-----------|-------------|-----------|-------------|----------|-------------|
| QTY | DESCRIPTION | QTY | DESCRIPTION | QTY | DESCRIPTION | QTY | DESCRIPTION | QTY | DESCRIPTION | QTY | DESCRIPTION | QTY | DESCRIPTION |
| 1 | ITEM 1 | 1 | ITEM 1 | 1 | ITEM 1 | 1 | ITEM 1 | 1 | ITEM 1 | 1 | ITEM 1 | 1 | ITEM 1 |
| 2 | ITEM 2 | 2 | ITEM 2 | 2 | ITEM 2 | 2 | ITEM 2 | 2 | ITEM 2 | 2 | ITEM 2 | 2 | ITEM 2 |
| 3 | ITEM 3 | 3 | ITEM 3 | 3 | ITEM 3 | 3 | ITEM 3 | 3 | ITEM 3 | 3 | ITEM 3 | 3 | ITEM 3 |
| 4 | ITEM 4 | 4 | ITEM 4 | 4 | ITEM 4 | 4 | ITEM 4 | 4 | ITEM 4 | 4 | ITEM 4 | 4 | ITEM 4 |
| 5 | ITEM 5 | 5 | ITEM 5 | 5 | ITEM 5 | 5 | ITEM 5 | 5 | ITEM 5 | 5 | ITEM 5 | 5 | ITEM 5 |
| 6 | ITEM 6 | 6 | ITEM 6 | 6 | ITEM 6 | 6 | ITEM 6 | 6 | ITEM 6 | 6 | ITEM 6 | 6 | ITEM 6 |
| 7 | ITEM 7 | 7 | ITEM 7 | 7 | ITEM 7 | 7 | ITEM 7 | 7 | ITEM 7 | 7 | ITEM 7 | 7 | ITEM 7 |
| 8 | ITEM 8 | 8 | ITEM 8 | 8 | ITEM 8 | 8 | ITEM 8 | 8 | ITEM 8 | 8 | ITEM 8 | 8 | ITEM 8 |

Figure 60. Pressure-Vessel Test Assembly

TABLE 35

PRESSURE-VESSEL DATA AND BURST-TEST RESULTS

| Vessel No. | Temp °F | Resin System | Weight, lb | | Internal Volume cu in. | Resin Content wt% | Burst Pressure psig | Type and Location of Failure |
|------------|---------|--------------|-------------|--------|------------------------|-------------------|---------------------|--|
| | | | Metal Liner | Vessel | | | | |
| B-2 | +75 | Control | 2.054 | 2.841 | 510.9 | 27.6 | 1425 | Longitudinal filaments in head area |
| B-8 | +75 | Control | 2.044 | 2.735 | 509.8 | 18.0 | 1461 | Liner leaks around boss |
| B-4 | +75 | 2 | 2.048 | 2.801 | 512.4 | 23.6 | 1506 | Liner leaks around boss |
| B-5 | +75 | 2 | 2.053 | 2.825 | 510.9 | 24.3 | 1551 | Same |
| B-13 | +75 | 3 | 2.058 | 2.854 | 508.7 | 27.8 | 1425 | Longitudinal filaments in head area |
| B-18 | +75 | 3 | 2.059 | 2.834 | 512.1 | 27.5 | 1380 | Same |
| B-12 | -320 | Control | 2.062 | 2.878 | 507.3 | 26.6 | 1770 | Longitudinal filaments in head area |
| B-14 | -320 | Control | 2.058 | 2.852 | 511.6 | 24.2 | 1933 | Same |
| B-9 | -320 | 2 | 2.065 | 2.860 | 510.6 | 27.4 | 1829 | Longitudinal filaments in head area |
| B-20 | -320 | 2 | 2.065 | 2.823 | 511.7 | 26.3 | 2011 | Same |
| B-7 | -320 | 3 | 2.059 | 2.914 | 510.4 | 28.3 | 1955 | Longitudinal filaments in head area |
| B-17 | -320 | 3 | 2.053 | 2.903 | - | - | - | Leaked during pressurization, no test* |
| B-1 | -423 | Control | 2.047 | 2.786 | 511.7 | 20.3 | 1850 | Longitudinal filaments in head area |
| B-6 | -423 | Control | 2.060 | 2.852 | 510.3 | 28.5 | 2030 | Ideal FWC pressure-vessel failure** |
| B-10 | -423 | 2 | 2.051 | 2.828 | 511.3 | - | - | Leaked at 440 psig around top boss |
| B-11 | -423 | 2 | 2.055 | 2.759 | 508.7 | 20.1 | 1890 | Small pinhole leak at top boss |
| B-15 | -423 | 3 | 2.040 | 2.869 | 511.0 | 28.2 | 1350 | Leaks around shoulder and boss welds |
| B-19 | -423 | 3 | 2.056 | 2.830 | 511.5 | 29.8 | 1951 | Longitudinal filaments in head area |

* Vessel B-17 was a substitute for B-16, which leaked at a very low pressure and could not be tested.

** Vessel B-10 was then internally sealed with a gel coat of Epon 828/WMA/BDMA. It was retested as Vessel B-10A with LH₂ developing a leak at 900 psig.

TABLE 36

STRUCTURAL-TEST RESULTS, PRESSURE VESSELS

| Vessel No. | Temp Of | Resin System | Performance Factor, pV/w in. | Stress, psi | | | | Lon-gitu-dinal | Hoop |
|------------|---------|--------------|------------------------------|--------------|-----------|----------|-----------|----------------|------|
| | | | | Longitudinal | | Hoop | | | |
| | | | | Filament | Composite | Filament | Composite | | |
| B-2 | +75 | Control | 0.53 x 10 ⁶ | 346,000 | 195,500 | 324,800 | 183,500 | 2.6 | 2.92 |
| B-8 | +75 | Control | 0.58 | 356,100 | 245,700 | 332,100 | 229,100 | 2.55 | 2.9 |
| B-4 | +75 | 2 | 0.57 | 367,200 | 201,000 | 343,100 | 200,700 | 2.85 | 2.60 |
| B-5 | +75 | 2 | 0.58 | 378,300 | 217,500 | 354,900 | 204,000 | 2.86 | 3.01 |
| B-13 | +75 | 3 | 0.52 | 347,600 | 192,900 | 325,500 | 180,600 | 2.76 | 2.20 |
| B-18 | +75 | 3 | 0.51 | 336,500 | 188,400 | 315,100 | 176,400 | 2.32 | 2.57 |
| B-12 | -320 | Control | 0.63 | 431,700 | 248,200 | 396,700 | 228,100 | 3.56 | 3.13 |
| B-14 | -320 | Control | 0.71 | 453,400 | 274,300 | 433,000 | 262,000 | 3.68 | 3.20 |
| B-9 | -320 | 2 | 0.67 | 429,000 | 229,500 | 412,100 | 220,500 | 3.88 | 3.13 |
| B-20 | -320 | 2 | 0.75 | 471,700 | 257,100 | 451,300 | 246,000 | 3.96 | 3.73 |
| B-7 | -320 | 3 | 0.69 | 458,600 | 250,800 | 437,900 | 239,500 | 3.91 | 3.49 |
| B-1 | -423 | Control | 0.71 | 423,600 | 278,700 | 408,800 | 269,000 | 3.12 | 3.1 |
| B-6 | -423 | Control | 0.71 | 464,800 | 257,900 | 447,600 | 248,400 | 3.78 | 3.6 |
| B-10 | -423 | 2 | - | - | - | - | - | - | - |
| B-11 | -423 | 2 | 0.74 | 432,800 | 283,500 | 420,600 | 275,500 | 3.00 | 3.43 |
| B-15* | -423 | 3 | 0.49 | 309,100 | 169,100 | 297,000 | 162,500 | 2.84 | 2.29 |
| B-19 | -423 | 3 | 0.73 | 445,400 | 236,000 | 430,300 | 228,000 | 4.17 | 3.75 |

* Vessel B-15 developed a leak during testing, and the results shown here are not included in averages reported elsewhere.

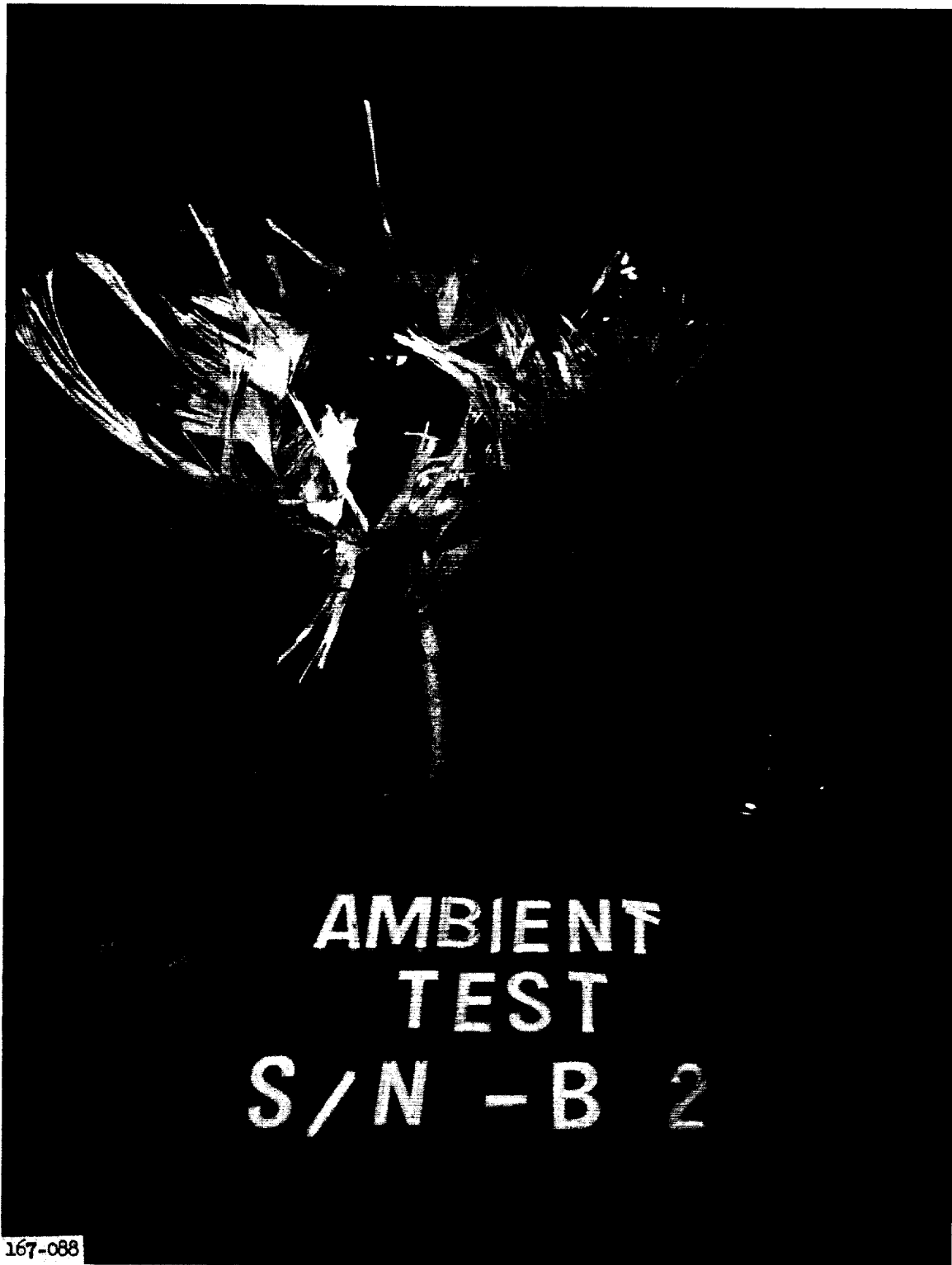


Figure 61. Vessel B-2 After Burst Test at Ambient Temperature

The pressure vessels made with the Resin 2 (Epon 828/DSA/Empol 1040/BDMA) yielded the highest burst pressures (1506 and 1551 psig). It is believed that higher strengths could have been obtained if the liners had not developed pinhole leaks (Figure 62). The performance of this system can be compared more significantly by noting in Table 36 that the average ultimate longitudinal and circumferential stresses were 372,800 and 349,000 psi, respectively. These values are higher by 5.8 and 5.9%, respectively, than those for the control resin (Epon 828/NMA/BDMA) and by 8.2 and 8.2% as compared with Resin 3 (Epon 826/Epon 871/DDI/Curalon L). The data, presented in Table 36 and Figures 63 and 64, failed to show a significant strength difference for the various resins. The average longitudinal-stress level for the six vessels (355,200 psi) was 7.1% above the minimum-allowable ultimate filament stress used for design purposes (330,000 psi).

The vessels may also be compared on the basis of the pressure-vessel performance factor, which is defined as the product of burst pressure and internal volume divided by vessel weight (pV/W).^{*} As shown in Table 36, the performance factors were 0.53 and 0.58×10^6 in. for the Resin 1 (control) vessels, 0.57 and 0.58×10^6 in. for Resin 2, and 0.52 and 0.51×10^6 in. for Resin 3. This similarity in vessel efficiency supported the conclusion that there was no significant difference in the room-temperature performance of the three resin systems.

Table 35 gives resin contents based on three samples from each vessel. The average contents were 22.8 wt% for Resin 1, 23.9 wt% for Resin 2, and 27.6 wt% for Resin 3.

Composite strengths, calculated from a knowledge of filament strengths and resin contents, are also presented in Table 36. The highest stresses attained in the cylindrical section for the longitudinal- and hoop-wound composites (245,700 and 229,100 psi, respectively) were exhibited by Vessel B-8. The hoop-composite stresses at failure were approximately 9.4% lower than the longitudinal because of the redundant design used to force the failure in the longitudinal fibers.

Longitudinal and hoop strains are shown in Figures 65 and 66 as a function of internal pressure. The maximum longitudinal strains, exhibited by Vessels B-2, B-5, and B-13, were 0.0260, 0.0286, and 0.0276 in./in.; the maximum hoop strains, for the same vessels, were 0.0292, 0.0301, and 0.0220 in./in.

The initial vessel pressurization to approximately 200 psig produced small strains as compared with those produced by the same pressure increment at higher total pressures. This condition is particularly apparent for the pressure/longitudinal-strain curves and was predicted by the design analysis. In Figure 67, the predicted pressure-strain relationship is compared with data obtained from the testing of Vessel B-4. As pressure was

^{*}In this calculation the weight of the metal bosses is not included because of their structural redundancy in the design.



Figure 62. Vessel B-5, Showing Leak Area

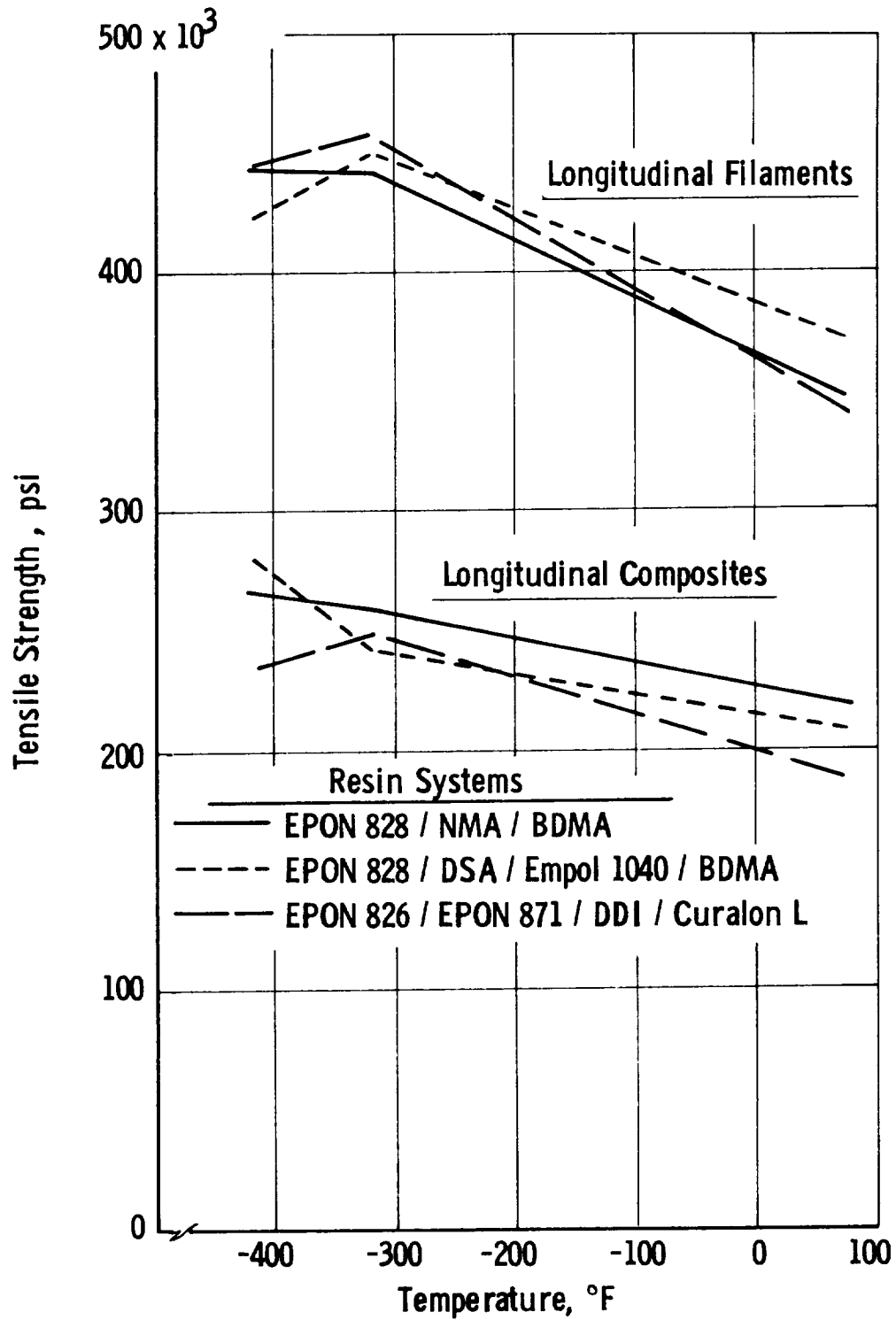


Figure 63. Longitudinal Tensile Strength
Pressure Vessels with Hi-stren Glass

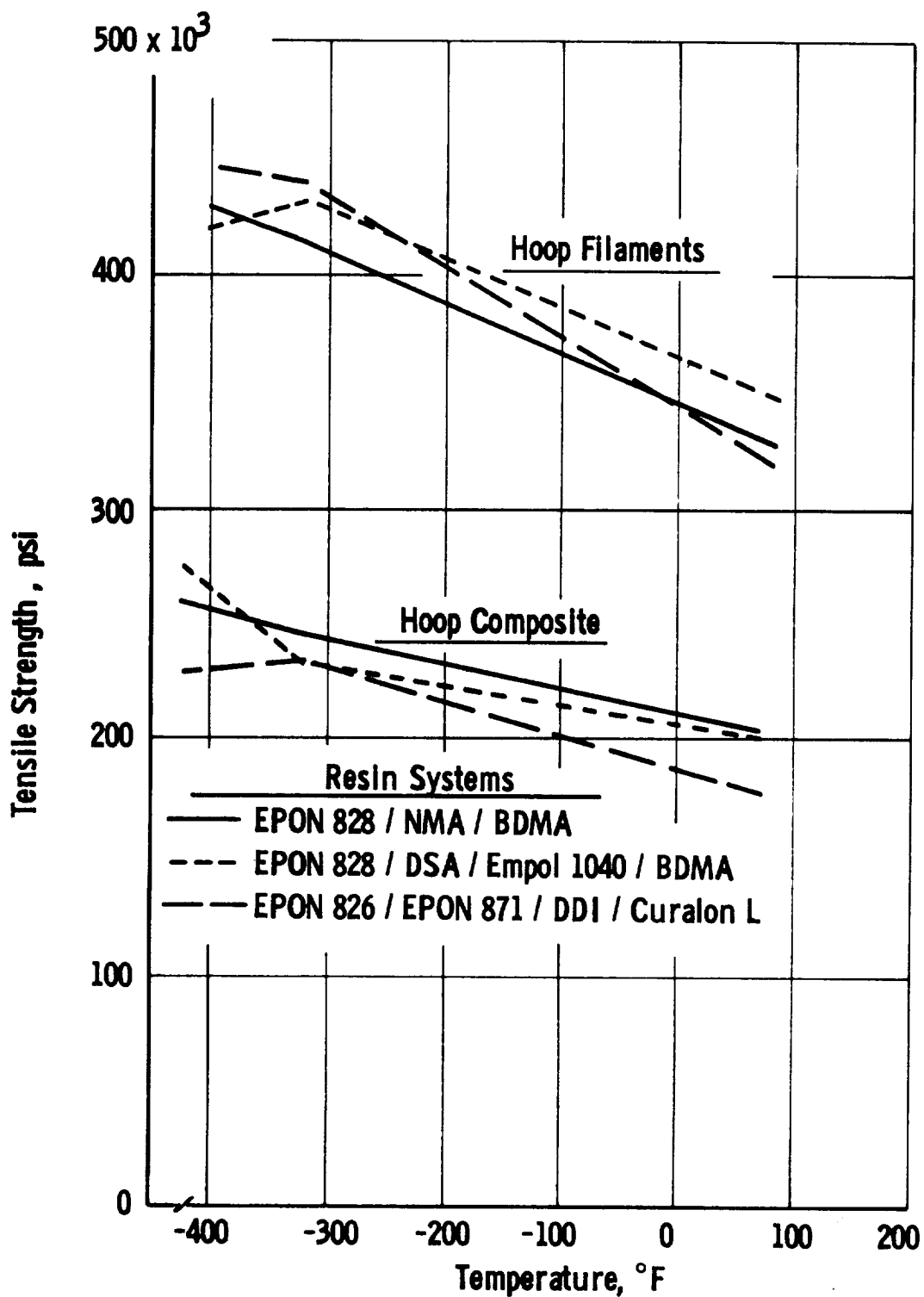


Figure 64. Hoop Tensile Strength, Pressure Vessels with Hi-Stren Glass

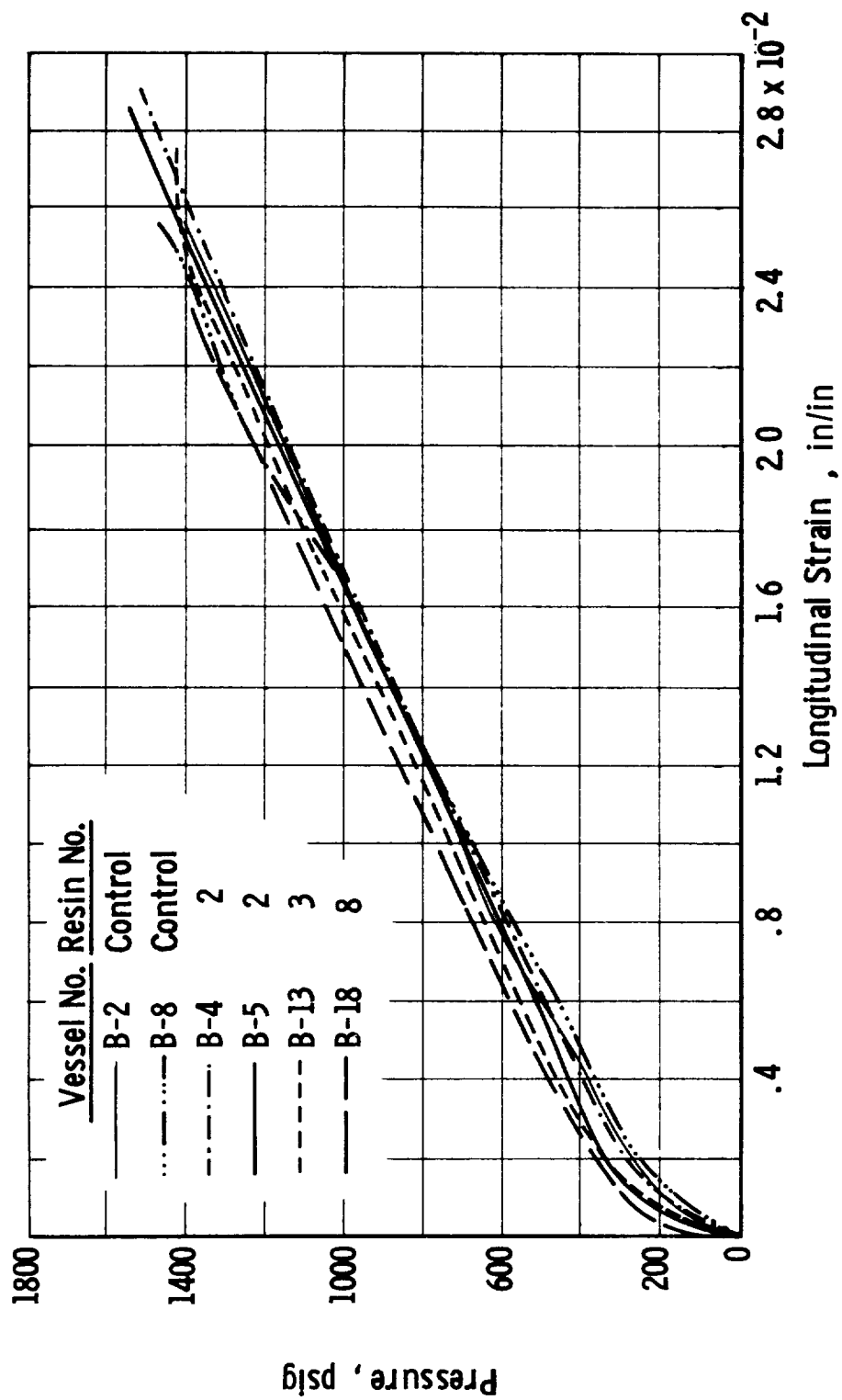


Figure 65. Pressure vs Longitudinal Strain
Pressure Vessels at +75°F

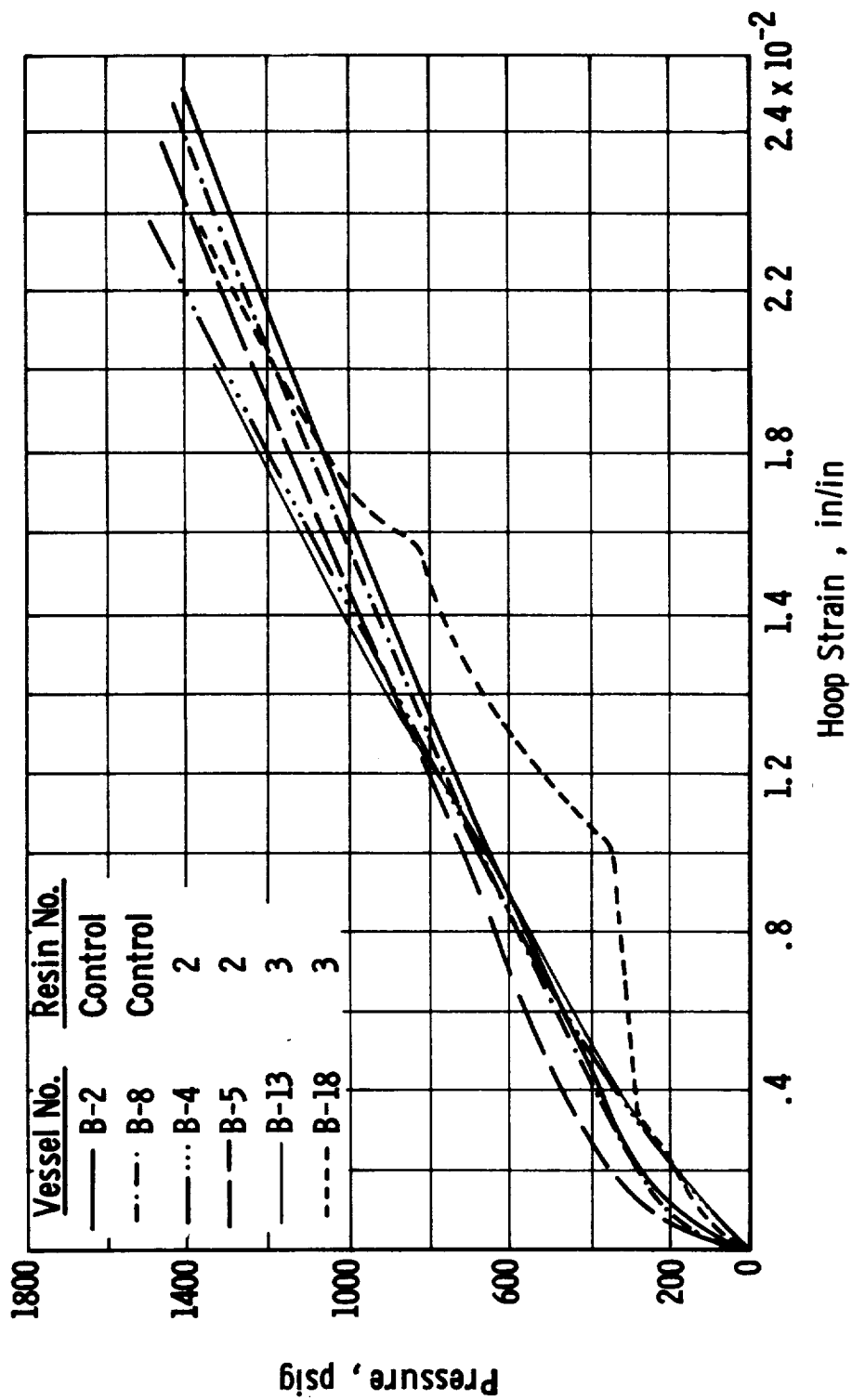


Figure 66. Pressure vs Hoop Strain, Pressure Vessels at +75°F

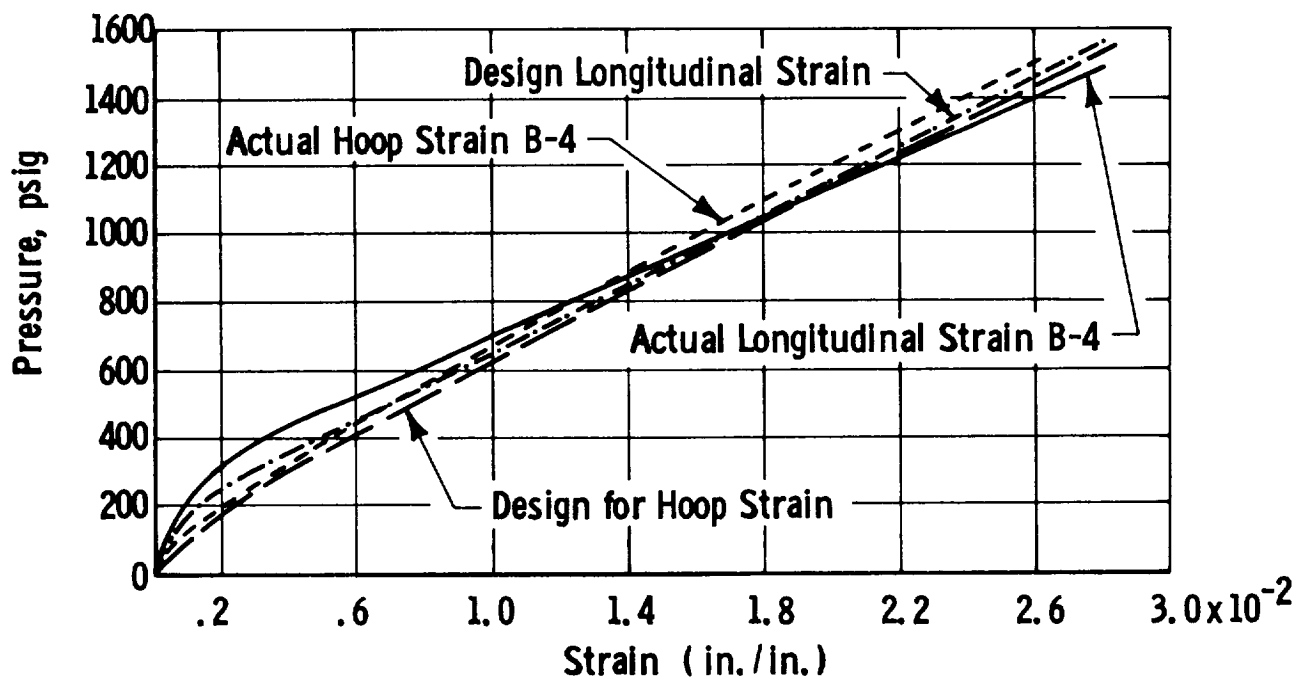


Figure 67. Design vs Actual Strain, Pressure Vessels at +75°F

increased from zero to approximately 200 psig, the cylinder strains produced in the hoop and longitudinal directions were small because of the load-carrying capability of the metal-foil liner. The yield point of the liner was exceeded at roughly 200 psig for the longitudinal direction and 100 psig for the hoop. At higher pressures, the liner deformed plastically and the increasing pressure load was carried almost entirely by the lower-modulus filament-wound composite, resulting in a greater strain-to-pressure ratio.

Data obtained in previous programs (Appendix B of Ref. 7) indicated that resin crazing is initiated at approximately 10% of the maximum pressure attained. Therefore, in addition to the load-carrying capability of the liner, the initial (precrazing) strength and toughness of the matrix may also contribute to the smaller strain produced at the start of pressurization.

2. LN₂ Temperature (-320°F)

Six pressure vessels (two with each resin system) were subjected to single-cycle burst tests at -320°F by increasing the internal pressure at an average rate of 700 psig/min until failure occurred. Burst-test data are presented in Table 35, and structural-strength data in Table 36. Longitudinal and hoop strains are plotted as a function of internal pressure in Figures 68 and 69.

Figure 70 shows a typical pressure vessel assembled for cryogenic testing with bow-tie extensometers in position. The vessels were mounted in a vacuum chamber provided with taps for deflection-measurement-instrument leads, thermocouples, and pressurization lines. The specimens were tested at 10^{-3} mm Hg in order to minimize heat input and assure attainment of the required cryogenic temperature. All equipment was operated remotely from a building that housed controls and instrumentation. The test vessels were filled with glass marbles to minimize the quantity of cryogen expended during a burst. The coolant flowed through the system and vessel assembly from a liquid-cryogen-transfer trailer until a liquid condition was obtained. The pressurizing gas was then liquefied and was supplied to the specimen through a heat exchanger.

The liquid-cryogen heat exchanger was acquired during this program and was installed to provide economical cryogenic testing. It employed high-pressure gaseous nitrogen for the LN₂ tests (or gaseous hydrogen for the LH₂ tests) supplied from an existing 20-cu-ft storage tank. The gas was passed through a series of coils surrounded by the low-pressure cryogen from the trailer. Operating on an extremely large supply reservoir, the heat exchanger was able to achieve and maintain a low cryogenic temperature in the test specimen and to assure a constant supply of cryogen during the test. Because difficulties were encountered in maintaining the desired low temperatures at the burst, comprehensive studies were made and are reported in Appendixes D and F.

Of the vessels tested at -320°F, one (Vessel B-16) failed prematurely when pinhole leaks developed in the liner; post-test examination

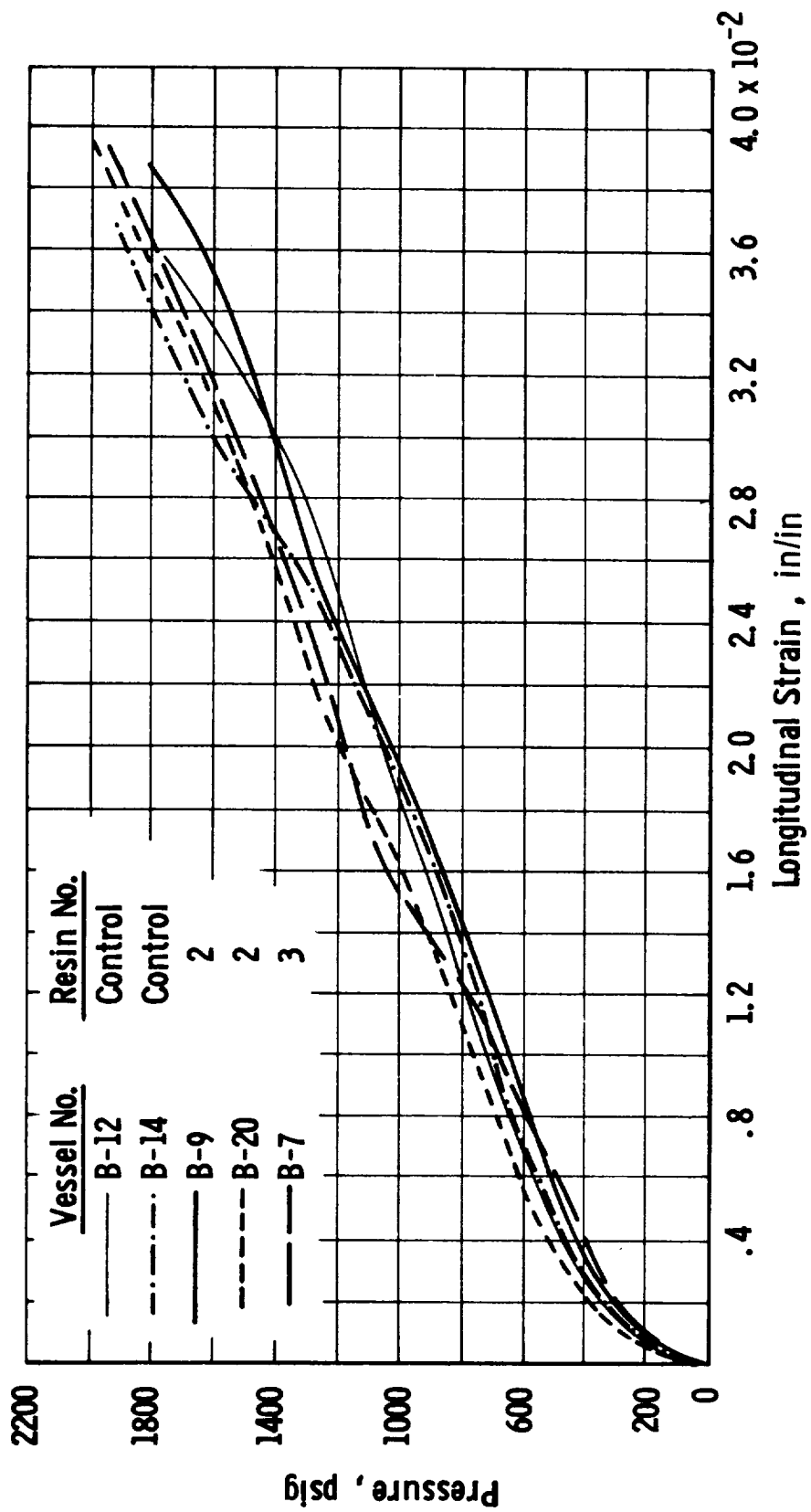


Figure 68. Pressure vs Longitudinal Strain, Pressure Vessels at -320°F

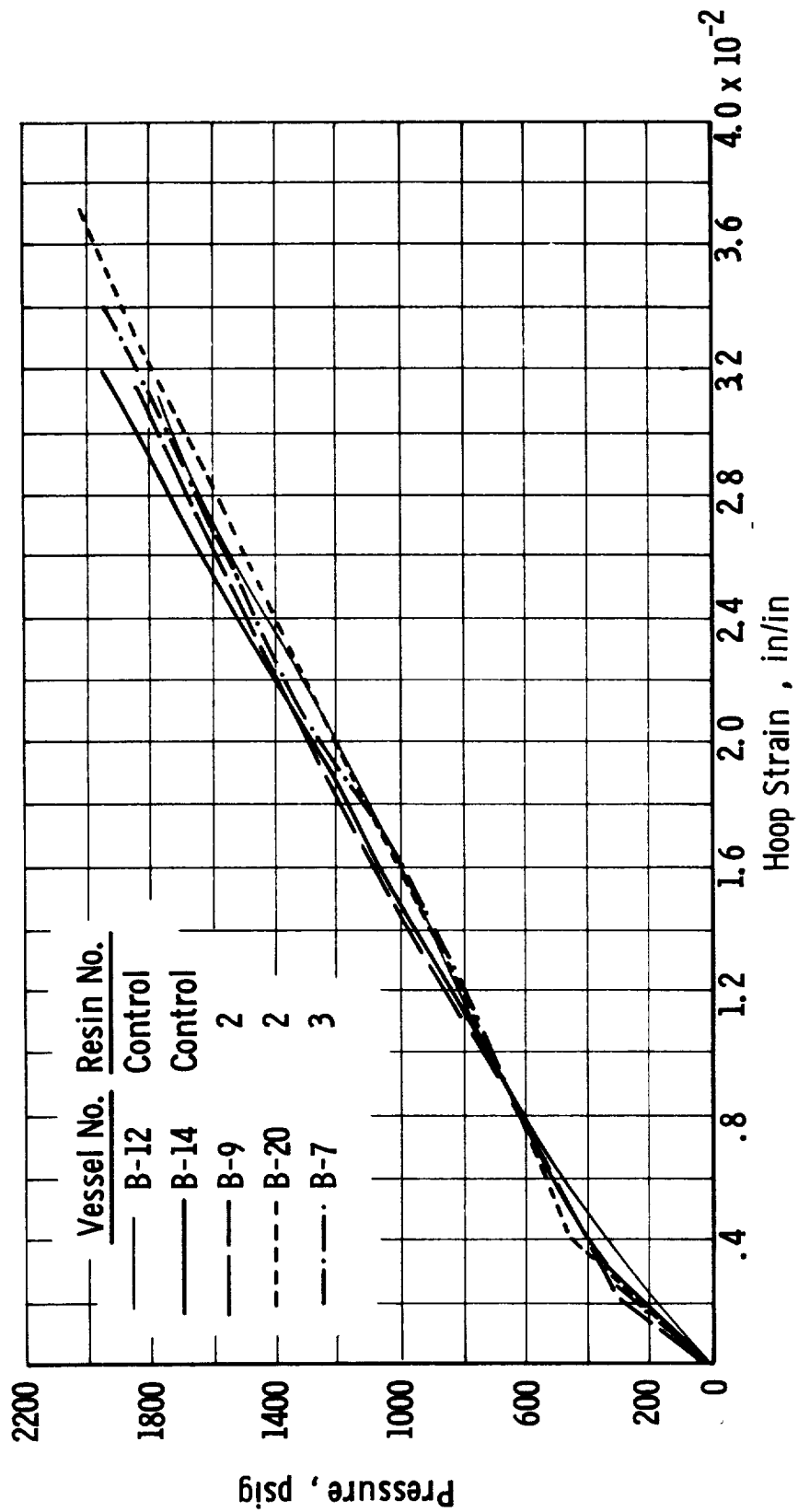


Figure 69. Pressure vs Hoop Strain, Pressure Vessels at -320°F

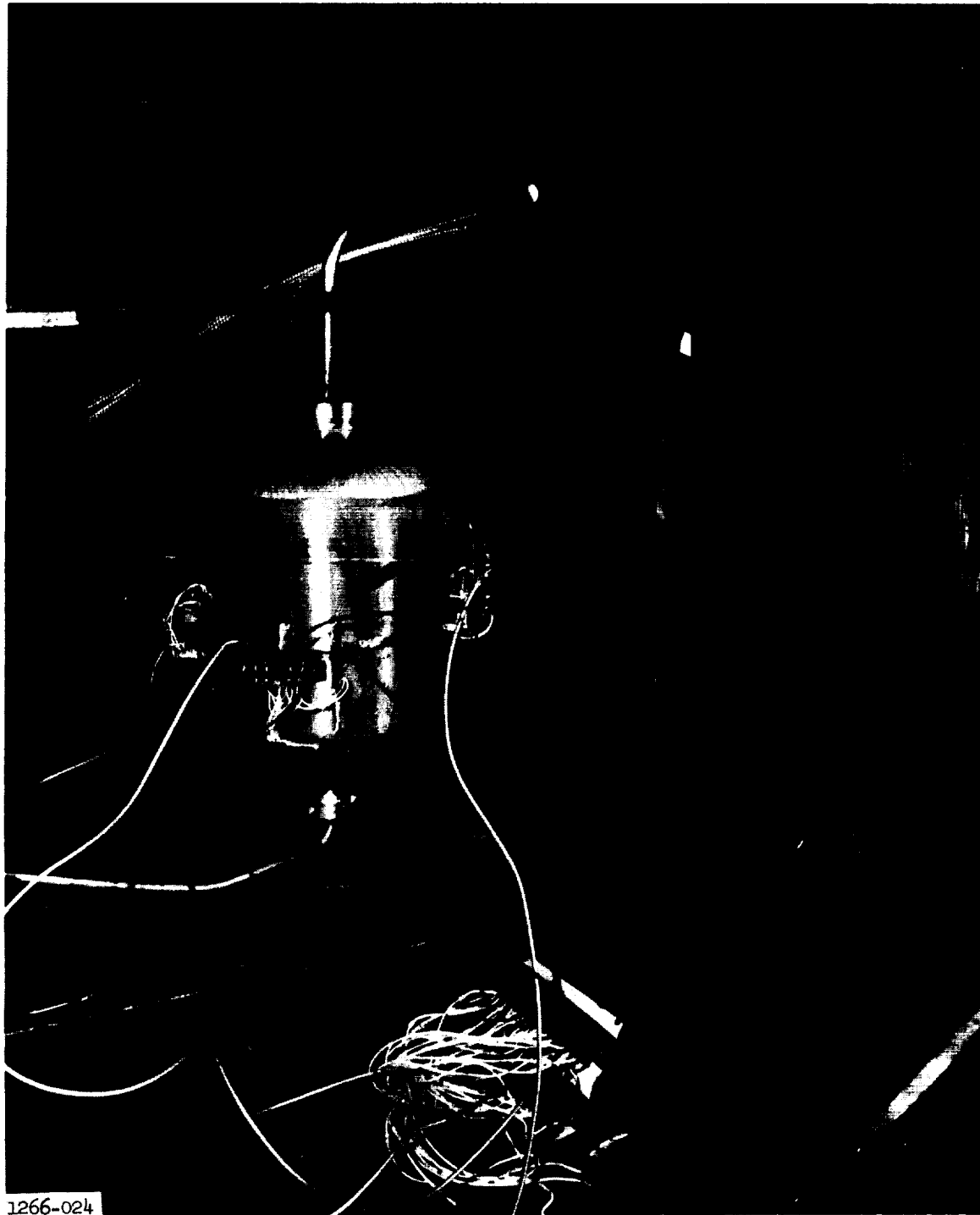


Figure 70. Pressure Vessel Assembled for Cryogenic Testing

revealed, however, that failure was not accompanied by glass-filament damage. The test-facility safety provisions were such that an increase in vacuum-chamber pressure to 5 psia (due to leakage or pressurization-line malfunction) would energize an automatic system that vented the specimen and vacuum chamber and closed the specimen pressure valve. The partial decay of chamber vacuum warned the test operator of vessel leakage and prompted him to increase the pressurization rate to overcome the leak. Unfortunately, the vacuum decay came too suddenly with this vessel to permit a sufficient increase in pressurization rate to achieve a burst. Examination of the interior of Vessel B-16 disclosed several pinholes in the cylinder near the longitudinal-seam-weld section. A spare liner was filament-wound and tested at -320°F . This vessel (B-17) also developed pinhole leaks in one head adjacent to the boss-to-head seam weld.

The other five vessels (B-7, B-9, B-12, B-14, and B-20) failed in the longitudinal filaments of the head area, as shown in Figure 71.

The Vessel B-20 test results are considered highly satisfactory in that the actual burst pressure of 2011 psig approached the predicted design value of 2087 psig. The highest longitudinal-filament stress (471,700 psi), as well as the maximum longitudinal and hoop strains (0.0396 and 0.0373 in./in., respectively), were obtained. The longitudinal-filament stress was 95% of the predicted level of 495,000 psi* and 30% above the average of the actual room-temperature longitudinal-filament stresses (355,200 psi).

As in the room-temperature tests, the strains occurring during initial vessel pressurization were small compared with those developed at higher pressures, due to the load-carrying capability of the liner. The resin contents of all the systems were consistent (see Table 35) and at a satisfactory level (24 and 28 wt%).

Post-test examination of the liner interiors revealed buckling in various areas; the higher the burst pressure attained, the more severe the liner buckling. The cause of the poor structural bond between the liner and composite is unknown; however, lack of an adhesive bond would have had little effect, if any, on the burst pressures attained in single-cycle pressurization.

3. LH₂ Temperature (-423°F)

Six pressure vessels (two with each resin system) were subjected to single-cycle burst tests at -423°F by increasing the internal pressure at an average rate of 700 psig/min until failure occurred. Burst-test data are presented in Table 35, and structural-strength data in Table 36. Longitudinal and hoop strains are plotted as a function of internal pressure in Figures 72 and 73.

*150% of the room-temperature design-allowable strength of 330,000 psi.

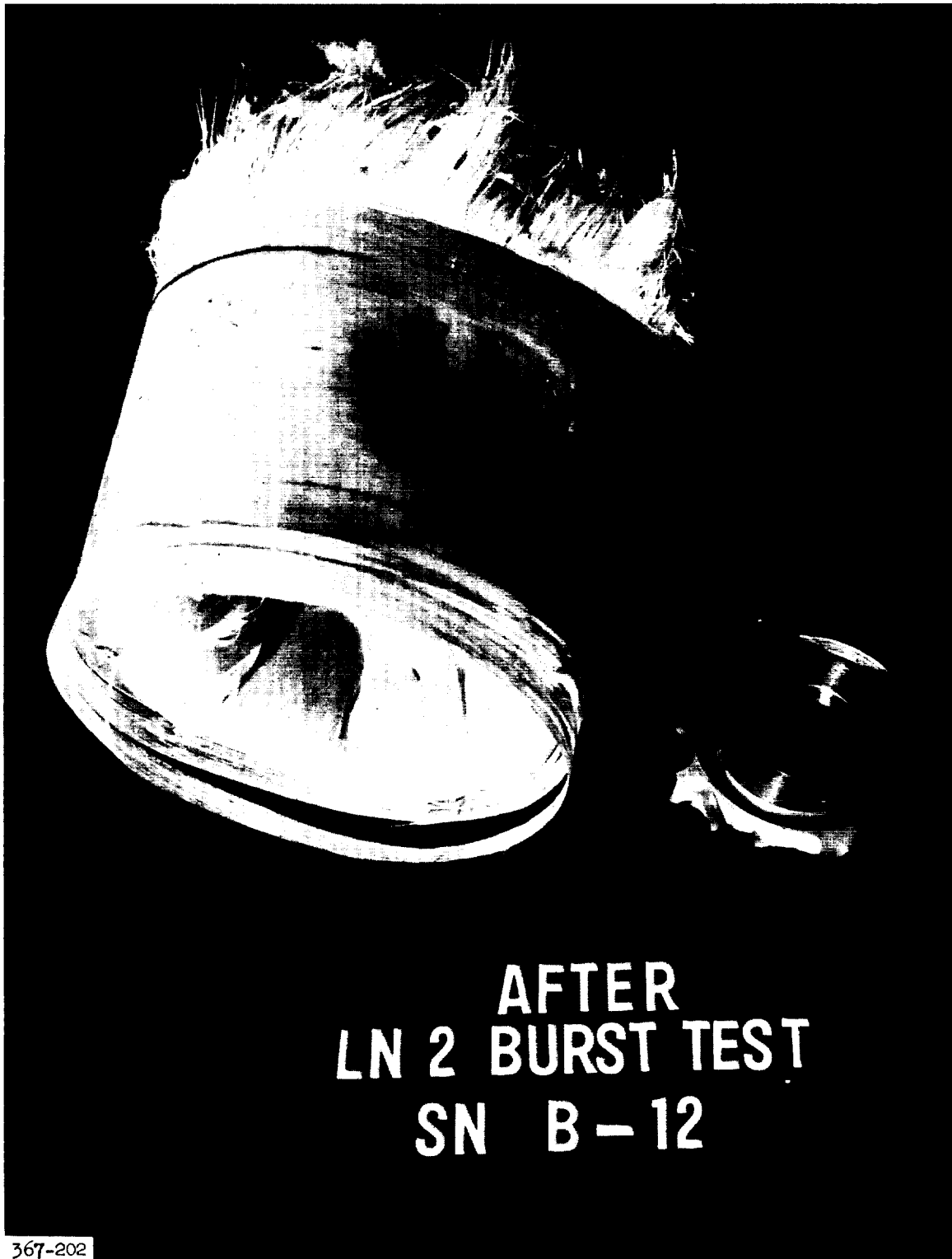


Figure 71. Pressure Vessel After Burst Test at -320°F

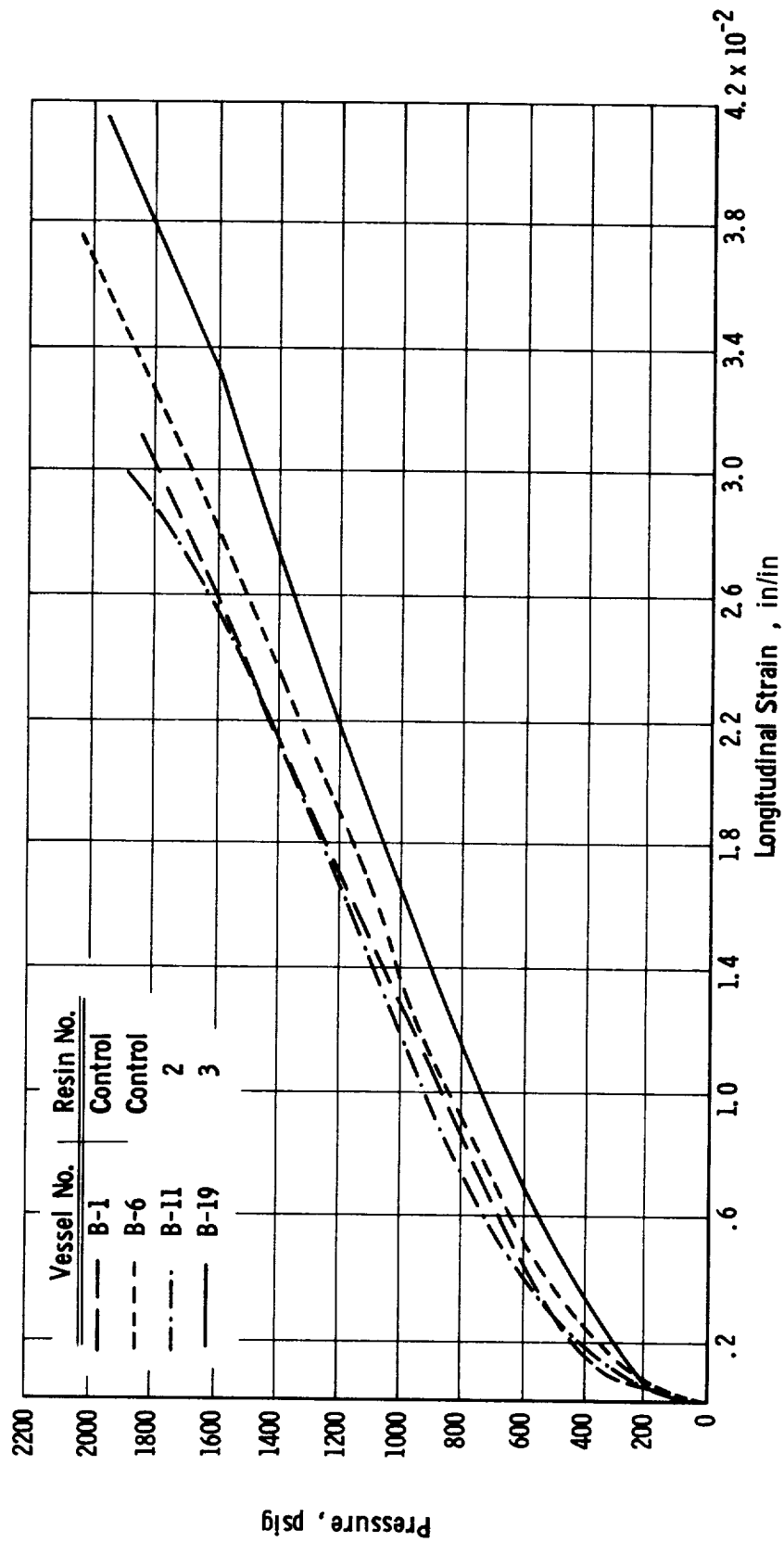


Figure 72. Pressure vs Longitudinal Strain, Pressure Vessels at -423°F

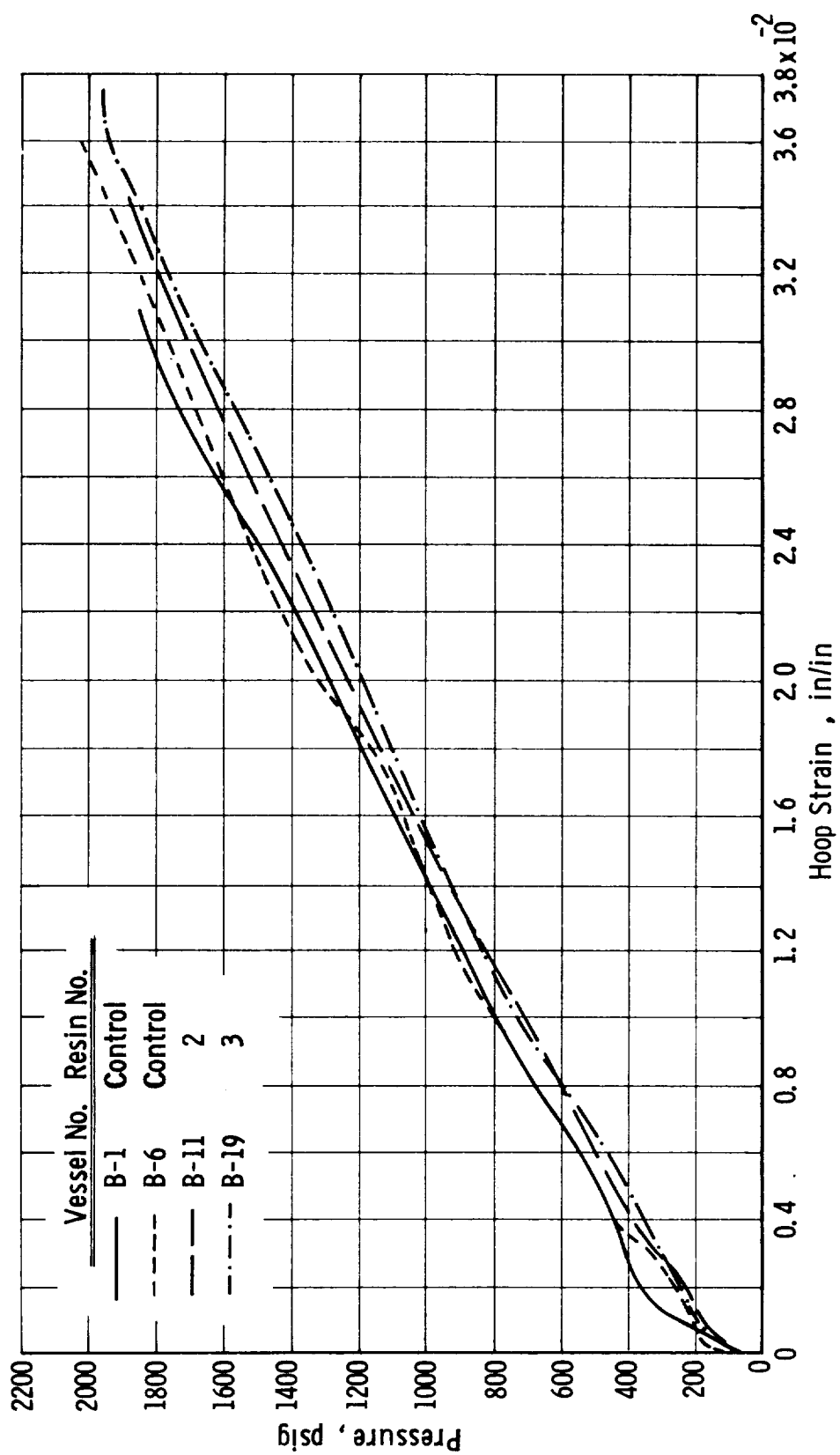


Figure 73. Pressure vs Hoop Strain, Pressure Vessels at -423°F

In three vessels, failure originated in the longitudinal filaments around the boss area. A typical failure is illustrated in Figure 74. A flower-type burst resulted when the filaments attained their maximum load-carrying capabilities. The metal boss in the burst head section was separated from the metal liner, and the opposite head collapsed inward. The hoop filaments did not fail but were damaged in the sudden explosive reaction. Pinhole leaks developed in the other three vessels. In Vessels B-10 and B-15, the leakage was so severe that pressures of only 440 and 1350 psig, respectively, were obtained. Vessel B-11 reached 1890 psig before leakage forced discontinuation of the test.

Post-test examination of the interiors revealed that liner wrinkling was more severe in these vessels than in those tested at room temperature, probably because of the higher pressures and strains reached at the burst.

Vessel B-6 (Resin 1) - with an ultimate longitudinal-filament stress of 464,800 psi, a hoop-filament stress of 447,600 psi, maximum longitudinal and hoop strains of 3.78 and 3.60%, and a performance factor of 0.71×10^6 in. - exhibited the highest structural performance of any of the vessels tested at -423°F .

As shown in Figures 72 and 73, the strains produced during initial vessel pressurization were small in comparison with those produced later by an equivalent pressure increment. As noted previously, this behavior was predicted by the design analysis and was due to the load-carrying capability of the high-modulus metal-foil liner. After the yield point of the liner was exceeded, the liner deformed plastically and the increasing loads were supported by the low-modulus composite structure. This change in the pressure-to-strain ratio occurred at relatively higher pressures because of the higher yield point and higher tensile modulus of the liner at cryogenic temperatures.

Temperatures were recorded continuously; they are presented in Table 37 for the start and end of each cryogenic test. Whereas the initial skin temperatures (TC_1 and TC_2) in the LH_2 tests were fairly close to -423°F , the analogous temperatures in the LN_2 tests were considerably higher than -320°F . To some extent, such temperature differentials are to be expected. When they occur at the start of pressurization, they may be due to (a) radiative heat transfer from the chamber wall to the pressure-vessel wall, (b) a poor bond between the sensor connection and the outer wall of the vessel, or (c) a lack of temperature equilibrium across the vessel wall.

Temperature differentials at or near the burst may have the same causes, or these additional ones: (a) During pressurization to burst, the vacuum pumps were turned off at about 700 psi, and a decay in test-chamber vacuum as pressure was further increased caused a rise in temperature increase at the outer wall of the vessel through convective heat transfer, or (b) during pressurization, the vessels were warmed by the work done on both the cryogen and the vessel (conductive heat transfer), in addition to warming from external radiative and convective heat transfer.



Figure 74. Pressure Vessel After Burst Test at -423°F

TABLE 37

TEST-TEMPERATURE MEASUREMENTS
CRYOGENIC PRESSURE VESSELS

| Vessel
No. | Resin
System | Monitor
Condition | Temperature, °F* | | | |
|---------------|-----------------|----------------------|------------------|----------------|-----------------|-----------------|
| | | | T _s | T _o | TC ₁ | TC ₂ |
| B-12 | Control | Start | -310 | -308 | -295 | -295 |
| | | Burst | -207 | -273 | -250 | -258 |
| B-14** | Control | Start | -312 | -322 | -302 | -305 |
| | | Burst | -305 | -312 | -287 | -290 |
| B-9 | 2 | Start | -310 | -314 | -300 | -305 |
| | | Burst | -139 | -261 | -223 | -231 |
| B-20 | 2 | Start | -316 | -315 | -285 | -319 |
| | | Burst | -316 | -312 | -247 | -302 |
| B-7 | 3 | Start | -317 | - | - | -230 |
| | | Burst | -311 | - | - | -217 |
| B-1 | Control | Start | -419 | -413 | -400 | -399 |
| | | Burst | -412 | -367 | -303 | -306 |
| B-6 | Control | Start | -416 | -412 | -402 | -403 |
| | | Burst | -416 | -391 | -347 | -323 |
| B-11 | 2 | Start | -417 | -417 | -402 | -399 |
| | | Burst | -408 | -382 | -364 | -366 |
| B-15*** | 3 | Start | -399 | -383 | -399 | -385 |
| | | Burst | -320 | -326 | -304 | -303 |
| B-19** | 3 | Start | -370 | -412 | -401 | -393 |
| | | Burst | -328 | -356 | -306 | -303 |

*Symbols defined in Figure 59.

T_s Reading taken from bottom boss (supply).*T_s and T_o Readings taken from bottom and top bosses.

4. Test Summation

Testing revealed that improved cryogenic filament-wound pressure vessels were produced with Hi-Stren/VHS glass and Resin System 2 (Epon 828/DSA/Empol 1040/BDMA). The highest cryogenic properties were obtained at -320°F with Resin System 2. The longitudinal-filament stress was 471,700 psi and the hoop-filament stress 451,300 psi.

A considerable increase in temperatures measured on the outer skin of the composite was encountered during pressurization in cryogenic testing. A study was undertaken to determine the cause and is reported in Appendix D. Further work, covered in Appendix F, revealed that, although skin-temperature measurements showed a large increase, thermometers incorporated within the composite wall during fabrication simultaneously showed a negligible increase (e.g., 13°F at the burst point).

VII. SUPPLEMENTARY WORK

Supplementary work was conducted in support of this program using Aerojet funds. The results are summarized below for the purpose of upgrading the state of the art.

A. GLASS-BORON COMPOSITES

Glass-boron filament-wound composites in the form of flat panels were fabricated of filament-wound sheets similar to the type used in Task III. They contained approximately 19 wt% of boron filaments. A single-end glass roving, impregnated with the control resin (epichlorohydrin/bisphenol A epoxy), was wound onto a take-up drum having an exact butt-joint layup. A boron filament was wrapped over the glass filaments with a 1/32-in. spacing. A subsequent layer of glass was wound over the boron, making a sandwich-type construction. The second layer of glass was used to hold the boron in place when the filament-wound sheets were cut from the take-up drum.

The glass-boron filament-wound sheets were laminated into a unidirectional (1:0) composite. Tensile, flexural, and short-span-shear tests were conducted at room temperature and at -320°F.

Although it was planned that the composite was to contain 15 wt% of boron, the boron content of the finished composite was determined to be 19 wt%. The test results are summarized in Table 38. The addition of boron fibers significantly improved the tensile modulus and the flexural and shear strength of the composite.

B. GLASS-FIBER/WHISKER COMPOSITES

1. Silicon Carbide Whiskers

a. Standard Quality

Initial experiments to evaluate the effects of adding whiskers to a composite were conducted with horizontal-shear NOL rings. The rings were fabricated with silicon-carbide whiskers incorporated in the glass-resin composite. Two methods were used: The whiskers were (a) vibrated onto the surface of the ring during fabrication, or (b) added to the resin matrix and held in suspension by ultrasonic agitation. Room-temperature and -423°F horizontal-shear-strength data reported in Table 39 indicate no improvement resulting from the use of whiskers. The whiskers used were suspected to be of low quality, and the experiment was repeated with a high-quality whisker material.

b. High Quality

Filament-wound composites were fabricated of single-end Hi-Stren glass roving and new silicon carbide whiskers impregnated with the control resin system (Epon 828/NMA/BDMA). The Task III fabrication

TABLE 38
COMPOSITE PROPERTIES, GLASS FIBERS/SILICON CARBIDE WHISKERS AND GLASS FIBERS/BORON FILAMENTS*

* Composite cure temperature: 1 hour at 200° F and 2 hours at 350° F. Silicon carbide whiskers were applied to the flat sheet by the salt-shaker method. The boron filaments were integrated with the glass fibers during filament winding.

TABLE 39

GLASS-FIBER/WHISKER-REINFORCED COMPOSITES, HORIZONTAL SHEAR
EPON 828/NMA/BDMA RESIN SYSTEM, * SINGLE-END HI-STRENGTH GLASS

| Ring No. | Type of Whiskers | Content, % | | Specific Gravity | Horizontal Shear Strength, psi | | Ratio of Strengths
-423°F/Room Temp |
|------------------|-------------------|------------|-------|------------------|--------------------------------|-----------|--|
| | | Whiskers | Resin | | At | | |
| | | | | | Room Temp | At -423°F | |
| S-1
(control) | None | - | 21.2 | 2.05 | 10,271 | 25,961 | 2.54 |
| W-1** | Silicon Carbide | 2.3 | 24.3 | 1.97 | 9,456 | 18,447 | 1.95 |
| W-2*** | Silicon Carbide | - | 26.0 | 1.95 | 10,530 | 23,941 | 2.27 |
| W-3** | Sapphire, Type 1B | 1.0 | 20.7 | 2.07 | 8,050 | 17,100 | 2.13 |
| W-4*** | Sapphire, Type 1B | 1.0 | 22.3 | 2.02 | 10,450 | 23,700 | 2.28 |

* Composite cure: 1 hour at 200° F and 2 hours at 350° F. Horizontal-shear values are averages as follows: at room temperature, five tests, and at -423° F, three tests.

** Whiskers vibrated onto composite during winding.

*** Whiskers mixed in the matrix resin and ultrasonically agitated.

procedure was used, and the whiskers were sprinkled onto one surface of each sheet. The whisker dispersion was considered uniform. The composite contained 1.9 wt% of whiskers. Tensile, flexural, and short-span-shear tests were conducted at room temperature and -320°F. The results are summarized in Table 38.

2. Sapphire Whiskers

Two NOL rings were fabricated with high-quality sapphire fibers incorporated into the composite by (1) vibration onto the ring surface during winding, or (2) addition to the matrix resin. Horizontal-shear-strength data reported in Table 39 indicate no improvement from the use of sapphire whiskers (up to 2.3% content in the composite).

C. VOID-FREE NOL RINGS

Two void-free NOL rings were fabricated (by McClean-Anderson, Inc.) of the Epon 828/NMA/BDMA resin system and single-end Hi-Stren roving coated with the VHS/A-1100 finish. Horizontal-shear specimens were cut from them for testing at room temperature and -423°F. The pertinent data are

| | |
|---------------------------|------------|
| Resin content | 33.8 wt% |
| Specific gravity | 1.84 |
| Voids | Negligible |
| Horizontal shear strength | |
| At +75°F | 10,200 psi |
| At -423°F | 16,500 psi |

The McClean-Anderson NOL rings were void-free, but the high resin content resulted in low horizontal shear strengths at room temperature and -423°F.

D. ULTRASONIC AGITATION

Two methods of ultrasonic agitation of the matrix resin (Epon 828, NMA/BDMA) were used during the fabrication of horizontal-shear NOL rings: (1) An ultrasonic horn was immersed in the resin bath, agitating the resin during filament impregnation, or (2) an ultrasonic wave was directed onto the winding surface of the ring during fabrication by placing the horn 1/2 in. from the mandrel. The reinforcement was VHS/A-1100/Hi-Stren glass. The room-temperature and -423°F horizontal-shear strength data reported below indicate that no improvements were achieved.

| Ring
No. | Resin
Content
wt% | Specific
Gravity | Voids
vol% | Horizontal
Shear Strength, psi | |
|-------------|-------------------------|---------------------|---------------|-----------------------------------|--------------|
| | | | | At
Room
Temp | At
-423°F |
| 52-A* | 16.3 | 2.12 | 0.15 | 9,000 | 14,200 |
| 52-B** | 15.1 | 2.15 | Negative | 9,600 | 13,300 |
| Control | 16.9 | 2.11 | 0.16 | 9,400 | 15,500 |

* Ultrasonic horn immersed in resin bath.

** Ultrasonic wave directed onto winding surface of ring.

VIII. CONCLUSIONS

A. Improved cryogenic filament-wound composites were produced with Hi-Stren/VHS glass and Resin System 2 (Epon 828/DSA/Empol 1040/BDMA). This resin, developed under NASA Contract NAS 3-6287, yielded the highest cryogenic properties: a longitudinal-filament stress of 471,700 psi and hoop-filament stress of 451,300 psi at -320°F .

B. Improvement in the bonding of glass filaments to resins was achieved through an improved finish treatment employing the matrix resin as the film former in the finish (sizing) system.

C. It was determined that coupling agents are effective only in improving the wet strength of filament-wound composites.

D. Aerojet Hi-Stren glass filaments were found to be highly effective reinforcements for cryogenic filament-wound structures, particularly when the glass was treated with an effective finish during the fiber-forming process. Although the tensile strength of Hi-Stren (700,000 psi) is chiefly responsible for the high vessel strength developed in this program, it is believed that the high tensile modulus (13.5×10^6 psi) played an important role in the performance of the metal-lined/FWC tanks.

E. Pinhole leaks that developed in metal liners are believed to have resulted either from poor techniques in liner manufacture or plaster-mandrel shrinkage that caused metal-liner wrinkling during filament winding.

F. The use of lubricants in the finish system has little or no effect on the finish performance at ambient or cryogenic temperatures.

IX. RECOMMENDATIONS

A. Based on the demonstrated performance of Hi-Stren/VHS filaments and Resin System 2 in this program, it is recommended that these materials be considered for use in glass-filament structures for current cryogenic applications.

B. Additional studies of metal-lined, FWC pressure vessels are needed to establish design, processing, and performance data at cryogenic temperatures. The recommended areas of investigation include

1. Methods and materials to provide a reliable adhesive bond between the metal liner and the composite wall
2. Liner-manufacture methods to overcome liner leakage
3. Development of a mandrel material that will eliminate metal-liner wrinkling or buckling during filament winding
4. Determination of the effects of winding temperature sensors in the composite to improve the measurement of cryogenic temperatures.

Sufficient test vessels should be used in these studies to assure a high degree of confidence in the data obtained on structural properties and performance levels.

C. It is recommended that filament-wound test vessels of the type used in this program (8 in. in diameter, metal-lined) be used for future evaluations of FWC strengths at cryogenic temperatures.

D. It is recommended that fatigue testing be considered as a potential technique for the evaluation of glass-FWC structures for use at cryogenic temperatures.

REFERENCES

1. J. Hertz, "The Effect of Cryogenic Temperatures on the Mechanical Properties of Reinforced Plastic Laminates," SPE Journal, 21, 181 (1965).
2. A. Lewis, G. E. Bush, and J. Creedon, Improved Cryogenic Resin/Glass-Filament-Wound Composites, NASA CR-54867 (Aerojet-General Report 3196), May 1966.
3. O. Weingart, "Development of Improved Processes for Filament-Wound Reinforced Plastic Structures," SPI Journal, 20th Section, 12-D.
4. W. D. Bascom, Some Surface Chemical Aspects of Glass-Resin Composites, Part 2 - The Origin and Removal of Microvoids in Filament Wound Composites, U. S. Naval Research Laboratory Report 6268, 24 May 1965.
5. Henry Lee and Kris Neville, Epoxy Resins, New York, McGraw-Hill, 1957.
6. R. F. Barnet, "NOL Rings for Composite Materials Research and Development," Trans. J. Plastics Inst., pp. 177 to 187, October 1965.
7. L. Soffer and R. Molho, Cryogenic Resins for Glass-Filament-Wound Composites, NASA CR-72114 (Aerojet-General Report 3343), January 1967.
8. R. W. Buxton, R. N. Hanson, and D. Fernandez, Design Improvements in Liners for Glass-Fiber Filament-Wound Tanks to Contain Cryogenic Fluids, NASA CR-54-854 (Aerojet-General Report 3141), January 1966.

APPENDIX A

TEST METHODS

The program goals required the determination of certain physical and mechanical properties of cast resin and of FWC specimens at ambient and cryogenic temperatures. Test methods for a number of mechanical and thermal properties of plastics at ambient and higher temperatures are described in ASTM and FTM standards, but new procedures were required for all tests at cryogenic temperatures and for some of the desired properties at ambient temperatures. Specimen fabrication and testing procedures were therefore developed for both resin and composite materials; whenever feasible, they were patterned after related procedures in ASTM Standards or FTM Standard No. 406. They are described below.

I. TENSILE STRENGTH AT FRACTURE, ELONGATION AT FRACTURE, AND MODULUS OF ELASTICITY OF CAST RESIN

Stress-strain measurements were used to determine the tensile strength at fracture, elongation at fracture, and modulus of elasticity of a cured resin.

A. Apparatus - Holding fixture, routing fixture (Figure A-1), clamp fixture (Figure A-2), No. 600 sandpaper, tensile-test machine, cryostat facility (Figures A-3 and A-4), extensometer.

B. Specimen Preparation - Each system was mixed according to its individual requirements (see Table 29 of the main text). The mixture was degassed for 30 min, and was then bottom-drained into a preheated, 0.125-in.-thick, flat-panel, molding fixture. The mold and contents were cured for 5 hours at 285°F and were then cooled. The panels were removed and routed to the configuration shown in Figure A-5. The specimen was carefully sanded with No. 600 sandpaper to promote a uniform surface.

C. Procedure - The test specimen was placed in the clamp fixture as shown in Figure A-6. It was stressed in tension until failure occurred, using a 0.05-in./min crosshead travel rate. A 2-in. extensometer was used in conjunction with a tensile machine and recorder to provide a load-vs-strain diagram. To determine the elongation at fracture, two reference marks were inked on the specimen and were accurately measured to the nearest 0.05 in. After specimen rupture, the broken portions were fitted together and the distance between the reference marks was measured.

D. Calculations - Methods used to calculate tensile strength, elongation, and elastic modulus are described below.

The tensile strength at fracture for the test specimens was determined from

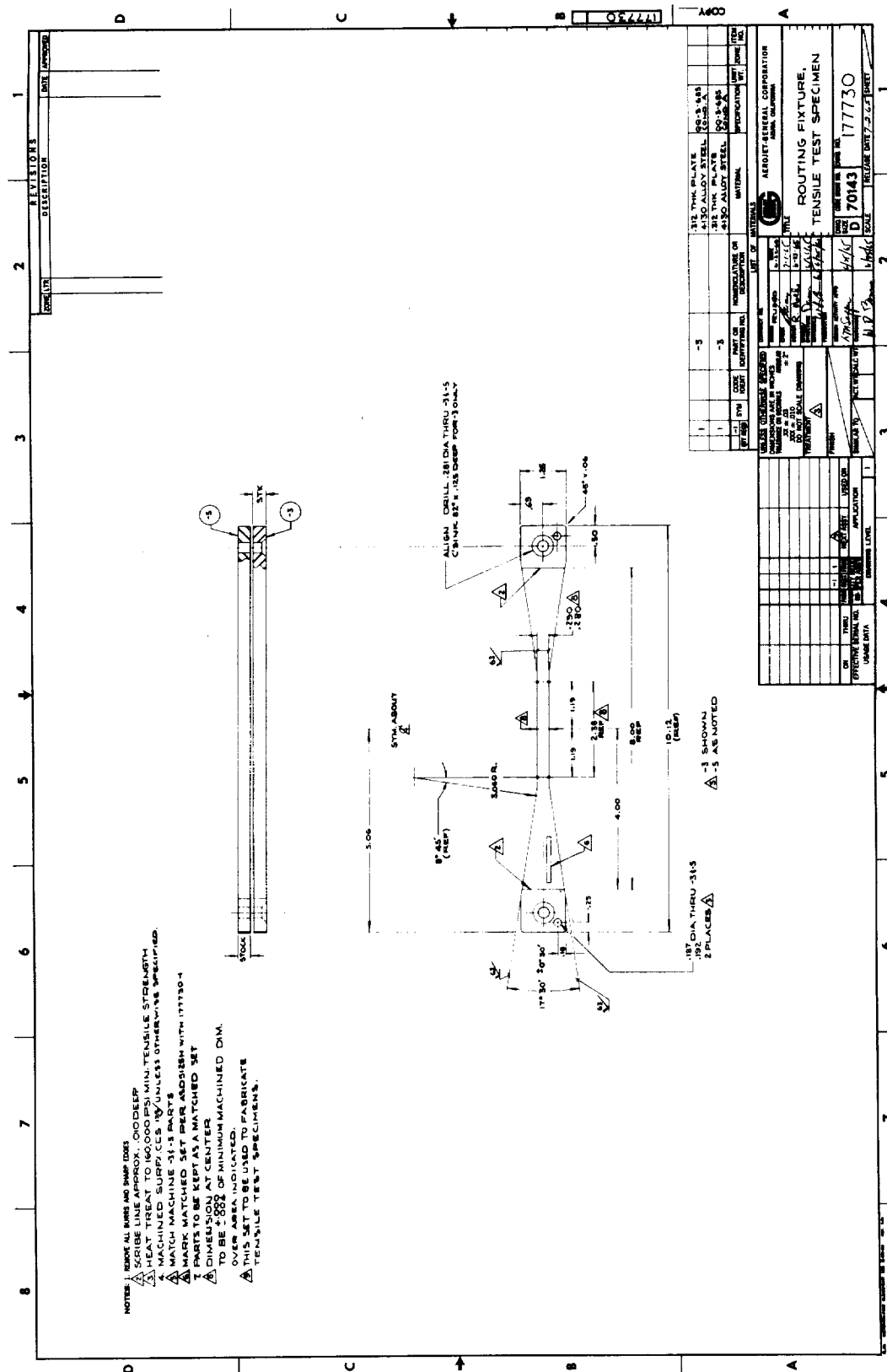




Figure A-2. Clamp Fixture, Tensile-Test Specimen

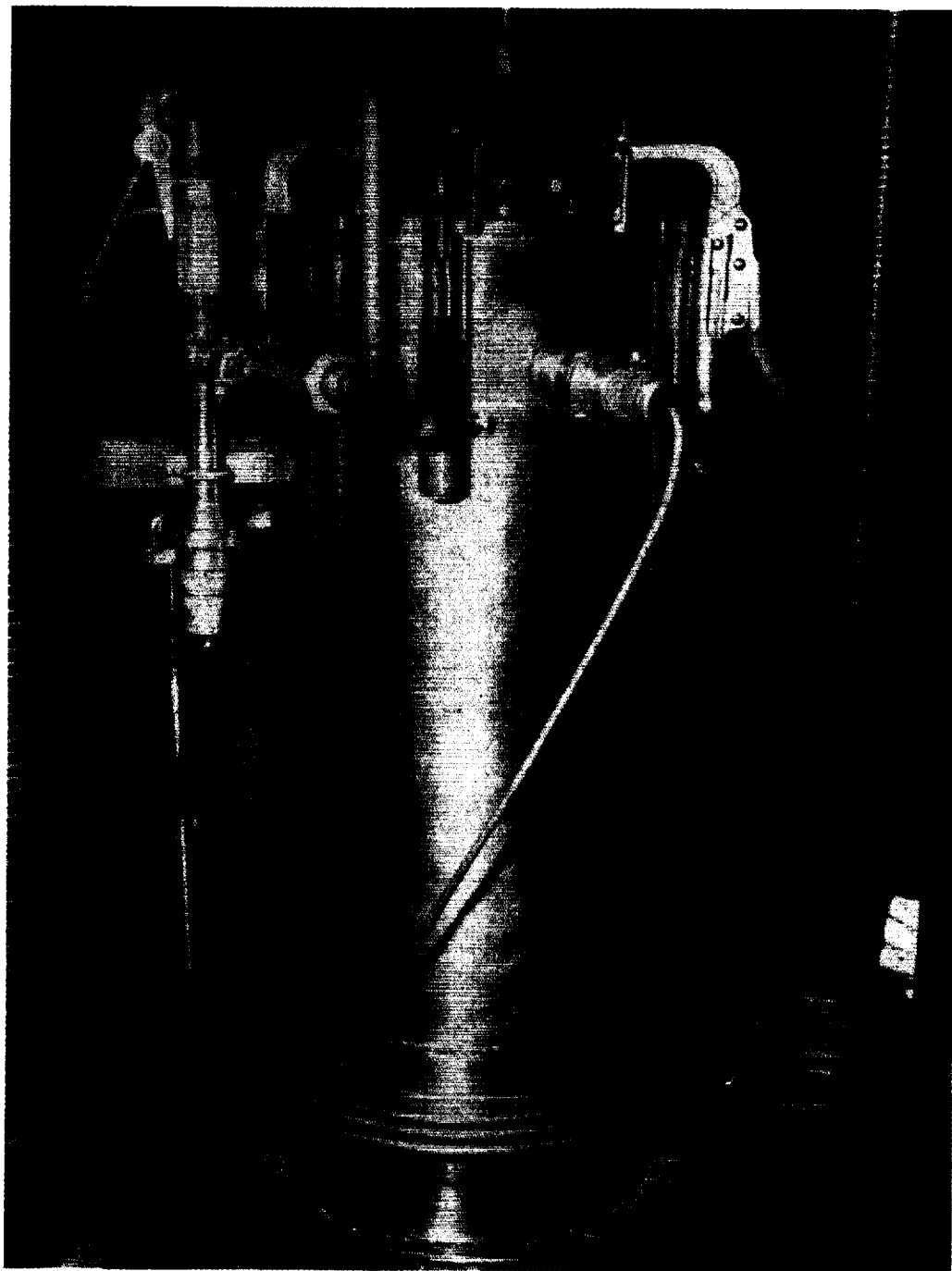


Figure A-3. Cryostat/Tensile-Machine Facility

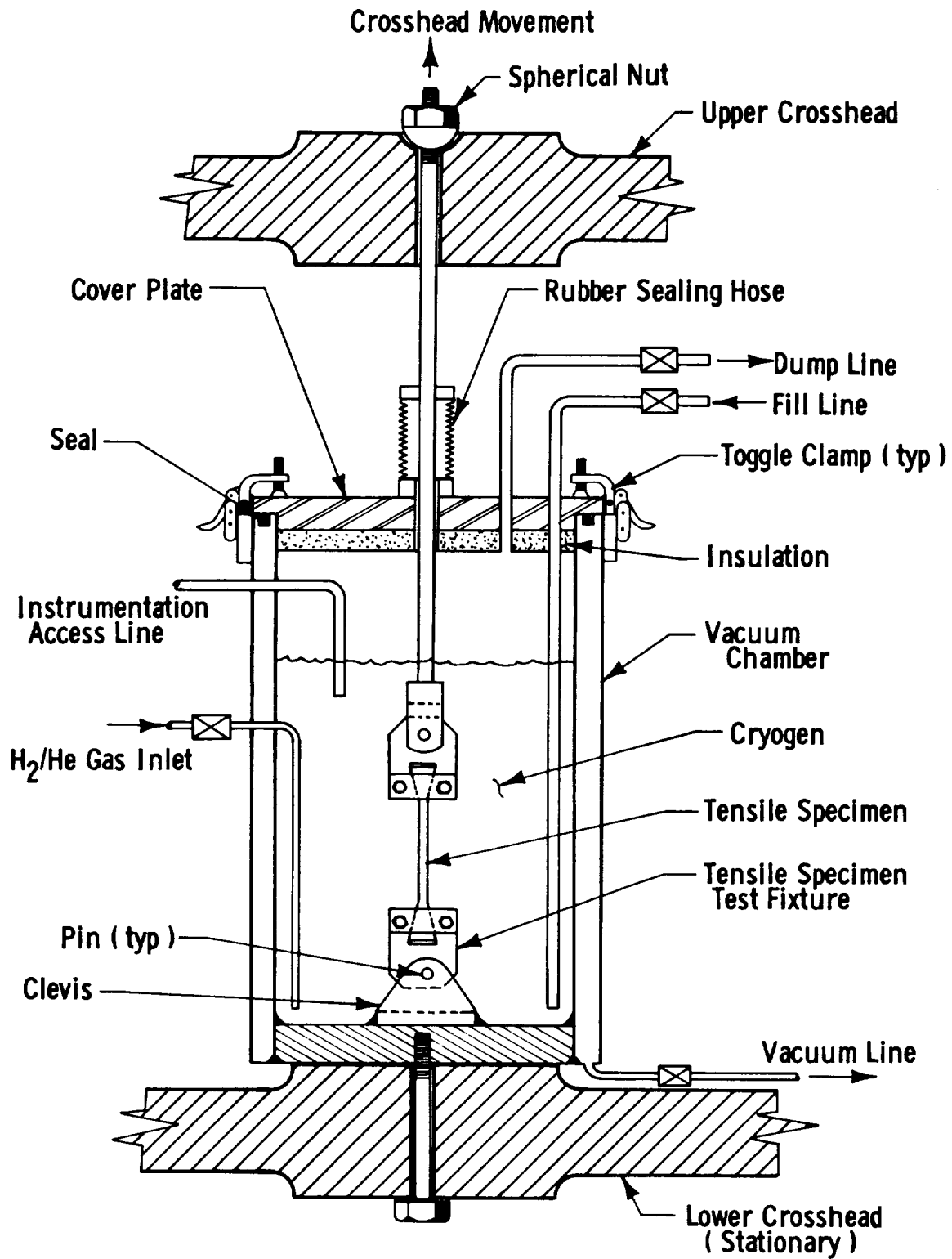


Figure A-4. Cryostat/Tensile-Test Machine



A-6

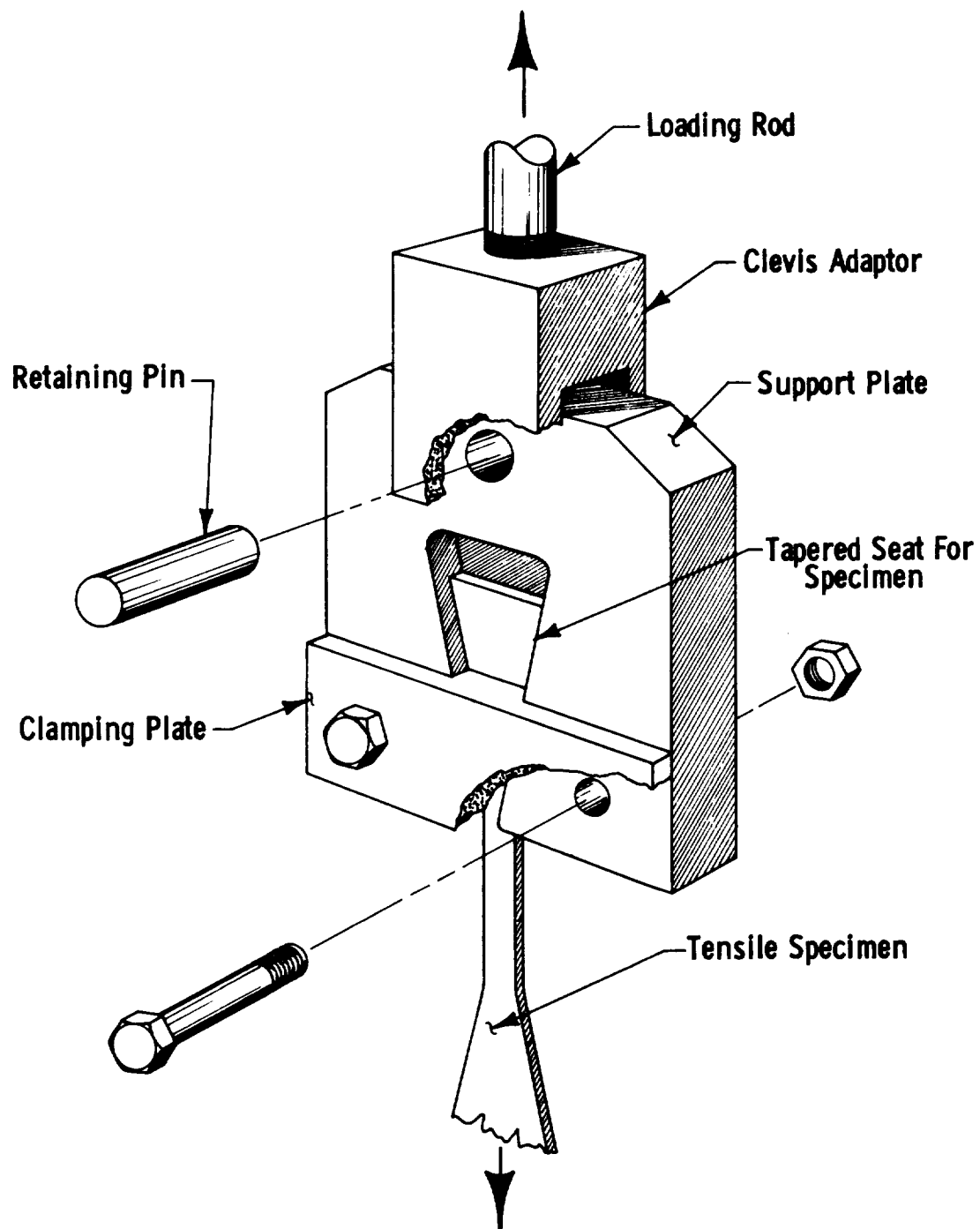


Figure A-6. Tensile-Test-Fixture Setup

$$S_F = \frac{P_F}{A}$$

where

S_F = tensile strength at fracture, psi

P_F = load at fracture, lb

A = original cross section, sq in.

The maximum tensile strength, if different from that at fracture, was calculated by substituting the maximum load for the load at fracture.

For test-specimen elongation at fracture,

$$e_F = \frac{L_1 - L}{L} (100)$$

where

e_F = elongation at fracture, %

L = distance between reference marks prior to testing, in.

L_1 = distance between reference marks after testing, in.

The modulus of elasticity was determined by extending the straight-line portion of the load-strain curve to any convenient point on the curve and noting the corresponding load at that point. A line for this point was dropped perpendicular to the base line. The distance from the intersection of the base line to the point where the load-strain curve crossed the base line was measured in inches and denoted as chart distance (C.D.). The modulus of elasticity was calculated from

$$E = \frac{L}{A} \bigg/ \frac{C.D.}{(mag)(gage\ length)}$$

where

L = load, lb

A = minimum cross section, sq in.

mag = magnification of extensometer

II. VISCOSITY OF UNCURED RESIN

The viscosity of the uncured resin was determined with the aid of a Brookfield Viscometer.

- A. Apparatus - Brookfield Viscometer (Model LVT), beaker, thermometer.
- B. Specimen Preparation - The test specimen was a sample (300 to 400 ml) of catalyzed resin system in a beaker.
- C. Procedure - The Viscometer spindle was positioned in the jar so that the sample surface was at the center of the shaft indentation and the spindle was in the center of the beaker. Viscometer rotation was started, and readings were taken (after 10 revolutions at each speed) at 6, 12, and 30 rpm. Measurements on the 100 scale of the dial were preferred because of their greater accuracy. The temperature after each set of readings was recorded.
- D. Calculation - Resin-specimen viscosity was determined by noting the dial factor on the Brookfield Model LVT viscosity chart, which relates the specific spindle being used and the spindle speed. The viscosity (poises) was calculated from

$$\text{Viscosity} = D_{100} F_D$$

where

D_{100} = dial reading on 100 scale

F_D = dial factor from Brookfield chart

III. INTERLAMINAR SHEAR STRENGTH OF GLASS/RESIN COMPOSITES

A. SHORT-SPAN-SHEAR METHOD

The interlaminar shear strengths of unidirectional and bidirectional glass-FWC specimens were determined by the short-span-shear method at +75, -320, and -423°F.

1. Apparatus - Filament-winding machine, tension-measuring device, drum-winding fixture, air-circulating curing oven, test fixture (Figure A-7), tensile-test machine, cryostat facility, brush.

2. Specimen Preparation - Resins were prepared according to the procedures given in Table 22 of the main text. Using the winding machine, single-end roving was passed through a dip tank containing the resin system and was then wound directly on the mandrel as unidirectional side-by-side filaments.


Technical drawing of a mechanical part, likely a bracket or support, showing dimensions and a table.

Dimensions and labels:

- 6: Dimension across the top flange.
- 7: 2 REGD (2 regular) - Dimension across the top flange.
- 2: Dimension across the top flange.
- 4: REGD (regular) - Dimension across the top flange.
- 10: Dimension across the bottom flange.

Table:

| | | | | | |
|----|---|--|--|-------|--|
| AR | | | | | |
| 8 | 8 | | | AN | |
| 1 | 1 | | | 150.0 | |

| | | | | | |
|--|--|---|--|--|--|
| UNLESS OTHERWISE SPECIFIED | | SHEET NO. | | LIST OF MATERIALS | |
| DIMENSIONS ARE IN INCHES
TOLERANCES ARE AS FOLLOWS
FRACTIONS
30 = ±.03
100 = ±.010
DO NOT SCALE DRAWINGS
TYPED PRINT | | REV. NO. 1
DATE 9-27-65
BY J. N. B. | |  AEROJET-GENERAL CORPORATION
Azusa, California | |
| TITLES | | TITLE | | TESTER-CRYOGENIC,
INTERLAMINAR SHEAR | |
| PROJECT | | PROJECT NUMBER | | Dwg No. 70143 | |
| DESIGN | | DESIGNER | | DATE 9-27-65 | |
| CHECKED | | CHECKED | | SCALE | |
| APPROVED | | APPROVED | | RELEASE DATE 9-27-65 | |
| APPLICATION | | SIMILAR TO | | PAGE 1 OF 1 | |
| VEL | | 1 | | | |

A-10

The windings were cut into 9-in. squares and were laid up so as to make a flat-panel laminate 0.125 in. thick and of the proper unidirectional or bidirectional orientation. The laminate was sandwiched between four plies of Dacron bleeder cloth and a layer of 181-glass cloth to facilitate release. The sandwich was placed on a steel plate that had been wrapped with Teflon-coated glass cloth. This assembly was then vacuum-bagged and cured under a vacuum according to the resin-system requirements. After curing, the laminate was removed and short-span-shear specimens 2.00 in. long by 1.00 in. wide by 0.125 in. thick were cut. The specimen width and thickness were measured to the nearest 0.001 in.

3. Procedure - The specimen was mounted in the test fixture in the calibrated testing machine, and was carefully aligned between the loading nose and supports (Figure A-8). The crosshead travel rate was 0.05 in./min, and the specimen was stressed until failure occurred.

4. Calculation - The short-span interlaminar shear strength was determined from

$$S = \frac{3 p}{4 b d}$$

where

S = interlaminar shear strength, psi

p = maximum load at failure, lb

b = specimen width, in.

d = specimen thickness, in.

B. HORIZONTAL-SHEAR METHOD

The interlaminar shear strengths of unidirectional glass-FWC specimens were determined by the horizontal-shear method at +75, -320, and 423°F.

1. Apparatus - NOL-ring winding machine, tension-measuring device, NOL-ring winding mandrel, air-circulating curing oven, test fixture (Figure A-7), tensile-test machine, cryostat facility.

2. Specimen Preparation - Resins were prepared according to the procedure given in Table 22 of the main text. Using the NOL-ring winding machine, the monofilament or single-end roving was passed through a resin bath and was then wound directly on the mandrel.

After cures according to individual requirements, the rings were removed from the winding fixture and were routed to a thickness of

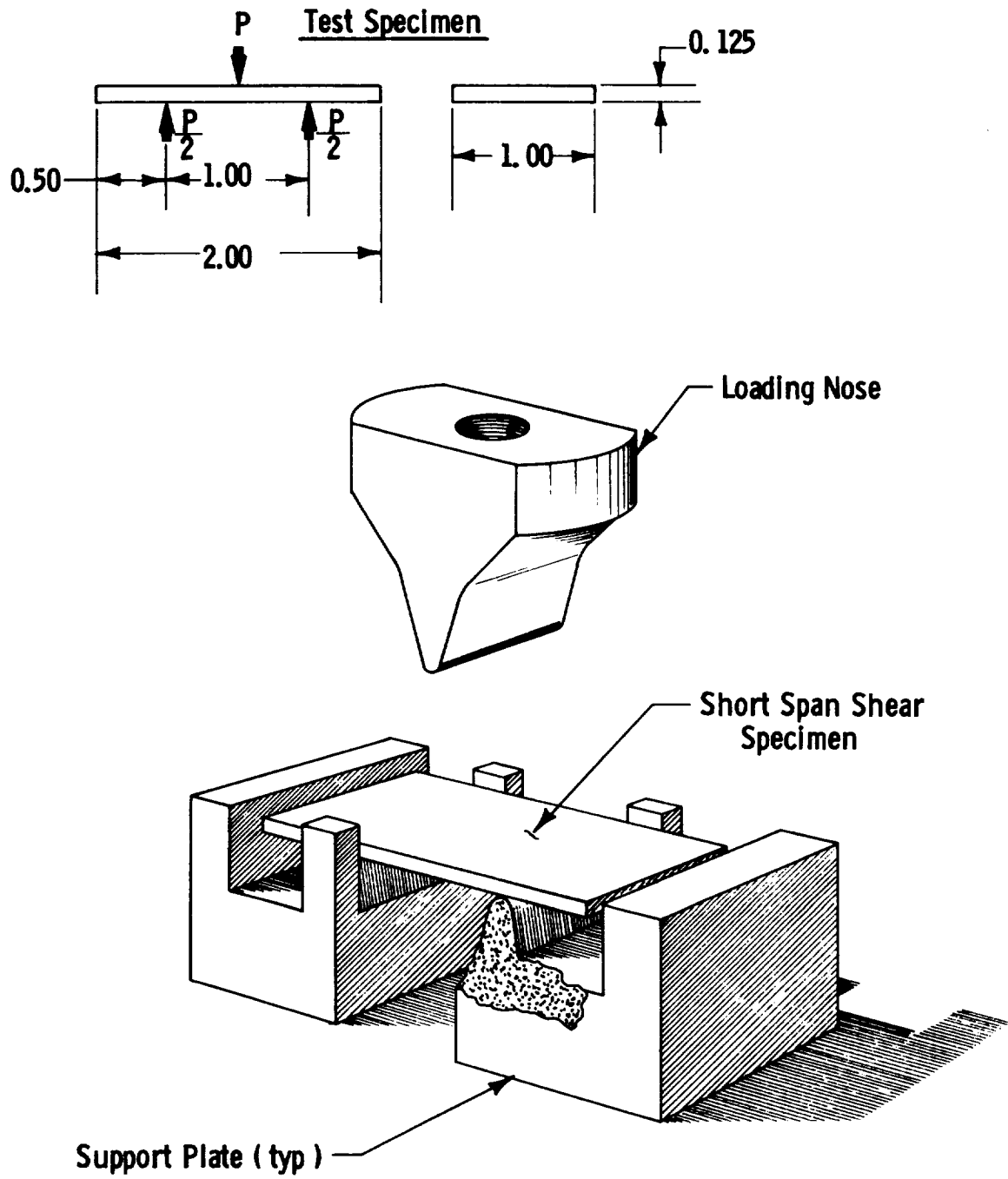


Figure A-8. Short-Span-Shear Test-Fixture Setup

approximately 0.125 in. The required arc segments (15) were cut from each ring, with the width and thickness being measured to the nearest 0.001 in. The finished specimen was 0.250 in. wide, 0.635 in. long, and 0.125 in. thick. These dimensions conformed to those recently approved in the tentative method for testing under ASTM Standard D2344-65 T.

3. Procedure - The specimen was aligned between the loading nose and supports, and was center-loaded on the convex side (Figure A-9). The crosshead travel rate was 0.05 in./min, and the specimen was stressed until failure occurred.

4. Calculation - The interlaminar shear strength (horizontal shear) was calculated from

$$S = \frac{3 p}{4 b d}$$

where

S = interlaminar shear strength, psi

p = maximum load at failure, lb

b = specimen width, in.

d = specimen thickness, in.

IV. COEFFICIENT OF LINEAR THERMAL CONTRACTION OF CAST RESIN

The linear thermal contraction of cured resin was determined between -400 and +70°F.

A. Apparatus - Fused-quartz-tube dilatometer, micrometer, thermocouple.

B. Specimen Preparation - Thermal-contraction specimens were prepared from the same batch of resin mix used for flexural-strength and shrinkage specimens. The individual cure schedules given in Table 22 of the main text were followed. After removal from the mold, the castings were cut and sanded into rectangular specimens. The finished specimens (three for each resin system) were 0.35 in. wide by 0.35 in. thick by 2.00 in. long. With a 1/16-in. bit, a hole was drilled halfway through the center of each specimen (normal to the length) for attachment of the thermocouple wire. The copper-constantan thermocouple was potted in the specimen with Shell 911F adhesive.

C. Procedure - The test-specimen length between the two quartz points was measured at room temperature to the nearest 0.001 in. The specimen was placed in a fused-quartz dilatometer tube, the quartz rod was brought into contact with it, and the dial gage was positioned. The assembled specimen and

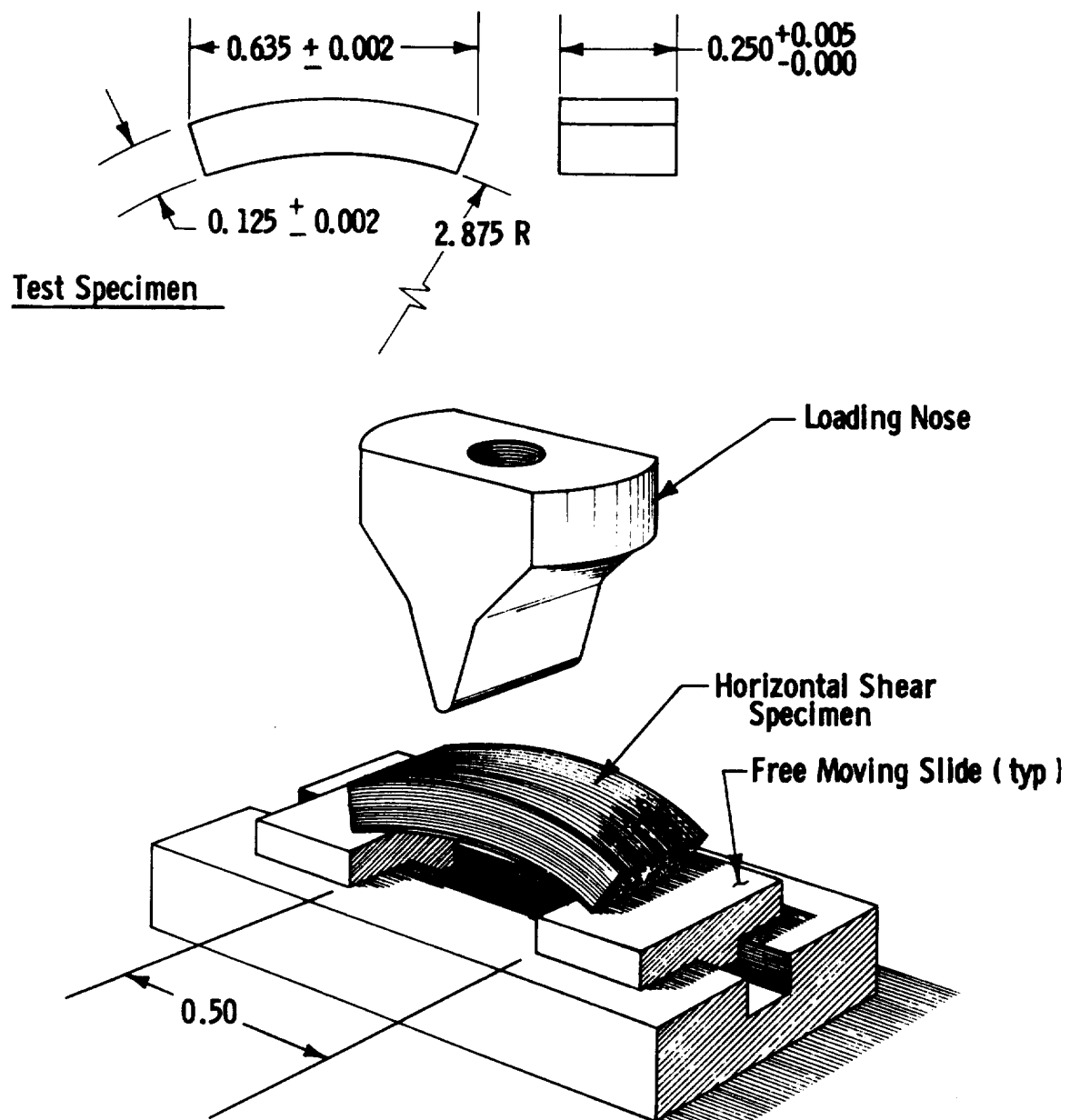


Figure A-9. Horizontal-Shear Test-Fixture Setup

tube were placed in the cryostat. The system was purged with helium gas and was then cooled with LH_2 to cryogenic temperatures. When the temperatures and dial-gage readings were recorded, the specimen was first permitted to stabilize at the cryogenic temperature for 15 min before being warmed to room temperature (by pressurizing the system with helium gas and replacing the LH_2). Dimensional changes were recorded at 10° intervals between -400 and $+70^\circ\text{F}$. Three test runs were made for each system. Before the specimens were tested, a 2-in.-long quartz sample was run in order to provide an instrument correction. A Leeds & Northrup Type K-3 universal potentiometer was used to monitor the temperature.

D. Calculation - The coefficient of linear thermal contraction was calculated from

$$\alpha = \frac{\Delta L}{L \Delta t}$$

where

- α = coefficient of linear thermal contraction, in./in./ $^\circ\text{F}$
- ΔL = change in length due to cooling, in./in.
- L = test length of specimen at room temperature, in.
- Δt = difference in temperature over which change in length was measured, $^\circ\text{F}$

V. SPECIFIC GRAVITY

The specific gravity of the resin was determined as the ratio of the weight of a given volume of the material at $73 \pm 4^\circ\text{F}$ to that of an equal volume of water at the same temperature.

A. Apparatus - Analytical balance, corrosion-resistant wire, beaker, thermometer.

B. Specimen Preparation - The test specimens were obtained from unused tensile or notch-toughness material. They were of any convenient size or shape, void-free, and not less than 0.2 cu in. in volume.

C. Procedure - A piece of corrosion-resistant wire about 12-in. long was fastened to the hook on a pan support of an analytical balance, and the weight was recorded to the nearest 0.1 mg. The test specimen was attached to the wire so that it was suspended about 1 in. above a beaker support; it was weighed to the nearest 0.1 mg. The suspended specimen was then immersed in a beaker of freshly boiled distilled water at a temperature of 72°F , and was weighed to the nearest 0.1 mg. The specimen was removed from the wire, and the weight of the wire immersed in water to the same depth was recorded.

D. Calculation - The specific gravity was calculated from

$$\text{Sp gr} = \frac{k - p}{(k - p) - (b - c)}$$

where

k = weight of specimen plus wire in air, g

p = weight of wire in air, g

b = weight of specimen in water plus partly immersed wire, g

c = weight of wire partly immersed in water, g

VI. RESIN SHRINKAGE (%) DURING CURE

The shrinkage of a castable resin during cure was determined from (a) volume measurements on the mold and on the cured casting, and (b) specimen weights in air and in water.

A. Apparatus - Semicylindrical mold.

B. Specimen Preparation - The mold (10 in. long and 1 in. in radius) was placed in the curing oven, was carefully leveled, and was preheated to the desired cure temperature. The individual resin mixes were the same degassed batches used in the preparation of flexural-strength and thermal-contraction specimens. The molds were filled in the oven and were heated in accordance with the applicable cure schedules.

C. Procedure - The dimensions of the mold cavity were carefully measured before the resin was cured. After removal from the mold, the volume of the cured specimen was determined (1) by direct measurement of the sample dimensions, and (2) by the difference in weight of the sample in air and while immersed in water.

D. Calculation - Specimen shrinkage (%) was calculated from

$$\text{Shrinkage} = \frac{V - V_i}{V} (100)$$

where

V = volume of cavity, cu in.

V_i = volume of cured resin, cu in.

VII. RESIN AND VOID CONTENTS OF GLASS/RESIN COMPOSITES

The resin and void contents of glass/resin composite specimens were determined by means of a resin-burnout procedure, and from the known specific-gravity values for resin, glass, and glass/resin composite.

A. Apparatus - Analytical balance, desiccator, heat-resistant non-reactive crucible, muffle furnace equipped with temperature control, corrosion-resistant wire, beaker.

B. Specimen Preparation - The test specimens were unused portions of the same NOL rings and short-span-shear panels from which horizontal- and short-span-shear specimens were cut. Each had a minimum weight of 3 g and maximum dimensions of 1 in. by 1 in. by the thickness supplied. The sides were square to the faces, and the edges were not frayed.

C. Procedure - The composite specimen was weighed on an analytical balance in a previously ignited and weighed crucible. It was placed in the furnace at a temperature below 650°F. The furnace temperature was raised to 1150 ± 50°F at a rate that would not cause a loss of glass filaments. The crucible was ignited to constant weight at this maximum temperature (20 min to 2 hours was required, depending on the sample thickness), and was permitted to cool in a desiccator. The weight loss was determined by weighing the residue.

Determination of the void content (vol%) required prior determination of the specific gravity of the resin and of the glass/resin composite by the method described in Section V, above. The specific gravity of the Hi-Stren glass filament that was used was 2.45.

D. Calculation - The resin content (wt%) of the glass/resin composite was calculated from

$$\text{Resin content} = \frac{W_a - W_g}{W_a} (100)$$

where

W_a = weight of glass/resin composite specimen in air, g

W_g = weight of glass after resin burnout, g

The void content (vol%) of the glass/resin composite was calculated from

$$\text{Voids} = \left[1 - \frac{SG_a}{W_a} \left(\frac{W_r}{SG_r} + \frac{W_g}{SG_g} \right) \right] (100)$$

where

SG_a = specific gravity of glass/resin composite

SG_g = specific gravity of glass = 2.45

SG_r = specific gravity of resin

W_r = weight of resin in composite specimen, g

VIII. TENSILE STRENGTH AT FRACTURE, ELONGATION AT FRACTURE, AND MODULUS OF ELASTICITY OF GLASS/RESIN COMPOSITES

The tensile properties of glass-FWC materials prepared with alternate filament orientations were determined by the method described below.

A. Apparatus - Laboratory filament-winding machine, routing fixture (Figure A-1), clamp fixture (Figure A-2), No. 600 sandpaper, tensile-test machine, cryostat facility, extensometer.

B. Specimen Preparation - Various steps in specimen preparation are considered individually below.

1. Resin Mixing - The resins were mixed in accordance with the formulations given in Table 22 of the main text.

2. Winding - A release film (Thalco 225) was applied to the mandrel of the winding machine. The single-end roving was led through a resin bath and was wound directly over a film of Teflon cloth.

3. Filament-Orientation Patterns - Three different patterns of filament orientation were used for each resin system (Figure 48 of the main text): (a) unidirectional, 1:0 longitudinal-to-transverse filament ratio, (b) bidirectional, 1:1 longitudinal-to-transverse filament ratio, and (c) bidirectional, 1:2 longitudinal-to-transverse filament ratio.

4. Layup and Cure - Each 10 by 20-in. layer was cut into two equal pieces, approximately 9 in. square. The resulting laminates were sandwiched between two layers of burlap (alternating orientation) and three layers of Dacron bleeder cloth on a Teflon-coated steel plate. (For the unidirectional laminate, cross plies of 181-glass cloth were placed between every third layer to reinforce the grip sections of the test specimens and prevent failure in these areas.) The laminate was fitted with a thermocouple in contact with the panel, was placed in a vacuum bag, and was cured according to the appropriate schedule (Table 22 of the main text).

5. Handling After Cure - After curing, the panels were cut and routed to a tapered-end specimen configuration (Figure A-5). The specimens were carefully smoothed with No. 600 sandpaper to provide a uniform surface and thereby reduce data scatter.

C. Test Procedure and Calculation - See paragraphs I, C and D, above.

IX. THERMAL-SHOCK RESISTANCE OF GLASS/RESIN COMPOSITES

Glass-FWC specimens in the form of arc segments from an NOL ring were tested in interlaminar shear after being cycled between room temperature and -423°F.

A. Apparatus - LH₂ Dewar flask, 2000-ml beaker, NOL-ring winding machine, tension-measuring device, NOL-ring winding mandrel, curing oven, interlaminar-shear test fixture (Figure A-9), tensile-test machine.

B. Specimen Preparation - The test specimen was a short beam in the form of an arc segment cut from an NOL ring. As finished, it was 0.250 in. wide, 0.635 in. long, and 0.125 in. thick. The NOL-ring winding machine was used to pass the single-end roving through a dip tank containing the resin system. The roving was then wound directly on the mandrel, which had been pretreated with Thaleco 225 mold release. The mandrel was held at approximately 150°F during winding. With a thermocouple as a temperature monitor, the rings were cured according to the individual-resin requirements (see Tables 4 and 22 of the main text). They were then removed from the winding fixture and were routed to a thickness of approximately 0.125 in. Excess resin was removed from the rings with No. 280 sandpaper. The required arc segments were cut from each ring, with the width and thickness measured to the nearest 0.001 in.

C. Procedure - The specimens were immersed for 15 min in a Dewar flask filled with LH₂. They were then removed and placed in a 2000-ml beaker of water at room temperature. After 15 min, they were removed from the water, were dried with compressed air, and were inspected visually for signs of thermal cracking. The test procedure was repeated for a total of five cycles.

Upon completion of temperature cycling, the specimens were mounted in the interlaminar-shear test fixture for testing in LH₂. The specimen was aligned between the loading nose and supports, and was center-loaded on the convex side. The crosshead travel rate was 0.05 in./min, and the specimens were stressed to failure. The interlaminar-shear-strength values obtained as described below were compared with noncycled -423°F data to determine the extent of degradation of the resin-to-glass bond caused by thermal cycling.

D. Calculation - The interlaminar shear strength (horizontal-shear method) was calculated from

$$S = \frac{3 p}{4 b d}$$

where

S = interlaminar shear strength, psi

p = maximum load at failure, psi

b = specimen width, in.

d = specimen thickness, in.

X. COEFFICIENT OF LINEAR THERMAL CONTRACTION OF GLASS/RESIN COMPOSITES

The linear thermal contraction of glass-FWC specimens with bidirectionally (1:2) oriented filaments was determined from measurements transverse to the direction of the majority of the filaments.

A. Apparatus - Filament-winding machine, tension-measuring device, flat mandrels, air-circulating oven, fused-quartz dilatometer, micrometer, thermocouple, brush.

B. Specimen Preparation - Various steps in preparation are considered separately below.

1. Resin Mixing - The resins were mixed as described in Table 22 of the main text.

2. Winding and Curing - The winding machine was used to pass the roving through a dip tank containing the resin and wind it as unidirectional side-by-side filaments on a winding drum. The flat sheets were cut and laid up to the proper filament orientation, and were cured in accordance with the required schedule.

3. Handling After Cure - After the cure, the panels were cut and sanded into rectangular beam specimens 2 in. long by 0.35 in. square. With a 1/16-in. bit, a hole was drilled halfway through the center of each specimen (normal to the length) for attachment of a copper-constantan thermocouple wire. The latter was potted in the specimen with Shell 911F adhesive.

C. Test Procedure and Calculation - See paragraphs IV,C and D, foregoing.

XI. FLEXURAL-FATIGUE TEST

A. Apparatus - LN₂ Dewar flask, filament-winding machine, NOL-ring mandrel, air-circulating oven, holding fixture, routing machine, cutting saw, and tensile-test machine.

B. Specimen Preparation - Individual NOL rings were fabricated on the winding machine by passing single-end roving through a dip tank containing the

appropriate resin and winding it onto the NOL-ring mandrel. Each ring was cured in accordance with Table 4 of the main text, was then routed to the desired dimensions (1/8 in. thick by 1/4 in. wide), and was sanded smooth. The test specimens cut from the ring were 2 in. long as measured on the inner circumference.

C. Procedure - One specimen of each ring was tested to determine the ultimate flexural strength at room temperature. Flexural-fatigue tests were then conducted on three specimens from each ring at -320°F as follows: a 1-in. span was used; each specimen was loaded to 80% of the ultimate strength found in the initial room-temperature flexural test, and was flexed 16 times per minute for a total of 48 cycles. The cross-head speed was 2 in./min. Upon completion of the fatigue test, each specimen was tested for ultimate flexural strength at room temperature.

D. Calculation - The flexural-fatigue test was used only for comparison of the systems evaluated in this program. Direct readings provided the necessary data.

XII. FLEXURAL PROPERTIES, FLAT SPECIMENS

This procedure was used to determine the flexural properties of rigid plastics (cast resin and composites) under standard room-temperature and cryogenic conditions.

A. Apparatus - Resin mold (cast resin), winding machine, air-circulating oven, diamond saw, tensile-testing machine.

B. Specimen Preparation - Cast-resin specimens were prepared at the same time as shrinkage and thermal-contraction specimens were cast. The resins were formulated and cured in accordance with Table 4 of the main text.

Composite specimens were cut from laminates of filament-wound sheets. The matrix-resin formulations and curing schedules are given in Table 22 of the main text.

The cast-resin specimens were cut to the standard 1 by 4-in. configuration. The composite specimens were reduced in length from 4 in. to 3 in. (i.e., 1 by 3 in.) to permit the use of existing cryogenic facilities.

C. Procedure - The width and thickness of each specimen were measured to the nearest 0.001 in. The span was measured to the nearest 0.01 in. The specimens were conditioned at the test temperature until equilibrium was attained. The rate of head travel was in the range from 0.20 to 0.25 in./min.

D. Calculation - The maximum stresses were calculated from

$$S = \frac{3 P L}{2 b d^2}$$

where

S = maximum stress, psi

P = load, lb

L = distance between points of support, in.

b = width of beam as tested, in.

d = depth of beam as tested, in.

XIII. FLEXURAL PROPERTIES, NOL SEGMENTS

This procedure was used to determine the flexural properties of NOL-ring segments at room temperature and cryogenic temperatures.

A. Apparatus - Winding machine, ring mandrels, air-circulating oven, holding fixture, router, diamond saw, tensile-testing machine.

B. Specimen Preparation - The NOL-ring composites were fabricated by passing a single end of Hi-Stren roving through a resin-dip bath and winding the end onto a ring mandrel. The resin formulations and curing schedules are given in Table 4 of the main text. After curing, the ring composite was routed and sanded smooth. Specimens were cut 2 in. in length as measured on the inside circumference.

C. Procedure - The width and thickness of each specimen were measured to the nearest 0.001 in. A span of 1 in. was measured to the nearest 0.01 in.

The specimens were conditioned at the test temperature until equilibrium was attained. Three-point loading was employed, and the rate of head travel was in the range from 0.20 to 0.25 in./min.

D. Calculation - The maximum stresses were calculated as outlined in paragraph XII,D, above.

XIV. COMPOSITE IMPACT RESISTANCE

This procedure was used to determine the relative susceptibility of uni-directional 1:0, bidirectional 1:1, and bidirectional 1:2 glass/resin composites to shock fracture at room temperature and -320°F. This susceptibility is indicated by the energy expended by a standard pendulum-type (Izod) impact machine in breaking a standard specimen in one blow.

A. Apparatus - Simple-beam (Izod) impact machine, winding machine, air-circulating oven, diamond saw.

B. Specimen Preparation - Composite panels were prepared at the same time as flexural and short-span-shear specimens. The formulations and cure schedules are given in Table 22 of the main text. Test specimens were cut 1/8 in. thick by 1/2 in. wide by 2 in. long.

C. Procedure - Each specimen was conditioned at the test temperature until equilibrium was attained. It was then transferred from the conditioning bath to the impact machine and tested. The maximum elapsed time between removal from the bath and testing was 6 sec. The specimen was supported vertically, with the top surface of the vise on a line with the center of the notch. The blow was struck on the notched side.

D. Calculation - The amount of energy expended in breaking each specimen, expressed in foot-pounds per inch of width of the specimen face hit by the hammer, was calculated.

APPENDIX B

DESIGN ANALYSIS, 8-IN.-DIA FILAMENT-WOUND PRESSURE VESSELS FOR CRYOGENIC-RESIN EVALUATION

This appendix summarizes the design and structural verification of various components of the 8-in.-dia cylindrical vessels employed in Task IV.

Experience acquired in previous development efforts (Ref. 8) led to the selection of a closed-end, cylindrical, test vessel fabricated from longitudinally and circumferentially oriented filaments wound over a 0.006-in.-thick metal liner (Type 304 stainless steel). The composite structure was adhesively bonded to the liner to minimize compressive liner buckling. The vessel, approximately 8 in. in diameter by 13 in. long, was designed to achieve a 2.5% strain with a longitudinal-to-circumferential strain ratio of 1.

I. DESIGN-ALLOWABLE STRENGTH

Aerojet has developed a systematic approach to the design of filament-wound vessels and is using it in a number of applications. The method involves the use of pressure-vessel design factors, corresponding to a range of dimensional parameters, to determine the allowable design strength for each configuration.

The factors are based on data collected over the past 6 years from Aerojet tests on several thousand pressure vessels, which ranged in diameter from 4 to 74 in. and had significant variations in their design parameters. Included as factors used for the selection of design-allowable values are the strength of the glass roving, resin content, envelope dimensions (length and diameter), internal pressure level, axial-port diameters, temperature, sustained-loading requirements, and cyclic-loading requirements. This method of analysis was used in the present program to establish realistic values for the allowable filament tensile strengths in the 8-in.-dia test vessel.

Because earlier investigations of glass/resin interaction in filament-wound pressure vessels had shown that the heads were more sensitive to the resin used than the cylindrical section, the test vessels were designed to fail in the longitudinal filaments of the heads. This allowable longitudinal-filament strength is given by

$$F_{f,1} = K_1 K_2 K_3 K_4 K_5 K_6 (\sec^2 \alpha) F_f^*$$

* From Structural Materials Handbook, Chemical and Structural Products Division, Aerojet-General Corporation, February 1964. These symbols are defined at the end of this appendix.

The following design factors* are based on the specific vessel parameters:

| <u>Parameter</u> | <u>Design Factor</u> |
|---------------------------|----------------------|
| $D_c = 7.789 \text{ in.}$ | $K_1 = 0.83$ |
| $D_b/D_c = 0.37$ | $K_2 = 0.95$ |
| $L/D_c = 1.58$ | $K_3 = 1.00$ |
| $t_{f,1}/D_c \cong 0.001$ | $K_4 = 0.96$ |
| $T = 75^\circ\text{F}$ | $K_5 = 1.00$ |
| $\eta = 3 \text{ min}$ | $K_6 = 1.00$ |
| $\alpha = 13^\circ$ | - |

The single-pressure-cycle allowable ultimate filament strength is therefore

$$F_{f,1} = (0.83)(0.95)(1.00)(0.96)(1.00)(1.00)(1.053)(415,000) = 330,000 \text{ psi}$$

II. DETERMINATION OF DESIGN BURST PRESSURE

The design burst pressures of the vessel (1338 psi at $+75^\circ\text{F}$, 2087 psi at -320°F , and 1922 psi at -423°F) were established on the basis of (a) a longitudinal-composite thickness of 0.011 in., which is the approximate composite thickness resulting from the use of 12-end, Hi-Stren glass roving, and (b) single-cycle design-allowable strengths for Hi-Stren glass filaments of 330,000 psi at $+75^\circ\text{F}$, 495,000 psi at -320°F , and 445,000 psi at -423°F .

These values were selected after a review of composite-property data indicating that the strength of glass laminates increases approximately 50% at -320°F and 35% at -423°F over the value at $+75^\circ\text{F}$. The dimensional coordinates of the pressure-vessel heads were established by the use of a computer program designed for metal-lined pressure vessels. This program, developed by Aerojet under Contract NAS 3-6292, also defined the filament and metal-shell stresses and strains at zero pressure and at the design pressure, the required hoop-wrap thickness for the cylindrical portion of the vessel, the filament-path length, and the weight and volume of the components and complete vessel.

* Ibid.

Because of the limited biaxial data available on filament-wound vessels at cryogenic test temperatures, a conservative approach was taken in the design of specific metal components (bolts, bosses, etc.) by employing the highest estimated burst pressure (2087 psi at -320°F) in conjunction with the lowest material strength (at +75°F).

III. WINDING-PATTERN DETERMINATION

The filament-wound vessel had two primary winding patterns: (a) a planar or end-for-end pattern designed to provide the total strength in the heads and longitudinal strength in the cylindrical section, and (b) a hoop pattern for circumferential strength in the cylindrical section.

The pattern developed for a pressure vessel requires the application of a specific quantity of glass in a predetermined orientation in order to obtain a desired burst pressure. The pattern is analyzed on the basis of actual winding data and laboratory tests of the glass roving and composite specimens. These data have shown that a cured single layer created by side-by-side orientation of Hi-Stren 12-end roving will produce an average composite thickness of approximately 0.0055 in. The minimum thickness for a cylindrical pressure vessel with meridional and circumferential filaments will therefore be 0.011 in. (one revolution, or two layers) for the longitudinal composite and 0.022 in. (four layers) for the hoop composite. Assuming these thicknesses and using the value of 20.0×10^{-6} sq in. determined for the area of a single end of Hi-Stren glass roving, the winding pattern for the 8-in.-dia vessel (Figure 57 of the main text) may be calculated as shown below.

A. LONGITUDINAL

The cross-sectional area of longitudinal-filament layers (A_1) is given by

$$\begin{aligned} A_1 &= \pi D_c t_{f,1} \\ &= A_{\text{end}} N_1 N_2 N_3 N_4 N_5 \frac{1}{\cos \alpha} \end{aligned}$$

where

- D_c = chamber diameter at longitudinal neutral axis = 7.789 in.
- A_{end} = area of single end = 20×10^{-6} sq in.
- N_1 = number of ends per strand = 12
- N_2 = number of strands per tape = 1
- N_3 = number of tapes per turn = 2

- N_4 = number of turns per revolution
 N_5 = number of revolutions = 1
 α = angle between filament and meridional direction = 13°
 $t_{f,1}$ = longitudinal-filament thickness, in. = $t_1 P_{vg}$
 t_1 = longitudinal-composite thickness = 0.011 in.
 P_{vg} = amount of glass filament in composite, volume fraction = 0.67 (based on desired resin content of 19 wt%)

Solving for N_4 ,

$$\begin{aligned}
 N_4 &= \frac{\pi D_c t_1 P_{vg} \cos \alpha}{A_{end} N_1 N_2 N_3 N_5} \\
 &= \frac{\pi (7.789) (0.011) (0.67) (0.97437)}{(20.0 \times 10^{-6}) (12) (1) (2) (1)} \\
 &= 366 \text{ turns/revolution}
 \end{aligned}$$

B. HOOP

The cross-sectional area of hoop layers (A_h) is given by

$$\begin{aligned}
 A_h &= t_{f,h} L_c \\
 &= A_{end} N_1 N_2 N_6 N_7
 \end{aligned}$$

where

- L_c = cylinder length = 7.28 in.
 N_6 = number of tapes per layer
 N_7 = number of layers = 4
 $t_{f,h}$ = hoop-filament thickness, in. = $t_h P_{vg}$
 t_h = hoop-composite thickness = 0.022 in.

Solving for N_6 ,

$$\begin{aligned}
 N_6 &= \frac{t_h P_{vg} L_c}{A_{end} N_1 N_2 N_7} \\
 &= \frac{(0.022) (0.67) (7.28)}{(20.0 \times 10^{-6}) (12) (1) (4)} \\
 &= 112 \text{ tapes/layer}
 \end{aligned}$$

IV. BOLTS

The load per bolt was calculated from

$$P = \frac{p_b \pi d^2}{4N}$$

where

P = load per bolt, lb

p_b = maximum design burst pressure = 2087 psi

d = bolt-circle diameter = 2.52 in.

N = number of bolts = 12

Therefore,

$$\begin{aligned}
 P &= \frac{(2087) (\pi) (2.52)^2}{(4) (12)} \\
 &= 868 \text{ lb/bolt}
 \end{aligned}$$

For MS 21279 bolts with a tensile strength of 130,000 psi (minimum), the ultimate tensile load per bolt (P_{tu}) is 2600 lb at ambient conditions. The margin of safety (M.S.) is given by

$$M.S. = \frac{P_{tu}}{P} - 1$$

Therefore,

$$\text{M.S.} = \frac{2600}{868} - 1 = +\underline{2.0}$$

V. THREADS

The shear stress in the threads was determined from

$$\sigma_s = \frac{P}{\pi d_t (0.5 l)}$$

where

σ_s = shear stress, psi

d_t = thread diameter = 0.164 in.

l = thread grip length = 0.25 in.

Therefore,

$$\begin{aligned}\sigma_s &= \frac{868}{(\pi) (0.164) (0.5) (0.25)} \\ &= 13,500 \text{ psi}\end{aligned}$$

The ultimate tensile strength (F_{tu}) for Type 304 stainless steel (annealed) is 70,000 psi (minimum). Assuming that

$$F_{su} = \frac{F_{tu}}{2}$$

where

F_{su} = ultimate shear strength, psi

$$F_{su} = \frac{70,000}{2} = 35,000 \text{ psi}$$

the margin of safety is

$$\begin{aligned} \text{M.S.} &= \frac{F_{su}}{\sigma_s} - 1 \\ &= \frac{35,000}{13,500} - 1 = \underline{+1.6} \end{aligned}$$

VI. BOSS FLANGE

The most critical section of the boss is located at the base of the flange. Stresses in this area are conservatively determined by assuming the flange to be a flat plate with a concentrated annular load and a fixed inner edge. The end-for-end wrap pattern of the longitudinal filaments produces a rigid band around the boss that supports the flange. Outside this band, the filaments are bridged and therefore offer no additional support. Because a single roll of 12-end roving is used to wrap the longitudinal pattern, the width of the band is 0.060 in., and the width used in calculating the bending stress is very small. Bending stresses are therefore neglected, with the shear loads at the juncture of the flange and boss predominating. The shear stress there was determined as follows:

$$\sigma_s = \frac{p_b d_f}{4 t_f}$$

where

d_f = diameter of flange-to-boss juncture = 2.75 in.

t_f = thickness of flange = 0.110 in.

Therefore,

$$\begin{aligned} \sigma_s &= \frac{(2087) (2.75)}{4 (0.110)} \\ &= 13,050 \text{ psi} \end{aligned}$$

With $F_{tu} = 70,000$ psi (minimum) for Type 304 stainless steel (annealed), assume

$$F_{su} = \frac{70,000}{2} = 35,000 \text{ psi}$$

Therefore,

$$\begin{aligned} \text{M.S.} &= \frac{F_{su}}{\sigma_s} - 1 \\ &= \frac{35,000}{13,050} - 1 = +1.68 \end{aligned}$$

VII. HYDROTEST PLUG

The stress at the center of the hydrotest plug resulting from the internal pressure is determined by assuming that the plug acts as a solid circular plate, with edges supported, and that a uniform load acts over the entire surface of the plug. The radial stress (σ_r) or tangential stress (σ_t) was calculated as follows:

$$\sigma_r = \sigma_t = \frac{3 W}{8 \pi m t_p^2} (3 m + 1)$$

where

$$\begin{aligned} W &= \text{total load on plug, lb} \\ &= \frac{\pi}{4} d^2 p_b \\ p_b &= \text{maximum design burst pressure} = 2087 \text{ psi} \\ m &= \text{reciprocal of Poisson's ratio} = 3.33 \\ t_p &= \text{thickness of hydrotest plug} = 0.50 \text{ in.} \end{aligned}$$

Therefore,

$$\begin{aligned} \sigma_r &= 0.310 \frac{d^2 p_b}{t_p^2} \\ &= \frac{(0.310) (2.52)^2 (2087)}{(0.50)^2} \\ &= 16,400 \text{ psi} \end{aligned}$$

and

$$\begin{aligned} \text{M.S.} &= \frac{F_{tu}}{\sigma_r} - 1 \\ &= \frac{70,000}{16,400} - 1 = +\underline{3.26} \end{aligned}$$

VIII. SAMPLE FILAMENT-STRESS CALCULATIONS

As indicated in the body of this report, design burst pressures for the vessel were established at each test temperature by a computer program. This was done on the basis of specific design criteria (see Table 31 of the main text) and selected single-cycle design-allowable strengths for longitudinal Hi-Stren filaments (330,000 psi at +75°F, 495,000 psi at -320°F, and 445,000 psi at -423°F) at a point on the head contour where the stresses are highest. The following values, taken from the computer-program printout, were used in calculating the actual longitudinal- and hoop-filament stresses at the burst pressure:

| Temperature
°F | Design Burst
Pressure
psi | Filament Stress, psi | |
|-------------------|---------------------------------|----------------------|---------|
| | | Longitudinal | Hoop |
| +75 | 1338 | 330,000 | 304,400 |
| -320 | 2087 | 495,000 | 467,500 |
| -423 | 1922 | 445,000 | 423,900 |

Because the computer-program analysis had already defined the stresses in the metal liner and in the filaments of the vessel, the reported stresses are corrected for that portion of the load supported by the liner. The design-allowable filament stresses from the computer analysis are factored by the direct ratio of actual to design burst pressure and the inverse ratio of actual to design number of winding turns, in order to permit calculation of the actual filament stresses attained at burst pressure. Sample calculations follow.

A. Example for actual stresses at +75°F (Vessel B-5):

$$\text{Longitudinal-filament stress} = 330.0 \left(\frac{1551}{1338} \right) \left(\frac{366}{370} \right) = 378,300 \text{ psi}$$

$$\text{Hoop-filament stress} = 304.4 \left(\frac{1551}{1338} \right) \left(\frac{448}{445} \right) = 354,900 \text{ psi}$$

B. Example for actual stresses at -320°F (Vessel B-20):

$$\text{Longitudinal-filament stress} = 495.0 \left(\frac{2011}{2087} \right) \left(\frac{366}{370} \right) = 471,700 \text{ psi}$$

$$\text{Hoop-filament stress} = 467.5 \left(\frac{2011}{2087} \right) \left(\frac{448}{447} \right) = 451,300 \text{ psi}$$

C. Example for actual stresses at -423°F (Vessel B-6):

$$\text{Longitudinal-filament stress} = 445.0 \left(\frac{2030}{1922} \right) \left(\frac{366}{370} \right) = 464,800 \text{ psi}$$

$$\text{Hoop-filament stress} = 423.9 \left(\frac{2030}{1922} \right) \left(\frac{448}{448} \right) = 447,600 \text{ psi}$$

The allowable hoop-filament stresses are somewhat lower because of the additional hoop filaments used in vessel fabrication to induce failure in the head. In the few instances when the hoop-filament stress was higher than the longitudinal, the number of hoop-filament-winding turns applied was less than the number calculated in paragraph III,B of this appendix.

SYMBOLS

| | |
|-----------|---|
| D_b | Boss diameter, in. |
| D_c | Mean diameter of cylinder, in. |
| F_f | Average ultimate tensile strength for glass roving, psi |
| $F_{f,1}$ | Allowable ultimate strength of longitudinal filaments, psi |
| K_1 | Design factor based on chamber diameter |
| K_2 | Design factor based on boss-diameter to chamber-diameter ratio |
| K_3 | Design factor based on chamber-length to chamber-diameter ratio |
| K_4 | Design factor based on approximation of thickness-to-diameter ratio |
| K_5 | Design factor based on operating temperature |
| K_6 | Design factor based on sustained pressurization loading |
| L | Chamber length, in. |
| T | Operating temperature, $^{\circ}\text{F}$ |
| α | Angle between line in axial direction and filament path, degrees |
| η | Time under sustained load, min |

APPENDIX C

PROCESSING, FABRICATION, AND TEST INSTRUCTIONS FOR IMPROVED RESIN/GLASS-FILAMENT-WOUND PRESSURE VESSELS

These instructions guided the fabrication of 19 filament-wound pressure vessels (18, plus one spare) and subsequent testing. The resin systems selected as the result of work in Tasks I, II, and III were used.

I. PROCESSING

A. HANDLING

Extreme care will be exercised in handling welded metal liners (0.006-in. wall thickness) throughout processing and fabrication. Clean, white, cotton gloves will be worn by all persons handling them after chemical cleaning of their outer surfaces.

B. METAL-LINER LEAK TEST

Each metal liner (Part No. 178155) will be mass-spectrometer leak-tested to verify its impermeability, and will be serialized in the boss area - B-1, B-2, etc. The liners will be delivered to the Glass Technology Laboratory for weighing.

C. WEIGHT RECORD

Each metal liner will be weighed to the nearest 0.01 g. Record the data as follows: Serial No. _____ Weight _____g.

D. PLASTER REINFORCEMENT

The inside of each metal-liner assembly will be reinforced with a plaster slush coat (Kerr DMM) approximately 1 in. thick to provide a support for the windings of glass filaments to be applied. Each metal-liner/plaster-mandrel assembly will be supported in a horizontally rotating position and placed in an approved oven to be dried for 24 hours at 200°F.

E. CLEANING OF METAL-LINER SURFACE

The outer surface of each metal liner will be cleaned to remove contaminants and provide a good bonding surface, in accordance with Aerojet Standard AGC-STD-1221 (Method of Pickling, Hot Nitric Acid). Clean, white, cotton gloves will be worn in handling after this step. The cleaned assemblies will be placed in individual polyethylene bags and sealed for delivery to the Filament Winding Laboratory.

F. GEL COATING

A gel coating, formulated as follows, will be applied to the outer surface of each metal liner to provide a structural bond with the glass-filament overwrap:

| | <u>Wt, g</u> |
|----------|--------------|
| Epon 828 | 100.0 |
| NMA | 80.0 |
| BDMA | 0.5 |

The resin system may be heated to 120°F in order to reduce the viscosity and provide a uniform coating. The gel coat will be "B" staged in a rotating horizontal position for 8 hours at 200°F.

G. GLASS-CLOTH APPLICATION

One layer of Type 104 glass cloth, 0.001 in. thick by 1 in. wide, will be applied over the weld area of the liner prior to filament winding. A doughnut-shaped layer of Type 112 glass cloth will be laid over the weld area of each boss.

II. FABRICATION AND PREPARATION FOR TESTING

A. LONGITUDINAL WRAP

The winding shaft will be assembled to the metal-liner/plaster-mandrel assembly for installation in the longitudinal-wrap position of the winding machine. All necessary adjustments and machine settings for the winding pattern will be made, and the winding angle, payoff roller, resin-impregnation tank, etc. will be checked. Gear ratios: A = 50, B = 60, C = 73, D = 61.

One roll of 12-end Hi-Stren glass roving will be weighed before the initiation of winding. Glass-roll weight before winding: _____g.

Longitudinal roving will be applied at a tension of 5 \pm 1 lb (one-strand tape). The longitudinal pattern will be one revolution with 366 turns (plus one turn for tieoff). Actual number of turns: _____.

The control resin will be a mixture of the following constituents in the quantities shown:

| | <u>Wt, g</u> |
|----------|--------------|
| Epon 828 | 100.0 |
| NMA | 80.0 |
| BDMA | 0.5 |

The NMA will be added to the Epon 828 and stirred until the mixture becomes homogeneous. The BDMA will be added prior to winding. The resin bath will be maintained at 100°F during filament winding.

Resin 2 will be a mixture of the following constituents in the quantities shown:

| | <u>Wt, g</u> |
|------------|--------------|
| Epon 828 | 200.0 |
| DSA | 231.8 |
| Empol 1040 | 40.0 |
| BDMA | 2.0 |

The Epon 828 and Empol 1040 will be mixed and warmed to 212°F and will then be cooled to room temperature for the addition of DSA and BDMA. The resin bath may be heated and maintained at approximately 95°F if it appears too viscous for filament winding.

Resin 3 will be a mixture of the following constituents in the quantities shown:

| | <u>Wt, g</u> |
|-----------|--------------|
| Epon 826 | 105 |
| Epon 871 | 45 |
| DDI | 44.1 |
| Curalon L | 105.3 |

The Epon 826, Epon 871, and DDI will be mixed together and heated to 150°F. The Curalon L will be melted at 200°F and added to the premix, with stirring. The resin system will be maintained at 150°F during filament winding.

The glass roll will be weighed after completion of the longitudinal-winding operation. Glass-roll weight after winding: _____g.

B. HOOP WRAP

Gear ratios: A = 52, B = 100, C = 40, D = 80.

Hoop pattern: four layers with 112 turns per layer over the 7.28-in. cylindrical distance.

Four instrumentation tacks (two sets of two), used to measure the axial cylindrical strain, will be positioned on the pressure vessel during the winding of the first hoop layer. Each set of two tacks will be placed 180° apart and in the plane of the cylinder axis. One set will be positioned 0.5 in. from the start of the first hoop layer and the other 0.5 in. before the end of the first hoop layer.

Glass-roll weight before hoop winding: _____g. Glass-roll weight after hoop winding: _____g. Actual number of turns in four layers: _____.

C. CURING OF COMPOSITE STRUCTURE

Curing cycles will be as follows: for the control resin (Epon 828/NMA/BDMA), 1 hour at 200°F followed by 2 hours at 350°F; for Resin 2 (Epon 828/DSA/Empol 1040/BDMA), 2 hours at 150°F followed by 4 hours at 300°F; and for Resin 3 (Epon 826/Epon 871/DDI/Curalon L), 5 hours at 285°F.

The pressure vessel will be rotated during the cure. For each resin system, the oven heat will be turned off and the chamber will be allowed to cool to room temperature. The oven door will be opened after the temperature drops to approximately 150°F.

D. PLASTER REMOVAL

The Kerr DMM plaster will be removed with an acetic-acid and hot-water solution (40% acetic acid and 60% water). The boss face, including the threaded holes and K-seal area, will be protected during these operations.

E. CLEANING, DIMENSIONAL CHECKING, AND WEIGHING

The interior of each pressure vessel will be washed with hot water (150°F maximum) until all foreign matter has been removed. (Do not use wire brushes or metal scraping tools.) The vessel will be air-dried at room temperature.

The boss-face to boss-face length will be measured and recorded:
_____ in.

The cylinder diameter will be measured (at three places) with pi tape and recorded: _____ in., _____ in., _____ in.

The pressure-vessel weight will be measured and recorded:
_____ g.

The vessel will be sent to Test Operations for cryogenic testing.

F. PREPARATION FOR TESTING

The test chamber (Part No. 178156), bolts, and plugs (Part No. 177413) will be assembled in accordance with the test-assembly drawing (Part No. 178169).

Test preparation, instrumentation, etc. will be in accordance with the Environmental Test Procedure for Cryogenic Pressure Vessels, 8-Inch-Diameter, for Contract NAS 3-6287.

III. TESTING

Tests will be conducted in accordance with the Environmental Test Procedure for Cryogenic Pressure Vessels, 8-Inch-Diameter, for Contract NAS 3-6287.

The internal volume of each tank will be determined and recorded before testing.

Single-cycle burst-pressurization tests will be conducted on all 18 vessels. Six will be tested at $+75^{\circ}\text{F}$, six at -320°F , and six at -423°F .

APPENDIX D

TEMPERATURE AND STRAIN MEASUREMENT, DATA AND ANALYSIS

I. GENERAL CONSIDERATIONS

Accurate measurement of the temperature of a glass/FWC skin under dynamic-strain conditions at cryogenic temperatures imposes problems that qualify the results to a degree. Some of these problems are as follows:

- The surface of the composite skin is rough and therefore forms a poor thermal-conduction path for an unbonded thermometer.
- No adhesives have been developed that are completely satisfactory for the bonding of thermometers at temperatures in the region of -400°F and 30,000 to 40,000 microstrain.*
- Inaccuracies inherent in the thermometer and data-processing system contribute to the overall system precision.

The wafer-thin platinum-resistance thermometers used in this program were bonded to the composite skin with a minimum thickness of Goodyear G207 cement to provide maximum surface contact with the irregular tank skin. A covering of Teflon, 1/16 in. thick by 1/2 in. square, was placed over the thermometer. A longitudinal band, independent of the bow-tie attachment bands, was used to spring-load the thermometer against the vessel wall. Various methods of attachment were used to bond 32-gage copper-constantan thermocouples against the composite wall.

A. For tests B-12, B-9, and B-20, the thermocouples were spot-welded to a 5-mil, 1/2-in.-square, stainless steel shim that was bonded (thermocouple toward composite wall) with Goodyear G207 cement. The plate was spring-loaded against the composite wall as for the platinum thermometers. This method appeared to be reasonably satisfactory (see Table D-1).

B. For Test B-7, the thermocouples were silver-brazed to a 0.1-in. by 0.3-in. by 3-mil stainless steel shim; they were calibrated in LN_2 and were found to be accurate within $\pm 3^{\circ}\text{F}$. The small shim was used in an attempt to improve the response of the thermometer as compared with the foregoing approach. The two thermometers were bonded and spring-loaded as above. Table D-1 shows that the bonding was not satisfactory, and this method was discontinued.

*Patrick T. Chiarito, Strain Measurements at Cryogenic Temperatures, NASA Lewis Research Center, Cleveland, Ohio, and John C. Tilinde, Investigation of Strain Gages at Cryogenic Temperatures, Douglas Missile & Space Systems Division.

TABLE D-1

TEMPERATURE MEASUREMENTS DURING BURST TESTING OF 8-IN.-DIA TANKAGE

| | Measured Test Temperature, °F | | | |
|--|-------------------------------|---------------------------|-----------------|---------------------------|
| | Vessel B-12 | | Vessel B-9 | |
| | Start (22 psig) | 1770 psig
Temp
Rise | Start (13 psig) | 1206 psig
Temp
Rise |
| Tank supply (LN ₂ line) | -310 | -287 23 | -310 | -223 87 |
| Tank outlet (LN ₂ line) | -308 | -302 6 | -314 | -313 1 |
| Skin Thermocouple 1 | -295 | -262 33 | -300 | -248 52 |
| Skin Thermocouple 2 | -295 | -275 20 | -305 | -255 50 |
| Skin, platinum-resistance
thermometer | -296 | -262 34 | -312 | -226 86 |
| | Vessel B-20 | | Vessel B-7 | |
| | Start (9 psig) | 2011 psig
Temp
Rise | Start (0 psig) | 1955 psig
Temp
Rise |
| Tank supply (LN ₂ line) | -316 | -316 0 | -317 | -311 6 |
| Tank outlet (LN ₂ line) | -315 | -312 3 | -329 | -329 0 |
| Skin Thermocouple 1 | -285 | -247 38 | -209 | -232 - |
| Skin Thermocouple 2 | -319 | -302 17 | -230 | -217 - |
| Skin, platinum-resistance
thermometer | -314 | -273 41 | -315 | -260 55 |
| Bottom-flange thermocouple | -310 | -312 - | -308 | -302 6 |
| | Vessel B-14 | | Vessel B-14 | |
| | Start (0 psig) | 1933 psig
Temp
Rise | Start (0 psig) | 1933 psig
Temp
Rise |
| Tank supply (LN ₂ line) | -318 | -310 8 | -310 | 8 |
| Tank outlet (LN ₂ line) | -322 | -312 10 | -312 | 10 |
| Skin Thermocouple 1 | -302 | -287 15 | -287 | 15 |
| Skin Thermocouple 2 | -305 | -290 15 | -290 | 15 |
| Skin, platinum-resistance
thermometer | - | - - | - | - |
| Bottom-flange thermocouple | -312 | -305 7 | -305 | 7 |

C. For Test B-14, the thermocouples were bonded with Epon 828/diethylenetriamine (DTA) (100/10 pbw). The composite vessel was prepared with No. 400 sandpaper and was cleaned. The bare soft-soldered thermocouples were secured to the composite with masking tape, which was used to form a dam. Resin was poured into the dam to a height of approximately 1/16 in. Following an ambient-temperature cure, the tapes were removed. The thermometers were then protected and spring-loaded as in I,A, above, and this method also appeared to be satisfactory.

The platinum-resistance thermometers used (Type 1371, Trans-Sonics, Inc. were originally proposed for all skin-temperature measurements, primarily on the basis of cost - \$15 each with a basic quoted accuracy of $\pm 3^{\circ}\text{F}$ uncalibrated. For increased accuracy, platinum-resistance or thermistor-type thermometers could be used, but would cost about \$100 each, primarily because of individual-thermometer-calibration requirements.

The quoted inaccuracy ($\pm 3^{\circ}\text{F}$) primarily results from the absence of cryogenic calibration. Additional inaccuracy is due to the strain sensitivity of the platinum wire.

George Hull of A. D. Little Company has stated that this thermometer could be in error by an additional $\pm 2^{\circ}\text{F}$ at 30,000 microstrain.

An accuracy of better than $\pm 5^{\circ}\text{F}$ is not required by this program, and the thermometer used is therefore satisfactory as well as cost-effective.

The installation of thermometers in the tank wrap during test-vessel fabrication is strongly recommended, to eliminate skin-surface-bonding problems and increase the reliability of wall-temperature data.

II. SKIN TEMPERATURE

By discarding the erroneous skin-surface temperature-rise data resulting from thermometer-bonding problems (Table D-1), an average increase of approximately 40°F in wall temperature is realized during the pressurization of 8-in.-dia tanks to the burst point at LN_2 temperatures while maintaining a temperature of -300°F (subcooled liquid) or lower at the tank inlet and outlet with the test-chamber pressure below 10 microns of Hg.

To substantiate this extreme temperature rise, a coil shroud (LN_2 -cooled, 13-1/2 in. in diameter) was fabricated from 50 ft of 1/4-in.-dia, 0.035-in.-wall, copper tubing covered with four layers of 10-mil aluminum foil for Test B-20. The vessel was placed inside this shroud so that only the flange ends of the tank were exposed to the ambient heat radiated by the vacuum-chamber wall. Heating by gas conduction was also minimized significantly by the proximity of the shield to the tank, with the shield cooling the gas between it and the tank.

A copper-constantan thermocouple was installed on the aluminum foil between the copper coils. It read -320°F during the burst test. Skin Thermocouple 2 indicated only a 17°F temperature rise during pressurization to the

burst (Table D-1), whereas Skin Thermocouple 1 and the platinum-resistance thermometer on the skin indicated 38 and 41°F increases, respectively. There was an apparent incomplete bond (conduction path) for Thermocouple 2, which left the thermocouple indicating a value intermediate between the -320°F shroud and that of the warm skin surface. This test verified that the walls become approximately 40°F warmer during the burst cycle; any unbonding from the tank skin would result in a lower indicated temperature rise because of a radiant-heat loss from the thermometer to the -320°F shroud heat sink.

The substantial skin-temperature rise during pressurization is probably caused by energy applied to the expanding tank and directly converted to heat in the tank wall due to yielding. This heat cannot be conducted back to the liquid inside the tank because of the short time involved (700-psi/min pressurization rate) and a poor conduction path due to a low heat-transfer film coefficient between the glass-filament wrap and the metal liner.

Assuming that no heat conduction occurs during testing and that the liner and the composite warm to the same temperature, the strain heating on an 8-in.-dia tank can be determined by calculation to cause a wall-temperature rise of 36°F at 140°R. At a temperature of 37°R this rise could be almost an order of magnitude greater, because of the rapid decrease in material specific heats with decreasing temperatures. The composite probably receives more strain heat than the metal liners; if all the strain heat is applied to the composite, a wall-temperature rise of 58°F is calculated at 140°R. These calculated figures should be considered as indicative only, because some heat conduction undoubtedly occurs and additional heat sources may be provided by sliding friction of the glass-overwrap layers. The possibility of an inconsistent heat-transfer film coefficient and load-carrying ratio between the liner and the composite from one tank to another during testing could account for some of the data scatter for the skin-temperature rise.

III. BOW-TIE STRAIN-GAGE TEMPERATURE MEASUREMENT AND CONTROL

The Aerojet bow-tie, strain-gage, displacement transducers (Figure D-1) are temperature-controlled by the manual adjustment of current through bifilar heater windings. Although the temperature-monitoring thermocouple is not located directly on the gage, the beryllium-copper reed offers a good conductive path to the gage and a poor one to the tank skin (attached by pins, not bonded); thus, the strain gage cannot be more than 10°F warmer than the thermocouple indication. (The relative locations of the thermocouple and heater windings make it impossible for the gage to be at a lower temperature than indicated by the thermocouple.)

The temperature gradient on the bow-tie extensometer, from directly above the tank attachment to a point adjacent to the strain-gage sensor was determined during LH₂ testing (Test B-19). It was found to be a maximum of 3°F. The bow-tie reeds are maintained at 70 ± 20°F during testing. The gage factor of the gages used on the bow-tie will change only 1% per 100°F change in temperature in the 70°F region. There is therefore a negligible loss in accuracy due to temperature effects.

IV. CALIBRATION OF BOW-TIE, STRAIN-GAGE, DISPLACEMENT TRANSDUCERS

A single-step, end-to-end calibration was performed on each bow-tie, strain-gage, displacement transducer used in testing. Each test employed three transducers, two for longitudinal displacement and one for hoop. The transducers were calibrated in place on the test vessel, with all instruments installed and connected to the data-acquisition equipment (a continuous-strip-chart recorder for each transducer). Laboratory conditions (ambient temperature) were employed, because the gages were maintained within the gage-compensation temperature range ($70 \pm 20^\circ\text{F}$) during cryogenic testing by manual adjustment of current. Additional instrumentation details are presented in Section III, above.

For use in calibration, a single washer was spot-welded at the end of each metal-foil support band (Figure D-2) attached to the longitudinal transducers. Two calibration tools (Figure D-2) were inserted between each attachment tack and the inner surface of the washer, and the signal-conditioning system was adjusted for a zero output reading on the recorder. The distance between the upper and lower attachment posts was accurately measured and recorded. Rotation of the calibration tools produced a displacement of 0.094 in. for each band, with a total displacement of 0.188 in. Strain was then calculated from

$$\text{Strain} = \frac{\Delta L}{L}$$

where

ΔL = total displacement between centers of washers = 0.188 in.
L = distance between centers of attachment tacks

Sample longitudinal-strain calculations for Vessel B-5 follow. For Strain Gage 2, L = 6.000 in. and

$$\text{Strain} = \frac{0.188}{6.000} = 0.3133 \text{ in./in.}$$

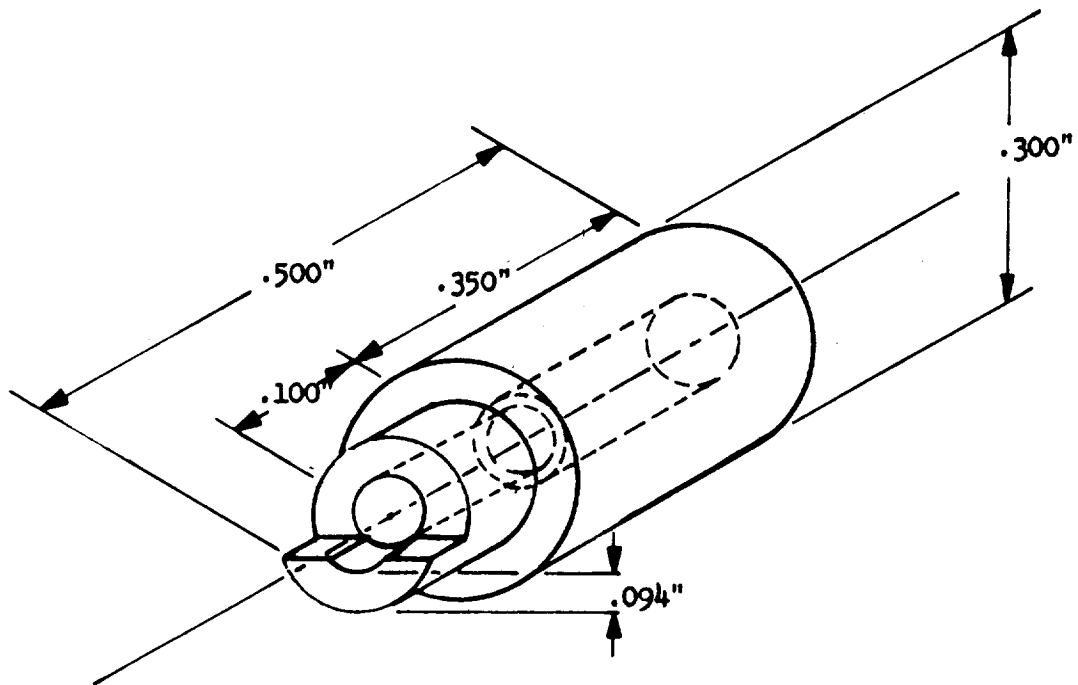
For Strain Gage 3, L = 5.937 in. and

$$\text{Strain} = \frac{0.188}{5.937} = 0.3166 \text{ in./in.}$$

The span control of the signal-conditioning equipment was adjusted so that the instrument would record 31.33 and 31.66% of full scale (based on the foregoing values), to permit strain to be read directly on each strip chart during the pressurization test. This procedure was repeated to ensure reliability.

The procedure used to calibrate the girth (hoop) transducer on each vessel (Strain Gage 1) was similar to that described above. The center of

CALIBRATION TOOL



SUPPORT BAND

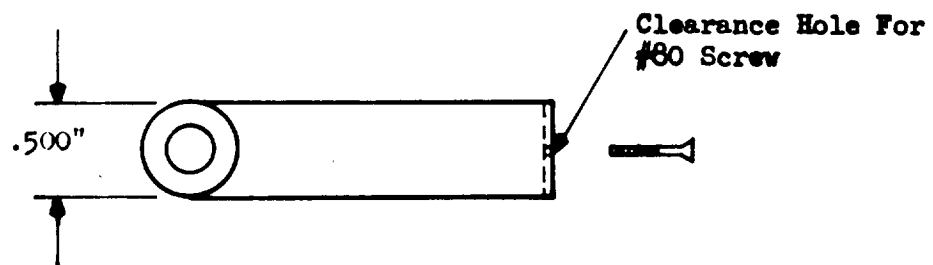


Figure D-2. Calibration Tool and Support Band

the girth band was displaced a predetermined distance on each side of the transducer (total amount, 0.500 in.). The calculations, and the zero and span adjustments, were performed as indicated above, except that values appropriate for girth measurements were used. A sample hoop-strain calculation for Vessel B-5 follows:

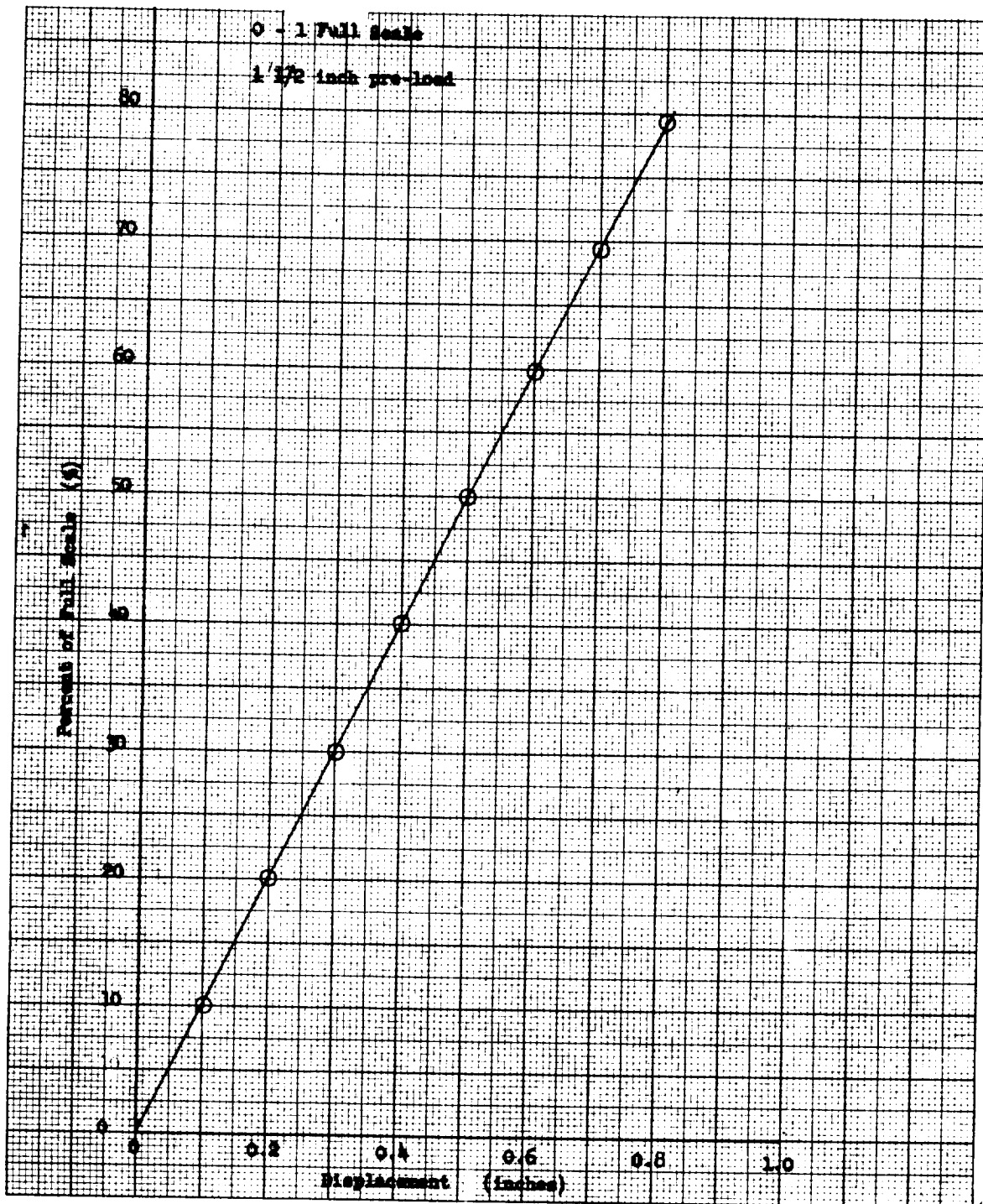
$$\begin{aligned}\Delta L &= \text{total hoop-band displacement} = 0.500 \text{ in.} \\ L &= \text{pressure-vessel circumference} = 24.875 \text{ in.}\end{aligned}$$

and

$$\text{Strain} = \frac{0.500}{24.875} = 0.02010 \text{ in./in.}$$

Detailed laboratory calibrations were also performed under ambient conditions to determine the degree of transducer linearity and reproducibility. Various displacements were set with the aid of a vernier caliper (reading accuracy, 0.001 in.), and transducer outputs for these displacements were measured with a recording potentiometer. The results are shown in Figure D-3. The curve for displacement vs recorder output as a percentage of chart scale was based on several data points for each configuration. Because all the transducers were linear and reproducible to 0.5% within a displacement range from 0.06 to 1.00 in., it was not necessary to perform multiple-point calibration for the individual transducers used in each test setup.

Vessel contraction during cryogenic conditioning before testing did not affect the accuracy of the strain data, because the transducer responses were linear and reproducible. As installed for testing, the transducers were pre-loaded for a displacement of approximately 1.50 in.



L-67-1186

Figure D-3. Calibration Curve for Bow-Tie Extensometer

APPENDIX E

CALCULATION OF FILAMENT AND COMPOSITE TENSILE STRESS

In analyzing filament-wound pressure vessels in this program, the assumption was made that the glass filaments are the primary structural material and therefore carry all the load.

A method based on the total number of glass fibers oriented in the direction of loading was used in determining the filament stress; modification of filament stress by the resin content yields composite stress. To determine these stress levels, an equivalent filament thickness was first calculated from the specific amount of glass roving laid in the test-specimen gage area during winding. This method was used in order to (1) provide a proper basis for comparison of data with regard to filament orientation and resin content, and (2) minimize differences in fabrication-processing effects. In this manner, the FWC test specimens were analyzed on the basis of actual winding data and laboratory tests, thus eliminating the effects of differences in specimen thickness caused by nonuniform resin contents. This calculated equivalent filament thickness is given by

$$t_f = A_e N_1 N_2 N_3 N_4$$

where

A_e = area of single end, sq in.

N_1 = number of ends per strand

N_2 = number of strands per turn

N_3 = number of turns per inch per layer

N_4 = number of layers in test specimen

Filament stress was determined by the ratio of load to area, factored by the fraction of filament layers oriented in the direction of loading. The lead of the winding machine and the width of the roving create an angular difference between the filament orientation and the direction of loading, but one so small that it may be ignored in the calculations:

$$\sigma_f = \frac{P}{t_f w} \left(\frac{N_4}{N_5} \right)$$

where

σ_f = ultimate filament stress, psi

P = ultimate load, lb

w = test-specimen width, in.

N_5 = number of layers oriented in direction of load

For composite stress,

$$\sigma_c = \frac{P}{t_c w} = \frac{P}{t_f w} \frac{V_g}{100}$$

where

σ_c = ultimate composite stress, psi

t_c = total equivalent composite thickness = $\frac{t_f}{V_g/100}$

V_g = amount of glass filament in composite, vol% (see Figure E-1).

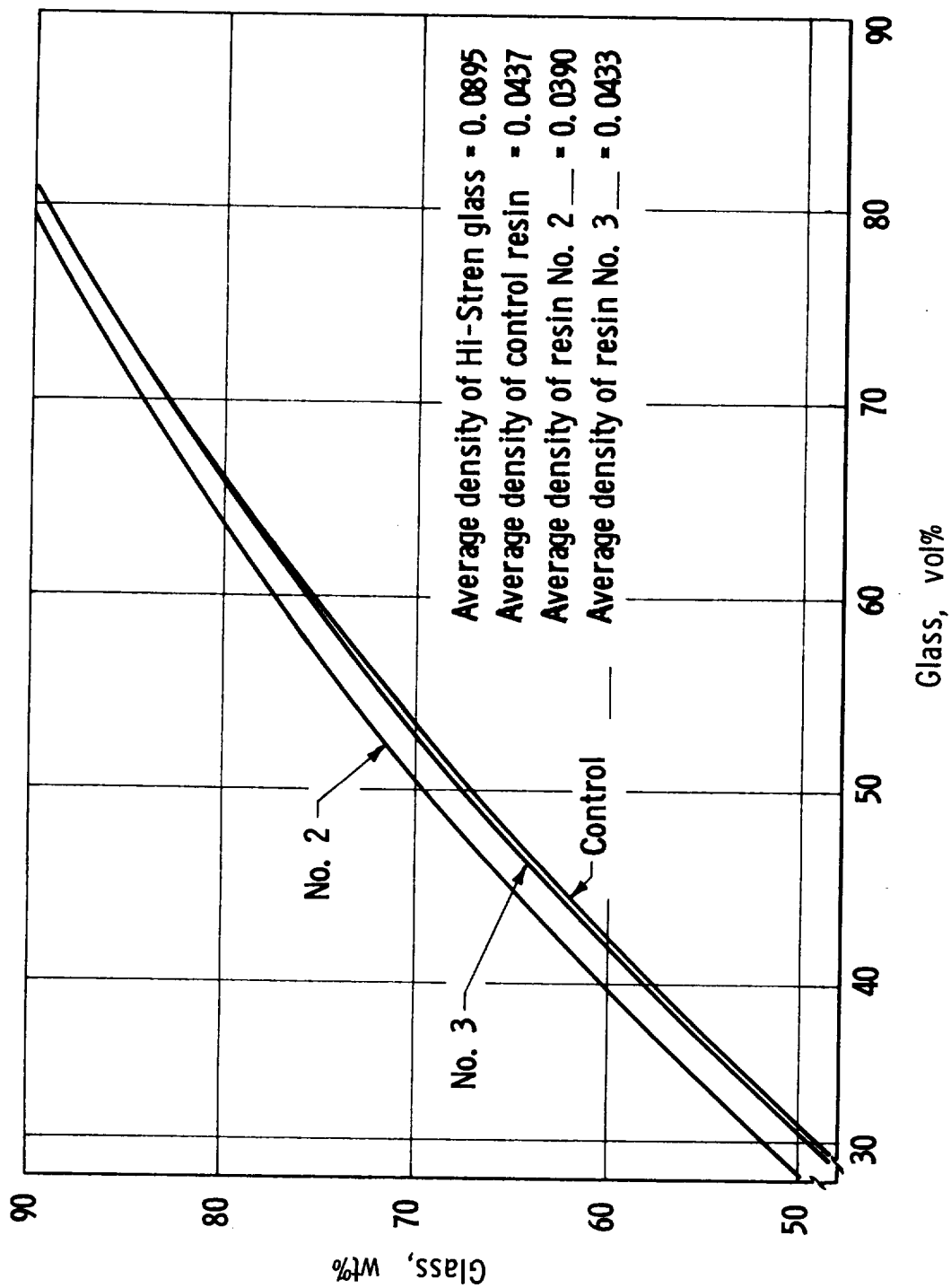


Figure E-1. Glass Weight/Volume Relationships in Resin Composites

APPENDIX F

EVALUATION OF PRESSURE-VESSEL WALL-TEMPERATURE MEASUREMENT

This special testing at liquid-nitrogen temperature was undertaken (1) to investigate installation techniques and the reliability of thermometers installed within the glass-composite wall for cryogenic-temperature measurement, and (2) to measure actual temperatures on the metal liner, at various distances from the liner in the glass-composite wall, and on the external surface of the glass-composite wall.

I. PROCEDURES

Platinum-resistance and copper-constantan thermometers were installed on the test vessel (Serial No. E-1) at locations shown in Figure F-1. The vessel was installed in the test stand and tested as described below.

Test 1: Two pressure cycles were conducted by pressurizing the vessel to 1800 psig and then venting to the atmosphere at a rate of approximately 1700 psi/min. Initial liquid-nitrogen equilibrium-temperature conditions were obtained prior to the first pressure cycle, and all temperatures were recorded continuously during the cycle. A liquid-nitrogen thermal shroud was used.

Test 2: A second, identical series of three pressure cycles were performed except that the liquid-nitrogen thermal shroud was not used.

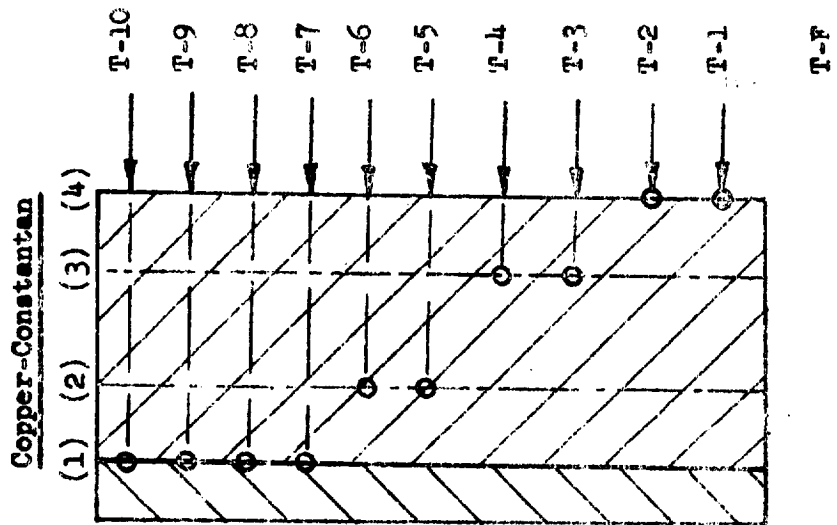
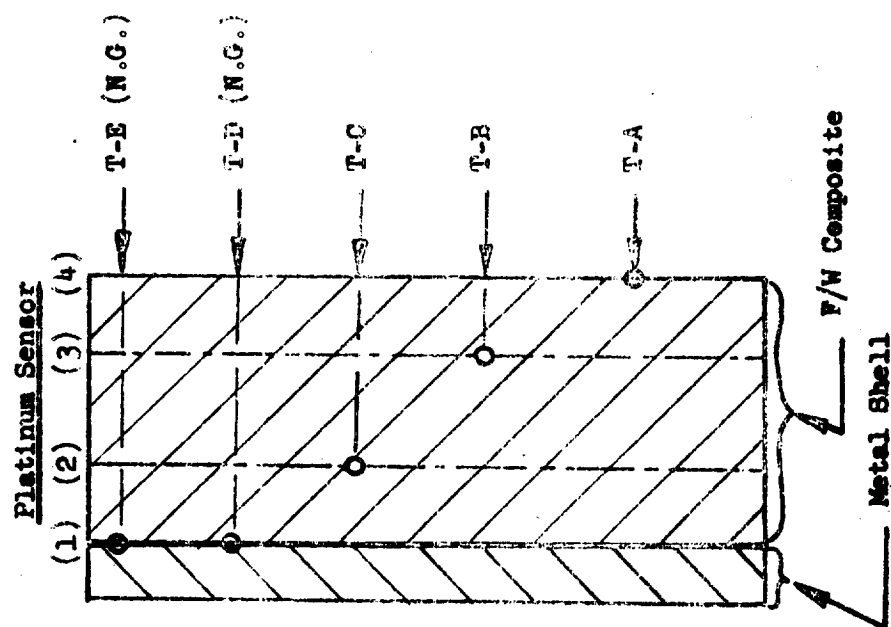
Test 3: A final test was performed, without the liquid-nitrogen thermal shroud, by pressurizing the vessel to failure. All thermometer outputs were recorded continuously during the test.

II. RESULTS

The platinum resistance thermometers T-E and T-D were not functional during the tests; shorting of the sensing elements to the metal liner occurred. The copper-constantan thermometer T-3 apparently partially open-circuited and the data were determined to be invalid.

The transient-temperature data were plotted against pressure for the first cycle of Test 1 and are shown in Figure F-2. The transient-temperature data were plotted against pressure for Tests 2 and 3 and are shown in Figures F-3 and F-4, respectively.

The plots for the external vessel-wall surface reveal progressively higher initial indicated temperatures between Tests 2 and 3. It is difficult to evaluate the validity of the external-wall-surface temperature for the cycles performed during Test 1, due to the presence of the thermal shroud. However, all other plotted temperatures for the various thermometer locations in all three tests indicate only a slight temperature increase during pressurization.



- (1) Installed on metal shell surface.
- (2) Installed on F/W composite after one revolution of windings.
- (3) Installed during last layer of winding.
- (4) Install on outer surface of F/W composite after resin cure.

Figure F-1. Temperature-Sensor Locations

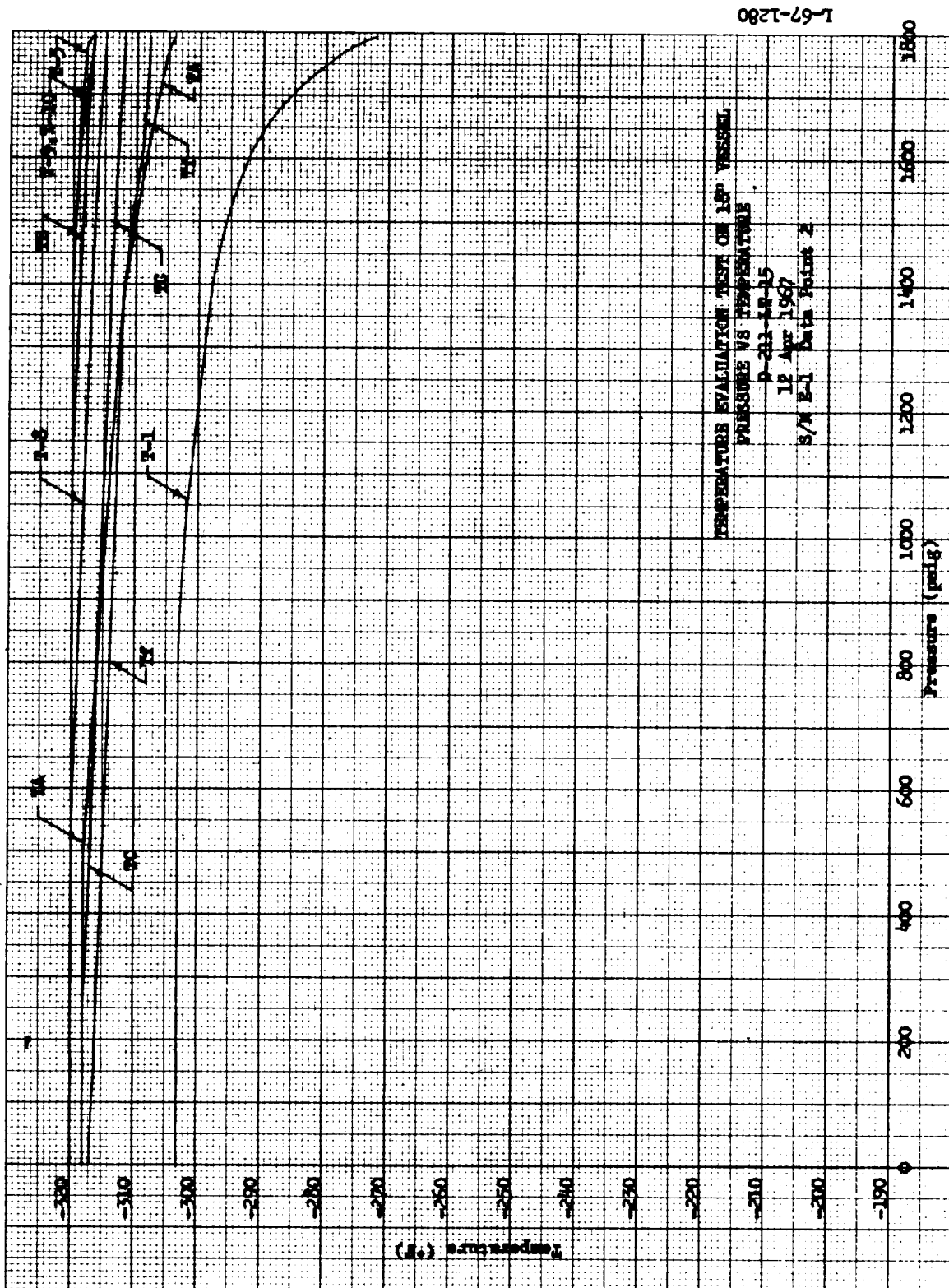


Figure F-2. Temperature Evaluation, Test 1

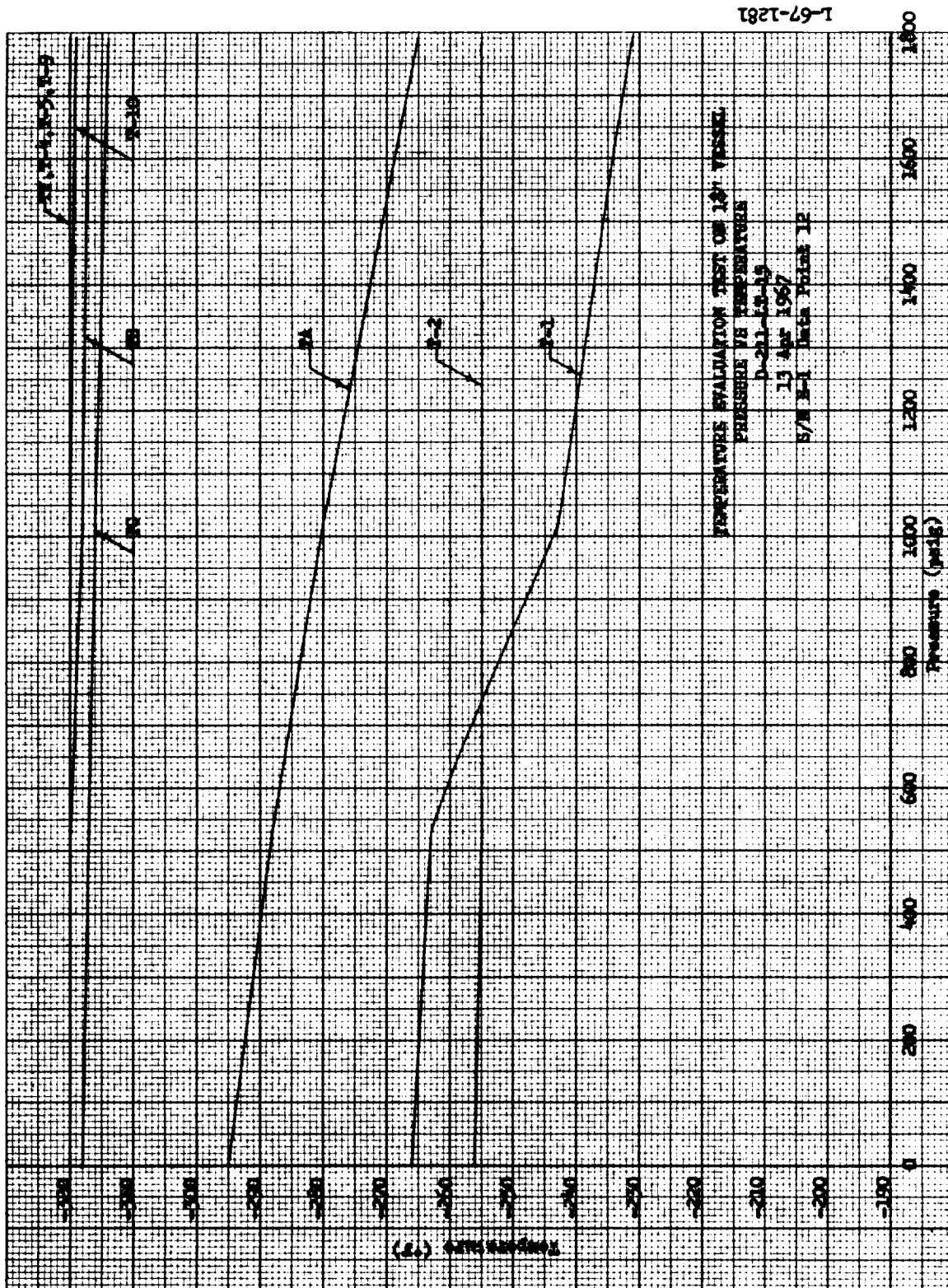


Figure F-3. Temperature Evaluation, Test 2

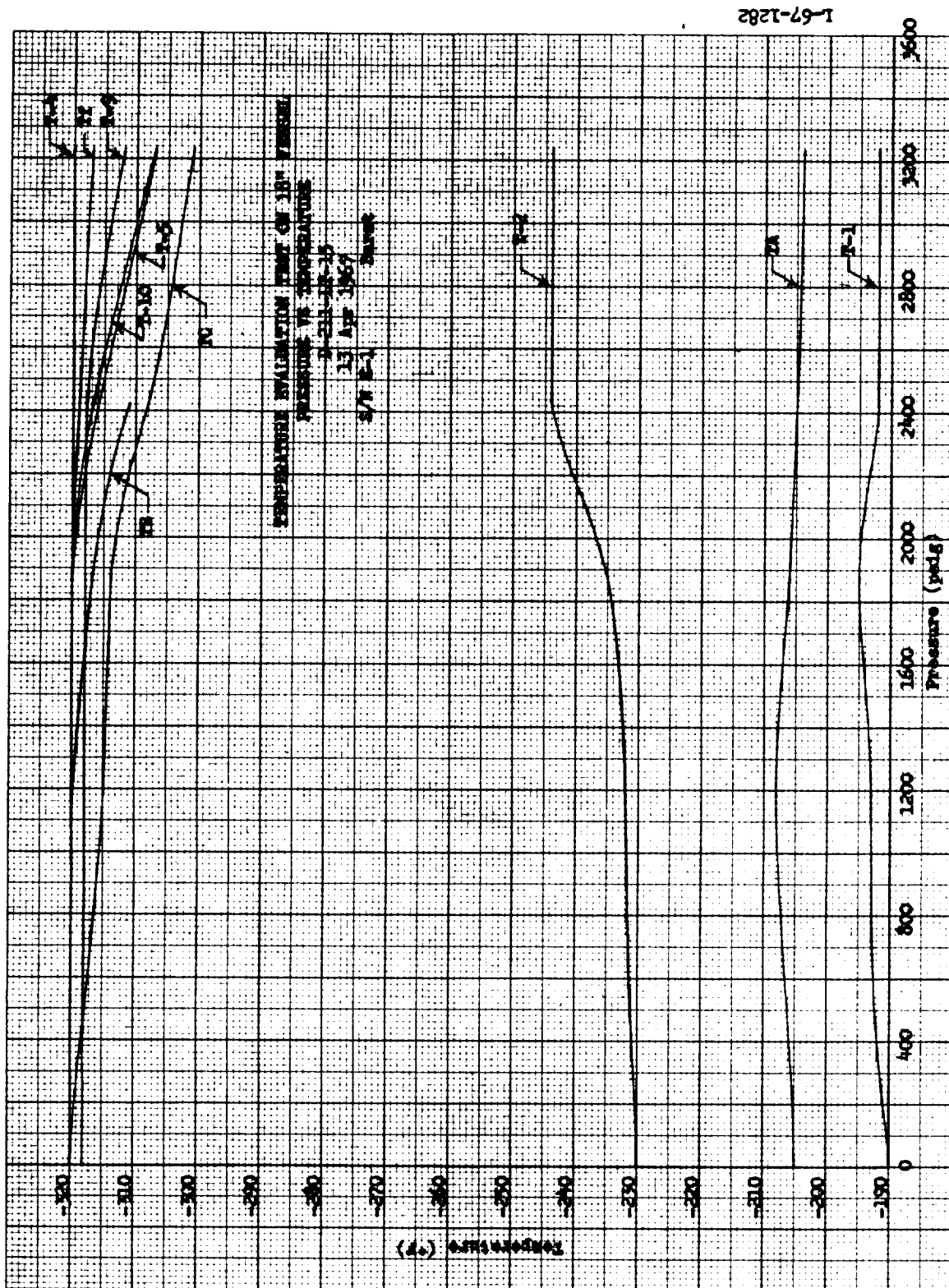


Figure F-4. Temperature Evaluation, Test 3

Between Tests 1 and 2 the test-vessel temperature was allowed to increase slowly to the ambient value while test-facility chamber vacuum was maintained.

The wall-surface thermometers during Tests 2 and 3 indicate erratic and invalid data due to effective bond degradation. The degradation was apparently caused by both the thermal cycling and the pressure-cycling tests conducted on the vessel. However, all other thermometers again indicated only a slight increase in temperature during vessel pressurization.

Vessel failure occurred during Test 3 at 3232 psig.

III. CONCLUSIONS

The tests indicated that thermometers can be practically and reliably placed within the glass-composite wall of a vessel.

They also indicated bond degradation, under simultaneous high strains and cryogenic temperatures, that resulted in considerably higher readings on surface thermometers than on thermometers incorporated within the composite wall.

FINAL REPORT DISTRIBUTION LIST FOR
CONTRACT NAS 3-6297

No. of Copies

| | |
|--|---|
| National Aeronautics and Space Administration | |
| Lewis Research Center | |
| 21000 Brookpark Road | |
| Cleveland, Ohio 44135 | |
| Attn: Contracting Officer, MS 500-210 | 1 |
| Liquid Rocket Technology Branch, MS 500-209 | 8 |
| Technical Report Control Office, MS 5-5 | 1 |
| Technology Utilization Office, MS 3-19 - John J. Weber | 1 |
| AFSC Liaison Office, MS 4-1 | 2 |
| Library | 2 |
| Office of Reliability & Quality Assurance, MS 500-203 | 1 |
| Structures Branch, M. & S. Division, MS 49-1 | 2 |
| E.W. Conrad, MS 100-1 | 1 |
| | |
| National Aeronautics and Space Administration | |
| Washington, D.C. 20546 | |
| Attn: Code MT | 1 |
| RPX | 2 |
| RPL | 2 |
| SV | 1 |
| RV-2 | 2 |
| | |
| Scientific and Technical Information Facility | |
| P.O. Box 33 | |
| College Park, Maryland 20740 | |
| Attn: NASA Representative | 6 |
| | |
| National Aeronautics and Space Administration | |
| Ames Research Center | |
| Moffett Field, California 94035 | |
| Attn: Library | 1 |
| C. A. Syvertson | 1 |
| | |
| National Aeronautics and Space Administration | |
| Flight Research Center | |
| P.O. Box 273 | |
| Edwards, California 93523 | |
| Attn: Library | 1 |
| | |
| National Aeronautics and Space Administration | |
| Goddard Space Flight Center | |
| Greenbelt, Maryland 20771 | |
| Attn: Library | 1 |

DISTRIBUTION LIST (cont.)

| | <u>No. of Copies</u> |
|---|----------------------|
| National Aeronautics and Space Administration
John F. Kennedy Space Center
Cocoa Beach, Florida 32931
Attn: Library | 1 |
| National Aeronautics and Space Administration
Langley Research Center
Langley Station
Hampton, Virginia 23365
Attn: Library | 1 |
| National Aeronautics and Space Administration
Manned Spacecraft Center
Houston, Texas 77001
Attn: Library
C. Yodzis, Code EPl | 1
1 |
| National Aeronautics and Space Administration
George C. Marshall Space Flight Center
Huntsville, Alabama 35812
Attn: Library
Keith Chandler, R-P&VE-PA
L. R. Moffett, Jr., R-P&VE-MNM
J. T. Shell, R-P&VE-NMR | 1
1
1
1 |
| National Aeronautics and Space Administration
Western Operations Office
150 Pico Boulevard
Santa Monica, California 90406
Attn: Library | 1 |
| Jet Propulsion Laboratory
4800 Oak Grove Drive
Pasadena, California 91103
Attn: Library
R. F. Rose | 1
1 |
| Office of the Director of Defense Research & Engineering
Washington, D.C. 20301
Attn: Dr. H. W. Schulz, Office of Asst. Dir. (Chem.Technology) | 1 |
| Defense Documentation Center
Cameron Station
Alexandria, Virginia 22314 | 1 |
| RTD(RTNP)
Bolling Air Force Base
Washington, D.C. 20332 | 1 |

DISTRIBUTION LIST (cont.)

| | <u>No. of Copies</u> |
|---|----------------------|
| U.S. Air Force
Washington 25, D.C.
Attn: Col. C. K. Stambaugh, Code AFRST | 1 |
| Commanding Officer
U.S. Army Research Office (Durham)
Box CM, Duke Station
Durham, North Carolina 27706 | 1 |
| U.S. Army Missile Command
Redstone Scientific Information Center
Redstone Arsenal, Alabama 35808
Attn: Chief, Document Section
Dr. W. Wharton | 1
1 |
| Bureau of Naval Weapons
Department of the Navy
Washington, D.C.
Attn: J. Kay, Code RTMS-41
Maxwell Stander, Code RRMA-32 | 1
1 |
| Commander
U.S. Naval Missile Center
Point Mugu, California 93041
Attn: Technical Library | 1 |
| Commander
U.S. Naval Ordnance Test Station
China Lake, California 93557
Attn: Code 45
Code 753
W. F. Thorm, Code 4562 | 1
1
1 |
| Commanding Officer
Office of Naval Research
1030 E. Green Street
Pasadena, California 91101 | 1 |
| U.S. Naval Research Laboratory
Washington, D.C. 20390
Attn: J. A. Kies, Code 6210
W. Zisman, Code 6100
J. E. Cowling, Code 6120 | 1
1
1 |
| Picatinny Arsenal
Dover, New Jersey
Attn: I. Forsten, Chief, Liquid Propulsion Laboratory | 1 |

DISTRIBUTION LIST (cont.)

No. of Copies

| | |
|---|--------|
| Arnold Engineering Development Center
Air Force Systems Command
Tullahoma, Tennessee 37389
Attn: AEOIM | 1 |
| Advanced Research Projects Agency
Washington, D.C. 20525
Attn: D. E. Mock | 1 |
| Aeronautical Systems Division
Air Force Systems Command
Wright-Patterson Air Force Base,
Dayton, Ohio
Attn: D. L. Schmidt, Code ASRCNC-2 | 1 |
| Air Force Missile Test Center
Patrick Air Force Base, Florida
Attn: L. J. Ullian | 1 |
| Air Force Systems Command (SCLT/Capt. S. W. Bowen)
Andrews Air Force Base
Washington, D.C. 20332 | 1 |
| Air Force Rocket Propulsion Laboratory (RPR)
Edwards, California 93523 | 1 |
| Air Force Rocket Propulsion Laboratory (RPM)
Edwards, California 93523 | 1 |
| Air Force FTC (FTAT-2)
Edwards Air Force Base, California 93523
Attn: Col. J. M. Silk | 1 |
| Air Force Office of Scientific Research
Washington, D.C. 20333
Attn: SREP, Dr. J. F. Masi | 1 |
| Department of the Air Force
Air Force Materials Laboratory (AFSC)
Wright-Patterson Air Force Base, Ohio 45433
Attn: T. J. Reinhart, Jr. (MAAE)
S. Litvak (MAAM) | 1
1 |
| Office of Research Analyses (OAR)
Holloman Air Force Base, New Mexico 88330
Attn: RRRT
Maj. R. E. Brocken, Code MDGRT | 1
1 |

DISTRIBUTION LIST (cont.)

No. of Copies

| | |
|--|-------------|
| Commander
U.S. Naval Ordnance Laboratory
White Oak, Silver Spring, Maryland 20910
Attn: Library
F. Robert Barnet | 1
1 |
| U.S. Atomic Energy Commission
Technical Information Services
Box 62
Oak Ridge, Tennessee
Attn: A. P. Huber, Code ORGDP, Box P | 1 |
| Air Force Aero Propulsion Laboratory
Research & Technology Division
Air Force Systems Command
United States Air Force
Wright-Patterson AFB, Ohio 45433
Attn: APRP (C. M. Donaldson) | 1 |
| Aerojet-General Corporation
11711 South Woodruff Avenue
Downey, California 90241
Attn: F. M. West, Chief Librarian | 1 |
| Aerojet-General Corporation
P.O. Box 15847
Sacramento, California 95813
Attn: Technical Library 2484-2015A
Dr. C. M. Beighley
D. T. Bedsole | 1
1
1 |
| Aeronutronic Division of Philco Corporation
Ford Road
Newport Beach, California 92600
Attn: Dr. L. H. Linder, Manager
D. A. Carrison
Technical Information Department | 1
1
1 |
| Aeroprojects, Incorporated
310 East Rosedale Avenue
West Chester, Pennsylvania 19380
Attn: C. D. McKinney | 1 |
| Aerospace Corporation
P.O. Box 95085
Los Angeles, California 90045
Attn: J. G. Wilder, MS-2293
Library-Documents | 1
1 |

DISTRIBUTION LIST (cont.)

| | <u>No. of Copies</u> |
|---|----------------------|
| Arthur D. Little, Inc.
Acorn Park
Cambridge 40, Massachusetts
Attn: Library | 1 |
| Astropower, Incorporated
Subs. of Douglas Aircraft Company
2968 Randolph Avenue
Costa Mesa, California
Attn: Dr. George Moc, Director, Research | 1 |
| Astrosystems, Incorporated
1275 Bloomfield Avenue
Caldwell Township, New Jersey
Attn: A. Mendenhall | 1 |
| ARO, Incorporated
Arnold Engineering Development Center
Arnold AF Station, Tennessee 37389
Attn: Dr. B. H. Goethert, Chief Scientist | 1 |
| Atlantic Research Corporation
Shirley Highway & Edsall Road
Alexandria, Virginia 22314
Attn: A. Scurlock | 1 |
| Security Office for Library | 1 |
| Battelle Memorial Institute
505 King Avenue
Columbus, Ohio 43201
Attn: Report Library, Room 6A | 1 |
| Bell Aerosystems, Inc.
Box 1
Buffalo, New York 14205
Attn: T. Reinhardt | 1 |
| W. M. Smith | 1 |
| Bendix Systems Division
Bendix Corporation
Ann Arbor, Michigan
Attn: John M. Bureger | 1 |

DISTRIBUTION LIST (cont.)

| | <u>No. of Copies</u> |
|--|----------------------|
| The Boeing Company
Aero Space Division
P.O. Box 3707
Seattle, Washington 98124
Attn: Ruth E. Peerenboom (1190) | 1 |
| J. Hoggatt, Kent Site | 1 |
| Chemical Propulsion Information Agency
Applied Physics Laboratory
8621 Georgia Avenue
Silver Spring, Maryland 20910 | 1 |
| Chrysler Corporation
Missile Division
Warren, Michigan
Attn: John Gates | 1 |
| Chrysler Corporation
Space Division
New Orleans, Louisiana
Attn: Librarian | 1 |
| Curtiss-Wright Corporation
Wright Aeronautical Division
Woodridge, New Jersey
Attn: G. Kelley | 1 |
| University of Denver
Denver Research Institute
P.O. Box 10127
Denver, Colorado 80210
Attn: Security Office | 1 |
| Douglas Aircraft Company, Inc.
Santa Monica Division
3000 Ocean Park Blvd.
Santa Monica, California 90405
Attn: J. L. Waisman
R. W. Hallet
G. W. Burge | 1
1
1 |
| Fairchild Stratos Corporation
Aircraft Missiles Division
Hagerstown, Maryland
Attn: J. S. Kerr | 1 |

DISTRIBUTION LIST (cont.)

| | <u>No. of Copies</u> |
|--|----------------------|
| General Dynamics/Astronautics
P.O. Box 1128
San Diego, California 92112
Attn: F. Dore | 1 |
| Library & Information Services (128-00) | 1 |
| Convair Division
General Dynamics Corporation
P.O. Box 1128
San Diego, California 92112
Attn: Mr. W. Fenning | |
| Centaur Resident Project Office | 1 |
| General Electric Company
Re-Entry Systems Department
P.O. Box 8555
Philadelphia, Pennsylvania 19101
Attn: F. E. Schultz | 1 |
| General Electric Company
Flight Propulsion Lab. Department
Cincinnati 15, Ohio
Attn: D. Suichu | 1 |
| Grumman Aircraft Engineering Corporation
Bethpage, Long Island,
New York
Attn: Joseph Gavin | 1 |
| Hercules Powder Company
Allegheny Ballistics Laboratory
P.O. Box 210
Cumberland, Maryland 21501
Attn: Library | 1 |
| IIT Research Institute
Technology Center
Chicago, Illinois 60616
Attn: C. K. Hersh, Chemistry Division | 1 |
| Kidde Aero-Space Division
Walter Kidde & Company, Inc.
675 Main Street
Belleville 9, New Jersey
Attn: R. J. Hanville, Director of Research Engineering | 1 |

DISTRIBUTION LIST (cont.)

No. of Copies

| | |
|--|--------|
| Lockheed Missiles & Space Company
P.O. Box 504
Sunnyvale, California
Attn: Y. C. Lee, Power Systems R&D
Technical Information Center | 1
1 |
| Lockheed-California Company
10445 Glen Oaks Blvd.,
Pacoima, California
Attn: G. D. Brewer | 1 |
| Lockheed Propulsion Company
P.O. Box 111
Redlands, California 92374
Attn: Miss Belle Berlad, Librarian
H. L. Thackwell | 1
1 |
| Lockheed Missiles & Space Company
Propulsion Engineering Division (D.55-11)
1111 Lockheed Way
Sunnyvale, California 94087 | 1 |
| Marquardt Corporation
16555 Saticoy Street
Box 2013 - South Annex
Van Nuys, California 91404
Attn: Librarian
W. D. Boardman, Jr. | 1
1 |
| Martin-Marietta Corporation
Martin Division
Baltimore 3, Maryland
Attn: John Calathes (3214) | 1 |
| McDonnell Aircraft Corporation
P.O. Box 6101
Lambert Field, Missouri
Attn: R. A. Herzmark | 1 |
| North American Aviation, Inc.
Space & Information Systems Division
12214 Lakewood Boulevard
Downey, California 90242
Attn: Technical Information Center, D/096-722 (AJ01)
H. Storms | 1
1 |

DISTRIBUTION LIST (cont.)

| | <u>No. of Copies</u> |
|---|----------------------|
| Northrop Space Laboratories
1001 East Broadway
Hawthorne, California
Attn: Dr. William Howard | 1 |
| Purdue University
Lafayette, Indiana 47907
Attn: Technical Librarian | 1 |
| AVCO Corporation
Research and Advanced Development Division
Wilmington, Massachusetts 01887
Attn: B. S. Horton | 1 |
| Bjorksten Research Laboratories, Inc.
Madison, Wisconsin
Attn: I. J. Leichtle | 1 |
| Brunswick Corporation
Defense Products Division
Marion, Virginia | 1 |
| Ferro Corporation
Fiber Glass Division
Fiber Glass Road
Nashville, Tennessee 37211
Attn: G. A. Stein | 1 |
| General Technologies Corporation
708 North West Street
Alexandria, Virginia
Attn: J. C. Withers | 1 |
| B. F. Goodrich Company
Aerospace and Defense Products
500 South Main Street
Akron, Ohio | 1 |
| Goodyear Aerospace Corporation
1210 Massillon Road
Akron, Ohio
Attn: L. M. Toth | 1 |
| Monsanto Company
Central Research Department
ARPA Program
St. Louis, Missouri
Attn: John D. Calfee | 1 |

DISTRIBUTION LIST (cont.)

No. of Copies

Monsanto Research Corporation
1515 Nicholas Road
Dayton, Ohio 45407
Attn: C. J. Eby

1

National Research Corporation
70 Memorial Drive
Cambridge, Massachusetts
Attn: R. W. Love

1

Radio Corporation of America
Astro-Electronics Division
Defense Electronic Products
Princeton, New Jersey
Attn: S. Fairweather

1

Republic Aviation Corporation
Farmingdale, Long Island
New York
Attn: Dr. William O'Donnell

1

Rocket Research Corporation
520 South Portland Street
Seattle, Washington 98108

1

Rocketdyne Division of
North American Aviation, Inc.
6633 Canoga Avenue
Canoga Park, California 91304
Attn: Library, Department 596-306
R. P. Frohmberg

1

1

Rohm and Haas Company
Redstone Arsenal Research Division
Huntsville, Alabama 35808
Attn: Librarian

1

Space-General Corporation
9200 E. Flair Dr.
El Monte, Calif. 91731
Attn: C. E. Roth

1

Stanford Research Institute
333 Ravenswood Avenue
Menlo Park, California 94025
Attn: Thor Smith

1

DISTRIBUTION LIST (cont.)

| | <u>No. of Copies</u> |
|--|----------------------|
| Texaco Experiment, Incorporated
P.O. Box 1-T
Richmond, Virginia 23202
Attn: E. B. Monteath
Librarian | 1
1 |
| Thiokol Chemical Corporation
Alpha Division, Huntsville Plant
Huntsville, Alabama 35800
Attn: Technical Director | 1 |
| Thiokol Chemical Corporation
Reaction Motors Division
Denville, New Jersey 07834
Attn: A. Sherman
Librarian | 1
1 |
| Thiokol Chemical Corporation
Redstone Division
Huntsville, Alabama
Attn: John Goodloe | 1 |
| TRW Systems, Incorporated
1 Space Park
Redondo Beach, California 90200
Attn: G. W. Elverum
STL Tech. Lib. Doc. Acquisitions | 1
1 |
| TRW, Incorporated
TAPCO Division
23555 Euclid Avenue
Cleveland, Ohio 44117
Attn: P. T. Angell | 1 |
| United Aircraft Corporation
Corporation Library
400 Main Street
East Hartford, Connecticut 06118
Attn: Dr. David Rix
Erle Martin | 1
1 |
| United Aircraft Corporation
Pratt & Whitney Division
Florida Research & Development Center
P.O. Box 2691
West Palm Beach, Florida 33402
Attn: R. J. Coar
Library | 1
1 |

DISTRIBUTION LIST (cont.)

| | <u>No. of Copies</u> |
|---|----------------------|
| United Aircraft Corporation
United Technology Center
P.O. Box 358
Sunnyvale, California 94088
Attn: Librarian | 1 |
| Vought Astronautics
Box 5907
Dallas 22, Texas
Attn: Warren C. Trent | 1 |
| Owens-Corning Fiberglas Corp.
Fiberglas Technical Center
Granville, Ohio
Attn: E. M. Lindsay | 1 |
| Princeton Chemical Research, Inc.
P.O. Box 652
Princeton, New Jersey 08540
Attn: F. W. Long | 1 |
| Shell Chemical Company
Plastics and Resins Division
Downey, California
Attn: Library | 1 |
| Union Carbide Corporation
Parma Technical Center
12900 Snow Road
Parma, Ohio 44101
Attn: Miss Marilyn McFerron, Assistant Librarian | 1 |
| Whittaker Corporation
Narmco Research & Development Division
3540 Aero Court
San Diego, California 92123
Attn: A. G. Larson | 1 |
| Martin Company
P.O. Box 5837
Orlando, Florida
Attn: Max Goldstein (MP-275) | 1 |

